

2014

The Nrf2 transcriptional target, OSGIN1, contributes to the cytoprotective properties of dimethyl fumarate

<https://hdl.handle.net/2144/15345>

"Downloaded from OpenBU. Boston University's institutional repository."

BOSTON UNIVERSITY
SCHOOL OF MEDICINE

Dissertation

**THE NRF2 TRANSCRIPTIONAL TARGET, OSGIN1, CONTRIBUTES TO THE
CYTOPROTECTIVE PROPERTIES OF DIMETHYL FUMARATE**

By

MELANIE SHACKETT BRENNAN

B.S., University of Connecticut, 2006

M.S., University of Hartford, 2008

Submitted in partial fulfillment of the
requirements for the degree of
Doctor of Philosophy

2014

© 2014 By
MELANIE SHACKETT BRENNAN
All rights reserved

Approved by

First Reader

Tsuneya Ikezu, M.D, Ph.D.
Professor of Pharmacology & Experimental Therapeutics, Neurology

Second Reader

Robert H. Scannevin, Ph.D.
Director of Neurology Research, Biogen Idec, MA, USA

DEDICATION

This dissertation is dedicated to my husband and best friend, Kyle. Without his unending patience and continuous support the completion of this dissertation would not have been possible.

ACKNOWLEDGMENTS

I would first like to thank Boston University and Biogen Idec for making this unique collaboration possible and giving me the opportunity to experience two amazing worlds of research. I have been able to learn and grow with a diverse group of remarkable scientists who have all contributed to my knowledge and curiosity in the field of Neuroscience. I would also like to thank my dissertation committee, Dr. Angela Ho, Dr. Tsuneya Ikezu, Dr. Shelley Russek, Dr. Don Mahad and Dr. Robert Scannevin for their insight, patience and ability to challenge me to think beyond what is known. A special thank you is due to Dr. Scannevin and Dr. Maria Matos who equally experienced the rises and falls of this research with me on a daily basis, and contributed many hours of thought and discussion to the research set forth in this dissertation. Finally, my gratitude is extended to my family and supporters outside of the research world who were always there by my side during the highs and lows of this unique journey.

**THE NRF2 TRANSCRIPTIONAL TARGET, OSGIN1, CONTRIBUTES TO THE
CYTOPROTECTIVE PROPERTIES OF DIMETHYL FUMARATE**

MELANIE SHACKETT BRENNAN

Boston University School of Medicine, 2014

Major Professor: Tsuneya Ikezu, Professor of Pharmacology & Experimental
Therapeutics, Neurology

ABSTRACT

Understanding how defense signaling pathways regulate neuronal protection in the compromised central nervous system (CNS) is essential for combating neurodegenerative disorders. This is apparent in the intrinsic activation of the transcription factor Nrf2 during periods of oxidative stress, a hallmark of neurodegeneration. This regulator of the antioxidant response induces the transcription of genes essential for protecting against oxidative stress-induced damage and is a prime target for drug discovery. Delayed-release dimethyl fumarate (DMF), currently approved for the treatment of relapsing-remitting forms of multiple sclerosis (MS), is believed to mediate its effect *via* the Nrf2 pathway; however, the exact mechanisms of action are unknown. The primary aim of the studies outlined in this dissertation was to identify the molecular mechanisms of Nrf2 regulation and subsequent cellular protection conferred by DMF and its bioactive metabolite, monomethyl fumarate (MMF). For this thesis study, transcriptional profiling studies following oral administration of DMF were conducted to characterize DMF pharmacodynamic responses in the central nervous system (CNS) and

peripheral tissues to understand the functional effects of DMF in vivo as well as explore the necessity of Nrf2 in this process. Data from these studies confirm earlier findings that DMF activates transcription of Nrf2 target genes in the CNS and periphery; however, tissue-specific gene expression was also observed, indicating additional levels of transcriptional control beyond Nrf2 activation. These findings suggest that there may be unique cytoprotective and immunomodulatory capabilities of DMF within specific tissues. In the CNS, a novel Nrf2 transcriptional target gene OSGIN1 was identified to be significantly upregulated following DMF treatment in vivo; however, the contribution of this gene to the pharmacodynamic properties of DMF or MMF has not been previously described. Therefore, the in vitro effects of MMF on OSGIN1 expression were characterized, and the necessity of OSGIN1 in mediating cytoprotective effects against toxic oxidative stress in human astrocytes was evaluated. These data identify a potential mechanism for MMF-mediated cytoprotection in human astrocytes that function in an OSGIN1 and p53-dependent manner. Overall, the experiments described in this dissertation allow for a broader understanding of endogenous cellular protection and how it can be used to combat CNS disorders.

TABLE OF CONTENTS

TITLE PAGE	i
COPYRIGHT PAGE	ii
READER'S APPROVAL PAGE	iii
DEDICATION	iv
ACKNOWLEDGMENTS	v
ABSTRACT	vi
TABLE OF CONTENTS.....	viii
LIST OF TABLES	xv
LIST OF FIGURES	xvi
LIST OF ABBREVIATIONS.....	xix
CHAPTER I: INTRODUCTION.....	1
1. OXIDATIVE/ELECTROPHILIC STRESS	1
1.1 Sources of ROS and Electrophiles	2
1.1.1 Cellular metabolism.....	3
1.1.2 Xenobiotic metabolism	7
1.1.3 Cell signaling	8
1.1.4 Immune defense	10
1.2 The Role of Oxidative and Electrophilic Stress in Neurodegenerative Disease.....	11

1.2.1 Multiple sclerosis	13
1.2.2 Parkinson’s disease	15
1.2.3 Alzheimer’s disease	17
1.2.4 Huntington’s disease	19
1.2.5 Amyotrophic lateral sclerosis	20
2. THE NRF2 PATHWAY IN RESPONSE TO STRESS	21
2.1 The NF-E2 Family of Transcription Factors	22
2.2 Nrf2	24
2.2.1 Functional domains of Nrf2	27
2.3 Activation of the Nrf2 Pathway	30
2.3.1 Keap1	33
2.3.2 Nrf2 targets genes	36
3. THE ROLE OF NRF2 IN DISEASE.....	40
3.1 Nrf2 and CNS-independent Diseases.....	40
3.2 Nrf2 and models of neurodegenerative disorders	41
3.2.1 Dysfunction of Nrf2 in human neurodegenerative disorders.....	41
3.2.2 Nrf2 and Models of Neurodegenerative Disorders	43
4. COMPOUNDS THAT REGULATE NRF2.....	46
4.1 Naturally Occurring Compounds	47
4.2 Synthetic Compounds	48
5. DIMETHYL FUMARATE.....	51
5.1 Origins of Dimethyl Fumarate	51

5.2 Structures and Interactions of DMF.....	51
5.3 Therapeutic Effect of DMF in Multiple Sclerosis	53
5.4 Preclinical Studies and the Mechanism of Action of DMF	54
5.4.1 Anti-inflammatory effects of DMF.....	54
5.4.2 DMF and the Nrf2 pathway	55
6. OSGIN1	57
6.1 Background.....	57
6.1.1 Characterization of the OSGIN1 gene	57
6.1.2 Transcripts (Splice Variants) of OSGIN1	58
6.2 OSGIN1 Function	61
6.2.2 OSGIN1 balances cell growth, differentiation and death	61
6.2.1 OSGIN1 as a regulator of inflammation	64
6.3 OSGIN1 and Disease	64
6.3.1 OSGIN1 and cancer	64
6.3.2 OSGIN1 and cardiovascular disease.....	66
6.4 OSGIN1 as a Transcriptional Target of Nrf2	66
7. RESEARCH HYPOTHESES	68
CHAPTER II: MATERIALS AND METHODS.....	69
1. MATERIALS.....	69
1.1 Animals	69
1.1.1 C57BL/6 wild type mice	69
1.1.2 Transgenic Nrf2 -/- knockout mice.....	69

1.2 Antibodies	70
1.2.1 Generation of OSGIN1 isoform-specific antibodies.....	71
1.3 Human siRNA constructs	73
1.4 Primers and Probes	73
1.4.1 Purchased primer/probe sets	73
1.4.2 Custom primer/probes sets.....	75
1.4.3 Primers for 3' and 5' RACE	75
2. METHODS	76
2.1 Pharmacokinetic Measure of MMF Exposure	76
2.2 Acute Oral Administration of DMF <i>in vivo</i>	77
2.2.1 Time course in wild type C57BL/6 mice.....	77
2.2.2 Dose response in wild type C57BL/6 mice.....	77
2.2.3 Modified time course in transgenic Nrf2 ^{-/-} knockout mice.....	77
2.2.4 Tissue harvest.....	78
2.3 Cell Culture.....	79
2.3.1 Primary human spinal cord astrocytes	79
2.3.2 Reverse transient transfection	79
2.4 Plate-based Cellular Assays	80
2.4.1 Compound handling.....	80
2.4.2 H ₂ O ₂ <i>in vitro</i> stress response assay.....	80
2.4.3 EdU proliferation assay.....	81
2.4.4 TiterTACS TM Assay for Apoptosis.....	81

2.4.5 Cellular extract preparation and Nrf2/p53 activity assays	82
2.4.6 Immunocytochemistry	82
2.5 RNA Extraction	83
2.5.1 Tissue RNA extraction.....	83
2.5.2 Whole blood RNA extraction (RBC and PBMC).....	83
2.5.3 RNA extraction from whole cells	83
2.5.4 Measure of RNA integrity, purity and quantity	84
2.6 Quantitative Real-Time Polymerase Chain Reaction (PCR).....	84
2.6.1 Quantitative Real-Time PCR using the Qiagen QuantStudio 12K-Flex	84
2.6.2 Fluidigm BioMark™ Real-Time PCR.....	85
2.7 Northern Blotting	86
2.7.1 RNA probe generation	86
2.7.2 Northern blot analysis	87
2.8 Rapid Amplification of cDNA Ends (RACE)	88
2.8.1 3' RACE.....	88
2.8.2 5' RACE.....	88
2.9 Protein Isolation	89
2.9.1 Protein isolation from tissue	89
2.9.2 Protein isolation from cells	89
2.9.3 Protein quantification.....	89
2.10 Western Blot Analysis	90
2.11 Thermo HCS Arrayscan Algorithm Creation and Analysis	90

2.12 Data Analysis and Statistics.....	90
2.12.1 Transcriptional profiling time course and dose response studies	91
CHAPTER III: DELAYED-RELEASE DIMETHYL FUMARATE	
PHARMACODYNAMIC RESPONSES ARE TISSUE-SPECIFIC AND NRF2-	
DEPENDENT	92
1. RATIONALE.....	92
2. RESULTS	94
2.1 DMF treatment leads to increased levels of MMF in all tissues of interest	94
2.2 DMF-induces differential gene expression across tissue types	96
2.3 The magnitude of DMF-induced gene expression is dose-dependent	106
2.4 DMF transcriptional regulation in whole blood.....	114
2.5 DMF-induced gene expression is Nrf2-dependent	116
2.6 DMF transcriptional regulation translates to protein expression	120
3. Discussion.....	123
CHAPTER IV: OSGIN1 CONTRIBUTES TO THE CYTOPROTECTIVE	
PROPERTIES OF MONOMETHYL FUMARATE (MMF).....	127
1. RATIONALE.....	127
2. RESULTS	128
2.1 MMF induces Nrf2 target genes and is protective against oxidative insult.....	128
2.2 Loss of Nrf2 abolishes MMF cytoprotection and depletes OSGIN1	132

2.3 Loss of OSGIN1 reduces MMF cytoprotection in the presence of oxidative insult	137
2.4 Identification of OSGIN1 isoform induction in the presence of MMF	141
2.5 p53 is downstream of OSGIN1 and contributes to OSGIN1-mediated cytoprotection	154
2.6 MMF time course of OSGIN1, p53, Nrf2 and NQO1.	162
2.7 MMF inhibits cell proliferation: preliminary studies.	166
3. Discussion	175
CHAPTER V: GENERAL CONCLUSIONS	184
1. General conclusions	184
2. Study limitations	185
3. Future directions	186
CHAPTER VI: BIBLIOGRAPHY	188
CURRICULUM VITAE	215

LIST OF TABLES

Table 1. <i>Reactive Oxygen Species and Electrophiles</i>	3
Table 2. <i>Characteristics of Neurodegenerative Disease</i>	12
Table 3. <i>Nrf knockout phenotypes</i>	24
Table 4. <i>Conserved domains of human Nrf2.</i>	29
Table 5. <i>Classical Nrf2-regulated genes</i>	39
Table 6. <i>Natural and Synthetic Nrf2 Inducers</i>	50
Table 7. <i>Antibodies</i>	70
Table 8. <i>siRNA constructs.</i>	73
Table 9. <i>Taqman Primer/Probe Assays</i>	74
Table 10. <i>Primer and probe sets for 5'UTR transcript variants of OSGIN1.</i>	75
Table 11. <i>Primers for 3' and 5' RACE.</i>	76
Table 12. <i>Gene selections for Fluidigm real-time PCR</i>	99
Table 13. <i>Transcriptional profiling time course statistical analysis.</i>	105
Table 14. <i>Transcriptional profiling dose response statistical analysis.</i>	112
Table 15. <i>DMF transcriptional time course in Nrf2^{-/-} mice.</i>	119

LIST OF FIGURES

Figure 1. Reactive Oxygen Species Generation <i>via</i> the Electron Transport Chain.....	6
Figure 2. Conserved domains of human Nrf2.....	29
Figure 3. Nrf2 degradation under homeostatic conditions.....	31
Figure 4. Activation of the Nrf2 pathway.	32
Figure 5. Human Keap1 protein domains.	36
Figure 6. Metabolites of dimethyl fumarate and monomethyl fumarate.	52
Figure 7. Genomic structure and protein isoforms of OSGIN1.....	60
Figure 8. Regulation of OSGIN1.	63
Figure 9. Epitope locations of human OSGIN1 isoform-specific antibodies.	72
Figure 10. MMF exposure in peripheral and CNS tissues following a single dose of DMF.....	95
Figure 11. DMF transcriptional profiling time course in peripheral tissues: kidney/jejunum.	101
Figure 12. DMF transcriptional profiling time course in peripheral tissues: spleen/liver.	102
Figure 13. DMF transcriptional profiling time course in CNS tissues: OSGIN1/BDNF.	103
Figure 14. DMF transcriptional profiling time course in CNS tissues: NQO1.	104
Figure 15. DMF transcriptional profiling dose-response in peripheral tissues: kidney/jejunum.	108

Figure 16. DMF transcriptional profiling dose-response in peripheral tissues: spleen/liver.	109
Figure 17. DMF transcriptional profiling dose-response in CNS tissues: cortex/cerebellum.....	110
Figure 18. DMF transcriptional profiling dose-response in CNS: hippocampus/striatum.	111
Figure 19. DMF transcriptional profiling dose-response in whole blood.....	115
Figure 20. Transcriptional time course with 100 mg/kg DMF in Nrf2 ^{-/-} and wild type mice: peripheral tissues.....	117
Figure 21. Transcriptional time course with 100 mg/kg DMF in Nrf2 ^{-/-} knockout and wild type mice: CNS tissues.	118
Figure 22. DMF induced Nrf2-dependent protein expression in peripheral tissues.	121
Figure 23. DMF induced protein expression in CNS tissues.....	122
Figure 24. MMF induces Nrf2 target gene expression in human astrocytes.	130
Figure 25. MMF protects human astrocytes from oxidative challenge.	131
Figure 26. Nrf2 knockdown.....	134
Figure 27. Loss of Nrf2 reduces OSGIN1 expression.	135
Figure 28. Loss of Nrf2 abolishes MMF-mediated cytoprotection.	136
Figure 29. OSGIN1 siRNA knockdown.	139
Figure 30. OSGIN1 siRNA knockdown inhibits MMF-mediated cytoprotection.....	140
Figure 31. Optimization of OSGIN1-52kDa and OSGIN1-61kDa antibodies.	144
Figure 32. OSGIN1 knockdown depletes OSGIN1 isoform specific immunoreactivity	145

Figure 33. The OSGIN1 61 kDa encoding isoform is regulated via MMF and Nrf2.	148
Figure 34. Immunocytochemical analysis of OSGIN1-52 kDa and OSGIN1-61 kDa antibodies.	149
Figure 35. 3' and 5' RACE of OSGIN1 transcript.	152
Figure 36. q-PCR analysis of identified 5'RACE transcripts.	153
Figure 37. q-PCR of p53 siRNA knockdown.	157
Figure 38. p53 protein is regulated by MMF in an Nrf2 and OSGIN1 dependent manner.	158
Figure 39. MMF induces nuclear translocation of p53.	159
Figure 40. MMF induces nuclear translocation of p53.	160
Figure 41. p53 contributes to MMF-mediated cytoprotection.	161
Figure 42. q-PCR time course of NQO1 and OSGIN1.	164
Figure 43. Protein time course of MMF-regulated proteins.	165
Figure 44. MMF inhibits cell proliferation.	168
Figure 45. Loss of OSGIN1 does not significantly induce apoptosis.	169
Figure 46. MMF mediated gene induction of PADI4.	172
Figure 47. PADI4 is regulated by OSGIN1 and p53.	173
Figure 48. PADI4 does not regulate OSGIN1 or p53.	174
Figure 49. OSGIN1 knockdown induces expression of TNF-alpha.	181
Figure 50. Potential mechanism of action of OSGIN1 mediated cellular protection.	182
Figure 51. Potential mechanism of action of OSGIN1 mediated cellular protection.	183

LIST OF ABBREVIATIONS

AATF	apoptosis antagonizing transcription factor
ABCA1	ATP-binding cassette, sub-family A (ABC1), member 1
ACTB	actin, beta
AD	Alzheimer's disease
ADP	adenosine diphosphate
AKR1B8	aldo-keto reductase family 1, member B8
ALS	Amyotrophic lateral sclerosis
ALS2	Amyotrophic lateral sclerosis 2 (juvenile)
APOE	apolipoprotein E
APP	amyloid precursor protein
ARE	antioxidant response element
ATG2A	autophagy related 2A
ATP	adenosine triphosphate
BACH1	BTB and CNC homology 1, basic leucine zipper transcription factor 1
BDGI	bone derived growth inhibitor
BDNF	brain-derived neurotrophic factor
BLAST	Basic Logical Alignment Search Tool
bZIP	Basic Leucine Zipper Domain
CCS	copper chaperone for superoxide dismutase
CDKN1A	cyclin-dependent kinase inhibitor 1A (p21)
cDNA	complementary DNA

CKD chronic inflammatory kidney disease
 CNC Cap'n'Collar
 CNS..... central nervous system
 CSFcerebral spinal fluid
 CUL3.....Cullin 3
 CYP..... cytochrome P450
 DAQ.....dopamine quinone
 DMF..... dimethyl fumarate
 DNAJA3 DnaJ (Hsp40) Homolog, Subfamily A, Member 3
 EAE.....experimental autoimmune encephalomyelitis
 EdU ethynyl-2'-deoxy-uridine
 EGR2.....early growth response protein 2
 EpRE.....electrophilic response element
 ETC.....electron transport chain
 GAB1GRB2-associated-binding protein 1
 GAPDH..... glyceraldehyde-3-phosphate dehydrogenase
 GCLCglutamate cysteine ligase, catalytic subunit
 GCLM.....glutamate cysteine ligase, modifier subunit
 GDF15.....growth differentiation factor 15
 GFAP glial fibrillary acidic protein
 GLUL..... glutamate-ammonia ligase
 GSH.....glutathione

GSTA2	glutathione S-transferase A2
HAEC.....	human aortic endothelial cells
H ⁺	hydrogen ion
HD.....	Huntington's disease
HCC	hepatocellular carcinoma
HCS.....	high content screening
HIF-1	hypoxia-inducible factor-1
HMOX-1/HO-1	heme oxygenase 1
HSP90	heat-shock protein 90
HTT.....	huntingtin
H ₂ O ₂	hydrogen peroxide
H ₂ O	water
IACUC	Institutional Animal Care and Use Committee
IGFBP	insulin-like growth factor binding protein 3
IL-1	interleukin 1
IS	internal standard
KEAP1	Kelch-like ECH-associated protein 1
LB	lysogeny broth
Maf.....	musculo-aponeurotic fibrosarcoma oncogene
MMF	monomethyl fumarate
MMO.....	methane monooxygenase
MMP11	matrix metalloproteinase 11

MPTP 1-methyl 4-phenyl-1,2,3,6-tetrahydropyridine
MRI.....magnetic resonance imaging
MS..... Multiple sclerosis
NADPH.....nicotinamide adenine dinucleotide phosphate-oxidase
NEPNew England Peptide
NETO2 neuropilin (NRP) and tolloid (TLL)-like 2
NF-E2..... nuclear-factor erythroid-derived 2
(NF)- κ B.....nuclear factor kappa-light-chain-enhancer of activated B cells
NFKBIB NK-kappa-B inhibitor beta
NGFG..... nerve growth factor, gamma
NINJ1 ninjurin 1
NMDAR..... N-methyl-D-aspartate receptor
NO..... nitric oxide
NOS..... nitric oxide synthase
NOS1..... nitric oxide synthase 1, neuronal
NQO1NAD(P)H dehydrogenase (quinone 1)
NRF1 nuclear factor (erythroid-derived 2)-like 1
NRF2..... nuclear factor (erythroid-derived 2)-like 2
NRF3..... nuclear factor (erythroid-derived 2)-like 3
NR2F6..... nuclear receptor subfamily 2, group F, member 6
NSG2.....neuron-specific protein family member 2
NUDT7 nudix (nucleoside diphosphate linked moiety X)-type motif 7

OKL38	ovary, kidney and liver protein 38
OLIG1	oligodendrocyte transcription factor 1
OSGIN1	oxidative stress induced growth inhibitor 1
OS	oxidative stress
OXNAD1	oxidoreductase NAD-binding domain containing 1
PADI4	peptidyl arginine deiminase type IV
PARK7	Parkinson disease (autosomal recessive, early onset) 7
PCR.....	polymerase chain reaction
PD	Parkinson's disease
PDI	protein-disulfide isomerase
PINK1	PTEN-induced putative kinase 1
PRDX1	peroxiredoxin 1
PRDX2.....	peroxiredoxin 2
PTGS2.....	prostaglandin-endoperoxide synthase 2
PUFA	polyunsaturated fatty acid
P53	tumor suppressor protein 53
RACE.....	rapid amplification of cDNA ends
RBP4.....	retinol binding protein 4, plasma
RIPA	Radio Immuno Precipitation Assay
ROS.....	reactive oxygen species
RRMS	relapsing remitting multiple sclerosis
SF	sulforaphane

SIAH1	seven in absentia homolog 1
SIRT1	sirtuin 1
SLC1A2	solute carrier family 1(glial high affinity glutamate transporter), member 2
SNAI1	zinc finger protein SNAI1
SNpc.....	substantia nigra pars compacta
SOD.....	superoxide dismutase
SQSTM1	sequestosome 1/p62
SRXN1	sulfiredoxin-1
STRA6	stimulated by retinoic acid gene 6 homolog (mouse)
TNF α	tumor necrosis factor alpha
TXNRD1.....	thioredoxin reductase 1, cytoplasmic
UBC	ubiquitin C
VEGFA	vascular endothelial growth factor A
uORF.....	upstream open reading frame
UFP	ultrafine particles
3-NP	3-nitropropionic acid
6-OHDA.....	6-hydroxydopamine
8-OHdG.....	8-Oxo-2'-deoxyguanosine

CHAPTER I

INTRODUCTION

1. OXIDATIVE/ELECTROPHILIC STRESS

Reactive oxygen species (ROS) and electrophiles are normal intermediates and/or byproducts produced during various physiological and pathophysiological processes. Although these molecules are known to play important roles in cellular and xenobiotic metabolism (Federico et al., 2012; Zangar et al., 2004), cell signaling (Finkel et al., 2009), immune defense (Mittal et al., 2014) and enzymatic reactions (Pendyala et al., 2010), uncontrolled production can have detrimental effects on cell homeostasis. Under normal conditions, the presence of ROS/electrophiles is regulated through intrinsic defense pathways that limit the highly reactive nature of these molecules; however, when this balance is disrupted and oxidative/electrophilic insult surpasses the cellular defense capacity, these toxic species can damage cells leading to oxidative and/or electrophilic stress (OS/ES) (Sies et al., 1985; Sies et al., 2014). This imbalance in the normal homeostatic state is associated with various forms of human disease and can cause disruptive modifications in lipids, proteins and nucleic acids, leading to cellular dysfunction and eventually cell death (Brieger et al., 2012). This section will provide an overview of intracellular sources and functions of ROS and electrophiles, as well as discuss their role specifically in neurodegenerative disease.

1.1 Sources of ROS and Electrophiles

Reactive oxygen species (ROS) are a collection of molecules and ions that are highly reactive based on the presence of an unpaired electron group (free radical) or the ability to generate these free radicals through various chemical reactions. The most common molecules that are considered to possess the characteristics of ROS and contribute to oxidative stress are listed in Table 1 (Sies et al., 2014; Melo et al., 2011). Although the classification of ROS does not tend to include electrophiles, positively charged species that are attracted to electrons, the high reactivity of ROS can initiate the production of molecules with electrophilic properties (Kansanen et al., 2011). A common example of electrophile production in the presence of ROS is *via* lipid peroxidation, which can result in the production of electrophiles such as 4-hydroxynonenal (4-HNE) and malondialdehyde (MDA) following oxidation of cell membrane lipids *via* oxygen free radicals (Table 1) (Vila et al., 2008; Kansanen et al., 2011). This process not only has the capability to propagate oxidative stress, but also to initiate electrophilic stress (Jacobs et al., 2010). As mentioned above, the molecular species that contribute to these types of stress are also generated during various physiological processes that are important for cell function; however, their production under normal conditions is tightly controlled in order to protect the cell from the reactive chemistry of these molecules (Dasuri et al., 2012). Therefore, understanding how and why endogenous pathways such as cellular metabolism, cell signaling and immune defense generate ROS and electrophiles is essential for identifying potential sites of disruption in cellular mechanisms that may contribute to oxidative and/or electrophilic stress.

Table 1. *Reactive Oxygen Species and Electrophiles*

OXYGEN FREE RADICALS	superoxide anion	$\bullet\text{O}_2^-$
	hydroxyl radical	$\bullet\text{OH}$
	alkoxy/peroxy radicals	$\text{RO}\bullet / \text{ROO}\bullet$
REACTIVE SPECIES	hydrogen peroxide	H_2O_2
	hypochlorous acid	HOCL
	peroxynitrite	ONOO^-
	singlet oxygen	O_2^*
	nitric oxide	NO
ELECTROPHILES	4-hydroxynonenal	$\text{C}_9\text{H}_{16}\text{O}_2$
	malondialdehyde	$\text{C}_3\text{H}_4\text{O}_2$

1.1.1 Cellular metabolism

A major source of ROS in cellular systems arises from endogenous metabolic processes such as oxidative phosphorylation in mitochondria, an aerobic pathway used for energy generation/recycling in the form of adenosine triphosphate (ATP) (Federico et al., 2012). During oxidative phosphorylation, protein complexes within the inner mitochondrial membrane transfer electrons from reducing agents (electron donors) to oxidizing agents (electron acceptors) in an oxidation-reduction reaction (redox reaction) (Figure 1). Together, these protein complexes create an electron transport chain (ETC) that generates energy from these redox reactions to transport protons into the intermembrane mitochondrial space. The shuttling of protons into the intermembrane space of the mitochondria generates a proton gradient and an electrical potential across the membrane that can be utilized by the ATP synthase, allowing proton passage back into the inner membrane which results in rotation of the enzyme and the ability to generate ATP from adenosine diphosphate (ADP) through a phosphorylation reaction.

This process is then repeated to continuously provide ATP as an energy source for the cell (Fernandez-Vizarra et al., 2009).

A common electron acceptor in oxidative phosphorylation is molecular oxygen (O_2), a strong oxidizing agent, which becomes negatively charged following acceptance of electrons in the electron transport system. The acceptance of four electrons by molecular oxygen normally reacts with four hydrogen ions (H^+) to be reduced to water (H_2O) in this system; however, in some instances, partially reduced intermediates can also be generated when only one or two electrons are transferred, resulting in the production of reactive oxygen species including superoxide anion ($\bullet O_2^-$) (Lass et al., 1997; Bryla et al., 1965) (Figure 1). The probability of superoxide anion production increases during oxidative phosphorylation when the proton concentration gradient generated from the ETC is disrupted (Apostolova et al., 2011). This can slow down electron transport and increase the half-life of reactive intermediates that generate superoxide. In most cases, mitochondrial generation of superoxide anion is rapidly neutralized by the enzyme superoxide dismutase (SOD), which breaks down superoxide to hydrogen peroxide (H_2O_2) and molecular oxygen (O_2) (Deby et al., 1990). Although a product of superoxide breakdown, H_2O_2 itself is a significant contributor to oxidative damage if not properly eliminated due to the ability of this molecule to easily penetrate cell membranes and induce damage, as well as decompose into the highly reactive hydroxyl radical ($\bullet OH$) (Miller et al., 2010). If not eliminated by certain enzymes such as catalase and glutathione peroxidase, H_2O_2 is a toxic threat to the cell (Sies et al., 2014).

Although there is an increased probability of ROS induced cell damage during oxidative phosphorylation, exposure of cellular components to reactive electrophiles is also increased during this biological process. A major example of electrophile exposure as a result of oxidative phosphorylation is through lipid peroxidation, or the oxidative degradation of lipids (Montuschi et al., 2004; Niki et al., 2008; Niki et al., 2012). As mentioned above, H_2O_2 can decompose into the reactive hydroxyl radical ($\bullet OH$), which can initiate lipid peroxidation by “stealing” electrons from lipids, leading to the propagation of a vicious cycle of fatty acid radical formation due to the instability of these molecules. Examples of electrophiles generated during lipid peroxidation are the reactive aldehydes, MDA and 4-HNE, which are considered end products of lipid peroxidation that can damage cell membranes and have potentially mutagenic properties (Vistoli et al., 2013). Therefore, the endogenous pathway of oxidative phosphorylation, which is crucial for normal cell functioning, is also a source of reactive species that can potentially contribute to oxidative and electrophilic stress if not tightly regulated.

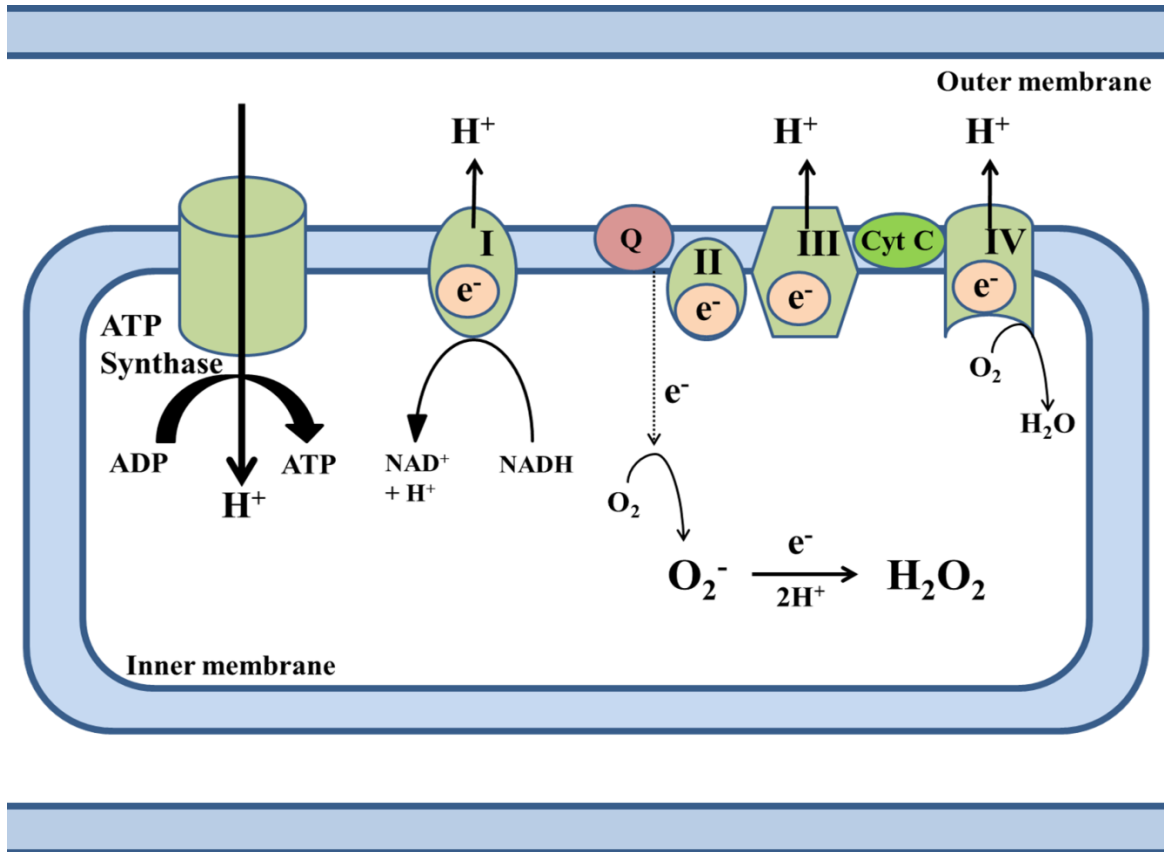


Figure 1. Reactive Oxygen Species Generation *via* the Electron Transport Chain.

ROS production in mitochondria through the process of oxidative phosphorylation by the electron transport chain (ETC). Leakage of electrons from the ETC can reactive with oxygen to generate superoxide and hydrogen peroxide leading to oxidative damage.

1.1.2 Xenobiotic metabolism

Another metabolic source of ROS is through the metabolism of exogenous xenobiotics; substances that are foreign to an organism. This process involves the deactivation and breakdown of chemicals, such as pharmaceutical agents and toxins, into products that are more easily eliminated through excretion; however, similar to oxidative phosphorylation, xenobiotic metabolism can also produce reactive intermediates that can be further damaging to cells (Zangar et al., 2004).

Xenobiotic metabolism of foreign substances occurs predominantly in the liver and can be divided into three phases: modification, conjugation and excretion (McKinnon et al., 1996). The first phase of xenobiotic metabolism, modification, utilizes enzymes to alter the structure of foreign compounds for detoxification and subsequent removal (Li et al., 2011). One common example of this is methane monooxygenase (MMO) reactions catalyzed by a family of heme proteins referred to as cytochrome P450 (CYP) enzymes. MMOs utilize molecular oxygen to incorporate one oxygen atom into a substrate to form a hydroxyl group and the other oxygen atom to water (Zangar et al., 2004). Since the reaction involves electron input as well as activated oxygen there are various leakage points for the production of ROS, including the release of superoxide anion radical due to oxygen release that does not couple to the substrate (Gorsky et al., 1984; Kuthan et al., 1982). The complex mechanisms of P450 enzymes can also result in other leakage points that generate H_2O_2 and other ROS during the breakdown of various endogenous and exogenous compounds, identifying this pathway as a potential contributor to cellular levels of ROS (Rashba-Step et al., 1994).

1.1.3 Cell signaling

A current focus of ROS and electrophilic research has been to understand the involvement of these reactive molecules in cellular signaling. Although ROS are largely described as toxic byproducts of cellular pathways, recent data suggests that ROS, as well as electrophiles, can be generated during normal physiological signaling and play an important role in cell regulation (Finkel et al., 1998; Moller et al., 2010; Mittler et al., 2011). The rapid production and scavenging of ROS, as well as the varying molecular properties of different reactive species make them ideal signaling molecules. Furthermore, the strong link between cell homeostasis and metabolism may also make ROS favorable signals for monitoring alterations in metabolic pathways (Ray et al., 2012).

In mitochondria, production of ROS is a controlled byproduct of metabolism; however, there is also evidence that production of ROS in these organelles may be induced by ligand binding and contribute to apoptotic signaling (Vernon et al., 2013). Cytokines such as tumor necrosis factor alpha (TNF α) and interleukin-1 (IL-1), which play important roles in immune responses, have been shown to induce mitochondrial ROS production following binding to their receptors and subsequent regulation of apoptosis in cells; however, the mechanism is not fully understood (Han et al., 2009). Furthermore, there is evidence to suggest that ROS production is required for activation of nuclear factor kappa-light-chain-enhancer of activated B cells (NF)- κ B and subsequent NF- κ B-dependent gene transcription, which plays important roles in response to stress and immune regulation (Wang et al., 2002). The role of ROS in transcriptional regulation

during oxidative and electrophilic stress has recently become of particular interest due to emerging studies that support ROS signaling as important regulators of glucose homeostasis, inflammation and cell survival (Kesarwani et al., 2013; Ma et al., 2010).

Another role for ROS signaling in mitochondria is through release of ROS from the ETC in response to hypoxia. In this scenario, the ETC functions as an O₂ sensor that releases ROS as a signaling molecule to induce expression of hypoxia-inducible factor-1 (HIF-1). HIF-1 can then regulate pathways involved with adaptive metabolic responses and bring cell functioning back to a normal homeostatic level, including reducing total ROS presence (Zepeda et al., 2013). The induction of HIF-1 activity is particularly important during tissue hypoxia, as this factor induces angiogenesis resulting in increased oxygen delivery to the deprived tissue to diminish hypoxia (Hadjipanayi et al., 2013).

One of the most investigated free radicals that functions as a cell signaling molecule is nitric oxide (NO). NO is synthesized in the body from the amino acid L-arginine by nitric oxide synthases and is an important regulator of various pathways in the immune system, nervous system and in cardiovascular functioning (Forstermann et al., 2012; Kobayashi et al., 2010). The most interesting role for NO involves the synthesis of this radical in the brain as a neuromodulator (Stefano et al., 2009). Potential roles for NO in the nervous system include nerve-mediated gut relaxation during digestion, neuronal immune response of macrophages and S-nitrosylation, a form of post-translation protein modification (Groneberg et al., 2011; Mouaward et al., 2013; Liu et al., 2013). NO mediated S-nitrosylation of the N-methyl-D-aspartate receptor (NMDAR), a predominant glutamate receptor in neurons involved in synaptic plasticity, may increase

neuronal survival during periods of excitotoxicity by inactivating this receptor (Qu et al., 2012). However, as with all ROS, the presence of NO in the nervous system can be detrimental and has been linked to various neurodegenerative diseases which will be discussed at the end of this section.

1.1.4 Immune defense

The production and signaling of ROS plays an important role during both aspects of immunological defense: innate and adaptive immunity (Matsuura et al., 2012). During innate immunity, one of the first defenses against environmental pathogens is through oxidative burst of activated phagocytes, which rapidly release ROS to non-specifically degrade pathogens that have been internalized (Forman et al., 2001). The release of ROS via immune cells is accomplished by nicotinamide adenine dinucleotide phosphate-oxidase (NADPH) oxidase, an enzyme that generates superoxide which can interact with other molecules to form free radicals (McGeer et al., 2002). The presence of ROS is also important during the second phase of immune defense, adaptive immunity, which is necessary for immunological memory. During this phase of immune defense, phagocytes present pathogen-specific antigens to T lymphocytes, which mount an immune response that specifically targets pathogens with the identified antigens (Langsdorf et al., 2012). ROS are important during this aspect of the immune response since free radicals continue to be released by phagocytes, which can enhance the intracellular signal transduction cascades within T lymphocytes (Nathan et al., 2013). The importance of ROS production during both aspects of immune response is supported by studies showing that individuals

who are deficient in ROS production are more susceptible to infection against various forms of bacterial invasion compared to healthy individuals.

The role of ROS in physiological signaling has expanded our understanding of the diversity of these compounds; however, further research is needed to thoroughly appreciate the importance of ROS in these pathways and to determine whether or not their functional role during signaling surpasses the potentially harmful nature of their structure.

1.2 The Role of Oxidative and Electrophilic Stress in Neurodegenerative Disease

The harmful effects of ROS and electrophiles can include damage to macromolecules such as proteins, lipids, polysaccharides and nucleic acids, as well as lead to the inactivation of enzymes (Schieber et al., 2014). Many studies have suggested that these damaging effects of oxidative stress are strongly associated with aging, most likely due in part to a reduced ability of cells to defend against these forms of stress (Szarka et al., 2014). In the brain, this loss of defense is particularly important since neurons are highly sensitive to oxidative and electrophilic stresses (Hamilton et al., 2001). The high metabolic rates of neurons place increased energy demands on mitochondria, thus leading to increased exposure of ROS. Oxidative and electrophilic stress resulting from ROS accumulation can affect mitochondrial efficiency and hence further propagate the production of ROS (Adam-Vizi et al., 2013). The low levels of antioxidants in neurons as well as their reduced ability to regenerate reduce their capacity to defend against the propagation of these reactive molecules (Dasuri et al., 2012).

Furthermore, the high fatty acid content in neurons, which is functionally necessary, makes them prone to lipid peroxidation by ROS (Tully et al., 2013). Therefore, the evidence that ROS overproduction is believed to be a common pathogenic mechanism in aging and neurodegenerative diseases is not particularly surprising (Reynolds et al., 2007). The last part of this section will discuss some of the evidence that links oxidative and electrophilic stress to neurodegenerative disease such as multiple sclerosis, Parkinson's disease, Alzheimer's disease, Huntington's disease and amyotrophic lateral sclerosis (Table 2).

Table 2. *Characteristics of Neurodegenerative Disease*

Disease	Heredity	Clinical Features	Pathology	Misfolded protein
Multiple Sclerosis	Sporadic	Neuroinflammation	White matter lesions; inflammation; BBB breakdown	N/A
Parkinson's disease	Mostly sporadic; rarely inherited	Movement disorder	Loss of DA neurons; Lewy bodies/NF subunits	α -synuclein
Alzheimer's disease	Sporadic (95%); inherited (5%)	Progressive dementia	Senile plaques; neurofibrillary tangles; loss of neurons/synapses	β -amyloid; tau
Huntington's Disease	Inherited	Dementia; motor and psychiatric problems	Loss of striatal neurons; inclusion bodies	Huntingtin
ALS	Sporadic (90%); inherited (10%)	Movement disorder	Motor neuron death; Spheroids/NF subunits	SOD

* *BBB-blood brain barrier; DA-dopaminergic; SOD-superoxide dismutase; ALS-amyotrophic lateral sclerosis; NF-neurofilament; N/A-not applicable*
References: Forman et al., 2004; Hafler et al., 2004; Dauer et al., 2003; Robberecht et al., 2013

1.2.1 Multiple sclerosis

As discussed in section 2.1.4 of this chapter, immune cells are known to contribute to endogenous ROS production and use these radicals as a first line defense against environmental pathogens. Multiple sclerosis (MS) is predominantly characterized as an inflammatory disease, and many suggest that the loss of neuronal myelin, the defining feature of MS, is due in part to destructive immune cells (Hohlfeld et al., 2004; Hafler et al., 2004). The resident immune cells in the brain, microglia, can release ROS during inflammation, which are toxic to oligodendrocytes, the cells that are responsible for myelin production in the CNS (Hafler et al., 2005). The demyelination associated with MS leads to nervous system damage and subsequent disruption in nerve communication.

One source of ROS generation associated with MS is the excessive production of the free radical nitric oxide (NO), which is a precursor for the highly unstable oxidant, peroxynitrite (ONOO⁻) (Pacher et al., 2007). NO is produced by a family of enzymes referred to as nitric oxide synthases (NOSs) which catalyze the formation of NO from the amino acid L-arginine (*section 2.1.3*). Four forms of NOS exist; neuronal (nNOS), which is produced in nervous tissue, inducible (iNOS), located in mitochondria and microglia for production of NO during inflammation, and endothelial (eNOS), produced in endothelial cells during various physiological conditions (Forstermann et al., 2012). The diverse production of NO is important for various signaling pathways; however, this diversity also creates more opportunities for excessive production of this biological molecule that can be toxic (Szabo et al., 2007). During periods of increased production,

NO can rapidly react with superoxide to produce ONOO^- and increase the production of further downstream reactive molecules (Beckman et al., 1996). Oligodendrocytes are particularly sensitive to ONOO^- and thus are vulnerable to damage induced by the presence of this oxidant (Jack et al., 2007). This can be exemplified by administration of ONOO^- directly into the rat corpus callosum, which resulted in the destruction of myelin and damage to neuronal axons similar to destruction seen in MS (Touil et al., 2001).

In experimental autoimmune encephalomyelitis (EAE), an animal model of brain inflammation that shares similarities with MS pathology, ONOO^- production can be detected early and correlates with the severity of disease activity (van der Veen et al., 1997). Furthermore, during periods of remission, where no disease symptoms are apparent, the presence of ONOO^- is undetectable in this model. The importance of this molecule in disease progression was confirmed experimentally when an ONOO^- catalyst used to neutralize its activity resulted in reduced disease severity and inflammation in this model (Cross et al., 2000). Although the presence of ONOO^- in the EAE model may be due in part to infiltrating immune cells, evidence suggests that ONOO^- may be a very early response to disease in this model. This is supported by studies that found ONOO^- production to occur before the infiltration of immune cells, resulting in damage to mitochondrial proteins and subsequent mitochondrial dysfunction (Li et al., 2011). These findings suggest that alterations in cell metabolism and mitochondrial membrane potential, which lead to ROS production, may be induced by ONOO^- synthesized directly from neuronal cell types.

In humans, gadolinium-enhancing lesions, which are indicative of damaged brain regions, have been shown to correlate with increased levels of NO metabolites identified in the cerebral spinal fluid (CSF) of MS patients (Rejdak et al., 2004; Rejdak et al., 2007). Furthermore, the presence of peroxynitrite has been identified in MS lesions, as well as the presence of reactive astrocytes that express high levels of the antioxidant, peroxiredoxin V (Cross et al., 1997; Holley et al., 2007). The damaging effect of these reactive molecules has also been detected in MS lesions, which show characteristics of oxidative damage including disruptions in mitochondrial DNA and enzymes (Van Horsen et al., 2008). These findings suggest that there is a continuous response to oxidative stress within brain lesions of MS patients.

1.2.2 Parkinson's disease

Parkinson's disease (PD) is a degenerative disorder of the CNS that results from the loss of dopamine-producing neurons within the substantia nigra leading to disruption in motor movements (Dawson et al., 2003). Literature suggests that mitochondrial dysfunction and oxidative stress may be important for the pathogenesis of PD and these factors may underlie the death of dopaminergic neurons in this disease (Jenner et al., 2003). Evidence for this is supported by findings using the MPTP (1-methyl 4-phenyl-1, 2, 3, 6-tetrahydropyridine) animal model, which specifically inhibits complex I of the electron transport chain and induces dopaminergic neuron loss. MPTP is first converted to toxic MPP⁺ in astrocytes followed by release into the extracellular space. MPP⁺ is then transported into dopaminergic neurons via the dopamine transporter, DAT, and inhibits complex I function. This inhibition leads to the buildup of free radicals and the death of

neurons within the substantia nigra similar to that observed in PD patients (Fox et al., 2010). Interestingly, complex I activity has been shown to be decreased specifically in the substantia nigra of postmortem patients with sporadic PD (Dexter et al., 2013). Furthermore, the inhibition of NOS, the catalyst for NO production, has been shown to slow progression of disease in the MPTP model and NOS-deficient mice are significantly more resistant to MPTP compared to controls (Kurosaki et al., 2002). These data suggest that mitochondrial dysfunction and free radical production are important factors in PD progression.

Further support for the importance of oxidative stress in PD stems from increased iron accumulation found in PD postmortem brains compared to healthy controls, specifically within dopaminergic neurons of the substantia nigra (Zecca et al., 2005). This increase in iron presence may be due to dysfunctional iron transport in the mitochondria and can be detrimental to dopamine neurons as iron can interact with H_2O_2 to generate toxic hydroxyl radicals (Mochizuki et al., 2012). The contribution of these free radicals to the disease state is further supported by the observation that antioxidant levels, including glutathione (GSH) and peroxiredoxin 2 (PRDX2), are reduced or altered in the substantia nigra of postmortem PD brains, leaving dopaminergic neurons more susceptible to the damaging effects of free radicals (Sofic et al., 2006).

A final example linking oxidative stress to PD, is genetic mutations that have been associated with familial PD, such as PTEN-induced putative kinase 1 (PINK-1), Parkinson disease (autosomal recessive, early onset) 7 (PARK7/DJ-1) and parkin, all of which are associated with mitochondria. Mutations in these genes have been shown to

result in mitochondrial mitophagy and increased oxidative stress (Geisler et al., 2010; Chien et al., 2012; Priyadarshini et al., 2013; Joselin et al., 2012).

1.2.3 Alzheimer's disease

One of the more highly studied neurodegenerative disorders associated with oxidative stress is Alzheimer's disease (AD). AD is the most common form of dementia that presents early with short term memory loss and advances to symptoms of confusion, mood swings and long term memory loss (Querfurth et al., 2010). Eventually, the disease progresses to loss of bodily function and ultimately death. The pathology associated with AD includes the loss of neurons and synapses in the cerebral cortex and the presence of protein accumulations of amyloid beta (plaques) and hyperphosphorylated tau (neurofibrillary tangles) (Tannenbergh et al., 2006; Loewen et al., 2010). Although the exact mechanisms associated with protein misfolding and aggregation are not fully understood in AD, various studies have correlated the disruption of these proteins with the presence of oxidative stress (Hoozemans et al., 2005; Lopez Salon et al., 2000; Behl et al., 1994). In postmortem AD patient brains, investigators found increased nitrosylation of proteins in areas of amyloid beta plaque formation (Honjo et al., 2010). Furthermore, the nitrosylation of heat-shock protein 90 (HSP90) was found to be increased in AD postmortem brains (Honjo et al., 2010). This alteration in protein structure due to NO has been shown to inhibit the ATPase activity of HSP90 and interrupt its chaperone function, which may be associated with the accumulation of tau amyloid.

Further evidence that oxidative damage may contribute to AD disease pathology can be found in transgenic animals and cell lines that overexpress beta amyloid or hyperphosphorylated tau as disease models for AD. In APP (amyloid precursor protein) transgenic mice that overexpress amyloid beta, increases in amyloid beta production correlated with defects in antioxidant defense systems, elevated levels of hydrogen peroxide and nitric oxide, as well as increased oxidative modification of proteins and lipids (Li et al., 2004; Nishida et al., 2006). Interestingly, these defects in antioxidant defense could be reversed by administration of antioxidants, suggesting that oxidative stress may play a role in amyloid beta induced toxicity (Lim et al., 2011). In regards to hyperphosphorylated tau, animal models that overexpress tau have shown increased susceptibility to oxidative stress (Stamer et al., 2002). For example, cortical neurons from a transgenic rat model overexpressing a human mutated tau variant, exhibited increased ROS levels compared to control and the administration of antioxidants to these animals protected neurons against ROS accumulation (Cente et al., 2006; Cente et al., 2009). Furthermore, P301S and P301L transgenic mouse models with human tau gene mutations that exhibit defects in tau and promote neurodegeneration, exhibit mitochondrial dysfunction, increased ROS production and reduced activity of the antioxidants (Yoshiyama et al., 2007; David et al., 2005; Dumont et al., 2011; Elipenahli et al., 2012).

Evidence of oxidative stress in human AD patients has been identified following analysis of markers for oxidative damage in postmortem brains. These markers include 3-nitrotyrosine, a product of peroxynitrite damage, protein carbonyls, which are products of protein oxidation, as well as the markers for oxidative damage of DNA (8-

hydroxydeoxyguanosine (8-OHdG)) and RNA (8-hydroxyguanosine) (Nunomura et al., 1999; Gabbita et al., 1998; Butterfield et al., 2001). Lipid peroxidation products, including MDA and 4-HNE have also been shown to be increased in AD brains as well as alterations in antioxidant production, such as SOD and catalase (Marcus et al., 1998; Omar et al, 1999; Furuta et al., 1995). These markers for oxidative damage also tend to be more localized to neuronal synapses and have been correlated to disease severity (Ansari et al., 2010).

1.2.4 Huntington's disease

Another neurodegenerative disease that has been correlated with oxidative stress is Huntington's disease (HD). HD is caused by an autosomal dominant mutation resulting in a CAG repeat extension in the huntingtin gene (HTT) and is characterized by disruptions in muscle coordination, cognitive decline and depletion of spiny neurons within the striatum (Dorsey et al., 2013). Evidence from postmortem studies of HD patients show accumulation of oxidative markers such as 3-nitrotyrosine and the lipid peroxidation marker, MDA, in the striatum and cortex compared to non-diseased controls (Browne et al., 1999). There is also evidence that levels of lipid peroxidation in HD patient plasma correlates with HD disease severity (Klepac et al., 2007; Chen et al., 2007). In experimental models using transgenic mice with mutated HTT, investigators found increases in DNA oxidative damage by measuring 8-OHdG in the brain and plasma, and also detected increased levels of 8-OHdG and lipid peroxidation markers (MDA, 4-HNE) in the striatum of these mice (Bogdanov et al., 2001, Lee et al., 2011).

These data suggest that metabolic dysfunction leading to oxidative stress in the CNS may be a contributor to HD pathogenesis.

A major piece of evidence that supports a role for oxidative damage via mitochondrial disruption in HD is the selective inhibition of succinate dehydrogenase in medium spiny neurons of the striatum by 3-nitropropionic acid (3-NP) and malonate. The damage induced by 3-NP and malonate has been described as sharing similar pathologic events as HD in animal models, including loss of locomotor function and selective striatal degeneration (Brouillet et al., 2005, Kumar et al., 2010). These compounds are mitochondrial inhibitors since they disrupt the transfer of electrons in the electron transport chain at complex II; therefore, a major factor of toxicity associated with these compounds is cellular and mitochondrial stress due to metabolic disruption. Use of these toxins both *in vivo* and *in vitro* results in increased oxidative damage.

1.2.5 Amyotrophic lateral sclerosis

Amyotrophic lateral sclerosis (ALS), also referred to as Lou Gehrig's disease, is a motor neuron disease that is characterized by muscle atrophy and rapid progressive weakness (Turner et al., 2013). Although there is not a strong correlation between ALS and oxidative damage in sporadic cases of this disease, approximately 20% of familial ALS cases are associated with a mutation in the superoxide dismutase-1 (SOD1) gene (Hand et al., 2002). SOD1 is an important antioxidant in the body that protects against the damaging effects of superoxide. Although the exact mechanisms behind motor neuron dysfunction induced by SOD1 mutations is not clear, researchers have suggested that free radicals may accumulate based on a loss of function of this gene (Saccon et al., 2013).

This theory is supported by studies with transgenic mice expressing mutant SOD1 that exhibit high rates of peroxynitrite damage in spinal cord motor neurons (Bruijn et al., 1997). Furthermore, other studies have indicated that oxidative damage may mediate mutant SOD1 toxicity. This is based on increased exposure of the active copper site in mutant SOD1 to external stimuli, which may induce copper-mediated conversion of hydrogen peroxide to hydroxyl radicals (Vehvilainen et al., 2014). Although there is data that support a loss of function role for SOD1, recent studies suggest SOD1 mutations may alternatively be associated with a gain of function mechanism (Vehvilainen et al., 2014). Therefore, further research is necessary to understand the involvement of SOD1 and other potential sources of oxidative damage in ALS pathology.

2. THE NRF2 PATHWAY IN RESPONSE TO STRESS

As exemplified in section two of this chapter, reactive oxygen species (ROS) and electrophiles possess unique properties that are beneficial for various physiological functions of the cell, including cell signaling, immune defense and metabolic processes. However, if not properly regulated, the reactive characteristics that make ROS/electrophiles ideal contributors to these pathways can also induce damage to the cell leading to a state of oxidative or electrophilic stress. This disruption has been described to play a role in neurodegenerative disease pathology which was reviewed in section 2.2 of this chapter. In order to maintain a homeostatic balance between ROS production and removal, cells have evolved various mechanisms to sense the presence of these molecules as well as regulate their existence. The primary cellular stress response pathway that

assists in maintaining cell homeostasis when threatened with oxidative and electrophilic stress is the Nrf2 (nuclear factor-erythroid 2-related factor 2) pathway (Miao et al. 2005; Nguyen et al., 2009). Initial activation of this pathway is mediated through redox sensing that initiates transcriptional activation of various genes involved with neutralization and removal of potentially harmful molecules.

2.1 The NF-E2 Family of Transcription Factors

Nrf2 is encoded by the *NFE2L2* gene and is a member of the NF-E2 (nuclear-factor erythroid-derived 2) family of basic region leucine-zipper (bZIP) transcription factors that possess a Cap'n'Collar (CNC)-type structure (Itoh et al., 1995). The CNC subfamily of bZIP transcription factors also includes the protein p45 NF-E2 (nuclear-factor erythroid-derived 2) and two other NF-E2 related transcription factors, Nrf1 (nuclear factor-erythroid 2-related factor 1) and Nrf3 (nuclear factor-erythroid 2-related factor 3). Although these family members share conserved domains that are distinct from other bZIP families, they also contain regions that make them functionally unique from one another (Toki et al., 1997).

The p45 NF-E2 transcription factor plays an important role in development, where it is specifically required for the proper development of platelets, and is the only one of these CNC genes to be hematopoietic specific (Shivdasani et al., 1995). In contrast to p45 NFE2, the three Nrf's are ubiquitous with partially overlapping expression patterns and functional characteristics (Sykietis et al., 2010). Although all three Nrf's can be activated under conditions of stress, their roles as transcription factors are not functionally redundant based on phenotype results from mouse knockout studies (Table

3). In these studies, *Nrf1*^{-/-} *knockout* mice were found to be embryonic lethal due to defects in erythropoiesis, while *Nrf2*^{-/-} and *Nrf3*^{-/-} were not required for development (Chan et al., 1998; Chan et al., 1996; Chen et al., 2003). Susceptibility to oxidative stress was exacerbated in both *Nrf1*^{-/-} and *Nrf2*^{-/-} mice, with no phenotypic changes observed in the absence of Nrf3 (Derjuga et al., 2004). In *Nrf1*^{-/-} and *Nrf2*^{-/-} double knockout studies, the loss of Nrf2 exacerbated embryonic lethality and susceptibility to oxidative stress in the absence of Nrf1, suggesting that Nrf2 may partially compensate for the loss of Nrf1 (Leung et al., 2003). The absence of *Nrf2*^{-/-} and *Nrf3*^{-/-} together was not reported to alter the phenotype of the *Nrf2*^{-/-} mouse (Derjuga et al., 2004). Interestingly, *Nrf2*^{-/-} single knockout mice also exhibited age related phenotypes including a lupus-like autoimmune syndrome that was observed in females and a distinct neurodegeneration characterized by myelin destruction in the CNS (Yoh et al., 2001; Ma et al., 2006; Hubbs et al., 2007). These findings support non-redundant functions for each of these transcription factors, specifically in regards to Nrf1 and Nrf2. Although there is evidence that both Nrf1 and Nrf2 function through an antioxidant response, the finding that the absence of Nrf2 is not compensated by Nrf1 suggests that Nrf2 itself is critical for defense against oxidative stress and is the major defense pathway against stress induction amongst these three transcription factors.

Table 3. *Nrf knockout phenotypes*

Genotype	Phenotype	Reference
<i>Nrf1</i> ^{-/-}	Mid to late embryonic lethal; defective erythropoiesis; oxidative stress	<i>Chan et al., 1998; Chen et al., 2003</i>
<i>Nrf2</i> ^{-/-}	Viable and fertile; sensitivity to oxidative and ER stress; aged related neurodegeneration and lupus-like autoimmune syndrome	<i>Hubbs et al., 2007; Yoh et al., 2001; Chan et al., 1996</i>
<i>Nrf3</i> ^{-/-}	No observable phenotype	<i>Derjuga et al., 2004</i>
<i>Nrf1</i> ^{-/-} , <i>Nrf2</i> ^{-/-}	Enhancement of <i>Nrf1</i> ^{-/-} phenotype; early embryonic lethal; increases oxidative stress	<i>Leung et al., 2003</i>
<i>Nrf2</i> ^{-/-} , <i>Nrf3</i> ^{-/-}	Viable and fertile	<i>Derjuga et al., 2004</i>

2.2 Nrf2

Since the discovery of Nrf2 through cloning experiments in 1994 by Moi et al., research has continuously provided evidence for this transcription factor as the major regulator of gene expression in response to oxidative/electrophilic stressors (Maher et al., 2010; Nguyen et al., 2009; van Muiswinkel et al., 2005). Early studies demonstrating Nrf2 to be an important regulator of the antioxidant response came from *in vitro* analysis of the ARE-driven regulation of the detoxification enzyme, NAD(P)H dehydrogenase (quinone 1) (NQO1) (Venugopal et al., 1996). In these studies, overexpression of Nrf2 cDNA was found to upregulate expression and induction of the NQO1 gene, which contains an antioxidant response element (ARE) in its promoter region. ARE sequences are found in the promoter regions of various detoxification enzymes and possess structural as well as biological characteristics that define their ability to respond to various forms of stress (Rushmore et al., 1993). Direct interaction of Nrf2 with the ARE

sequence was confirmed in 2005 via chromatin immunoprecipitation that demonstrated a direct interaction between endogenous Nrf2 and the ARE (Nguyen et al., 2005). Over the years, other ARE-driven genes under the control of Nrf2 have been identified which will be discussed in further detail in section 3.3.3.

Later studies investigating the role of Nrf2 in response to oxidative and electrophilic stress were conducted *in vivo* utilizing *Nrf2*^{-/-} mice. ARE-dependent gene regulation both at the basal level and in the presence of an inducing agent was found to be severely impaired in these knockout mice, confirming that Nrf2 is responsible for both constitutive and inducible expression of ARE-driven genes (Itoh et al., 1997; Chanas et al., 2002). Subsequent studies have shown that Nrf2 is crucial for cells to cope with oxidative stress and that transcriptional induction via Nrf2 may be differentially regulated in specific cell types. This is in contrast to early theories that suggested activation of the Nrf2 pathway was cell intrinsic, where each cell regulates its own internal Nrf2 to control transcription of ARE-driven genes (Lee et al., 2004). Although this is apparent for certain cell types, there is little data supporting Nrf2 regulation in specific cells such as neurons. Recent studies propose that Nrf2-mediated neuronal protection is through a bystander effect where support is provided primarily by local astrocytes (Bell et al., 2011; Miao et al., 2011; Vargas et al., 2008; Vargas et al., 2009). This can be seen in studies where neuron-rich cultures lack the ability to activate Nrf2 in the presence of oxidative stress and Nrf2-activating compounds, resulting in cellular death (Li et al., 2009; Murphy et al., 2001). In contrast, activation of Nrf2 in mixed neuronal/astrocyte cultures can be localized to astrocytes leading to protection of neighboring neurons, suggesting that Nrf2

neuronal protection is mediated through astrocytes (Braun et al., 2009). This can be further demonstrated in studies conducted by Carole Escartin et al. where Nrf2 activation is shown to increase production of the antioxidant glutathione (GSH) by astrocytes, which is then released into the extracellular space and cleaved to cysteine. Since neurons cannot take-up extracellular GSH, free cysteine is collected through the Nrf2-activated EAAT3 (excitatory amino acid transporter 3) transporter to initiate de novo synthesis of GSH (Escartin et al., 2011). These data suggest that the protection inferred by Nrf2 regulation is broad and may have different functions across cell types.

The broad functions of Nrf2 also expand outside of its ability to regulate transcription of antioxidant related genes. Investigation into the diversity of Nrf2 has uncovered the ability of this protein to cross-talk with other signaling pathways involved in biological processes such as differentiation, proliferation and apoptosis (Li et al., 2012). Studies using *Nrf2*^{-/-} mice show that Nrf2 protects against tumor formation in various tissues based on the increased susceptibility of Nrf2-null mice to chemical inducers of cancer compared to control mice (Ramos-Gomez et al., 2001; Xu, et al., 2006; Osburn et al., 2007). Furthermore, humans with a single nucleotide polymorphism (SNP) in the Nrf2 promoter region exhibit reduced Nrf2 expression that correlates with an increased risk of lung cancer (Suzuki et al., 2013). In contrast to the latter studies, elevated levels of Nrf2 in cancer cells have also been shown to promote cell proliferation (Mitsuishi et al., 2012). Together, these findings suggest that Nrf2 may play multiple roles within the cell, especially in regard to cell cycle regulation. Further evidence for Nrf2 contribution to cellular proliferation and differentiation arises from the Nrf2-

dependent transcriptional regulation of the cell cycle regulators p21 (cyclin-dependent kinase inhibitor 1) and OSGIN1 (oxidative stress induced growth inhibitor 1), as well as the autophagy protein, SQSTM1/p62 (sequestosome/nucleoporin 62), which is also important for the formation of bone cells (DeNicola et al., 2012, Rea et al., 2013; Yan et al., 2014; Lau et al., 2010). The identification of these non-classical Nrf2 target genes sparks interest in the multifunctional aspects of this transcription factor and the probability that characteristics within the conserved domains of Nrf2 may contribute to these functions.

2.2.1 Functional domains of Nrf2

There are seven known functional domains within the 605 amino acid protein of Nrf2 that contribute to its biological activities (Itoh et al., 1999) (Figure 2; Table 4). The first defined domain, Neh1, also known as the DNA binding domain, contains the CNC-type bZIP region that characterizes the NF-E2 family of transcription factors. The presence of a bZIP domain is common amongst DNA binding proteins and allows transcriptional regulators, such as Nrf2, to mediate sequence specific DNA binding as well as dimerization of DNA binding regions (leucine zipper) to regulate transcription. This region is where Nrf2 can heterodimerize with Maf recognition elements (MARE) within small Maf transcription proteins which have been identified as co-regulators of Nrf2-mediated gene regulation. The characterization of Nrf2 as a CNC-type bZIP transcription factor is defined by the presence of a 43-amino acid CNC domain that is conserved across multiple species, including worms, insects, fish, birds and mammals,

and has functional roles in development and homeostatic maintenance (Mohler et al., 1991).

The Neh2 domain is a negative regulatory domain located towards the N-terminus of this protein where Nrf2 binds to its specific repressor, Keap1 (Kelch-like ECH-associated protein 1). The Neh6 domain is also important for the role of Nrf2 repression since it represents a second negative regulatory domain which mediates Keap1-independent degradation of Nrf2 (Chowdhry et al., 2013; Rada et al., 2012). The functional and structural importance of Keap1 will be discussed in more detail in section 3.3.

The Neh3, Neh4 and Neh5 domains are considered transactivation domains that enhance transcriptional regulation of Nrf2 due to the ability of these regions to interact with components of the transcriptional apparatus. The Neh3 domain, located on the carboxy-terminal of Nrf2, is required for Nrf2 transcriptional activation and has been shown to interact with CHD6 (a chromo-ATPase/helicase DNA binding protein family member), which may function as a transcriptional co-activator to induce Nrf2-dependent gene regulation (Nioi et al., 2005). The Neh4 and Neh5 domains also act as transactivation domains, but act synergistically to bind the protein CBP (cAMP Response Element Binding Protein). This protein functions as another transcriptional co-activator and possesses intrinsic histone acetyltransferase activity, which is important for enhancing gene expression (Kato et al., 2001)

In 2013, a seventh domain, Neh7, was identified and shown to contain a recognition site for retinoid X receptor alpha (RXR α). These studies verified that RXR α

can bind to Nrf2 and repress ARE-driven gene expression; therefore, the Neh7 domain is considered a negative regulatory region of the Nrf2 protein (Wang et al., 2013).

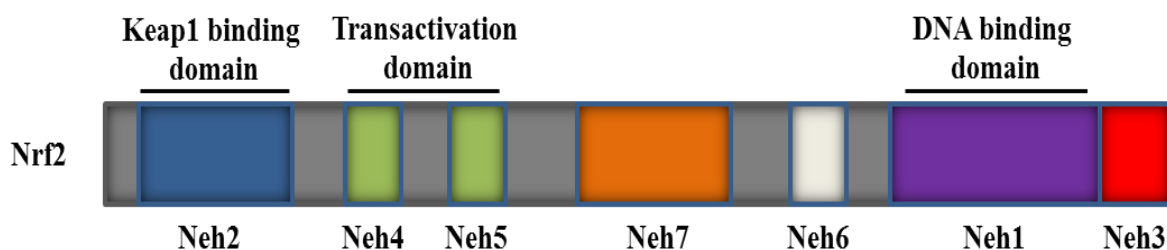


Figure 2. Conserved domains of human Nrf2.

There are seven functional domains of human Nrf2 summarized in Table 4 below.

Table 4. Conserved domains of human Nrf2.

DOMAIN	FUNCTION
Neh1	CNC-bZIP domain that allows Nrf2 to heterodimerize with small Maf proteins
Neh2	Allows Nrf2 binding to its cytosolic repressor Keap1
Neh3	Potential role in Nrf2 stability; may act as a transactivation domain
Neh4 and Neh5	Transactivation domain; binds cAMP Response Element Binding Protein (CREB)
Neh6	May play a role in Nrf2 degradation
Neh7	Regulatory region for RXR α interaction

2.3 Activation of the Nrf2 Pathway

Under normal physiological conditions, constitutively expressed Nrf2 is sequestered in the cytoplasm by the actin-associated Keap1 (Kelch-like ECH-associated protein 1). Keap1 targets Nrf2 for ubiquitination and subsequent proteasomal degradation via a Cullin 3 (Cul3) ubiquitin ligase complex (Itoh et al., 2003; Kobayashi et al., 2004). Under steady state conditions Nrf2 is not readily detected in the cytoplasmic pool based on its continual degradation; however, this allows Nrf2 protein to be quickly accessed when needed (Itoh et al., 2003) (Figure 3). During periods of stress when reactive molecules can inhibit the degradation of Nrf2 by interacting with cysteine residues located on the Keap1 protein, resulting in an allosteric conformational change in Keap1 that alters the binding capacity of the Nrf2-Keap1 complex (Dinkova-Kostova et al., 2002). This alteration in Keap1 disrupts ubiquitin tagging of Nrf2, which allows Nrf2 to translocate into the nucleus. Once inside the nucleus, Nrf2 dimerizes with members of the small Maf (musculo-aponeurotic fibrosarcoma oncogene) family of transcription factors to regulate gene transcription. These small Maf-Nrf2 dimers bind to specific sequences located in the promoter region of cytoprotective genes referred to as Antioxidant and Electrophilic Response Elements (ARE/EpRE), leading to the regulation of specific genes involved in the induction of a Phase II antioxidant response (Itoh et al., 1997; Nguyen et al., 2003) (Figure 4). This tightly controlled pathway allows Nrf2 to be utilized rapidly under periods of stress and exemplifies the critical role of Nrf2 in maintaining basal and inducible expression of antioxidant defenses.

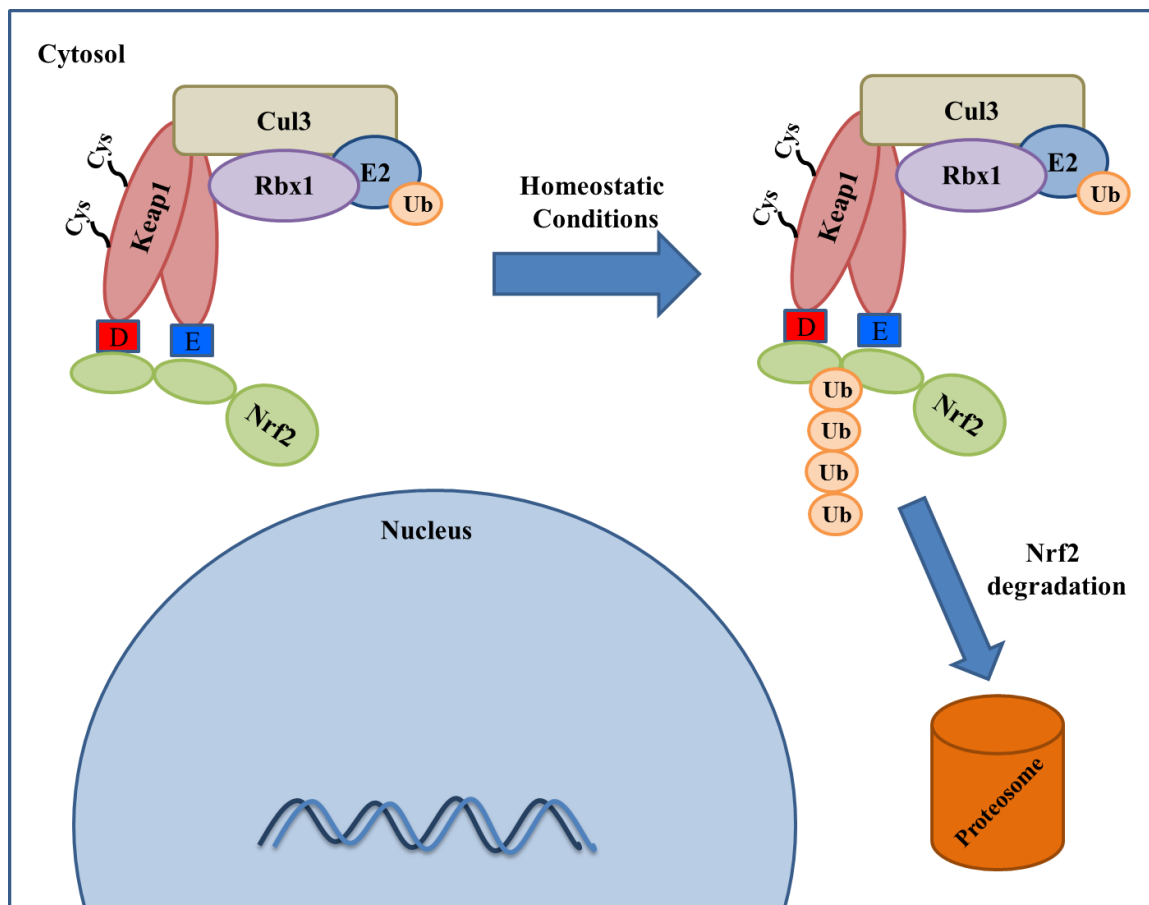


Figure 3. Nrf2 degradation under homeostatic conditions

Under basal conditions, constitutively expressed Nrf2 is sequestered in the cytoplasm by the protein Keap1 through dimeric binding via two motifs within the N-terminal domain of Nrf2 referred to as the “ETGE” (E) and “DLG” (D) motifs. In collaboration with a Cul3-ubiquitin ligase system, Keap1 targets Nrf2 for ubiquitination and subsequent proteasomal degradation.

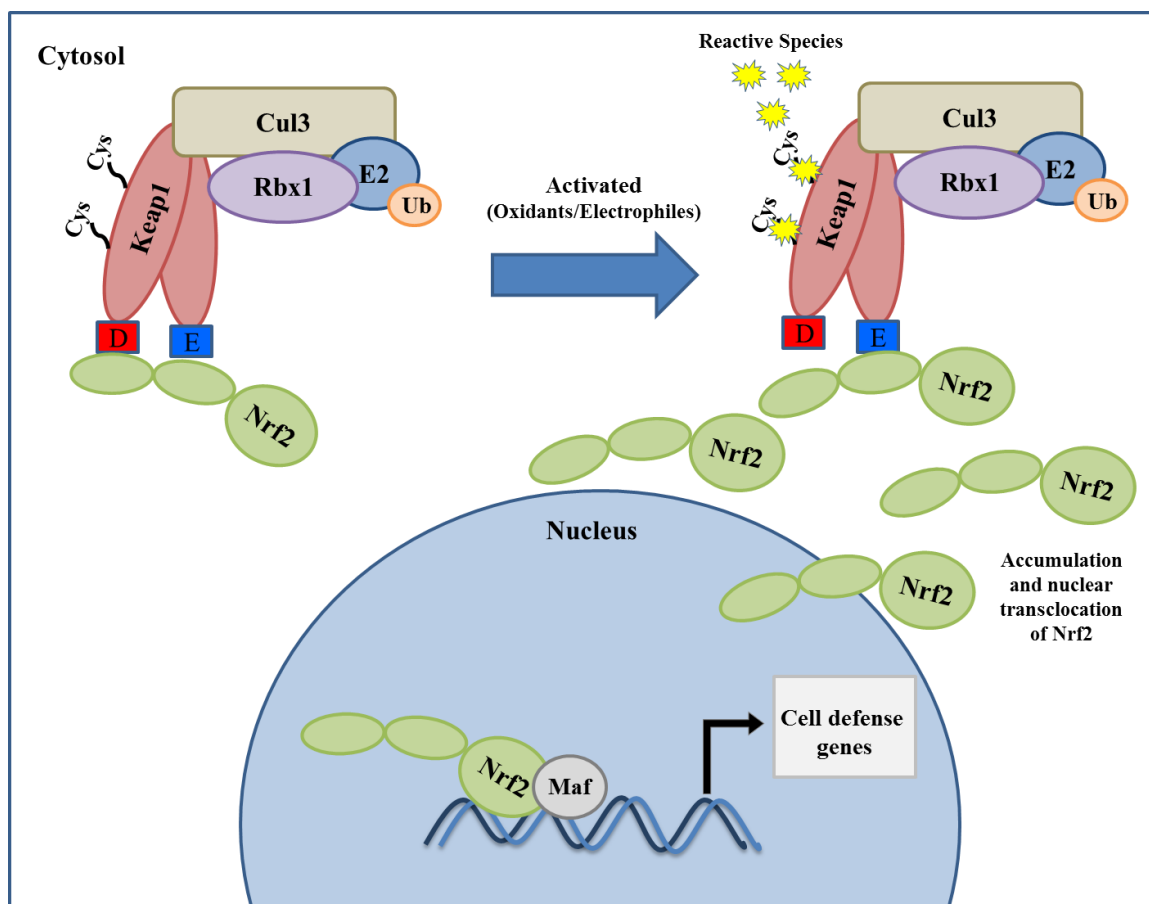


Figure 4. Activation of the Nrf2 pathway.

In the presence of electrophiles or reactive oxygen species (ROS), these molecules interact with the cysteine residues on Keap1 leading to an allosteric protein modification and the inability of Keap1 to bind to the “DLG” (D) motif of Nrf2. Nrf2 is less degraded, leading to accumulation of Nrf2 and its ability to translocate to the nucleus. Once inside the nucleus, Nrf2 works with other cognate transcription factors such as Maf to induce the transcriptions of various cellular defense genes.

2.3.1 Keap1

Nrf2 is predominantly regulated by the protein Keap1, which is a substrate for a Cul3-containing E3 ubiquitin ligase and was identified to be a regulator of Nrf2 following deletion of the Neh2 domain of Nrf2 by Itoh et al. in 1999. Itoh et al. discovered that this deletion resulted in increased Nrf2 activity and initiated the proposal that this region negatively regulated Nrf2 via a repressor. Using protein-protein interaction studies with the Neh2 domain as bait, a mouse protein homologous to the *Drosophila* protein Kelch was identified and named Keap1 (Itoh et al., 1999). Further studies using Keap1-deficient (*Keap1*^{-/-}) mice confirmed the importance of Keap1 due to the constitutive activation of Nrf2 in these mice following loss of Keap1 as well as embryonic lethality (Wakabayashi et al., 2003).

The Keap1 protein contains four discrete domains (Figure 5). The N-terminus contains a BTB (Broad complex, Tramtrack and Bric-à-Brac) domain through which Keap1 forms a homodimer and can interact with Cul3 to target Nrf2 for ubiquitination (Zipper et al., 2002). Within this domain, Keap1 binds to Nrf2 to form a RING E3-ubiquitin ligase with Cul3/Rbx1 which leads to the proteasomal degradation of Nrf2 (Itoh et al., 2003). The BTB domain is particularly important since it contains the cysteine 151 residue (Cys151) that has been implicated as a major Keap1 cysteine important for stress sensing (Yamamoto et al., 2008). The intervening region (IVR) of Keap1 which is particularly cysteine-rich contains eight cysteine residues, including Cys273 and Cys288. These two cysteine's, like Cys151, have been implicated as stress sensors (Holland et al., 2008; Yamamoto et al., 2008). The DGR (double glycine repeat) domain of Keap1 is a

Kelch domain which is composed of six Kelch motifs that fold together to create a β -propeller structure that aids in protein-protein interactions. In collaboration with the CTR (C-terminal region) domain, the DGR forms a region specific for Nrf2 binding termed the DC domain (Bryan et al., 2013).

As mentioned above, Nrf2 is primarily localized in a complex with Keap1 under basal conditions that consists of one Nrf2 molecule bound to two Keap1 molecules. In this complex, monomeric Nrf2 binds to dimeric Keap1 via two motifs within the N-terminal Neh2 domain of Nrf2 referred to as the “ETGE” and “DLG” motifs (Figure 3/4) (Tong et al., 2006). Studies investigating the importance of these regions found that both motifs were required for Keap1-mediated ubiquitination of Nrf2 by Cul3–Rbx1 and that Keap1 affinity for the ETGE motif was 200-fold greater than for the DLG motif (McMahon et al., 2006; Tong et al., 2006). Original theories of the Keap1-Nrf2 degradation pathway believed that Nrf2 was either bound to Keap1 and degraded or unbound following conformational changes in Keap1 that no longer supported Nrf2 binding (Kang et al., 2004). However, studies conducted by Baird et al. in 2013 found that the Keap1-Nrf2 complex existed in two distinct conformations (Baird et al., 2013). The first conformation consists of the “ETGE” motif of Nrf2 bound to Keap1, referred to as the “open” state, and the second where both the “DLG” and “ETGE” motifs are bound to the Keap1 dimer, referred to as the “closed” state. When the complex is in the closed state, Nrf2 is in the correct orientation to be targeted by the Keap1-dependent E3 ligase for ubiquitination, which is the orientation that is predominant under basal conditions (McMahon et al., 2006; Tong et al., 2006). In the presence of electrophiles or compound

inducers, these molecules react with Keap1 cysteine residues to alter the conformation of the Keap1-Nrf2 complex and switching Keap1 from a closed to an open state (Holland et al., 2010). These data suggest that Nrf2 is not released from Keap1 following alteration of the complex but instead blocks the binding of newly synthesized Nrf2 which can then translocate to nucleus (Li et al.; 2012, Baird et al.; 2013, Egger et al., 2005).

Although classical activation of the Nrf2-Keap1 pathway is believed to be modulated through electrophilic and reactive compound modifications of cysteine residues, there is evidence that alternate Keap1 binding partners as well as Keap1-independent mechanisms exist to activate Nrf2. Sequestosome 1 (p62/SQSTM1) has been shown to interact with the Nrf2-binding site on Keap1 to inhibit its interaction with Nrf2 during selective autophagy to facilitate regulation of Nrf2 (Jain et al., 2010, Lau et al., 2010, Copple et al., 2010, Ichimura et al., 2013). In Keap1-independent mechanisms, Nrf2 has been shown to be phosphorylated by protein kinases that assist in Nrf2 release from Keap1 and subsequent activation of the ARE. Studies have identified phosphorylation of Nrf2 by protein kinase C (Huang et al., 2002), mitogen-activated protein kinase (MAPK) (Yu et al., 1999), phosphoinositide 3-kinase (PI3K) (Lee et al., 2001) and protein kinase R (PKR)-like endoplasmic reticulum kinase (PERK) (Cullinan et al., 2003), leading to increased Nrf2 activity; however, the mechanisms behind this Keap1-independent pathway is unknown. Furthermore, Nrf2 has been shown to be activated independently of Keap1 by caspase-3 cleavage (Ohtsubo et al., 1999), oncogene activation (DeNicola et al., 2011) and blockage by miRNA's (Sangokoya et al., 2010). Finally, other transcription factors, such as nuclear factor kappa-light-chain-enhancer of

activated B cells (NF- κ B) can affect the expression of Nrf2 mRNA (Rushworth et al., 2012; Miao et al., 2005; Ramachandran et al., 2008; Nair et al., 2008). Thus, control of Nrf2 basal expression and stability is highly complex and involves multiple pathways that translate to diverse functions.

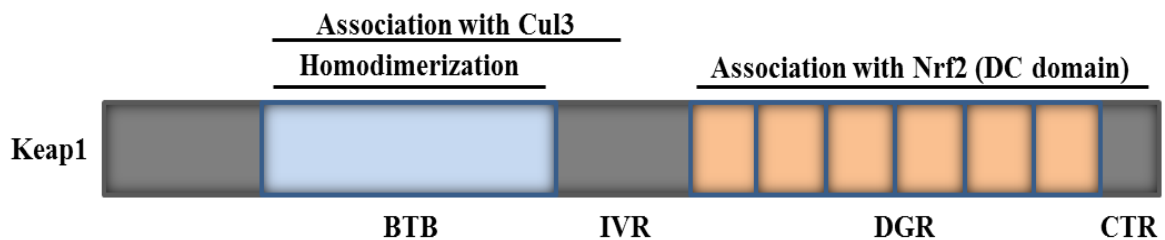


Figure 5. Human Keap1 protein domains.

BTB=Broad complex, Tramtrack and Bric-a-Brac; IVR=Intervening Region; DGR=Double Glycine Repeat; CTR=C-Terminal Region.

2.3.2 *Nrf2* targets genes

Following Nrf2 accumulation via Keap1-dependent or independent mechanisms, Nrf2 is able to translocate to the nucleus where it can regulate the transcription of many genes involved in the antioxidant response (Itoh et al., 1997) (Table 5). Subsequent studies confirmed that Nrf2 binding to ARE/EpRE elements regulates basal expression and coordinates induction of numerous antioxidant response genes that possess a core ARE (Nguyen et al., 2003). Interestingly, Nrf2 also possesses an ARE sequence in its

promoter region that may allow Nrf2 to activate its own transcription to enhance the cellular defense response against stress (Nguyen et al., 2003).

Nrf2 induction of ARE-driven genes includes the transcription of the direct antioxidants NAD (P) H-quinone oxidoreductase 1 (NQO1), heme oxygenase 1 (HO-1) and thioredoxin (TXNRD1), which are important for the neutralization of reactive molecules (Alam et al., 1999). Along with direct antioxidants, Nrf2 mediates the expression of other detoxifying enzymes including aldo-keto reductases (AKRs) and Uridine Diphosphoglucuronosyltransferases (UGTs) (Nishinaka et al., 2005; Paonessa et al., 2011). One major downstream product of the Nrf2 pathway is the biosynthesis of glutathione (GSH), an antioxidant that is expressed ubiquitously throughout the CNS and periphery. GSH serves as an electron donor during the reduction of peroxides by glutathione peroxidases and is believed to play an important role in cellular protection against oxidative damage (Liu et al., 2009; Dringen et al., 2000). Nrf2 is responsible for inducing a number of genes involved with glutathione synthesis and regeneration such as glutamate cysteine ligase (GCL), the first rate limiting step in glutathione synthesis (Wild et al., 1999), glutathione-s-transferases (GST) (Hayes et al., 2000), glutathione reductase (GSR) (Shih et al., 2003) and glutathione peroxidase (GPX) (Thimmulappa et al., 2002). Each of these genes described in Table 5 are considered classical targets of Nrf2 and emphasize the importance of Nrf2 induction during periods of oxidative and electrophilic stress.

As previously mentioned, the activation of ARE-driven genes has been shown to include Nrf2 heterodimerization with small Maf proteins (MafG, MafK and MafF) as

well as heterodimerization with Jun proteins (c-Jun, Jun-D and Jun-B) (Li et al., 1992; Dhakshinamoorthy et al., 2000). Interestingly, Maf-Nrf2 heterodimers have also been shown to repress ARE-mediated expression and induction of antioxidant enzymes, suggesting an additional level of Nrf2 gene regulation that may be controlled through transcriptional complexes of Nrf2 (Nguyen et al., 2000, Dhakshinamoorthy et al., 2000). Therefore, although Nrf2-mediated induction of ARE gene regulation is well established, further investigation into the transcriptional machinery of Nrf2 is necessary to fully understand how heterodimeric partners regulate Nrf2 function.

Although Nrf2 is considered the “master regulator” of the antioxidant response, evidence supporting transcriptional regulation of genes involved in disparate processes also exists. These include immune and inflammatory processes, carcinogenesis and tissue remodeling. There is even evidence for a role of Nrf2 in cognition and addiction. This divergence in Nrf2 target gene functions may provide insight into the numerous diseases that share oxidative damage as a common pathogenesis. Even though the downstream targets of Nrf2 associated with these pathways will not be discussed in detail in this section, it is important to understand that there are diverse targeted pathways of Nrf2 that have a physiological significance and may be contributing to the progression of different diseases.

Table 5. *Classical Nrf2-regulated genes*

Classical Nrf2-regulated Genes	
Target Genes	Function
NAD(P)H dehydrogenase (quinone 1) (NQO1)	Direct antioxidant; catalyzes 2-electron reduction of quinones to hydroquinones
Heme oxygenase-1 (HO-1)	Direct antioxidant; catalyzes the degradation of heme
Aldo-Keto Reductases (AKRs)	NAD(P)H-dependent reduction of aldehydes
Ferritin	Direct antioxidant; sequesters free iron
Uridine Diphosphoglucuronosyltransferases (UGTs)	Encode enzymes that directly inactivate oxidants or electrophiles
Glutathione S-transferases (GSTs)	Encode enzymes that directly inactivate oxidants or electrophiles
Glutathione Reductase	Increase GSH synthesis and regeneration; catalyzes the recycling of GSH
γ -Glutamylcysteine Ligase (GCL)	Increase GSH synthesis and regeneration; catalyzes rate limiting step in GSH synthesis
χ -CT (creatine transporter)	Increase GSH synthesis and regeneration; transporter that aids in GSH synthesis
malic enzyme	Stimulates NADPH synthesis
Glutathione peroxidase 2 (GPX2)	Antioxidant enzyme; detoxification of H ₂ O ₂ and peroxynitrite
peroxiredoxin	Antioxidant enzyme; detoxification of H ₂ O ₂ and peroxynitrite
Multi-Drug Resistance Associated Protein (MRP)	Role in multidrug resistance
Sulfotransferases (SULFs)	Catalyze sulfation of xenobiotics sulfation of xenobiotics
Phosphogluconate Dehydrogenase	Stimulates NADPH synthesis
G6PD	Provides NADPH to GSH reductase for GSH reduction
Metallothioneins	Protection against metal toxicity
Thioredoxin reductases/thioredoxins	Direct antioxidants; reduce proteins by cysteine thiol-disulfide exchange

NADPH- nicotinamide adenine dinucleotide phosphate; GSH-glutathione

3. THE ROLE OF NRF2 IN DISEASE

3.1 Nrf2 and CNS-independent Diseases

As previously mentioned, oxidative and electrophilic stressors have become increasingly recognized as contributing factors to various forms of disease. Since Nrf2 is the central mediator of antioxidant balance within the cell, alterations in the functionality of this pathway are likely to play a role in diseases that exhibit oxidative damage. Chronic inflammation, cancer and cardiovascular diseases can all be induced by biological, physical and chemical factors that are associated with an increased risk to overall oxidative stress (Wohlgemuth et al., 2014, Csiszar et al., 2007, Martien et al., 2007). These diseases have been associated with increased production of ROS/electrophiles and/or a diminished antioxidant capacity which in some cases have been correlated with an impaired activation of Nrf2 (Singh et al., 2006). For example, genetic mutations in Keap1 and Nrf2 that inhibit the formation of the Nrf2-Keap1 complex have been observed in various tumor types (Abazeed et al., 2013; Sato et al., 2013). In CKD, severe oxidative stress indicated by oxidized lipid burden is markedly correlated with suppression of Nrf2 activity and its gene targets (Kim et al., 2011, Kim et al., 2009). Furthermore, several downstream Nrf2 target genes have been implicated in protection against the pathogenesis of each of these diseases, suggesting that this pathway may be impaired (Joshi et al., 2012).

3.2 Nrf2 and models of neurodegenerative disorders

3.2.1 Dysfunction of Nrf2 in human neurodegenerative disorders

Based on the unifying aspect of oxidative stress in neurodegenerative disorders, the role of the Nrf2 pathway in the CNS is of particular interest. As previously described in section 2.2, the high prevalence of oxidative damage observed in postmortem tissues of diseased patients is due in part to the brain being particularly vulnerable to oxidative and electrophilic stressors. This vulnerability is not only a result of reduced antioxidant levels, high lipid content and increased oxygen consumption within the brain, but also the imbalance of oxygen defense abilities across cell types (Hamilton et al., 2001). In the CNS, activation of the Nrf2 pathway and subsequent GSH production is preferentially regulated in astrocytes compared to neurons, leaving neurons highly dependent upon neighboring astrocytes for protection during periods of stress (Escartin et al., 2011). A loss of function of Nrf2 has been described in the pathogenesis of various neurodegenerative disorders which may contribute to the specific neuronal loss that is characteristic of these diseases (Itoh et al., 2009, Johnson et al., 2008).

In post-mortem tissues of AD patients, significant increases in the expression of the Nrf2 target genes, HO-1 and NQO1, have been identified in cortical and hippocampal regions compared to controls. Furthermore, the expression of Nrf2 itself was found to be predominantly localized within the cytoplasm of AD hippocampal neurons from post-mortem tissue (Schipper et al., 2006, Ramsey et al., 2007). These findings spark interest based on their partially contradictory results. The accumulation of antioxidants would suggest that activation of the Nrf2 pathway is functional in AD brains but the oxidative

load exceeds the capabilities of detoxifying agents. However, the localization of Nrf2 to the cytoplasm and not the nucleus of hippocampal neurons of AD patients suggests that translocation of Nrf2 is hindered leading to a dysfunctional pathway. Additional evidence that Nrf2 may be dysregulated in AD comes from measurement of SQSTM1/p62 levels in AD postmortem tissue where expression of this gene and its cytoplasmic levels were found to be significantly reduced in the frontal cortex. As previously mentioned SQSTM1/p62 can interact with the Nrf2 binding site on Keap1 and inhibit the Nrf2-Keap1 complex (Salminen et al., 2012). Therefore, a decline in the level of SQSTM1 protein could potentially inhibit the signaling pathway of Nrf2 leading to increases in oxidative stress and impaired neuronal survival.

Similar to AD, post-mortem analysis of PD brain tissue has identified increases in NQO1 and HO1 to be predominantly localized to reactive astrocytes (van Muiswinkel et al. 2004, Schipper et al. 2004). However, in contrast to the latter AD brain analysis, Nrf2 was localized predominantly within the nucleus of PD brain tissue astrocytes (Ramsey et al., 2007). These findings correlate better with an overall state of oxidative stress which is consistent with the mitochondrial dysfunction identified within dopaminergic neurons of PD post-mortem brains (Alam et al., 1997, Clements et al., 2006). Interestingly, analysis of postmortem brain tissue from the primary motor cortex and spinal cord of ALS patients identified overall reductions in Nrf2 mRNA and protein expression, suggesting that Nrf2 may be dysregulated in ALS (Pehar et al., 2007). Alterations in Nrf2 regulation across CNS disorders elicits further understanding of the role of Nrf2 in disease pathogenesis, some of which has been made clear through research models.

3.2.2 *Nrf2 and Models of Neurodegenerative Disorders*

Although analysis of postmortem brain tissue has given insight into the Nrf2 pathway during neurodegeneration, most of the knowledge regarding Nrf2 and neurodegenerative disorders stem from *in vivo/vitro* research models. The following section will individually present evidence for Nrf2 dysregulation in experimental models that mimic PD, AD, HD, ALS and MS; diseases that exemplified oxidative burden as a unifying pathology in section 2.2.

i. Nrf2 and Models of Parkinson's Disease

A previously described, PD is characterized by the loss of dopaminergic neurons within the substantia nigra pars compacta as well as increases in mitochondrial dysfunction. This pathology exacerbated in *Nrf2*^{-/-} mouse models in the presence of the neurotoxic dopamine analogues 6-hydroxydopamine (6-OHDA) and MPTP (Chen et al., 2009, Innamorato et al., 2010). The damaging effects of these toxins could be rescued via astrocyte specific over-expression of Nrf2 in these models (Chen et al., 2009). Activation of the Nrf2 pathway *in vitro* was also able to restore metabolic deficiencies observed in olfactory-derived cells from sporadic PD patients (Cook et al., 2011). Furthermore, in *Drosophila* fruit fly models of PD, genetic activation of Nrf2 signaling is sufficient to ameliorate disease phenotypes (Misra et al., 2011).

ii. Nrf2 and Models of Alzheimer's Disease

Mouse models of AD that overexpress the pathogenic protein beta-amyloid precursor protein (APP) exhibit reduced mRNA levels of Nrf2 and its target genes,

NQO1 and GCL, as well as reductions in Nrf2 protein expression (Resende et al., 2008). Additionally, overexpression of Nrf2 via injection of lentiviral-Nrf2 expression vector into the hippocampus of APP transgenic mice improved spatial learning compared to control animals even though it did not alter amyloid beta peptide (A β) levels (Kanninen et al., 2009). However, *in vitro* Nrf2 overexpression or activation of the Nrf2 pathway has shown to significantly protect neuronal and astroglial cell lines against A β -mediated toxicity (Wruck et al., 2008).

iii. Nrf2 and Models Huntington's Disease Models

Common models of HD *in vivo/vitro* include administration of the mitochondrial complex II inhibitors, 3-nitropropionic acid (3-NP) and malonate, which are particularly damaging to striatal neurons and result in increased oxidative damage (Beal et al., 1993, Briouillet et al., 1999). Various research labs have demonstrated that Nrf2-deficient mice are more susceptible to the damage invoked by these mitochondrial inhibitors in striatal tissue leading to increases in lesions within this brain region (Shih et al., 2005). The overexpression or activation of Nrf2 specifically in astrocytes has been shown to protect the striatum from these toxins and reduce lesion size. Additionally, the overexpression of Nrf2 *in vitro* has been shown to confer significant protection against 3-NP and malonate toxicity (Calkins et al., 2005).

iv. Nrf2 and Models of Amyotrophic Lateral Sclerosis

A significant percentage of familial ALS cases are caused by a toxic gain of function in SOD1, a potent scavenger of free radicals (Rosen et al., 1993). Rodent models

that express the mutant form of SOD1 (mSOD1) share many features with ALS including mitochondrial dysfunction and oxidative stress; however, the decreased expression of Nrf2 demonstrated in ALS postmortem tissue is not paralleled in rodent mSOD1 models (Ischiropoulos et al., 2003; Kraft et al., 2007). Despite this discrepancy, there is supporting evidence that Nrf2 activation is protective against the toxicity induced within mSOD1. For example, astrocytes isolated from transgenic mSOD1 animals are toxic to neurons in co-culture, a phenomenon that can be reversed by overexpressing Nrf2 in these astrocytes (Vargas et al., 2006). Furthermore, over-expression of Nrf2 *in vivo* in mSOD1 rodents delays the onset of disease and prolongs lifespan in this model (Vargas et al., 2008). Therefore, it is possible that Nrf2 is expressed in mSOD1 mouse astrocytes but may not be functional.

v. Nrf2 and Models of Multiple Sclerosis

One of the most widely studied *in vivo* models of MS is the inflammatory EAE (experimental autoimmune encephalomyelitis) model, which is characterized by severe demyelination and inflammation. Induction of EAE pathology in *Nrf2*^{-/-} mice has been shown to exacerbate the development and severity of EAE characteristics (Linker et al., 2011). These include increased myelin loss, increased immune cell infiltration into the spinal cord, as well as altered expression of proinflammatory, cytokine and chemokine genes compared to control mice.

The combined evidence from both human postmortem tissues and experimental models of neurodegeneration, identify the Nrf2 pathway as an important response mechanism during disease. This correlates with the evidence presented in section 2.2 that

oxidative stress is a unifying factor across neurodegenerative disorders and neuroinflammation and strengthens the notion that Nrf2 is important for protection against these stresses. Thus, activation of the Nrf2 pathway may be a suitable therapeutic target that could be utilized across multiple disease types, especially in regards to neurodegenerative disease (Copple et al., 2012).

4. COMPOUNDS THAT REGULATE NRF2

As previously described in detail (section 3, Chapter 1), cells sense and adapt to the presence of oxidants and electrophiles through a combined Nrf2-Keap1 mechanism. In this pathway, the key signaling protein that senses and transduces the effects of electrophiles is Keap1. Through modifications of Keap1 cysteine residues, electrophiles alter the conformation of this protein leading to changes in the binding affinity of Keap1 for Nrf2 and subsequent accumulation of Nrf2 protein (Cooper et al., 2002). These steps are important to ensure that Nrf2 has a longer half-life and is free to translocate to the nucleus and induce gene transcription. Some of the most interesting research regarding the Nrf1-Keap1 pathway identifies various naturally occurring and synthetic compounds that can regulate the Nrf2 transcription factor most likely through interactions with Keap1 cysteine residues (Balogun et al., 2003; Garg et al., 2008; Chen et al., 2005; Juge et al., 2007; Nguyen et al., 2000; Kraft et al., 2004). The discovery of these compounds has sparked considerable interest in using these molecules to regulate the Nrf2 pathway as a potential therapeutic target molecule.

4.1 Naturally Occurring Compounds

The first molecules that were investigated as potential activators of stress signaling pathways were derived from plant products, including the broccoli extract sulforaphane [1-isothiocyanato-(4R)-(methylsulfinyl)butane] (Matusheski et al., 2004). Sulforaphane (SF) was originally isolated using bioassays based on its ability to induce NQO1, which was later identified to be one of the classical transcriptional targets of Nrf2 (Tarozzi et al., 2013) (Table 6). Further studies confirmed that SF regulated the Nrf2 pathway by modifying multiple Keap1 domains leading to increased expression of Nrf2-mediated cytoprotective genes (Juge et al., 2007; Angeloni et al., 2009; Dinkova-Kostova et al., 2002). The ability of SF to interact with Keap1 stems from its electrophilic chemistry and thus functions in a similar manner as endogenous electrophiles to regulate Nrf2. Activation of ARE-dependent genes by SF can be exemplified in cell lines where the addition of this compound leads to the increased production of HO1, NQO1 and glutathione (GSH) related precursors (Negi et al., 2011; Mas et al., 2012). More specifically, SF prevented oxidative-stress induced cytotoxicity in striatal neuronal cultures by increasing GSH levels following Nrf2-induced expression of γ -glutamylcysteine ligase (GCL) (Mizuno et al., 2011). Furthermore, activation of Nrf2 by SF was shown to be localized within astrocytes compared to neurons in primary mixed cultures of astrocytes and neurons, even though this lead to the protection of both cell types in the presence of oxidative and excitotoxic stressors (Kraft et al., 2009; Innamorato et al., 2008).

The protective effects of SF have also been demonstrated against chronic neurodegeneration using *in vitro* and *in vivo* models. AD *in vitro* models have been used to demonstrate the ability of SF to protect neuronal cells from A β -induced cytotoxicity as well as increase proteasomal activities, suggesting that SF may aid in proteasomal degradation of A β accumulation (Park et al., 2009; Gan et al., 2010). These findings were extended in *in vivo* mouse models of AD where SF ameliorated cognitive impairment of A β toxicity (Kim et al., 2013). In PD models, SF has been demonstrated to protect dopaminergic neurons from the toxic effects of 6-OHDA in various *in vitro* cultures (Han et al., 2007; Yoon et al., 2010; Siebert et al., 2009). Furthermore, the loss of neurons in the PD *Drosophila* model of α -synucleinopathy can be reduced in the presence of SF (Trinh et al., 2008). Finally, SF induces Nrf2 cytoprotective genes and protects against dopaminergic neuronal cell death and astrogliosis in the MPTP mouse model of PD (Jazwa et al., 2011; Morroni et al., 2013).

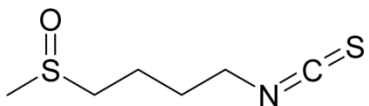
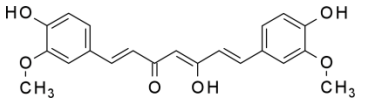
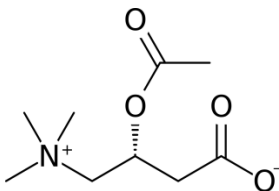
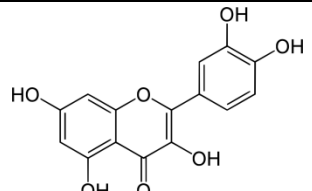
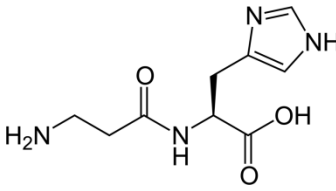
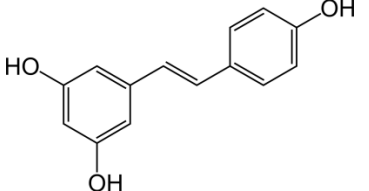
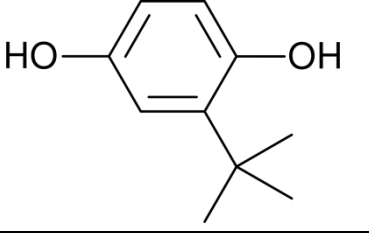
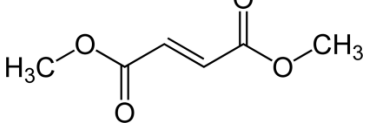
Although not as potent as SF, other naturally occurring dietary antioxidants such as curcumin, acetyl-L-carnitine, quercetin, resveratrol and carnosine have also been identified as similar activators of the Nrf2 pathway (Balogun et al., 2003; Garg et al., 2008; Chen et al., 2005) (Figure 6). These compounds have also been shown to be protective in various models of neurodegeneration and have been used as starting points for identifying therapeutic analogues that specifically target Nrf2.

4.2 Synthetic Compounds

Along with the above mentioned naturally occurring activators of Nrf2, synthetic compounds such as tert-butylhydroquinone (tBHQ) and dimethyl fumarate (DMF) have

also been found to modify Keap1 to activate the Nrf2 pathway (Nquyen et al., 2000; Kraft et al., 2004) (Figure 6). Similar to SF and other natural antioxidants, synthetic tBHQ can induce ARE-driven gene expression in neuronal cultures as well as protect these cell types from various forms of degenerating toxins. Furthermore, *in vivo* administration of t-BHQ in mouse models results in protection against dopaminergic cell degeneration, A β -induced apoptosis and traumatic brain injury. In regards to DMF, the next section in this Chapter will highlight DMF in detail and discuss its importance in activating the Nrf2 pathway.

Table 6. *Natural and Synthetic Nrf2 Inducers*

Compound	Chemical Name	Source	Structure
Sulforaphane	[1-isothiocyanato-(4R)-(methylsulfinyl)butane]	cruciferous vegetables	
Curcumin	(1E,6E)-1,7-Bis(4-hydroxy-3-methoxyphenyl)-1,6-heptadiene-3,5-dione	turmeric spice	
Acetyl-L-carnitine	(R)-3-Acetyloxy-4-trimethylammonio-butanoate	acetylated L-carnitine	
Quercetin	2-(3,4-dihydroxyphenyl)-3,5,7-trihydroxy-4H-chromen-4-one	plant pigment	
Carnosine	(2S)-2-[(3-Amino-1-oxopropyl)amino]-3-(3H-imidazol-4-yl)propanoic acid	animal protein	
Resveratrol	3,5,4'-trihydroxy-trans-stilbene	grapes	
tBHQ	2-(1,1-Dimethylethyl)-1,4-benzenediol	synthetic	
DMF	dimethyl (E)-butenedioate	synthetic	

5. DIMETHYL FUMARATE

5.1 Origins of Dimethyl Fumarate

In the 1950's the German chemist W. Schweckendiek discovered that topical application of fumaric acid esters (FAE) improved the outcome of his psoriatic lesions. Schweckendiek theorized that psoriasis was due to an underlying metabolic disorder caused by disruptions in the citric acid cycle that could be corrected with FAEs (Schweckendiek et al., 1959). Years later, DMF was combined with three fumaric acid esters, monoethyl fumarate-calcium (MEF-Ca), monoethyl fumarate-magnesium (MEF-Mg) and monoethyl fumarate-zinc (MEF-Zn), and licensed as an oral therapy for the treatment of psoriasis under the name Fumaderm (Altmeyer et al., 1994). More than a decade following the approval of Fumaderm, DMF as a single therapy was advanced through clinical trials for the treatment of relapsing-remitting MS (RRMS).

5.2 Structures and Interactions of DMF

Dimethyl fumarate (DMF) (*trans*-1, 2-ethylenedicarboxylic acid dimethyl ester) is the di-methylester of fumaric acid. It is a $\alpha\beta$ -unsaturated compound that is highly electrophilic and rapidly reacts with nucleophiles in a Michael addition reaction. Upon oral administration, DMF is believed to be rapidly metabolized by intestinal esterases to its bioactive metabolite monomethyl fumarate (MMF) (Litjens et al., 2004). MMF is more resistant to metabolism by esterases and thus can be absorbed and distributed throughout the body, including across the blood brain (BBB) into the brain. Eventually MMF is metabolized to fumaric acid within cells, which fuels the citric acid cycle leading to increased CO₂ expiration (Litjens et al., 2004) (Figure 6).

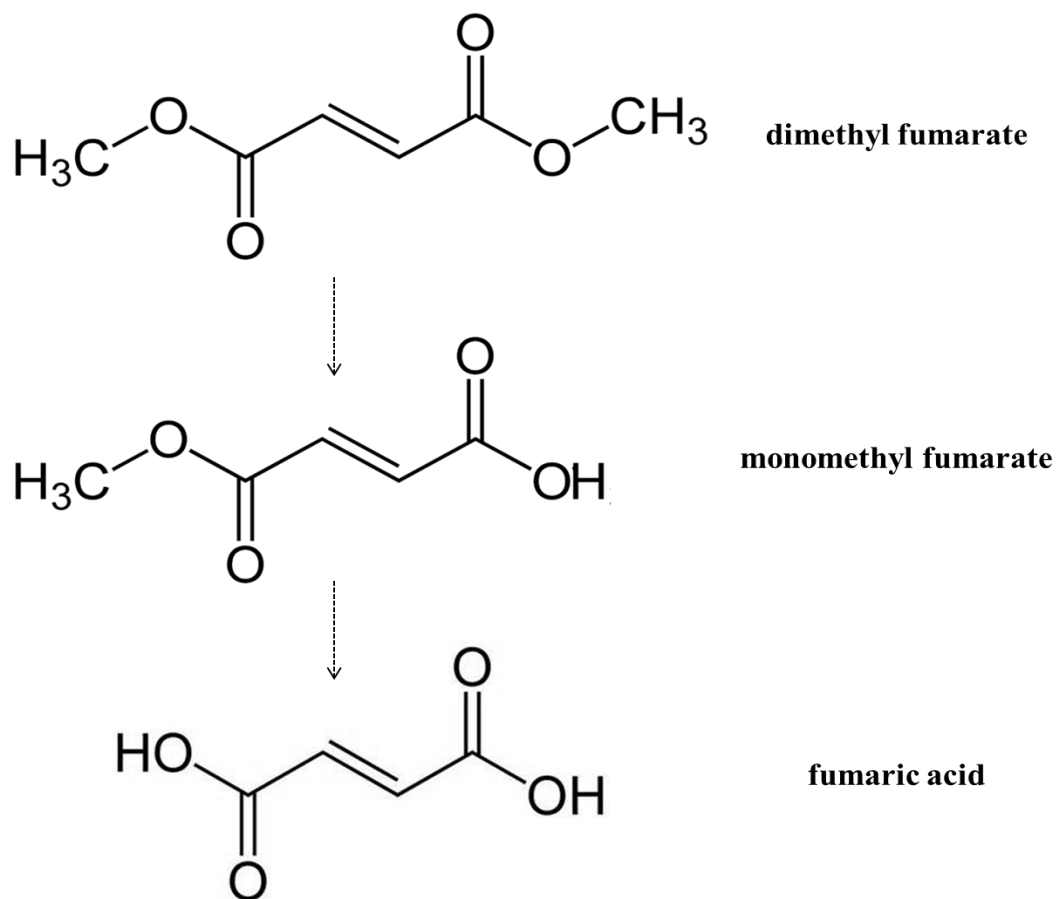


Figure 6. Metabolites of dimethyl fumarate and monomethyl fumarate.

Dimethyl fumarate (DMF) is rapidly metabolized by intestinal esterases to its bioactive metabolite, monomethyl fumarate (MMF) *in vivo*. MMF is more slowly metabolized *in vivo* within cells to fumaric acid, which fuels the citric acid cycle leading to increased CO₂ respiration.

5.3 Therapeutic Effect of DMF in Multiple Sclerosis

More than a decade following the approval of fumarates for use in psoriasis, Fumaderm was administered to patients with RRMS in a small magnetic resonance imaging (MRI)-based study (Schimrigk et al., 2006). In this trial, oral intake of Fumaderm was able to reduce the total number of gadolinium-enhancing lesions as well as reduce lesion volume. Although the MRI endpoint of this initial study was remarkable, tolerability was mainly reduced due to gastrointestinal side effects. To increase the tolerability of fumarate administration, an oral formulation containing only DMF in an enteric-coated tablet (BG-12) was developed and investigated in a multicenter, randomized, double-blind phase-II trial (Kappos et al., 2008). This phase II clinical trial significantly reduced new gadolinium-enhancing lesions and new T2-hyperintense lesions compared to placebo controls. Both of these lesion types are representative of damaged cell tissue indicated by MRI analysis (Kappos et al., 2012, MacManus et al., 2011).

Following these promising results from phase II trials, BG-12 was further investigated clinically in RRMS in a phase III trial that lasted 2 years and included clinical measurement of relapse rate (Gold et al., 2012). Completion of this trial resulted in a 51% reduction in relapses in the highest dose group, increased the overall time between relapses for patients and significantly reduced the number of gadolinium-enhancing and T2-hyperintense lesions. In 2013, BG-12 was approved as a monotherapy for the treatment of RRMS and marketed under the name Tecfidera.

5.4 Preclinical Studies and the Mechanism of Action of DMF

5.4.1 Anti-inflammatory effects of DMF

Early studies investigating the therapeutic potential of DMF were conducted with a focus on understanding the effects of this compound on the immune system. Experimental studies both *in vitro* and *in vivo* determined that DMF could induce a shift in cytokine production from a Th1/Th17 to a Th2 pattern (Ockenfels et al., 1998, Zoghi et al., 2011). This pattern shift is characterized by the loss of interferon-gamma and tumor necrosis factor alpha (TNF- α) production to an increase in interleukin (IL)-4 and IL-5 (Oreja-Guevara et al., 2012). These findings correlate with Th2 cytokine patterns being associated with reduced inflammation and symptom improvement in MS patients while expression of Th1 cytokines have been shown to increase inflammation (Murphy et al., 2002, Segal et al., 2003, Sharief et al., 1991, Miller et al., 2004, Imitola et al., 2005). Further evidence that supports a role for DMF in anti-inflammatory effects stems from the ability of DMF to inhibit the translocation of the transcription factor NF- κ B. This suppression results in the reduction of NF- κ B target genes leading to a reduction in pro-inflammatory cytokines and adhesion molecules, as well as a reduction in apoptotic induction (Mrowietz and Asadullah 2005; Stoof et al., 2001). Additional *in vivo* studies utilizing the EAE rodent model of MS resulted in amelioration of disease onset and reductions in overall clinical score, particularly in later stages of the disease, following DMF treatment (Linker et al., 2011). This amelioration of disease was correlated with a reduction in infiltrating macrophages into the spinal cord, which may be due in part to the reduction of NF- κ B mediated cytokine expression described above (Schilling et al.,

2006). However, the mechanisms behind the anti-inflammatory effects of DMF are still under investigation.

Recently, studies conducted by Chen et al. have identified the hydroxycarboxylic acid receptor 2 (HCA₂) as a contributor to the protective effects of DMF in the EAE model. In these studies investigators compared the treatment effect of DMF in *HCA₂*^{-/-} and wild-type animals induced with EAE and found HCA₂ to be necessary for the therapeutic potential of DMF (Chen et al., 2014). Since the HCA₂ is a G_i-coupled membrane receptor expressed on immune cells such as macrophages and neutrophils, and infiltration of these immune cells is reduced in DMF-treated EAE animals, the activation of this receptor may be an important mediator of the anti-inflammatory effects of DMF. Further investigation into this receptor and how it is regulated by DMF are needed to better understand the mechanisms behind DMF and inflammation.

5.4.2 DMF and the Nrf2 pathway

Along with its anti-inflammatory effects, DMF has also been identified as a regulator of the Nrf2 pathway. *In vitro* studies using both DMF and its bioactive metabolite, MMF, show Nrf2 stabilization and increased antioxidant protein expression of Nrf2 targets including NQO1 and HO-1 (Scannevin et al., 2012). These findings were identified in various cell types including human astrocyte and oligodendrocyte cultures. Furthermore, treatment of cell cultures with DMF and MMF resulted in direct modifications of Keap1 cysteine residues, confirming that DMF/MMF activate the Nrf2 pathway through a similar mechanism as other electrophilic compounds (Linker et al., 2011, Liu et al., 2007). Most interestingly, administration of DMF/MMF was shown to

induce cytoprotection in cultures of neurons and astrocytes challenged with oxidative insults, an effect that was lost in the absence of Nrf2 (Scannevin et al., 2012). Lastly, *in vivo* experiments using the EAE model of MS displayed increased levels of Nrf2 in the CNS following DMF treatment. These alterations in Nrf2 levels correlated with the ability of DMF to ameliorate EAE symptoms as well as preserve myelin, axons and neurons. In Nrf2-deficient mice, DMF was unable to protect against the disease course of EAE (Gold et al., 2006, Linker et al., 2011).

Taken together, these studies support regulation of the Nrf2 pathway as an important mechanism of action for DMF, especially in regards to neuroprotection. However, although there is strong evidence that DMF increases cellular levels of Nrf2 resulting in antioxidant gene up-regulation, it is not known how these changes result in protection of neurons or if DMF solely functions through this pathway or another. Therefore, understanding the specific sequence of events involved with Nrf2-mediated cellular protection is crucial for delineating the endogenous pathways that are in place to protect neurons and will assist in determining the role DMF and other potential neuroprotective compounds play in these pathways.

Transcriptional profiling studies conducted within our lab have begun to uncover the diverse functions of the Nrf2 pathway across tissue types in response to DMF treatment; which will be discussed further in Chapter III. These studies have begun to unveil the mechanisms associated with DMF-mediated regulation of the Nrf2 pathway, particularly in regards to the CNS. One potential pathway that has been identified involves the induction of oxidative stress induced growth inhibitor 1 (OSGIN1), which

has been observed to be uniquely regulated in the CNS following DMF treatment. The evidence for OSGIN1 involvement in DMF mediated protection will be addressed in detail in Chapters IV; however, an introduction to OSGIN1 will first be presented in the next section.

6. OSGIN1

6.1 Background

6.1.1 Characterization of the OSGIN1 gene

Oxidative stress induced growth inhibitor 1 (OSGIN1), also referred to as bone marrow stromal cell (BMSC)-derived growth inhibitor 1 (BDG1) or ovary, kidney and liver protein 38 (OKL38), was first identified in 2001 by Huynh et al. as a novel induced pregnancy complementary DNA (cDNA) from a human ovary cDNA library. Huynh originally named the gene OKL38 based on the predominant expression of its protein product in ovary, kidney and liver and its predicted size of around 38 kDa (Huynh et al., 2001). However, additional aliases arose from identification of different isoforms of this gene that resulted in the discovery of a 52 kDa and a 61 kDa protein product from the same gene (Wang et al., 2005). For simplicity, we will refer to this gene and its protein product as OSGIN1 throughout this discussion and reference the individual isoforms by size.

The human OSGIN1 gene is located on chromosome 16, spans approximately eighteen kilo-base pairs (kb) and contains eight exons and seven introns (Figure 7). Multi Tissue Expression array (MTE) and Multi Tissue Northern blot (MTN) analysis indicated

that OSGIN1 was ubiquitously expressed across all tissue types, with higher expression in specific tissues such as the liver and kidney (Ong et al., 2004). Two conserved domains have been found within the OSGIN1 protein (Marchler-Bauer et al., 2013); a NAD (P)-binding Rossmann-like domain and a Bthiol_YpdA domain. These two domains overlap within the C-terminal region of OSGIN1 and are associated with oxidoreductase protein families. The NAD(P)-binding Rossmann-like domain is found in the putative NADP oxidoreductase coenzyme F420-dependent proteins and/or NAD-dependent glycerol-3-phosphate dehydrogenase-like proteins, while the Bthiol_YpdA domain is found within a protein family of oxidoreductases present only in bacteria (Marchler-Bauer et al., 2013, Huang et al., 2004). The presence of these conserved oxidoreductase domains within OSGIN1 support a role of this gene in response to oxidative stress.

6.1.2 Transcripts (Splice Variants) of OSGIN1

In addition to OSGIN1~38kDa, researchers had identified two additional transcripts by northern blot analysis; however, whether these transcripts were precursory to the originally cloned transcript or arose from differential splicing from the gene was unknown (Huynh et al., 2001). In 2004, Ong et al. identified and cloned two transcript variants along with the OSGIN1 gene that correlated with the 52 and 61kDa isoforms (Ong et al., 2004, Wang et al., 2005). Alternative splicing of OSGIN1 was found to occur at the 5' end of this gene to generate these variants and the splicing pattern was identified to be similar to that of the human thioredoxin reductase 1 (TXNRD1) gene (Rundlof et al., 2007, Osborne et al., 2001). This similarity in splicing suggests that these two genes

may be regulated in a similar manner and be family members, which is supported by the presence of similar oxidoreductase domains found in both genes (Ong et al., 2004, Osborne et al., 2001).

Interestingly, two variants were also cloned in these studies that encode for the same open reading frame (ORF) corresponding to the 52 kDa protein product of OSGIN1 (Ong et al., 2004). These variants were identified to be expressed from different promoters and therefore contain different 5' untranslated regions (UTR). These findings suggest that OSGIN1 may be regulated at the translational level and that the 5'UTR may play an important role in regulation of OSGIN1 protein. The involvement of the 5'UTR in OSGIN1 regulation was further supported by Ong and colleagues in 2007 when they discovered that OSGIN1 could be downregulated via translational suppression involving the 5'UTR of OSGIN1 mRNA (Ong et al., 2007). They found that small upstream ORFs (uORF) were present in the 5'UTR of all three identified transcripts and that disruption of these small uORF's resulted in increased OSGIN1 protein expression. These findings suggest that uORF's within OSGIN1 transcripts could result in the translational suppression of OSGIN1 mRNA. The presence of uORF and upstream AUG (uAUG) sites in 5'UTR regions has previously been described to decrease the frequency of AUG starts sites to initiate transcription in the main ORF (Morris and Geballe, et al., 2000), suggesting that OSGIN1 expression could potentially be regulated by weaker upstream AUG starts.

Over the years a total of seven potential OSGIN1 transcripts have been identified; six of which have evidence for protein encoding. Interestingly, the originally identified

OSGIN1-38kDa transcript is not recognized in genome browsers such as Ensembl as a known splice variant of the cloned full length OSGIN1, suggesting that the originally identified cDNA was incomplete. Although original experimental analysis has included the 38 kDa form, more recent investigation has focused on the two isoforms that encode for 52 and 61 kDa ORFs. However, the presence of other identified transcripts suggests that the regulation of the OSGIN1 gene may be complex and result in differential biological functions downstream.

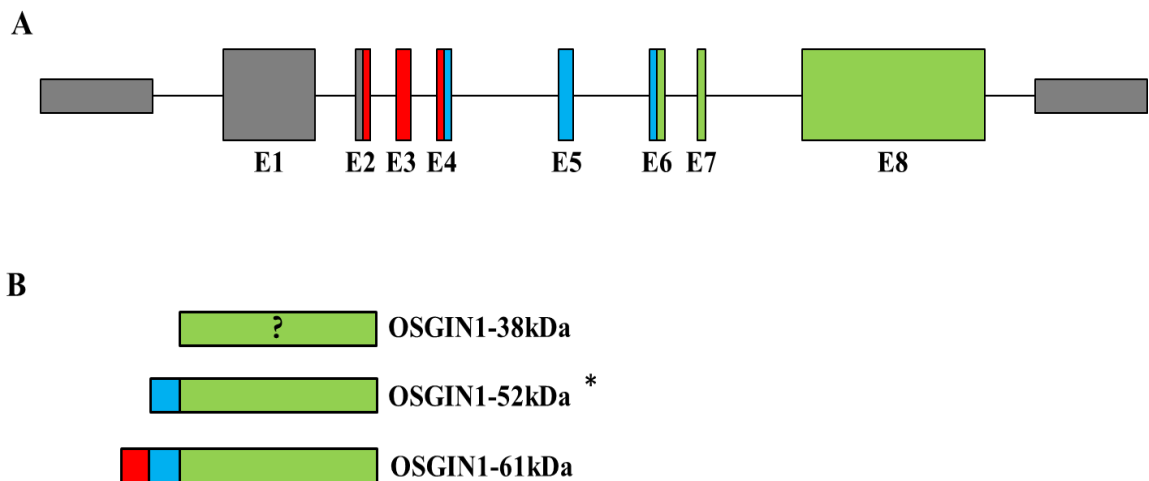


Figure 7. Genomic structure and protein isoforms of OSGIN1.

A, genomic structure of OSGIN1 with eight labeled exons. B, translated protein products of OSGIN1 correlating (by color) with transcribed exons. Currently there is no strong evidence supporting the 38 kDa protein product as an isoform of OSGIN1. **there are two identified OSGIN1 transcripts that encode for the same 52 kDa protein product (see section 6.1.2 of introduction)*

6.2 OSGIN1 Function

6.2.2 OSGIN1 balances cell growth, differentiation and death

As mentioned above, OSGIN1 was originally identified as a novel pregnancy gene. Studies by Huynh and colleagues localized OSGIN1 to rat breast epithelial cells and found that it was induced during pregnancy and lactation. Further analysis of OSGIN1 in human breast cancer cell lines found that expression of this protein was abnormally low in these cells. To investigate the importance of this loss, human breast cancer cells overexpressing the 38 kDa isoform of OSGIN1 were administered to mice and monitored for tumor formation. Interestingly, the researchers found that OSGIN1 overexpression reduced tumor formation in these mice, suggesting that this protein may play an important role in the differentiation and growth of cells (Huynh et al., 2001). Further studies by Ong et al. found that overexpression of the 52 kDa OSGIN1 isoform protein could also inhibit cell proliferation, induce cell death and reduce the migration of multiple cancer cell lines (Ong et al., 2004). Furthermore, comparison studies between the three identified isoforms found that the 52 kDa form was more potent at inducing cell death than the 38 kDa or 61 kDa forms and was lethal to certain cell types, suggesting that these variants may have divergent functions (Ong et al., 2004, Wang et al., 2002). The 61 kDa isoform is now considered to be the canonical OSGIN1 transcript sequence; however, expression of the 52 kDa isoform is most recognized in the literature.

Further investigation into the specific pathways associated with OSGIN1 mediated cell cycle regulation found that OSGIN1 specifically induces cell cycle arrest in the S phase resulting in the induction of apoptosis in breast cancer cells (Wang et al.,

2004). In 2008, Yao et al. expanded upon these findings in experiments involving DNA damage and confirmed that OSGIN1 regulates apoptosis through mitochondrial localization and cytochrome C release that involves the transcriptional control of tumor suppressor protein (p53) and peptidylarginine deiminase 4 (PADI4) (Yao et al., 2008) (Figure 8). In these studies, OSGIN1 and p53 levels were found to be repressed before DNA damage which correlated with high PADI4 expression at the OSGIN1 promoter. In contrast, increased DNA damage resulted in increased p53 at the OSGIN1 promoter, increased OSGIN1 expression and suppression of PADI4. Previous data has identified PADI4 to suppress the transcriptional activity of p53 by counteracting protein arginine methyltransferase co-activators of p53 via deimination (Li et al., 2008). Together, PADI4 and p53 may alternately regulate the expression of OSGIN1 to mediate apoptosis during periods of cell damage (Figure 8).

In 2012, Hu et al further investigated the role of OSGIN1 and p53 on regulating mitochondrial structure and function (Hu et al., 2012). In these studies, the overexpression of OSGIN1 was found to co-localize with p53 within mitochondria, suggesting that p53 can both transcriptionally regulate OSGIN1 as well as mediate its function at a protein level. Together, p53 and OSGIN1 were found to induce changes in mitochondrial morphology and increase ROS levels within the cell, as well as induce apoptosis via a cytochrome C release dependent mechanism (Figure 8). These findings provide evidence that OSGIN1 plays an important role in regulating pathways involved with cell cycle regulation and induction of cell death.

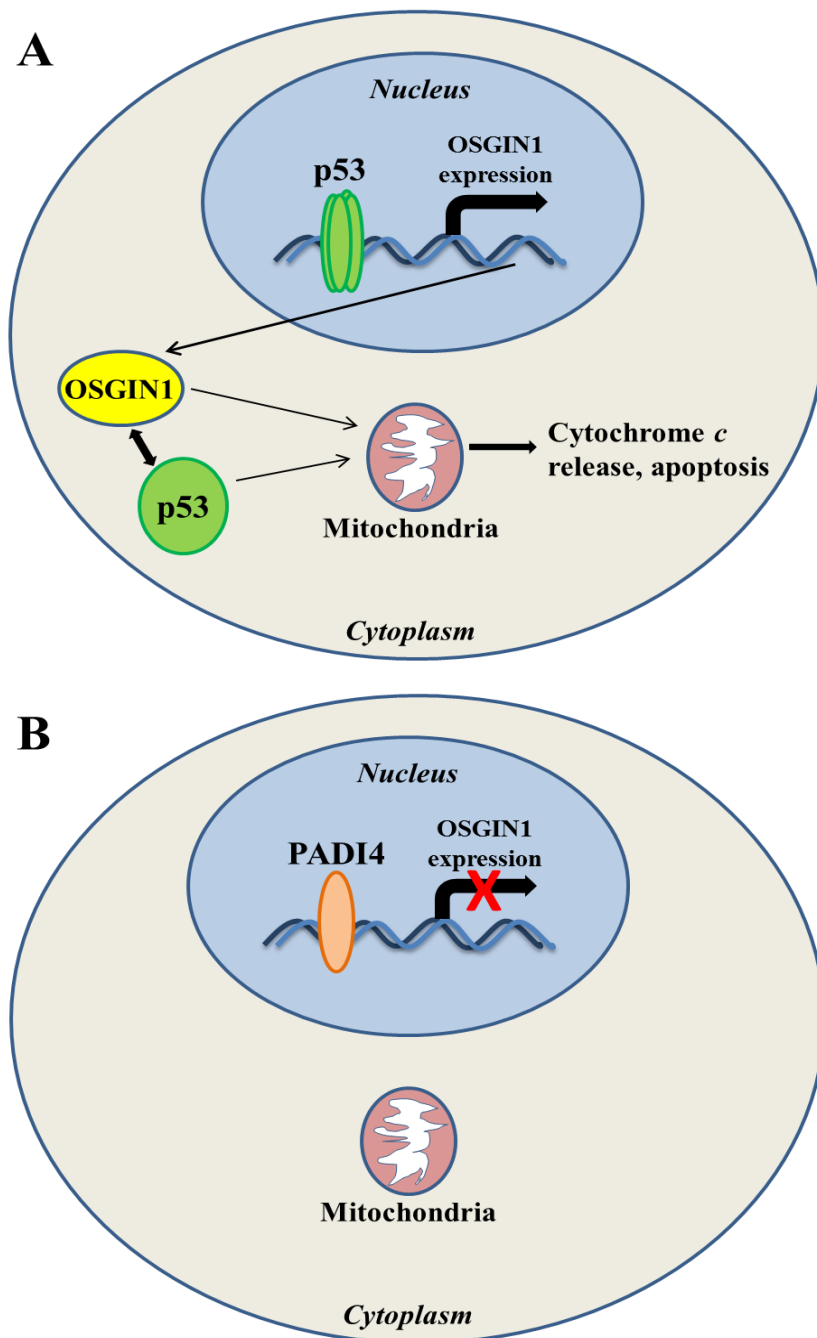


Figure 8. Regulation of OSGIN1.

A, p53 binds to the promoter of OSGIN1 to regulate transcription of this gene. Translated OSGIN1 protein can then interact with p53 in the cytoplasm to regulate apoptosis via cytochrome *c* release from mitochondria (Hu et al. 2012). B, PADI4 can also bind to the promoter of OSGIN1, but works to suppress OSGIN1 expression (Yao et al. 2008).

6.2.1 OSGIN1 as a regulator of inflammation

Along with mediating cell cycle, OSGIN1 has also been shown to be an important regulator of inflammation. Using primary human epithelial cells, OSGIN1 was found to be a major hub gene that regulates major pathways in response to oxidized 1-palmitoyl-2-arachidonoyl-sn-glycero-3-phosphocholine (Ox-PAPC), a product of lipid oxidation that tends to accumulate in atherosclerotic lesions and other chronic inflammatory sites (Romanoski et al, 2011, Yia-Herttuala et al., 1989). In these studies, the loss of OSGIN1 was found to increase the expression of interleukin-8 (IL-8), activating transcription factor 4 (ATF-4) and kruppel-like factor 4 (KLF4), all molecules previously identified to be involved in the endothelial inflammatory response (Romanoski et al., 2010, Irizarry et al., 2003). These data support a protective role for OSGIN1 against the induction of inflammation in the presence of Ox-PAPC and potentially oxidative stress due to the generation of Ox-PAPCs by oxidation reactions. Furthermore, loss of OSGIN1 was also shown in these studies to increase the levels of HO-1 induced by Ox-PAPC, suggesting a close relationship between these molecules in regulating responses to Ox-PAPC (Romanoski et al., 2011).

6.3 OSGIN1 and Disease

6.3.1 OSGIN1 and cancer

A large portion of data supporting OSGIN1 as a regulator of cell cycle stems from studies investigating tumorigenesis. Some of the first investigations of OSGIN1 found OSGIN1 to be down-regulated in 70% of kidney tumors using cancer gene profiling

arrays (Ong et al., 2004). These findings were also paralleled in hepatocellular carcinoma (HCC) where the loss of OSGIN1 correlated with advanced tumor stages of HCC (Ong et al., 2005). This was also confirmed by Liu et al. in 2014 when they analyzed 400 paired HCC and adjacent non-tumor tissues and found OSGIN1 to be down regulated or altered in human HCC's. Lower expression levels of OSGIN1 in these tissues correlated with decreased survival times and disease-free states in patients. Further investigation of these tumors also identified amino acid substitutions in OSGIN1 that were retained in tumor tissues. These altered forms of OSGIN1 protein resulted in a reduced ability to translocate to mitochondria and induce apoptosis compared to the common form (Liu et al., 2014). On the contrary, one study reported OSGIN1 transcripts to be overexpressed in HCC and adjacent benign tissue compared to tissues from healthy normal controls; however, supporting protein analysis was not included in this study (Riou et al., 2002).

Many studies investigating the importance of OSGIN1 in tumorigenesis have been conducted using breast cancer cell lines (Hu et al., 2012, Ong et al., 2004, Yao et al., 2008). As previously mentioned, OSGIN1 was originally identified as an important gene regulated during pregnancy and is believed to contribute to mammary gland cell growth and death needed during stages of lactation (Huynh et al., 2001). This role suggests that fluctuations in the OSGIN1 gene may be required for the cellular changes that transition a cell from a normal to a malignant state. The fluctuations of OSGIN1 in breast cells contrast with the more stable expression of this gene in other tissue types, suggesting dysregulation of OSGIN1 in this tissue type may be causative of disease. This can be exemplified in breast cancer cell lines treated with the natural compound Taheebo

(inner bark of the *Tabebuia avellanae* tree), which is shown to have anti-proliferative effects in cancer cell lines. Global gene expression profiling conducted on cancer cells treated with Taheebo identified cell growth arrest and initiation of apoptosis in these cells to be correlated with increased OSGIN1 expression (Mukherjee et al, 2009). These studies indicate OSGIN1 as a tumor suppressor and thus a potential therapeutic target in cancer.

6.3.2 *OSGIN1 and cardiovascular disease*

Less investigation has been conducted on the role of OSGIN1 in non-carcinogenic diseases; however, some studies target OSGIN1 as regulated during models of cardiovascular disease (Omura et al, 2009). Exposure to ultrafine particles (UFP), associated with ambient air pollution, has been shown to be associated with cardiovascular disease (Kumar et al., 2008). Microarray studies showed OSGIN1 to be upregulated upon exposure to diesel exhaust particles which can adversely affect health (Omura et al., 2009). These findings were confirmed in a study by Li et al in 2010 that showed that UFP induced superoxide and resulted in increased OSGIN1 expression in human aortic endothelial cells (HAEC) (Li et al., 2010). Further research is necessary to understand the role of OSGIN1 in cardiovascular disease as well as other unstudied diseases.

6.4 OSGIN1 as a Transcriptional Target of Nrf2

Of particular interest to this discussion is the identification of OSGIN1 as a transcriptional target of Nrf2. In 2006, Li et al. suggested that OSGIN1 was regulated via

an oxidative signal induced by Ox-PAPC since these lipid oxidation products could induce expression levels of OSGIN1 that correlated with superoxide production. This theory was strengthened by the finding that the presence of superoxide scavengers prevented Ox-PAPC induced expression of OSGIN1 (Li et al, 2006). Involvement of Nrf2 was also identified in this scenario when siRNA knockdown of Nrf2 resulted in the inability of Ox-PAPC to induce OSGIN1, suggesting that this gene is a direct target of the Nrf2 pathway. These findings were confirmed by Yan et al. in endothelial cells showing that OxPAPC can induce OSGIN1 and is an Nrf2 mediated target (Yan et al., 2014).

Recently, new data suggests that miRNAs may be involved with the transcriptional control of OSGIN1. MiR-320a was recently found to regulate induction of the Nrf2 target genes HO-1, GCLM, and OSGIN1 by electrophilic molecules in endothelial cells and this miRNA was shown to be critical for regulating Nrf2 transcriptional induction by OxPAPC (Schrottmaier et al., 2014).

The identification of OSGIN1 as a gene regulated in response to stressful stimuli as well as in biological pathways such as cell cycle, suggests that this gene is important for not only endogenous pathway regulation but also stress. Whether OSGIN1 is controlled by Nrf2 in all of its functions or its transcripts are differentially regulated by different transcriptional regulators (suggested by differential promoter usage) is unknown and warrants further research.

7. RESEARCH HYPOTHESES

The activation of the Nrf2 pathway plays a crucial role in the defense against oxidative and electrophilic stress; however, the mechanisms that lead to Nrf2-mediated cytoprotection are still under investigation. Using the known Nrf2 regulators, DMF and MMF, the primary aim of the research set forth in this dissertation was to identify the molecular mechanisms of Nrf2 regulation and subsequent cellular protection conferred by activation of this pathway. Using *in vivo* transcriptional profiling studies, the differential regulation of DMF-target genes was assessed across time and dose followed by confirmation of Nrf2 involvement. Following identification of the Nrf2-transcriptional target gene OSGIN1 in the CNS, further experiments attempted to elucidate the role of this gene and its importance in defending against oxidative damage. These proposed experiments allow for a broader understanding of endogenous cellular protection in the presence of oxidative stress and how it can be used to combat various disorders of the CNS. This research is defined by three major hypotheses:

- 1: Activation of the Nrf2 pathway via DMF/MMF results in differential regulation of Nrf2 target genes across tissue types.
- 2: OSGIN1 is an Nrf2 transcriptional target that is important for the cytoprotective properties of MMF.
- 3: Alternative splicing of the OSGIN1 gene results in unique biological functions.

CHAPTER II

MATERIALS AND METHODS

1. MATERIALS

1.1 Animals

All procedures involving animals were performed in accordance with standards established in the Guide for the Care and Use of Laboratory Animals as adopted by the U.S. National Institutes of Health. All animal protocols were approved by the Biogen Idec Inc. Institutional Animal Care and Use Committee (IACUC), which is accredited by the Association for Assessment and Accreditation of Laboratory Animal Care International.

1.1.1 C57BL/6 wild type mice

6-8 week-old male C57BL/6 wild-type mice were used for experimentation. Mice were purchased from Jackson Laboratories (Bar Harbor, ME) and maintained on a 12-hour light/dark cycle and given access to food and water ad libitum.

1.1.2 Transgenic Nrf2^{-/-} knockout mice

Transgenic *Nrf2*^{-/-} knockout mice were obtained from Masayuki Yamamoto at the University of Tsukuba (Tsukuba, Japan). Generation of these mice was obtained by a target vector designed to replace the b-Zip region of the *Nrf2* gene with a SV40 nuclear localization signal (NSL)- β -galactosidase (*lacZ*) recombinant gene. To select for transformants a neomycin resistance (*neo*) gene was inserted downstream of the NSL-*lacZ* gene. The diphtheria toxin gene was placed upstream of the *Nrf2* gene for negative

selection against non-homologous recombinants (Itoh et al., 1997). Heterozygote males were shipped to Jackson Laboratories (Bar Harbor, ME), bred to female C57Bl/6J and maintained on the 6J background. 6-8 week-old male *Nrf2*^{-/-} and aged matched C57BL/6 wild-type mice from the same colony were used for all experimentation.

1.2 Antibodies

All purchased and custom generated antibodies used for experimentation are listed and described in Table 7.

Table 7. Antibodies

ANTIBODY	MANUFACTORER	CATALOG NUMBER	DILUTION
β-ACTIN	MP Biomedicals	69100	1:5000
BDNF	Abcam	ab108383	1:5000
GCLC	Abcam	ab41463	1:500
NQO1	Epitomics	2618-1	1:1000
NRF2	Epitomics	2178-1	1:1000
OSGIN1	NEP	Custom*	1:200
OSGIN1-1a/2a	NEP	Custom*	1:1000
OSGIN1-2b	NEP	Custom*	1:500
OSGIN1 C-terminal	Abcam	ab173766	1:250
OSGIN1 N-terminal	Abcam	ab90128	1:1000
PADI4	Abcam	ab96758	1:500
P53	Cell Signaling	9282	1:1000
SQSTM1	Abcam	ab56416	1:250
TXNRD1	Abcam	ab124954	1:1000

*NEP-New England Peptide; *please see section 1.2.1 of Materials and Method*

1.2.1 Generation of OSGIN1 isoform-specific antibodies

Three isoform specific rabbit polyclonal antibodies were generated by New England Peptide (NEP) based on the sequences identified and cloned by Ong et al. (Ong 2004). Peptides were generated against human specific sequences in the OSGIN1 38 kDa, 52 kDa and 61 kDa protein regions (Figure 9). Based on the methods of NEP, antibodies were generated and affinity purified using OSGIN1 isoform-specific peptides. Due to the overlapping homology of the sequences only the longest 61 kDa peptide sequence resulted in a unique antibody (Figure 9).

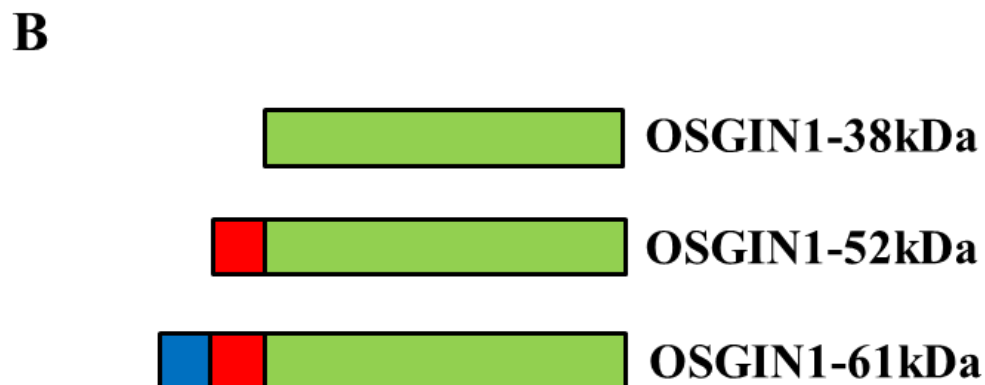
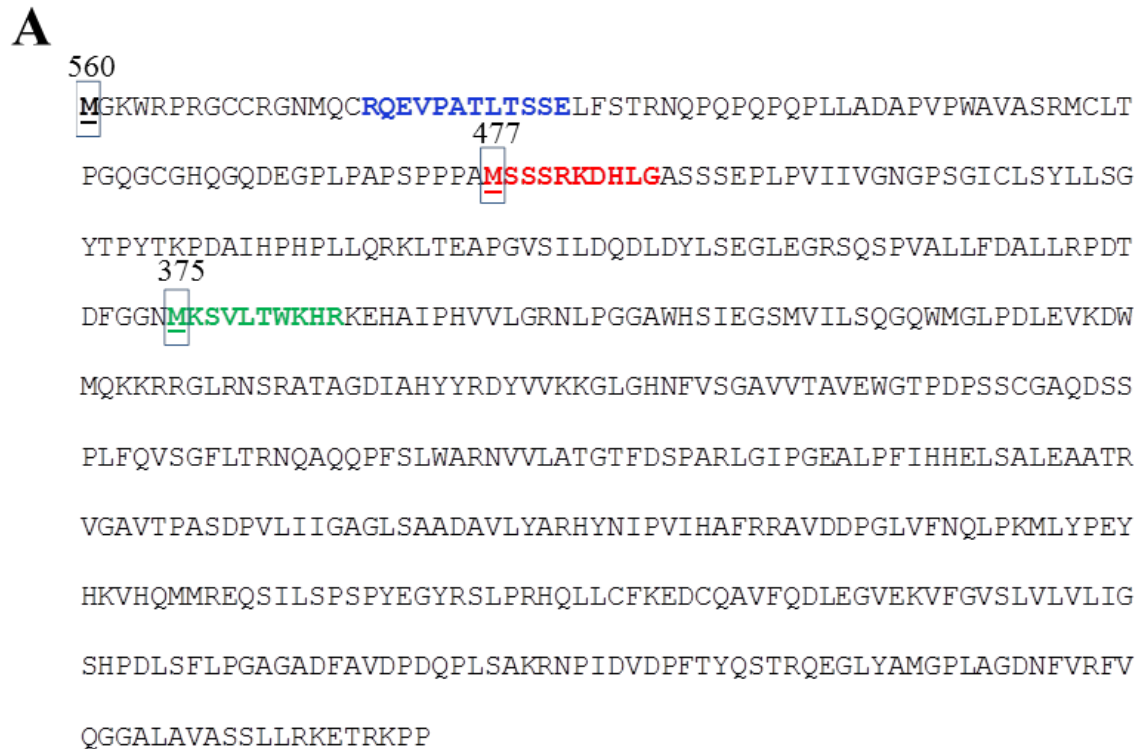


Figure 9. Epitope locations of human OSGIN1 isoform-specific antibodies.

Boxes represent translational start sites of each OSGIN1 isoform labeled with the corresponding amino acid length protein; 560aa (OSGIN1~61kDa), 477aa (OSGIN1~52kDa) and 375aa (OSGIN1~38kDa). Colored amino acids indicate region of peptide generation for antibody creation; blue: OSGIN1~61kDa, red: OSGIN1~52kDa and green: OSGIN1~38kDa.

1.3 Human siRNA constructs

Human siRNA constructs were purchased from OriGene technologies (Rockville, MD) or Invitrogen (Grand Island, NY) and are listed and described in Table 8. For all siRNA transfection studies, constructs were transfected into cells at a final concentration of 10nM. If multiple duplexes were used, the total addition of combined duplexes equaled 10nM.

Table 8. *siRNA constructs.*

siRNA	MANUFACTORER	CATALOG NUMBER	DUPLEX USED
OSGIN1	OriGene	SR309301	A and C* (5nM each)
PADI4	OriGene	SR308375	A,B,C* (3.3nM each)
Trilencer-27 Scrambled Negative Control	OriGene	SR30004	10nM
Scrambled Negative Control Stealth RNA	Invitrogen	13750-047	10nM
p53 Pos Control Stealth RNA	Invitrogen	13750-047	10nM
NRF2	OriGene	SR303156	A,B,C* (3.3nM each)

**A, B, C represent different siRNA duplexes from Origene used for transfection.*

1.4 Primers and Probes

1.4.1 Purchased primer/probe sets

All manufactured primer/probe sets were purchased from Life Technologies (Grand Island, NY) at a concentration of 20X and are listed in Table 9.

Table 9. *Taqman Primer/Probe Assays*

Gene	Species	Taqman Assay ID
AATF	Mouse	Mm00498160_m1
ACTB	Mouse	Mm00442646_m1
ACTIN	Human	Hs01060665_g1
AKR1B8	Mouse	Mm00484314_m1
ALS2	Mouse	Mm01255664_m1
APOE	Mouse	Mm01307193_g1
ATG2A	Mouse	Mm01212087_m1
BDNF	Mouse	Mm04230607_s1
CCS	Mouse	Mm00444148_m1
CDKN1A	Mouse	Mm04205640_g1
DNAJA3	Mouse	Mm00469723_m1
EGR2	Mouse	Mm00456650_m1
GAB1	Mouse	Mm00491216_m1
GAPDH	Human Mouse	Hs02758991_g1 Mm99999915_g1
GCLC	Human Mouse	Hs00155249_m1 Mm00802655_m1
GCLM	Mouse	Mm00514996_m1
GDF15	Mouse	Mm00442228_m1
GFAP	Mouse	Mm01253033_m1
GLUL	Mouse	Mm00725701_s1
GSTA2	Mouse	Mm03019257_g1
HMOX1	Human Mouse	Hs01110250_m1 Mm00516005_m1
IGFBP	Mouse	Mm01187817_m1
MMP11	Mouse	Mm00485048_m1
NETO2	Mouse	Mm01245002_m1
NFKBIB	Mouse	Mm00456849_m1
NGFG	Mouse	Mm01203825_gH

Gene	Species	Taqman Assay ID
NINJ1	Mouse	Mm00479014_m1
NOS1	Mouse	Mm00435175_m1
NQO1	Human Mouse	Hs02512143_s1 Mm01253561_m1
NR2F6	Mouse	Mm01340321_m1
NSG2	Mouse	Mm00476554_m1
NUDT7	Mouse	Mm01240093_m1
OLIG1	Mouse	Mm00497537_s1
OSGIN1	Human Mouse	Hs00203539_m1 Mm00660947_m1
OXNAD1	Mouse	Mm00520913_m1
PADI4	Human	Hs00202612_m1
P21	Human	Hs00355782_m1
PRDX1	Mouse	Mm01621996_s1
PTGS2	Mouse	Mm00478374_m1
P53	Human	Hs01034249_m1
RBP4	Mouse	Mm00803264_g1
SIRT1	Mouse	Mm00490758_m1
SLC1A2	Mouse	Mm00441457_m1
SNAI1	Mouse	Mm00441533_g1
SOD1	Mouse	Mm01344233_g1
SQSTM1	Mouse	Mm00448091_m1
SRXN1	Human Mouse	Hs00607800_m1 Mm00769566_m1
STRA6	Mouse	Mm00486457_m1
TNF-α	Human	Hs01113624_g1
TXNRD1	Human Mouse	Hs00182418_m1 Mm00443675_m1
UBC	Mouse	Mm02525934_g1
VEGFA	Mouse	Mm01281449_m1

1.4.2 Custom primer/probes sets

Custom primers for 5'UTR analysis were generated using primer express software to distinguish between two nucleotide substitutions identified within the 5'UTR of two human OSGIN1 transcripts (Table 10; *section 2.4 of results*). These transcripts were identified from RACE analysis and encode for the same protein. Generated primers and probes were analyzed using BLAST (Basic Logical Alignment Search Tool) to confirm specificity.

Table 10. *Primer and probe sets for 5'UTR transcript variants of OSGIN1.*

	Forward Primer	Reverse Primer	Probe
WT	CTTCCCTCTGGCCTCT- CAGA	GAGATCGGGACACCCAT- TACC	CCTCTTGGATC- CCC
ALT	AATGGGTGTCCCGAT- GTCA	CCGGCCAAGTTGTGCAC- TA	ACTCTGTGATC- CGTGTC

WT-Represents canonical sequence; ALT-represents nucleotide alteration identified in 5'RACE

1.4.3 Primers for 3' and 5' RACE

All primers for RACE were generated against the human OSGIN1 sequence and were analyzed using BLAST (Basic Logical Alignment Search Tool) to confirm specificity.

Table 11. *Primers for 3' and 5' RACE.*

3' RACE Primers	
Primer	Sequence
GSP1	GCTCCCGGACCTGGAGGT
Nested GSP2	ACTGGATGCAGAAGAAGCGA
5' RACE Primers	
Primer	Sequence
GSP1	CGCTTCTTCTGCATCCAGTCC
GSP2	GCATCCAGTCCTTGACCTCCA
Nested GSP3	TGACCTCCAGGTCCGGGAGC

2. METHODS

2.1 Pharmacokinetic Measure of MMF Exposure

Whole blood and tissues (brain, liver, kidney, jejunum and spleen) were collected in a separate cohort of mice 30 minutes after dosing. Whole blood was collected via cardiac puncture and collected in lithium heparin tubes (Fisher Scientific, Cambridge MA) with an addition of 10 mg sodium fluoride. Tubes were immediately inverted several times and stored on wet ice until processed (no longer than 30 min). Whole blood was then centrifuged (15 minutes @ 1500xg, 4 °C), and plasma was immediately collected and stored on dry ice until transfer to -80°C for storage. Tissues of interest were also collected at 30 minutes after dosing, snap frozen and stored at -80°C. A liquid chromatography–mass spectrometry/mass spectrometry (LC-MS/MS) based bioanalytical assay was used to determine MMF concentration levels in plasma and tissue samples. Stable isotope labeled ¹⁴C-MMF was employed as an internal standard (IS). Study samples were thawed on ice and MMF, as well as the IS, were extracted from plasma samples using protein precipitation followed by separation from endogenous components using a liquid

chromatography column. Detection was conducted by mass spectrometry using negative electrospray and the multiple reaction monitoring mode. Concentrations of MMF in study samples were calculated using peak area ratios of MMF to the IS against the standard curve relating the peak area ratios to spiked MMF concentrations.

2.2 Acute Oral Administration of DMF *in vivo*

2.2.1 Time course in wild type C57BL/6 mice

Wild type mice were dosed with a single suspension of 100 mg/kg DMF in 0.8% hydroxypropyl methylcellulose (HPMC) or vehicle solution alone. 100 mg/kg was selected based on previous animal studies with DMF. Drug was delivered by oral gavage at 10 μ L/gram and dosed at 5 minute intervals to ensure proper timing and reduction of RNA variability following tissue collection. Tissues were harvested 2, 4, 6, 8, 12.5, 16.5, 23 or 37.5 hours after dosing with each time point including a vehicle control group and DMF group with an *n* of 6 animals.

2.2.2 Dose response in wild type C57BL/6 mice

Experimental procedures for the DMF dose response study parallel those stated for the time course study unless noted otherwise. Wild type C57BL/6 mice were dosed with a suspension of 50, 100, 200, 400 or 600 mg/kg DMF in 0.8% HPMC or vehicle solution alone. Drug was delivered by oral gavage and tissues harvested 7 hours after dosing. This time point was selected following analysis of the DMF time course data.

2.2.3 Modified time course in transgenic Nrf2^{-/-} knockout mice

Wild type and Nrf2^{-/-} mice were dosed with a single suspension of 100 mg/kg DMF in 0.8% HPMC or vehicle solution alone. 100 mg/kg was selected based on previous animal studies with DMF. Drug was delivered by oral gavage at 10 μ L/gram and dosed at 5 minute intervals to ensure proper timing and reduction of RNA variability following tissue collection. Tissues were harvested at 4, 8, 16 and 32 hours post-dose with an *n* of 6 per group. The time points for the Nrf2^{-/-} study were selected following analysis of the first time course study in wild type mice. Tissue samples were also collected for protein analysis at 6 hours post DMF administration in Nrf2^{-/-} and wild type mice based upon gene regulation changes identified in the latter study.

2.2.4 Tissue harvest

Animals were exposed to CO₂ and whole blood collected via cardiac puncture. Two 100 μ l aliquots of whole blood were collected in 1.5 ml microcentrifuge tubes and snap frozen in liquid nitrogen. Peripheral (liver, spleen, kidney and jejunum) and CNS brain (cerebellum, hippocampus, striatum and cortex) tissues were harvested and snap frozen in liquid nitrogen with special care taken to collect tissues of similar size and from the same location. Two samples were collected for each tissue, one for RNA extraction and one for protein extraction, and protein tissue samples were weighed in pre-tarred tubes before snap freezing. All samples were stored at -80°C until RNA and protein extraction was conducted (see *sections 2.5 and 2.11 of Materials and Methods*).

2.3 Cell Culture

2.3.1 Primary human spinal cord astrocytes

Primary cultures of human spinal cord astrocytes were purchased from ScienCell Research Laboratories (Carlsbad, CA) and grown in Astrocyte Medium (AM; ScienCell). Cultures were maintained according to the supplier specifications. Cells for plate based assays were seeded into clear-bottom poly-D-lysine tissue culture 12-or 24-well plates (BD Biosciences, San Jose, CA).

2.3.2 Reverse transient transfection

Human spinal cord astrocytes were transfected with X-tremeGENE siRNA transfection reagent (Roche, Indianapolis, IN) using the reverse transfection method. siRNA complexes were created according to the manufacturer's protocol and consisted of 1.5ul of X-tremeGENE transfection reagent and 10nM of either OSGIN1 siRNA (Origene), PADI4 siRNA (Origene), Nrf2 siRNA (Origene), p53 siRNA (Invitrogen) or scrambled siRNA (Origene, Invitrogen). Using the reverse transfection method, complexes were added to poly-d-lysine coated 24-well tissue culture plates (BioCoat) and astrocytes were added on top of the complex at a concentration of 60,000 cells/well in human spinal cord astrocyte medium (ScienCell). Cells were incubated with complex for 12 hours at 37°C followed by replacement of complex media with fresh human astrocyte media. Knockdown was assessed at 48 hours post-transfection for q-PCR analysis (see *section 2.6.1 of Materials and Methods*) and western blotting (see *section 2.12 of Materials and Methods*). For analysis with MMF, cells were treated with a titration of MMF 24 hours

post-transfection and analyzed in plate-based assays as described in *section 2.4* of *Materials and Methods*.

2.4 Plate-based Cellular Assays

2.4.1 Compound handling

MMF was prepared in 100mM solutions of DMSO, titrated in DMSO, and then diluted into normal growth media for cell treatments. The final concentration of DMSO (0.03%) was consistent for all treated cells.

2.4.2 H₂O₂ in vitro stress response assay

24 hours post-transfection, human astrocytes were treated with 0, 10 or 30uM of MMF compound in DMSO for 20 hours at 37°C with 5% CO₂. Since DMF is rapidly metabolized to its bioactive metabolite, MMF, following oral administration, cells will likely be exposed to MMF rather than DMF. Therefore, we used MMF in these in vitro studies. Following 20 hour treatment with MMF compound, media was removed from human astrocytes and replaced with 0, 200 or 300uM of hydrogen peroxide (H₂O₂) diluted in Hanks balanced salt solution plus 20 mM HEPES, pH 7.4. Astrocytes were challenged with hydrogen peroxide for 2 hours at 37°C with 5% CO₂ followed by recovery for 20 hours in human astrocyte media. Following 20 hour recovery from oxidative challenge, cellular viability was assessed using a LIVE/DEAD viability stain according to the manufacturer's protocol (Invitrogen). LIVE stain was quantified by fluorescence intensity from calcein AM fluorescence in live cells (excitation wavelength,

488 nM; emission wavelength, 525 nM) and in parallel by counting Hoechst-labeled nuclei using automated imaging and counting (see *section 2.14 of Materials and Methods*). In the LIVE/DEAD assay, dead cells were labeled with ethidium homodimer and appear red in fluorescent images (excitation wavelength, 550 nM; emission wavelength, 575 nM). Live images from LIVE/DEAD labeled cells were imaged as above. Cell nuclei from Hoechst dye labeled cells were quantitated in an automated fashion on the Thermo ArrayScan VTi platform (Thermo Fisher Scientific).

2.4.3 EdU proliferation assay

Human astrocytes were treated with a titration of MMF and incubated for 20-24 hours at 37°C with 5% CO₂. Cells were incubated with EdU to measure proliferation according to the manufacturer protocol outlined for the Click-iT[®] EdU HCS Assay (Invitrogen). EdU was added to cells at a 1:1000 fold dilution in growth media and pulse labeled for 1 hour. Following EdU incorporation, cells were fixed in 4% paraformaldehyde (PFA)/4% sucrose in PBS and EdU detected by immunostaining according the manufacturer. Immunostained plates were quantitated for EdU incorporation using an automated fashion on the Cellomics ArrayScan VTI platform and correlating algorithm analysis (see *section 2.14 of Materials and Methods*).

2.4.4 TiterTACSTM Assay for Apoptosis

Human astrocytes were transfected with siRNA according to the protocol in *section 2.3.2* of this chapter. Following 20-24 hours incubation with MMF, cells were fixed in 4%

PFA/4% sucrose and the HT TiterTACS™ Assay Kit (Trevigen, Gaithersburg, MD) was used to detect cellular apoptosis according to the manufacturer's protocol.

2.4.5 Cellular extract preparation and Nrf2/p53 activity assays

For Nrf2 and p53 activity assays, human astrocytes were treated for 6 or 24 hours with MMF. Cytosolic and nuclear extracts were prepared by using a nuclear extract kit from Active Motif Inc. (Carlsbad, CA). TransAM Nrf2 and TransAM p53 assays (Active Motif Inc.) were used according to the manufacturer's instructions.

2.4.6 Immunocytochemistry

Localization of p53 signal and OSGIN1 positive staining were analyzed via immunocytochemistry following treatment with MMF after 24 hours. Cells were fixed in 4% PFA/4% sucrose, permeabilized in .1% Triton X-100 and labeled with primary anti-p53 antibody or NEP antibodies generated against the 52 kDa and 61 kDa isoforms of OSGIN1 (see *section 1.2 of Materials and Methods*). Primary labeled cells were tagged with a secondary fluorescence antibody and DAPI nuclear stain. Images were acquired using the Thermo HCS Arrayscan VTI platform and an algorithm generated to measure p53 nuclear versus cytoplasmic signal and total OSGIN1 positive puncta (see *section 2.11 of Materials and Methods*).

2.5 RNA Extraction

2.5.1 Tissue RNA extraction

For RNA preparation, frozen tissues were placed in 2 mL RNase-free 96-well blocks with 1.5 ml QIAzol Lysis Reagent (QIAGEN) and a 3.2 mm stainless steel bead (BioSpec Products, Bartlesville, OK). Tissues were disrupted for four cycles of 45 seconds in a Mini-Beadbeater (Biospec Products). RNA was extracted in chloroform and the aqueous phase was mixed with an equal volume of 70% ethanol. Extracted RNA was applied to RNeasy 96 plates and purified by the spin method according to the manufacturer's protocol (RNeasy 96 Universal Tissue Protocol, QIAGEN, Hilden Germany).

2.5.2 Whole blood RNA extraction (RBC and PBMC)

RNA extraction from whole blood was conducted using the Agencourt RNAdvance Blood kit according to the manufacturer's protocol (Beckman Coulter, CA). To begin, frozen whole blood samples were arranged on dry ice in a 96-well tube rack and 520 µl Proteinase K/Lysis buffer was added to each blood aliquot. Samples were then simultaneously inverted at room temperature until all were mixed directly into solution. Agencourt RNAdvance Blood protocol was then followed using the Agencourt SPRIPlate 96R Super Magnet Plate (Beckman Coulter) for RNA extraction.

2.5.3 RNA extraction from whole cells

Total mRNA was isolated from cells using an RNeasy kit (QIAGEN) according to the manufacturer's protocol for spin technology.

2.5.4 Measure of RNA integrity, purity and quantity

For initial optimization of RNA extraction and all transcriptional profiling studies, RNA was analyzed for purity and integrity by capillary electrophoresis on an Agilent Bioanalyzer 2100 (Agilent Technologies, Santa Clara, CA). For optimized studies

2.6 Quantitative Real-Time Polymerase Chain Reaction (PCR)

2.6.1 Quantitative Real-Time PCR using the Qiagen QuantStudio 12K-Flex

qPCR was performed from total mRNA isolated from tissues and reverse-transcribed into cDNA according to manufacturer protocols (Life Technologies, Carlsbad, CA). For *in vivo Nrf2*^{-/-} analysis (see section 2.2.3 of *Materials and Methods*), target gene mouse primers (see section 1.4.1 of *Materials and Methods*) and 6-FAMTM dye-labeled TaqMan[®] MGBTM probes (Applied Biosystems) were custom dried onto 384-well PCR plates and mixed with 10 µl of cDNA and 10 µl 2X Taqman Universal Master Mix II, no ung (Applied Biosystems), to yield a final reaction volume of 20µl. For all other studies, qPCR was performed using 20X Taqman target gene human primer/probe sets (see section 1.4.1 of *Materials and Methods*) mixed with cDNA and 2X Taqman Universal Master Mix II, no UNG, to a final volume of 20 µl. All final reactions contained 100 ng of cDNA, 900 nM of each primer, and 250-nM TaqMan[®] probes and were cycled on a QuantStudioTM 12K Flex system (Life Technologies) once for 10 minutes at 95°C, followed by 40 cycles of 95°C for 15 seconds and 60°C for 1 minute. All samples were measured in duplicate using GAPDH or β-Actin as a normalizing gene. Final analysis

was performed using the comparative CT method to calculate fold changes and samples were normalized relative to vehicle control conditions within each data set.

2.6.2 Fluidigm BioMarkTM Real-Time PCR

RNA was analyzed for purity and integrity by capillary electrophoresis using the Agilent Bioanalyzer 2100 (Agilent Technologies, Santa Clara, CA). Total RNA (125 ng) was DNase-treated for 15 minutes at room temperature and EDTA heat inactivated at 65°C for 10 minutes using Dnase I Amp Grade from Invitrogen. Samples were then reverse transcribed using the High Capacity cDNA Reverse Transcription Kit according to the manufacturer's protocol (Applied Biosystems). High-throughput qPCR was conducted to study gene expression in 5 ng cDNA using 96.96 Dynamic Arrays for the microfluidic BioMarkTM System (Fluidigm Corporation, CA, USA). A panel of 48 genes measured in duplicate, were selected based on previous DMF gene profiling studies conducted *in vivo* and *in vitro*, as well as published experimental and computational literature of identified Nrf2 regulated genes (Table 12). Real time PCR probe sets were designed using Primer Express 3.0 (Applied Biosystems) with TaqMan MGB Quantification default settings. A 20X Assay stock of the primer probe set of each gene to be investigated was made (900 nM for primers and 200 nM for Probe in 1X TE Buffer [10 mM Tris pH 8 (Ambion), 1 mM EDTA pH 8 (Sigma)]) and then diluted to a 0.2X assay pool. 2 µl of 0.2X assay pool was combined with 2ul of the reverse-transcribed total RNA and 4ul of 2x Taqman® PreAmp Master Mix (Applied Biosystems) for a final reaction volume of 8ul. Pre-amplification of cDNA was performed in the Tetrad thermocycler [at 95°C for a 10 minute activation step followed by 10 cycles: 95°C, (15 s), 60°C, (4 minutes)]. Following

pre-amplification, 32 μ l 0.1X TE Buffer was added to each sample and then mixed at an 11:9 ratio of 2X Taqman® Gene Expression Master Mix (Applied Biosystems) with 1% 20X GE Sample Loading Reagent (Fluidigm) to create the Sample Mix. In a separate mixture, 2X of Assay Loading Reagent (Fluidigm) was mixed with each pre-made 20X Assay at a 1:1 ratio to yield a 10X Assay mix. 5 μ l of each Sample Mix and 5 μ l of each 10X Assay Mix were loaded and mixed into dedicated wells of a 96.96 Dynamic Array using the Integrated Fluidic Circuits (IFC) Controller HX (Fluidigm). The loaded Dynamic Array was then transferred to the BioMark™ real-time PCR instrument and the Fluidigm GE 96x96 Standard v1 PCR Thermal Protocol was run [Thermal Mix at 50°C (2 minutes), 70°C (30 minutes), and 25°C (10 minutes); UNG and Hot Start at 50°C (2 min), and 95°C (10 minutes); cycling was performed using 95°C (15 second), and 60°C (1 minutes) for 40 cycles]. Samples were measured in duplicate and normalized to Gapdh, Actb and Ubc housekeeping controls. Final analysis was performed using the comparative CT method to calculate fold changes and samples were normalized relative to vehicle control conditions within each data set.

2.7 Northern Blotting

2.7.1 RNA probe generation

RNA probes were generated using primers that covered the primer/probe sequence of the OSGIN1 Taqman assay used for q-PCR analysis (see *section 1.4 of materials and methods*). PCR was conducted using human spinal cord astrocyte cDNA as a template and PfuUltra II Hotstart PCR Master Mix according to the manufacturer's protocol (Agilent). PCR products were separated on 2% SeaKem® LE Agarose DNA gels

(Lonza), appropriate bands excised and purified using QIAquick Gel Extraction Kit (Qiagen). Purified DNA was digested, re-purified and inserted into a pBluescript II KS+ Vector using a Quick Ligation Kit (Invitrogen). The vector-DNA ligation was then transformed into One Shot Chemically Competent *E. coli* (Invitrogen) by heat shock at 42°C for 30 seconds. Transformed cells were spread on ampicillin resistant selection plates and incubated overnight at 37°C. Following overnight incubation, eight colonies were collected in lysogeny broth (LB) medium plus ampicillin and shaken for eight hours at 37°C. Plasmid DNA was then purified using the Nucleospin 8 Plasmid Kit according to the manufacturer's protocol (Machery-Nagel, Bethlehem PA). Purified plasmid was checked for correct insertion by restriction digest and submitted for DNA sequencing. Plasmid DNA containing the appropriate insert was linearized and transcribed into RNA probes using a MAXIscript *in vitro* Transcription Kit (Invitrogen) according to the manufacturer's protocol. Unincorporated nucleotides were removed by column purification using NucAway Spin Columns (Ambion) and biotin labeled using a BrightStar Psoralen-Biotin Kit (Ambion).

2.7.2 Northern blot analysis

Northern blot analysis was conducted using the Ambion[®] NorthernMax[®]-Gly Kit (Life Technologies) according to the manufacturer's protocol. RNA was transferred to Ambion BrightStar Plus Membranes (Ambion) using an iBlot Transfer System (Invitrogen) and detection was accomplished using the BrightStar BioDetect Kit (Ambion).

2.8 Rapid Amplification of cDNA Ends (RACE)

2.8.1 3' RACE

3' RACE was conducted using the Invitrogen 3' RACE Kit (Invitrogen) with the primers listed in *section 1.4 of Materials and Methods*. The manufacturer's protocol was followed other than for target cDNA amplification which was accomplished using Platinum PCR Supermix (Invitrogen). 3' RACE products were separated by gel electrophoresis, excised and inserted into a TOPO vector. Generated plasmids were transformed into bacteria and purified according to the protocol mentioned in *section 2.7.1 of Materials and Methods*. Purified DNA was checked by restriction digest and submitted for DNA sequencing.

2.8.2 5' RACE

5' RACE was conducted using the Invitrogen 5' RACE Kit (Invitrogen) with the primers listed in *section 1.4 of Materials and Methods*. 5' RACE primer starting points were determined based on the sequence identified from 3' RACE. 5' RACE products were separated by gel electrophoresis, excised and inserted into a TOPO vector. Generated plasmids were transformed into bacteria and purified according to the protocol mentioned in *section 2.7.1 of Materials and Methods*. Purified DNA was checked by restriction digest and submitted for DNA sequencing.

2.9 Protein Isolation

2.9.1 Protein isolation from tissue

For protein extraction, frozen tissues were placed on wet ice and Radio Immuno Precipitation Assay (RIPA) buffer containing protease inhibitors was immediately added to samples at a volume of ~300 μ l per 5 mg of tissue. Tissues were homogenized in buffer for 20 seconds using an F60 Sonic Dismembrator (Fisher Scientific) at setting 8 in a 4°C walk-in fridge. Homogenized samples were incubated for 2 hours at 4°C with constant agitation and then centrifuged for 20 minutes at 13,000 rpm in a microcentrifuge maintained at 4°C. Following centrifugation, the supernatant was collected and the pellet discarded. Supernatants were analyzed for total protein concentration using the Thermo Scientific Pierce BCA Protein Assay Kit (Thermo Scientific) and diluted to yield equal concentrations of 2 μ g/ μ L. Samples were diluted 1:1 in 2X Laemmli denaturing buffer and boiled at 100°C for 5 minutes.

2.9.2 Protein isolation from cells

For protein isolation from whole cells, cells were scraped directly in 1X Laemmli denaturing buffer, disrupted using an F60 Sonic Dismembrator (Fisher Scientific) and boiled at 100°C for 5 minutes.

2.9.3 Protein quantification

Protein was quantified using the Pierce[®] BCA Protein Assay Kit (Pierce) and samples diluted to equal loading volumes.

2.10 Western Blot Analysis

Thirty μg of total denatured protein was loaded on Criterion™ TGX™ precast gels (Bio-Rad Laboratories) and ran at a constant voltage of 200V for ~45 minutes. Gels were transferred to nitrocellulose membranes using the Invitrogen iBlot system (Invitrogen). Membranes were blocked in 5% milk in TBST (tris-buffered saline, tween 20) for 1 hour followed by incubation with primary (overnight at 4°C) and secondary (1 hour at room temperature) antibodies in 5% milk in TBST. Signal was developed using SuperSignal® Chemiluminescent Substrate (Thermo Scientific). Primary antibodies can be found in *section 1.2 of Materials and Methods*.

2.11 Thermo HCS Arrayscan Algorithm Creation and Analysis

Plate-based cell assays were imaged using the Thermo HCS Arrayscan (Thermo Scientific) and quantified by algorithm generation. Templates were used to generate algorithms using HCS Studio software and included the *Nuclear Translocation* algorithm template for p53 translocation analysis and *Target Activation* algorithm template for DAPI nuclear count and the EdU proliferation assay.

2.12 Data Analysis and Statistics

Method of statistical analysis and corresponding p values are stated within individual figures other than for transcriptional profiling time course and dose response studies which are described below.

2.12.1 Transcriptional profiling time course and dose response studies

Statistical analysis was performed using Wilcoxon signed-rank test using SAS software for the transcriptional profiling time course study, with each statistical comparison occurring between vehicle and DMF-treated per time point. For the transcriptional profiling dose response study, one-way analysis of variance (ANOVA) was performed with Dunnett's multiple comparison test. Significance is indicated in Tables 13 and 14 as either $p < .01$ (dark gray) or $p < .05$ (light gray).

CHAPTER III

DELAYED-RELEASE DIMETHYL FUMARATE PHARMACODYNAMIC RESPONSES ARE TISSUE-SPECIFIC AND NRF2-DEPENDENT

1. RATIONALE

A potential mechanism to treat neurodegenerative disease is to utilize and enhance the activity of existing cellular defense mechanisms to overcome the degenerative and toxic effects of pathogenic stimuli. Elucidating how these defensive signaling pathways regulate cellular protection at the molecular level can contribute to the development of therapeutic approaches for combating neurodegenerative disease. The major cellular defense system activated during periods of oxidative and electrophilic stress is the Nrf2 pathway, which regulates the expression of genes that are pro-survival in nature and enable cells to better mitigate potentially toxic stimuli. DMF is believed to mediate its effect, at least in part, via the Nrf2 pathway; however, the exact mechanism of action is unknown. Therefore, evaluating the detailed pharmacodynamic responses to DMF treatment would provide important insight into the molecular nature of the DMF mechanism of action. Although there is strong evidence that DMF regulates Nrf2 expression resulting in target gene up-regulation, it is not known how these changes result in immunomodulation and/or cellular protection or if DMF activity is mediated solely through Nrf2, or if non-Nrf2 mechanisms exist. To begin exploring these possibilities, we measured transcriptional changes in wild type and Nrf2 knockout mice treated with DMF to compare the pharmacodynamic responses throughout the central nervous system (CNS) and periphery in order to understand how changes in target gene

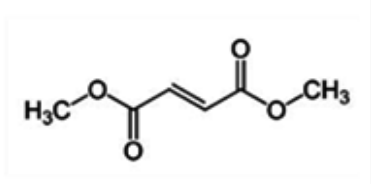
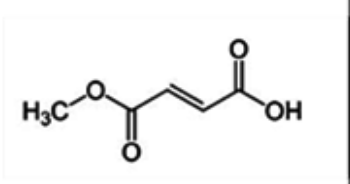
expression may confer DMF functional activity, and also to determine the necessity for Nrf2 in these processes.

2. RESULTS

2.1 DMF treatment leads to increased levels of MMF in all tissues of interest

DMF is known to be rapidly hydrolyzed to its bioactive metabolite, MMF, within minutes following oral intake (Werdenberg et al., 2003). To confirm that DMF was present at tissue sites analyzed for gene expression, MMF concentrations were measured in these tissues as an indicator of compound exposure. Following a single dose of 100 mg/kg DMF in wild type C57BL/6 mice, MMF exposure was detected in all six tissues of interest; liver, spleen, kidney, jejunum, brain and plasma (Figure 10). The highest level of MMF exposure was seen within plasma samples and the lowest levels were found to be in the liver. In the remaining tissues, comparable exposure levels were seen between the peripheral organs and the brain. These findings confirm that DMF administration can result in effects within the CNS and that the metabolite of MMF can cross the blood brain barrier to contribute to DMF-mediated mechanisms.

A

Compound Name	Dimethyl Fumarate	Monomethyl Fumarate
Abbreviation	DMF	MMF
Structure		
Molecular Weight	144.13	130.1
Molecular Formula	C ₆ H ₈ O ₄	C ₅ H ₆ O ₄

B MMF Exposures 30 min Post Oral Dosing
DMF 100 mg/kg in Mice

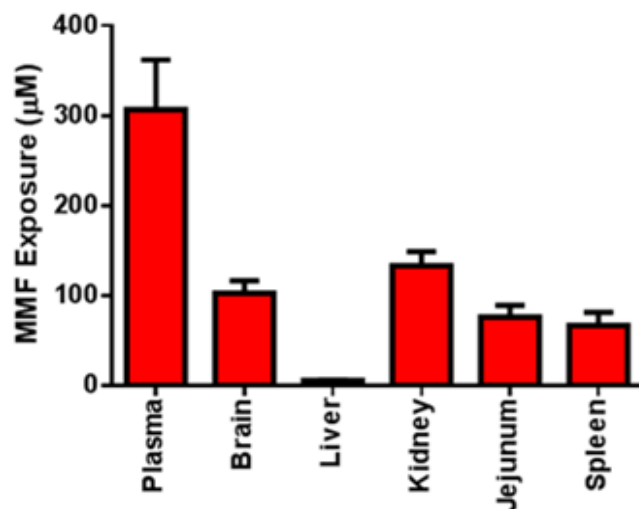


Figure 10. MMF exposure in peripheral and CNS tissues following a single dose of DMF.

A, structure and basic properties of dimethyl fumarate (DMF) and monomethyl fumarate (MMF). B, drug exposure levels were measured in mouse tissue samples collected 30 minutes post-dose of oral DMF and were analyzed for levels of MMF, the active metabolite of DMF.

2.2 DMF-induces differential gene expression across tissue types

To determine the effects of a single 100 mg/kg DMF dose on transcription regulation, a detailed gene transcriptional profiling study was conducted that measured the expression of 48 genes (Table 12) across eight time points using the Fluidigm BioMark™ HD System. This system maintains the sensitivity of classical real time PCR analysis while utilizing nanofluidic technology to collect larger data sets (upwards of 9,000 data points) in a single run. After receiving a single dose of DMF or vehicle, cohorts of animals were harvested at 2, 4, 6, 8, 12.5, 16.5, 23 or 37.5 hours. DMF and vehicle treated animals were harvested in parallel at each time point to eliminate the effects of diurnal variation, as all DMF samples were compared directly to time-matched vehicle controls to determine fold-changes in target gene expression. Data collected using this system identified time-dependent transcriptional changes following DMF treatment within peripheral (liver, spleen, kidney, jejunum and whole blood) and CNS (cerebellum, hippocampus, striatum and cortex) tissues. DMF-dependent transcription differed between the genes regulated within these tissue types as well as the onset and duration of the response (Figures 11-14; Table 13).

DMF-dependent transcription differed between the specific genes regulated within tissue types, with each tissue exhibiting a fairly distinct profile of the 48 genes selected for analysis. In Figures 11 and 12, identified DMF-regulated genes in peripheral tissues were graphed to show the differential expression of these genes in various tissues types against VEGFA, a non-regulated baseline control gene. Identified genes included ARB18, GCLC, GDF15, NQO1, SRXN1, SQSTM1, TXNRD1, OSGIN1 and RBP4.

Within peripheral tissues, less regulation in these genes was seen to occur in the liver and spleen compared to the kidney and jejunum, with the largest number of genes being regulated in the kidney and the largest magnitude of response occurring within the jejunum (Figure 11). Classical Nrf2-regulated genes such as AKRB18, GCLC, NQO1, SRXN1 and TXNRD1 showed fairly universal expression across the four analyzed peripheral tissues compared to more localized expression in specific peripheral regions for GDF15, SQSTM11, RBP4 and OSGIN1 (Figures 11 and 12).

Gene regulation following DMF treatment in CNS tissues was defined by a smaller subset of gene changes compared to the periphery, with gene transcription only affecting levels of NQO1, OSGIN1 and BDNF (Figure 13 and 14). Furthermore, as was seen in the periphery, the expression of these genes was differentially regulated in the four analyzed brain regions. NQO1 levels only changed slightly (1.5 to 2 fold) within brain tissues, with the exception of the striatum where no expression of NQO1 could be detected at the selected time points. The largest and most universal transcriptional changes within the brain were seen with OSGIN1 gene regulation, which expressed changes up to 4-5 fold above vehicle values in the hippocampus and cortex. OSGIN1 changes could also be detected within the cerebellum and striatum albeit at lower expression levels. In contrast to OSGIN1 and NQO1 in the brain, BDNF expression was unique to the striatum following DMF treatment.

Transcriptional changes following DMF treatment also resulted in distinct patterns in the onset and duration of the response. Within peripheral tissues, gene regulation peaked between 4 and 8 hours post-dose with the exception of OSGIN1 and

GDF15 in the kidney, which exhibited an earlier peak regulation of around 2 hours (Figure 11). For the few genes regulated within CNS tissues, gene expression also tended to peak at a slightly earlier time point between 2 and 6 hours following DMF dosing (Figures 13 and 14). For most regulated genes in most tissues, overall expression gradually decreased to baseline between 12 and 24 hours; however, when expressed, NQO1 and AKR1B8 tended to have more prolonged response in tissues. This can be seen in the small change in NQO1 within the CNS, as well as the more pronounced regulation of NQO1 and AKR1B8 within the kidney and jejunum. Although CNS regulation of NQO1 was slight, the prolonged expression tended to last out to 16.5 hours. In the kidney and jejunum prolonged expression continued past 24 hours. A unique time course following DMF could also be seen for BDNF expression in the striatum and RBP4 in the spleen, with peak regulation of these genes occurring at 4 hours post-dose and then dropping below normal levels before returning to baseline at around 16 hours.

Table 12. *Gene selections for Fluidigm real-time PCR.*

GO TERM	GO ID	Gene Name	Gene Symbol
Autophagy	GO:0006914	ATG2 autophagy related 2 homolog A sequestosome 1 (p62)	ATG2A SQSTM1
Cell cycle	GO:0007049	cyclin-dependent kinase inhibitor 1A (P21) growth differentiation factor 15	CDKN1A GDF15
Cell differentiation	GO:0030154	vesicular endothelial growth factor	VEGFA
Cellular matrix organization	GO:0030198	matrix metalloproteinase 11 (stromelysin 3)	MMP11
Cell migration	GO:0016477	snail homolog 1	SNAI1
Cholesterol homeostasis		ATP-binding cassette, sub-family A (ABC1), member 1	ABCA1
Developmental growth	GO:0048589	stimulated by retinoic acid gene 6 homolog (mouse)	STRA6
Dopamine receptor signaling pathway	GO:0007212	neuron-specific protein family member 2	NSG2
Glutamine biosynthesis process	GO:0005642	glutamate-ammonia ligase	GLUL
L-glutamate transport	GO:0015813	solute carrier family 1, member 2 (EAAT2)	SLC1A2
Metabolic process	GO:0008152	glutathione S-transferase alpha 2	GSTA2
Myelination	GO:0042552	early growth response 2	EGR2
Negative regulation of apoptotic process	GO:0043065	DnaJ (Hsp40) homolog, subfamily A, member 3 apoptosis antagonizing transcription factor nerve growth factor- γ	DNAJA3 AATF NGFG
Negative regulation of cell growth	GO:0008083	Oxidative stress induced growth inhibitor 1 nitric oxide synthase 1 sirtuin 1	OSGIN1 NOS1 SIRT1
Neuron development	GO:0048666	nuclear receptor subfamily 2, group F, member 6	NR2F6
Neuron fate commitment	GO:0048663	oligodendrocyte transcription factor 1	OLIG1
Nucleoside diphosphate metabolic process	GO:0009132	nudix (nucleoside diphosphate linked moiety X)	NUDT7
Oxidation-reduction process	GO:0055114	aldo-keto reductase family 1, member B8 copper chaperone for superoxide dismutase oxidoreductase NAD-binding domain containing 1	AKR1B8 CCS OXNAD1
Positive regulation of excitatory postsynaptic membrane potential	GO:2000463	neuropilin (NRP) and tolloid (TLL)-like 2	NETO2

Table 12 continued. Gene selections for Fluidigm real-time PCR.

GO TERM	GO ID	Gene Name	Gene Symbol
Regulation of cell growth	GO:0001558	insulin-like growth factor binding protein	IGFBP
Regulation of synaptic plasticity	GO:0048167	brain-derived neurotrophic factor	BDNF
Response to oxidative stress	GO:0006979	amyotrophic lateral sclerosis 2 (juvenile)	ALS2
		apolipoprotein E	APOE
		GRB2-associated binding protein 1	GAB1
		glutamate-cysteine ligase, catalytic subunit	GCLC
		glutamate-cysteine ligase, modifier subunit	GCLM
		NAD(P)H dehydrogenase, quinone 1	NQO1
		peroxiredoxin 1	PRDX1
		prion protein	PRNP
		prostaglandin-endoperoxide synthase 2	PTGS2
		superoxide dismutase	SOD1
		sulfiredoxin 1	SRXN1
		thioredoxin reductase 1	TXNRD1
		glial fibrillary acidic protein	GFAP
Retinol metabolic process	GO:0042574	retinol binding protein 4, plasma	RBP4
Signal transduction	GO:0007165	NF-kappa-B inhibitor, beta	NFKBIB
Tissue regeneration	GO:0042246	ninjurin 1	NINJ1

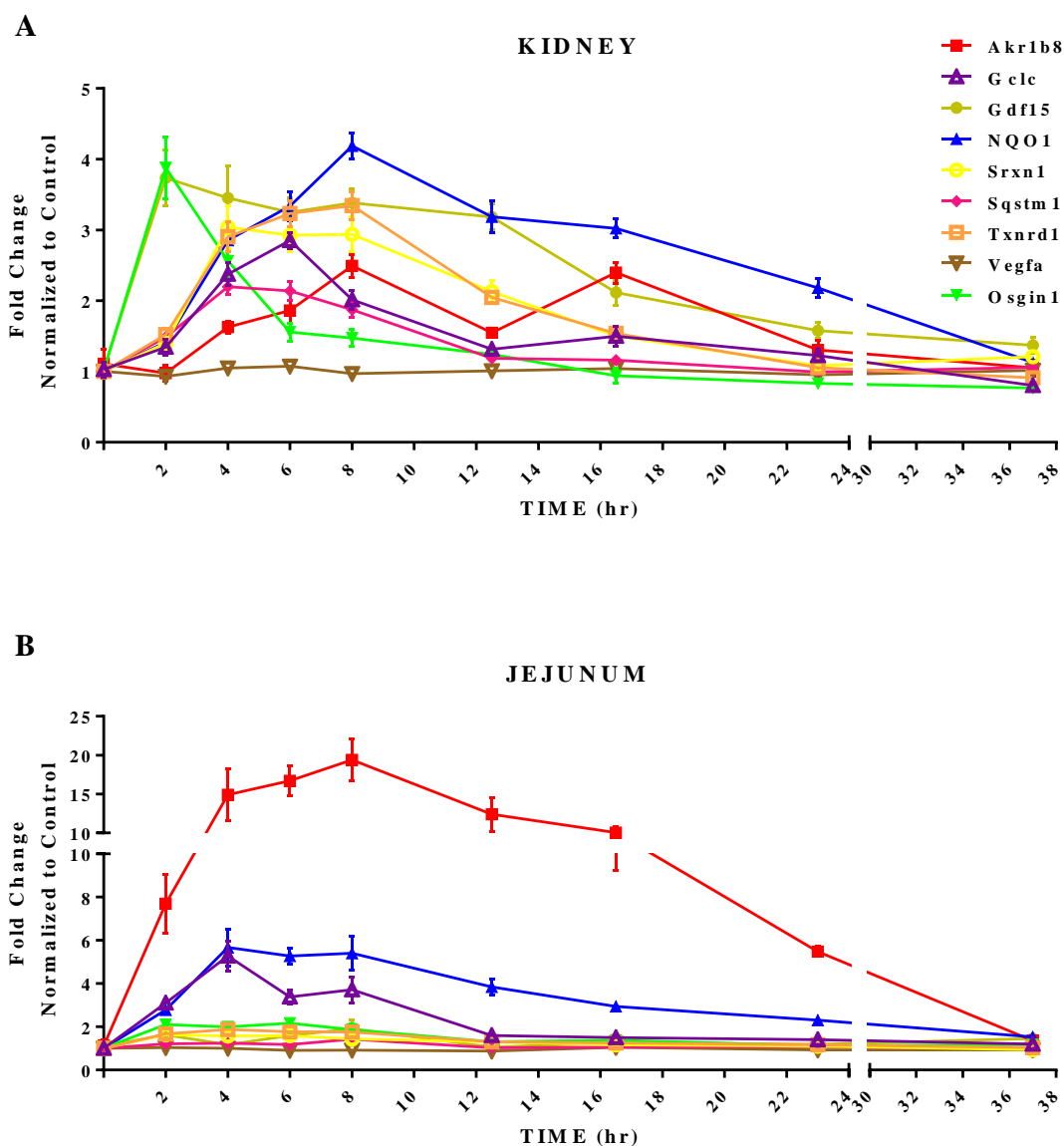


Figure 11. DMF transcriptional profiling time course in peripheral tissues: kidney/jejunum.

Transcriptional changes following single 100 mg/kg oral dose of DMF in kidney (A) and jejunum (B), graphed as changes in selected genes over time. Data are graphed as fold change values normalized to vehicle treated animals, with the starting value of 1 equivalent to the normalized baseline of vehicle animals. Graphed genes represent only those that were found to be regulated in peripheral tissues, with Vegfa as a baseline control gene. Refer to Table 13 for statistical analysis.

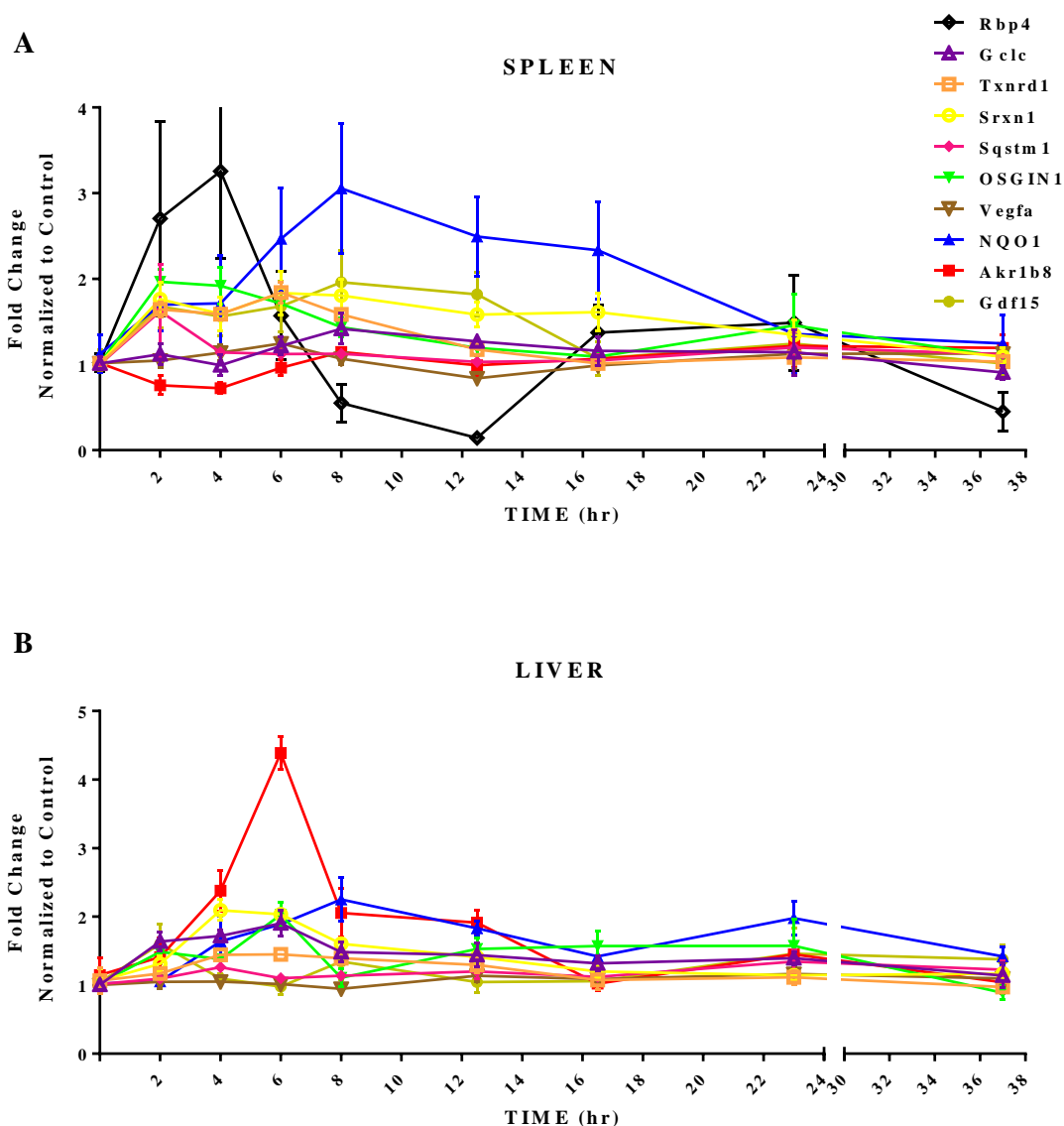


Figure 12. DMF transcriptional profiling time course in peripheral tissues: spleen/liver.

Transcriptional changes following single 100 mg/kg oral dose of DMF in spleen (A) and liver (B), graphed as changes in selected genes over time. Data are graphed as fold change values normalized to vehicle treated animals, with the starting value of 1 equivalent to the normalized baseline of vehicle animals. Graphed genes represent only those that were found to be regulated in peripheral tissues, with Vegfa as a baseline control gene. Refer to Table 13 for statistical analysis.

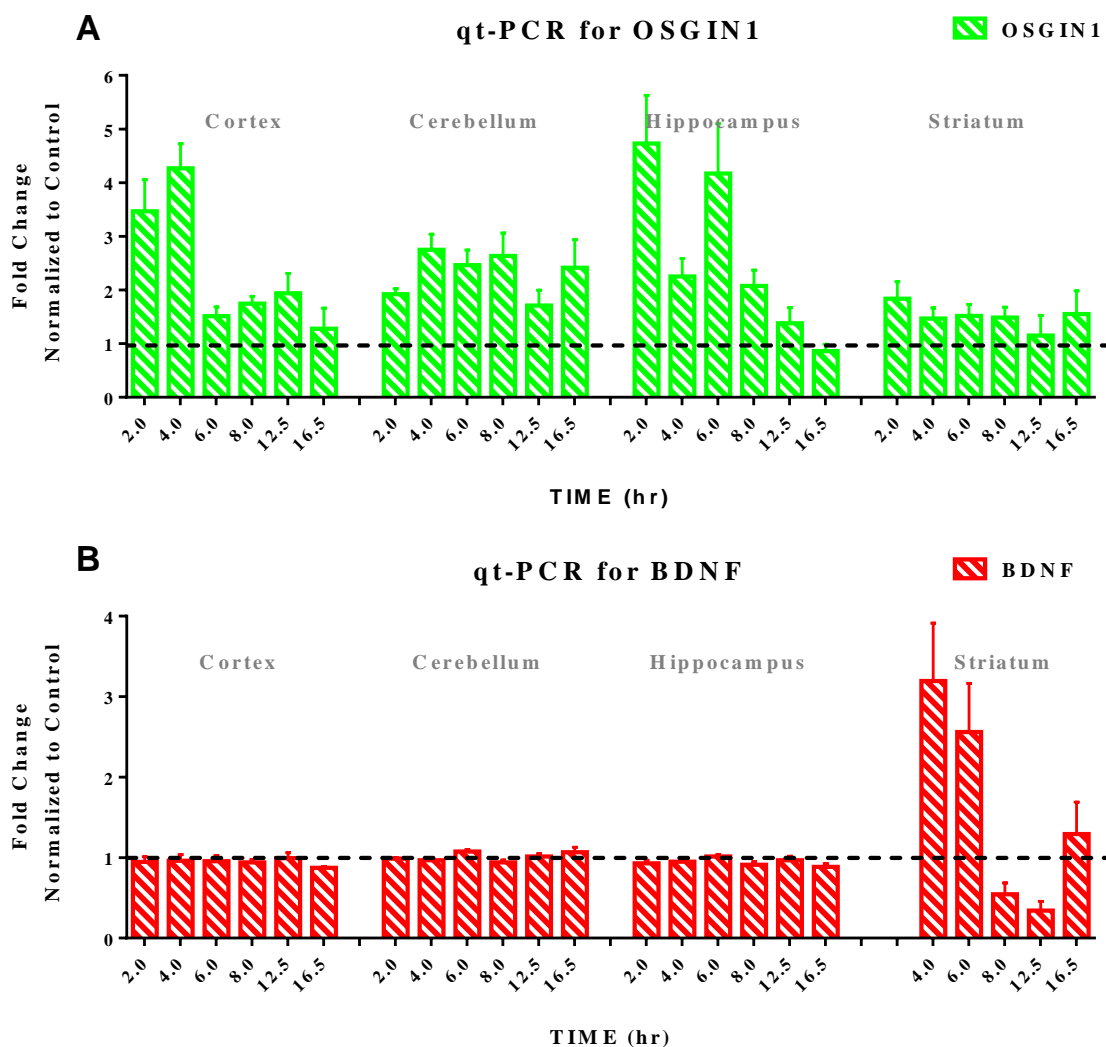


Figure 13. DMF transcriptional profiling time course in CNS tissues: *OSGIN1*/*BDNF*.

Transcriptional changes following single 100 mg/kg oral dose of DMF for two genes found to be regulated in the brain: *Osgin1* (A) and *Bdnf* (B). Data are graphed as fold change values normalized to vehicle treated animals, with the dashed line at 1 equivalent to the normalized baseline of vehicle animals. Later time points are not included since regulation of the graphed genes is consistent with the graphed 16.5 hour time point. Refer to Table 13 for statistical analysis.

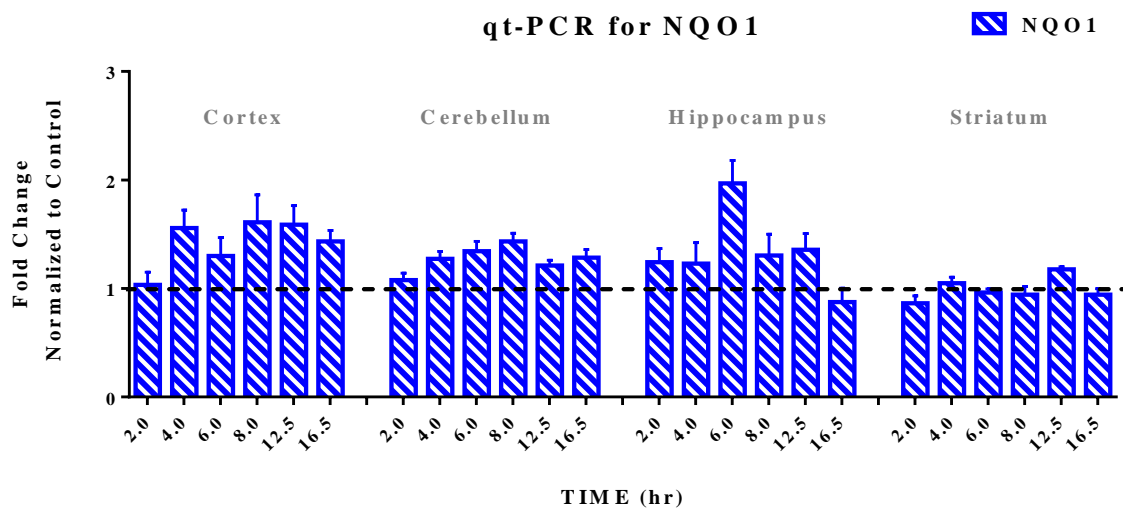


Figure 14. DMF transcriptional profiling time course in CNS tissues: NQO1.

Transcriptional changes following single 100 mg/kg oral dose of DMF Nqo1 in the brain. Data are graphed as fold change values normalized to vehicle treated animals, with the dashed line at 1 equivalent to the normalized baseline of vehicle animals. Later time points are not included since regulation of the graphed genes is consistent with the graphed 16.5 hour time point. Refer to Table 13 for statistical analysis.

Table 13. *Transcriptional profiling time course statistical analysis.*

Tissue	Gene	P-value 2 hrs	P-value 4 hrs	P-value 6 hrs	P-value 8 hrs	P-value 12.5 hrs	P-value 16.5 hrs	P-value 23 hrs	P-value 37 hrs
Liver	AKR1B8	0.51	0.008	0.0011	0.013	0.010	0.99	0.15	0.88
	GCLC	0.0007	0.0005	0.0016	0.029	0.021	0.027	0.0056	0.74
	NQO1	0.88	0.15	0.0081	0.0042	0.0015	0.14	0.0059	0.013
	OSGIN1	0.0048	0.21	0.19	0.79	0.022	0.13	0.27	0.30
	SRXN1	0.17	< 0.0001	< 0.0001	0.0005	0.0007	0.36	0.21	0.021
Spleen	NQO1	0.14	0.98	0.064	0.0046	0.046	0.038	0.99	0.93
	OSGIN1	0.078	0.0012	< 0.0001	0.0039	0.29	0.44	0.31	0.76
	SQSTM1	0.44	0.032	0.041	0.0035	0.38	0.70	0.35	0.010
	SRXN1	0.050	0.030	0.017	0.0008	0.011	0.029	0.22	0.54
	TXNRD1	0.0087	< 0.0001	< 0.0001	< 0.0001	0.0091	0.98	0.57	0.67
Kidney	AKR1B8	0.82	0.082	0.0061	0.0075	0.0012	0.028	0.31	0.86
	GCLC	0.081	0.0003	0.0001	0.0026	0.019	0.098	0.14	0.028
	GDF15	< 0.0001	< 0.0001	< 0.0001	< 0.0001	< 0.0001	0.0001	0.0041	0.038
	NQO1	0.0001	< 0.0001	< 0.0001	< 0.0001	< 0.0001	< 0.0001	< 0.0001	0.18
	OSGIN1	< 0.0001	< 0.0001	0.066	0.0056	0.015	0.50	0.025	0.088
	SQSTM1	0.0001	< 0.0001	< 0.0001	< 0.0001	0.0047	0.19	0.84	0.45
	SRXN1	0.0009	< 0.0001	< 0.0001	< 0.0001	< 0.0001	0.0052	0.16	0.026
	TXNRD1	0.0002	< 0.0001	< 0.0001	< 0.0001	< 0.0001	0.0030	0.28	0.002
Jejun.	AKR1B8	< 0.0001	< 0.0001	< 0.0001	< 0.0001	< 0.0001	< 0.0001	< 0.0001	0.22
	GCLC	< 0.0001	< 0.0001	< 0.0001	< 0.0001	< 0.0001	0.0001	0.0007	0.060
	NQO1	< 0.0001	< 0.0001	< 0.0001	< 0.0001	< 0.0001	< 0.0001	< 0.0001	0.003
	OSGIN1	.0002	< 0.0001	0.011	0.017	0.13	0.012	0.56	0.22
	SRXN1	0.0029	0.0003	0.0002	0.0011	0.0051	0.037	0.28	0.31
	TXNRD1	0.0009	< 0.0001	< 0.0001	0.0017	0.0019	0.0039	0.056	0.68
Cortex	OSGIN1	0.0019	0.0020	0.097	0.16	0.036	0.36	0.37	0.36
Cereb.	OSGIN1	< 0.0001	< 0.0001	0.0033	0.0048	0.99	0.36	0.028	0.12
Hippo.	NQO1	0.28	0.51	0.0035	0.26	0.30	0.35	0.79	0.65
	OSGIN1	0.0005	0.012	0.0044	0.052	0.55	0.50	0.37	0.61

Jejun. =jejunum; Cereb. =cerebellum; Hipp. =hippocampus. Gray shading representative of $p < .01$ based on Wilcoxon signed-rank test. p values calculated using vehicle control samples.

2.3 The magnitude of DMF-induced gene expression is dose-dependent

Dose-dependent changes in DMF-induced gene expression were also measured against the gene panel (Table 12) analyzed in the above mentioned time course using the Fluidigm BioMark™ HD System. This study aimed to capture DMF-dependent transcriptional changes with increasing concentrations of DMF that ranged from 50 to 600 mg/kg. DMF concentrations were administered at a constant time point of 7 hours that was selected based on optimal gene regulation across tissues identified in the previous time course. Data from this study shows the magnitude of DMF transcriptional response to be dose-dependent for all genes in all tissues tested except for the BDNF response in striatal tissue (Figures 15-18; Table 14). In contrast to all other regulated genes in the periphery and CNS which showed dose-dependent expression of genes previously identified in the time course, BDNF expression in the striatum increased at lower doses of 50 and 100 mg/kg but returned to baseline at concentrations above 100 mg/kg.

In the presence of higher DMF concentrations, genes not identified in the time course study were found to be induced. The most obvious example of this is the expression of CDKN1A at concentrations above 100 mg/kg within the liver, kidney and all CNS tissues (Figures 15-18). Interestingly, the liver, which did not express large transcriptional changes in the time course study, amplified CDKN1A over 40-fold at the highest dose following DMF treatment (Figure 16B). Furthermore, AKR1B8, which had the most profound expression in the jejunum in the time course study, was surpassed in expression by GSTA2 at concentrations above 200 mg/kg (Figure 15B). Other genes that

increased in expression at higher doses with DMF included NETO, IGFBP3 and NINJ1 in the spleen and GSTA2 in the jejunum. Reductions in gene expression were also seen at higher doses of DMF including NUDT7 in the liver and OLIG1 in the kidney (Figure 15A and 16B).

In the CNS, the cortex, cerebellum and hippocampus portrayed similar gene regulation patterns for CDKN1A, OSGIN1 and NQO1 following higher concentrations of DMF, with the largest magnitude of expression seen in OSGIN1 (Figures 17 and 18A). In contrast to the latter tissues and as seen in the time course data, the striatum continued to show differential regulation of genes in the presence of DMF compared to other CNS brain regions (Figure 18B). As mentioned above, BDNF regulation was only present in the striatum and only at low doses; however, there were also reductions in GAB1 and EGR2 seen within the striatum with increasing concentrations of DMF that reduced the expression of these in half. Furthermore, unlike neighboring brain regions, the striatum did not show dose-dependent increases in NQO1.

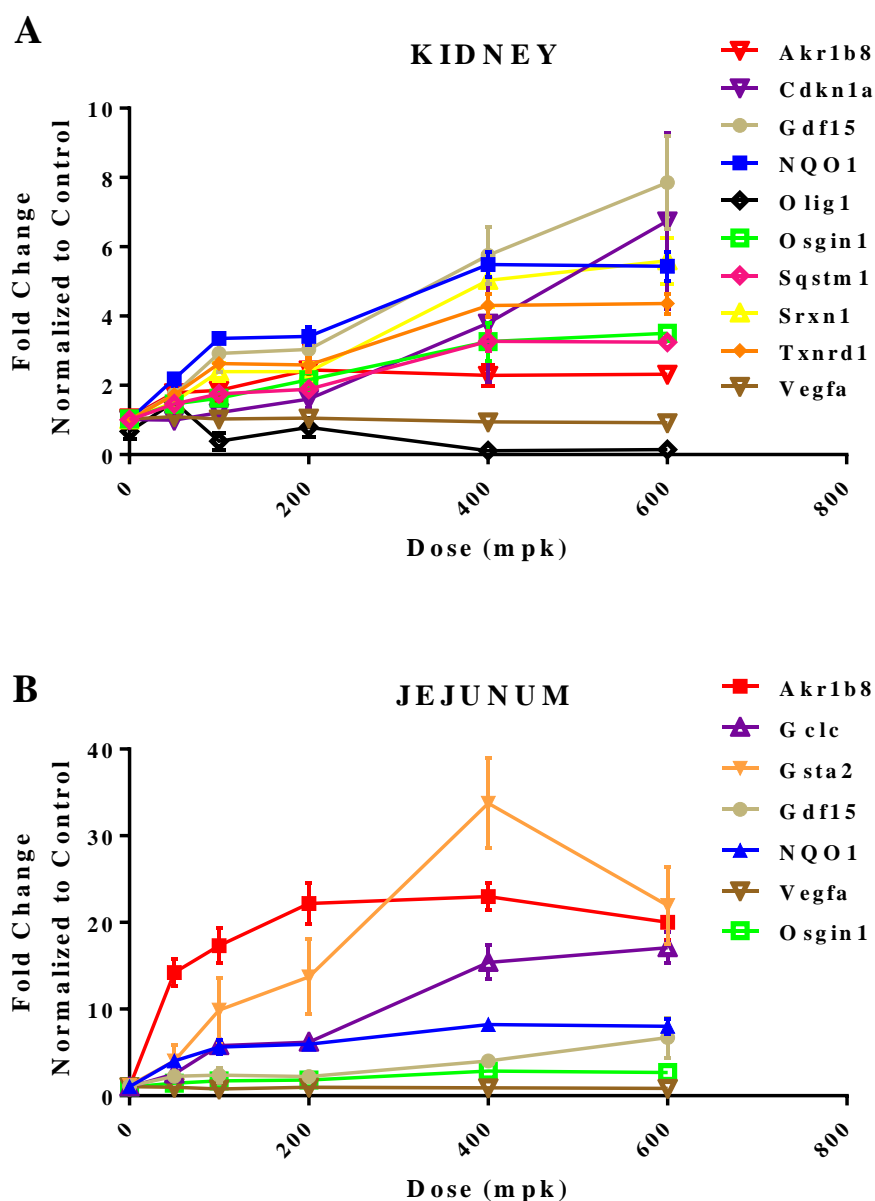


Figure 15. DMF transcriptional profiling dose-response in peripheral tissues: kidney/jejunum.

Transcriptional changes following multiple doses of DMF in kidney (A) and jejunum (B), graphed as changes in selected genes across doses. Data are graphed as fold change values normalized to vehicle treated animals, with the starting value of 0 equivalent to the normalized baseline of vehicle animals. Graphed genes represent only those that were found to be regulated in peripheral tissues, with Vegfa as a baseline control gene. Refer to Table 14 for statistical analysis.

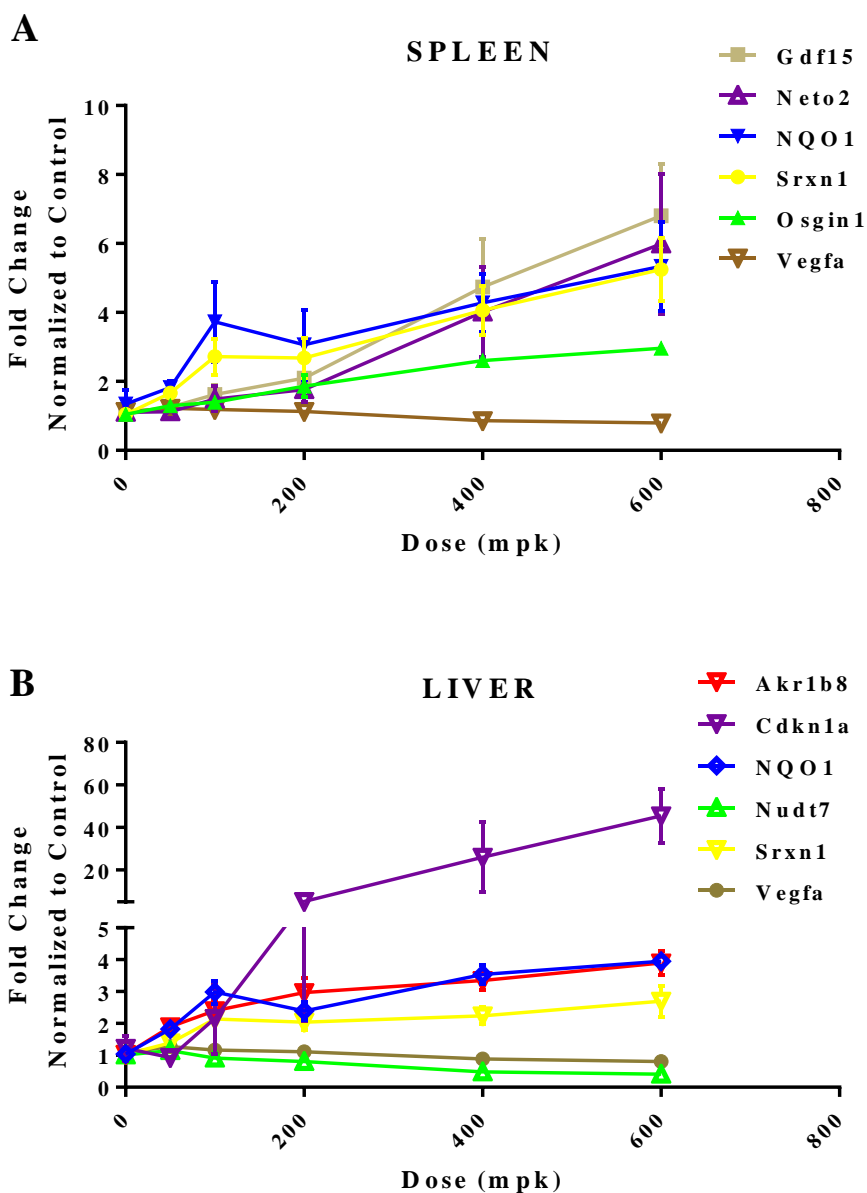


Figure 16. DMF transcriptional profiling dose-response in peripheral tissues: spleen/liver.

Transcriptional changes following multiple doses of DMF in spleen (A) and liver (B), graphed as changes in selected genes across doses. Data are graphed as fold change values normalized to vehicle treated animals, with the starting value of 0 equivalent to the normalized baseline of vehicle animals. Graphed genes represent only those that were found to be regulated in peripheral tissues, with Vegfa as a baseline control gene. Refer to Table 14 for statistical analysis.

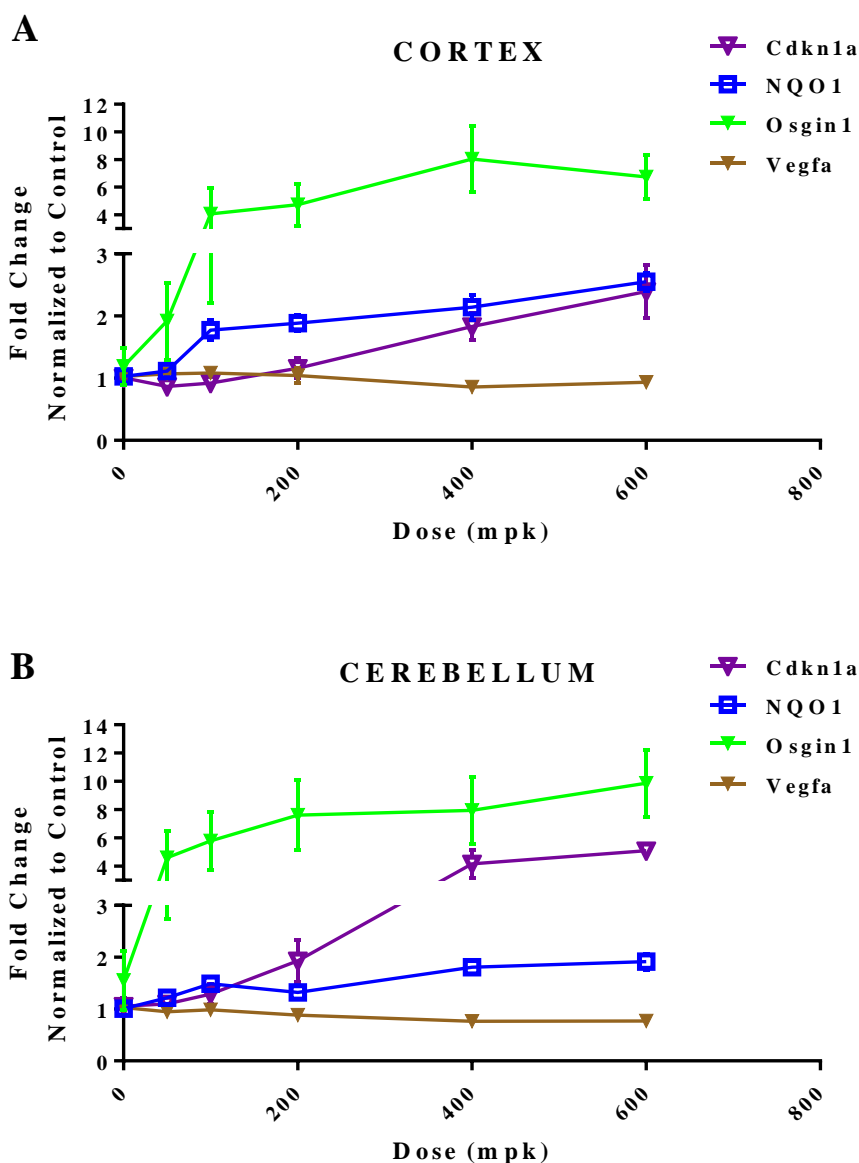


Figure 17. DMF transcriptional profiling dose-response in CNS tissues: cortex/cerebellum.

Transcriptional changes following multiple doses of DMF in Cortex (A), Cerebellum (B), graphed as changes in selected genes across doses. Data are graphed as fold change values normalized to vehicle treated animals, with the starting value of 0 equivalent to the normalized baseline of vehicle animals. Graphed genes represent only those that were found to be regulated in CNS tissues, with Vegfa as a baseline control gene. Refer to Table 14 for statistical analysis.

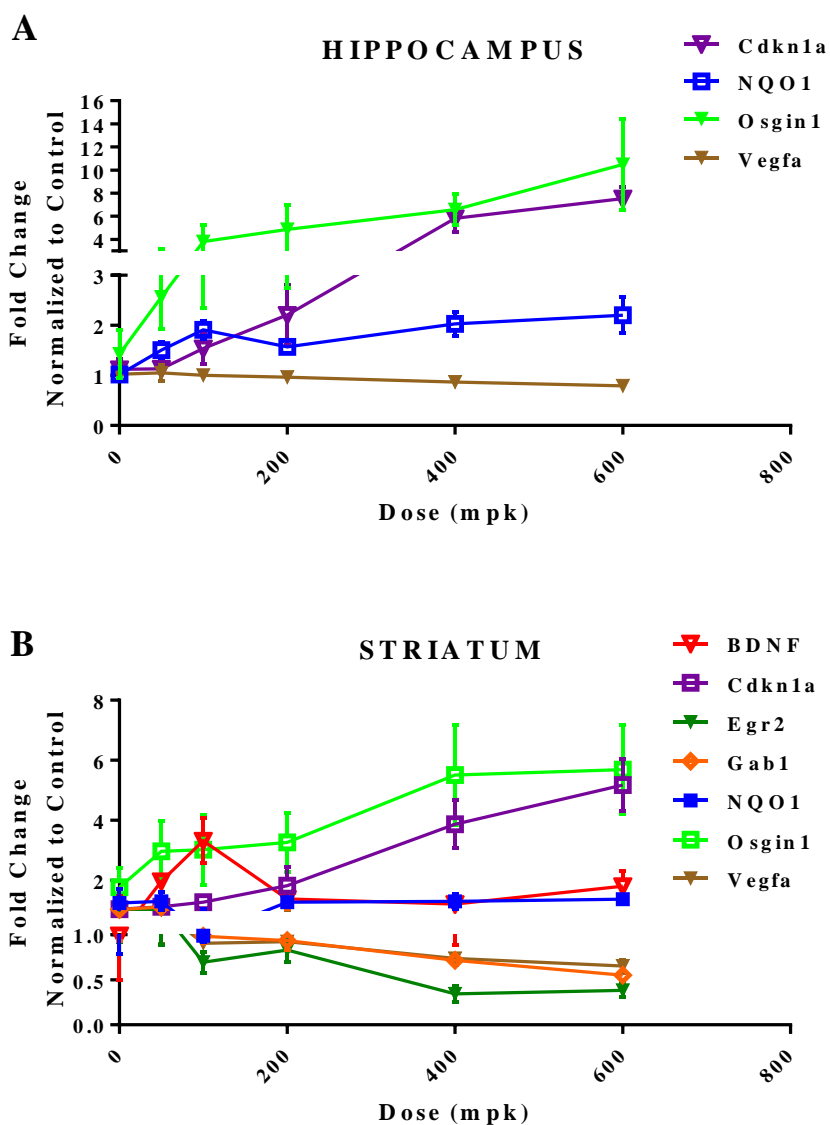


Figure 18. DMF transcriptional profiling dose-response in CNS: hippocampus/striatum.

Transcriptional changes following multiple doses of DMF in Hippocampus (A), Striatum (B), graphed as changes in selected genes across doses. Data are graphed as fold change values normalized to vehicle treated animals, with the starting value of 0 equivalent to the normalized baseline of vehicle animals. Graphed genes represent only those that were found to be regulated in CNS tissues, with Vegfa as a baseline control gene. Refer to Table 14 for statistical analysis.

Table 14. *Transcriptional profiling dose response statistical analysis.*

Tissue	Gene	p-value 50mpk	p-value 100mpk	p-value 200mpk	p-value 400mpk	p-value 600mpk
Liver	AKR1B8	0.2078	0.0180	0.0006	< 0.0001	< 0.0001
	CDKN1A	> 0.9999	0.9999	0.9958	0.1512	0.0019
	GCLC	0.3035	0.1414	0.1571	0.0007	< 0.0001
	NQO1	0.1285	< 0.0001	0.0028	< 0.0001	< 0.0001
	NUDT7	0.6611	0.8941	0.3174	0.0006	0.0001
	SQSTM1	0.7532	0.3684	0.1855	0.0041	0.0026
	SRXN1	0.8096	0.0288	0.0502	0.0149	0.0006
Spleen	GDF15	0.9999	0.9957	0.9179	0.0373	0.0006
	GLUL	0.9946	0.5730	0.4302	0.0019	< 0.0001
	NINJ1	0.6906	0.0910	0.0240	< 0.0001	< 0.0001
	NQO1	0.9579	0.5392	0.3811	0.0632	0.0088
	OSGIN1	0.9673	0.8205	0.0392	< 0.0001	< 0.0001
	SQSTM1	0.9997	0.2289	0.3902	0.0081	< 0.0001
	SRXN1	0.9922	0.4780	0.5188	0.0456	0.0022
Kidney	TXNRD1	0.9997	0.1512	0.2418	0.0005	< 0.0001
	GCLC	0.5500	0.0357	0.1326	< 0.0001	0.0002
	GCLM	0.0159	0.0004	0.0003	< 0.0001	< 0.0001
	GDF15	0.9164	0.2127	0.1689	0.0002	< 0.0001
	GSTA2	0.7974	0.0005	0.0260	0.0040	< 0.0001
	NQO1	0.0183	< 0.0001	< 0.0001	< 0.0001	< 0.0001
	OSGIN1	0.7770	0.5161	0.0548	< 0.0001	< 0.0001
	PRDX1	0.1131	0.0086	0.0307	0.0012	0.0036
	PRNP	0.2796	0.1519	0.1220	0.0046	0.0410
	SQSTM1	0.1257	0.0044	0.0008	< 0.0001	< 0.0001
Jejunum	SRXN1	0.8774	0.1240	0.1268	< 0.0001	< 0.0001
	TXNRD1	0.0692	< 0.0001	< 0.0001	< 0.0001	< 0.0001
	AKR1B8	< 0.0001	< 0.0001	< 0.0001	< 0.0001	< 0.0001
	CDKN1A	0.9997	0.9813	0.5640	0.0921	0.0104
	GCLC	0.8189	0.0265	0.0142	< 0.0001	< 0.0001
	GCLM	0.3128	0.0194	0.0005	< 0.0001	< 0.0001
	GDF15	0.9054	0.8633	0.9174	0.2186	0.0036
	GSTA2	0.9806	0.3975	0.1193	< 0.0001	0.0037
	NQO1	0.0186	0.0002	< 0.0001	< 0.0001	< 0.0001
	OSGIN1	0.5395	0.3733	0.0596	< 0.0001	0.0003
SRXN1	0.4836	0.1905	0.0461	0.0047	0.0007	

Light grey= $p < .05$ and dark grey= $p < .01$ based on one-way analysis of variance (ANOVA) performed with Dunnett's multiple comparison test. p values calculated using vehicle control samples. (Table continued on page 113)

Table 14 continued. *Transcriptional profiling dose response statistical analysis.*

Tissue	Gene	P-value 50mpk	P-value 100mpk	P-value 200mpk	P-value 400mpk	P-value 600mpk
Jejunum	TXNRD1	0.0717	0.0050	0.0015	< 0.0001	< 0.0001
	Cortex	CDKN1A	0.9867	0.9984	0.9786	0.0358
	GCLC	0.3499	0.5443	0.4165	0.0060	0.0002
	IGFBP3	0.9981	0.8788	0.9918	0.0358	0.0006
	NQO1	0.9914	0.0036	0.0008	< 0.0001	< 0.0001
	OSGIN1	0.9949	0.9763	0.1509	0.0062	0.0321
Cerebellum	CDKN1A	0.9999	0.9938	0.4639	0.0002	< 0.0001
	GAB1	0.8488	0.8932	0.6950	0.0346	0.0099
	NQO1	0.4832	0.0133	0.1517	< 0.0001	< 0.0001
	OSGIN1	0.6673	0.4070	0.1447	0.1406	0.0292
Hippocampus	CDNK1A	> 0.9999	0.9915	0.7042	0.0002	< 0.0001
	GAB1	0.9997	0.6539	0.7792	0.0890	0.0322
	GCLC	0.4169	0.0009	0.2017	< 0.0001	0.0013
	NQO1	0.3692	0.0241	0.2579	0.0091	0.0021
	OSGIN1	0.9936	0.8693	0.6327	0.2702	0.0146
Striatum	BDNF	0.4307	0.0062	0.8007	0.9594	0.3467
	CDKN1A	0.9999	0.9982	0.7790	0.0051	< 0.0001
	EGR2	0.9999	0.1539	0.5928	0.0008	0.0016
	GAB1	0.9025	0.9934	0.8852	0.0431	0.0011
Whole Blood	GCLC	0.9998	0.7210	0.0478	0.0010	0.0041
	NINJ1	0.7168	0.9965	0.1031	0.0236	0.0006
	NGFG	> 0.9999	0.9719	0.5310	0.0098	0.0016
	NQO1	0.9986	0.9877	0.5893	0.6577	0.0434
	SRXN1	0.8727	0.8770	0.0374	0.0350	0.0038
	TXNRD1	0.3182	0.4550	0.1012	0.0248	0.0260

Light grey= $p < .05$ and dark grey= $p < .01$ based on one-way analysis of variance (ANOVA) performed with Dunnett's multiple comparison test. p values calculated using vehicle control samples.

2.4 DMF transcriptional regulation in whole blood

Gene regulation following DMF treatment in the time course and dose response paradigms was also measured in whole blood samples for each animal analyzed. Whole blood data tended to be more variable than results detected in peripheral and CNS tissues; however, 2-fold increases in GFAP, PRDX1, OSGIN1 and NQO1 could be detected after a single 100 mg/kg dose of DMF (Figure 19A). These gene expression increases peaked at 2 hours for OSGIN1, between 4 and 6 hours for GFAP and PRDX1, and 8 hours for NQO1. Differential gene regulation in whole blood could also be detected with higher concentrations of DMF (Figure 19B) in a dose-dependent manner at a single 7 hour time point. Increased expression of GCLC and NINJ1 were detected at concentrations ≥ 200 mg/kg and decreased expression of NFKBIB and NSG2 were also identified at higher concentrations of DMF.

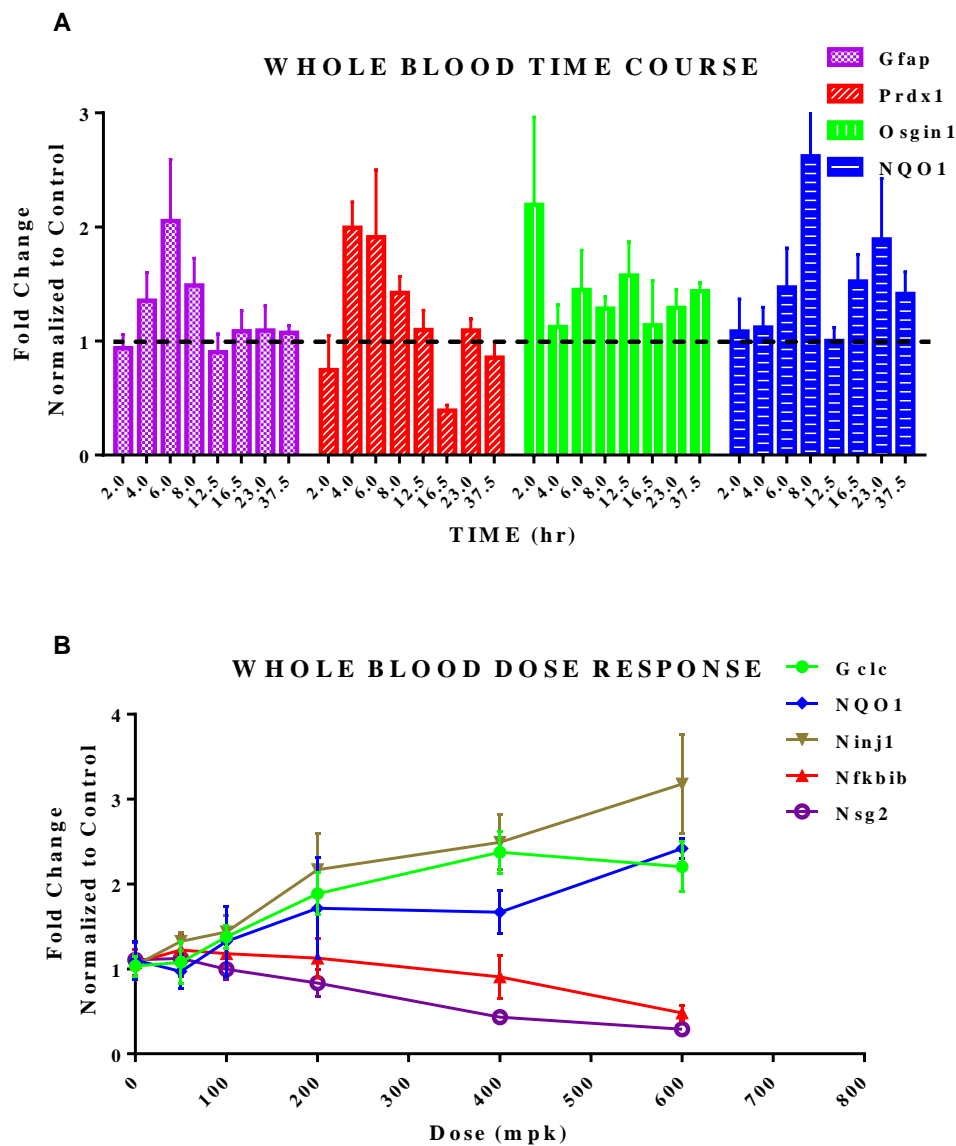


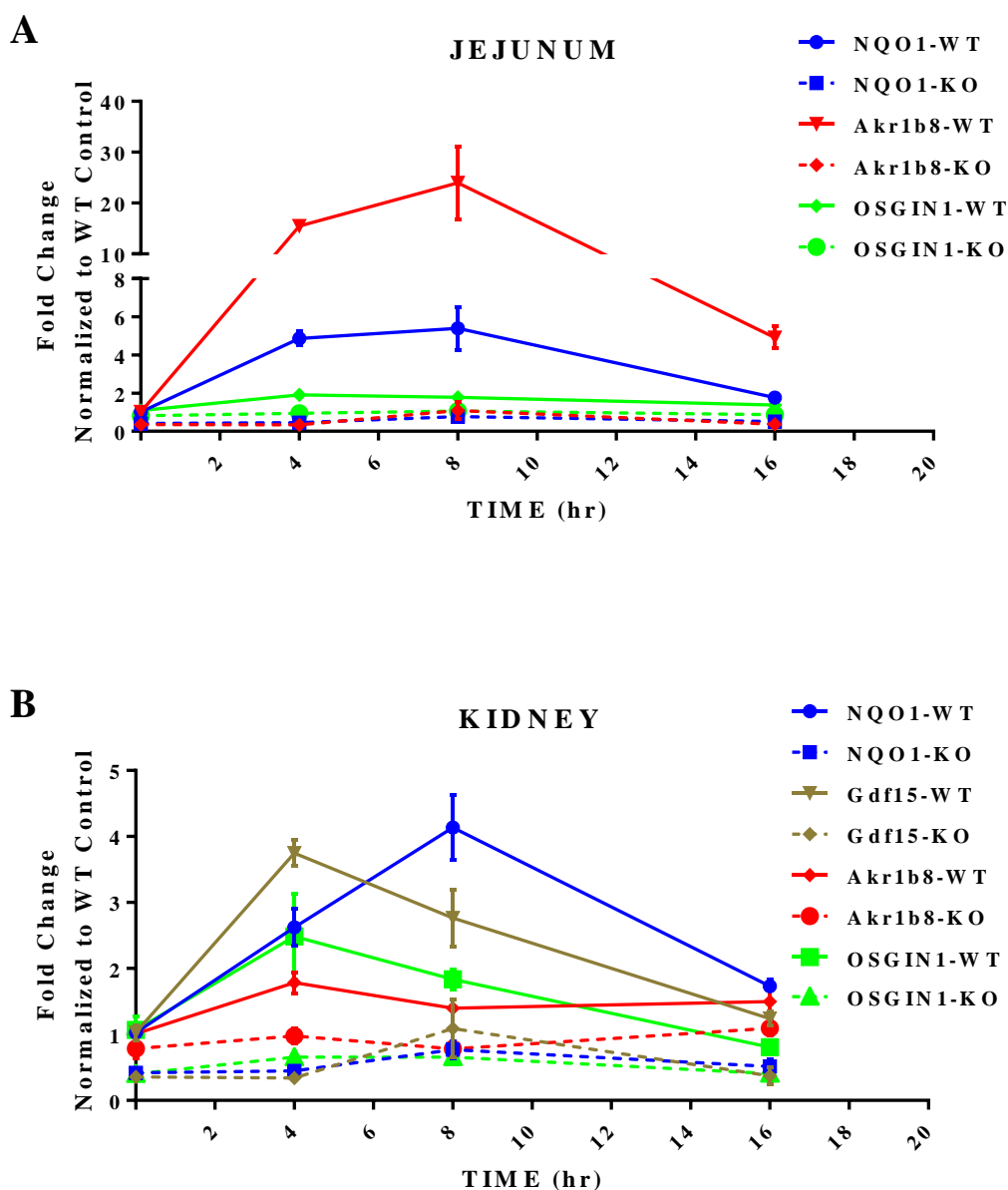
Figure 19. DMF transcriptional profiling dose-response in whole blood.

Transcriptional changes following a single dose of 100 mg/kg DMF across 8 time points in whole blood samples (A). Data are graphed as fold change values normalized to vehicle treated animals, with the dashed line at 1 equivalent to the normalized baseline of vehicle animals. Transcriptional changes following multiple doses of DMF in whole blood (B). Data are graphed as fold change values normalized to vehicle treated animals, with the starting value of 0 equivalent to the normalized baseline of vehicle animals. Graphed genes represent only those that were found to be regulated in whole blood. Refer to Tables 13 and 14 for statistical analysis.

2.5 DMF-induced gene expression is Nrf2-dependent

To determine if the DMF-induced transcriptional changes identified in the aforementioned time course and dose response studies were Nrf2-dependent, we measured the regulation of five of these identified genes in an Nrf2 knockout mouse. The panel of five genes included NQO1, AKR1B8, GDF15, OSGIN1 and BDNF, and were measured for transcriptional regulation at 4, 8 and 16 hours post 100 mg/kg DMF. This small gene panel was selected to specifically measure genes that were of particular interest and/or genes that had not been previously identified as classical Nrf2-regulated genes in the literature. In the absence of Nrf2, our results indicate a loss of NQO1, AKR1B8, GDF15 and OSGIN1 expression following dosing with a single concentration of DMF in the periphery and the CNS (Figures 20 and 21). Furthermore, the baseline expression of these genes in the knockout animals was decreased below endogenous expression levels of wild type controls in tissues where these genes could be induced by DMF.

Of these five analyzed genes BDNF was the only target that did not result in a complete loss of DMF-induced signal (Figure 21B). Although variable, loss of Nrf2 resulted in increased levels of BDNF expression at baseline, and in the presence of DMF these increases were gradually returned to the level of wild type values over time.



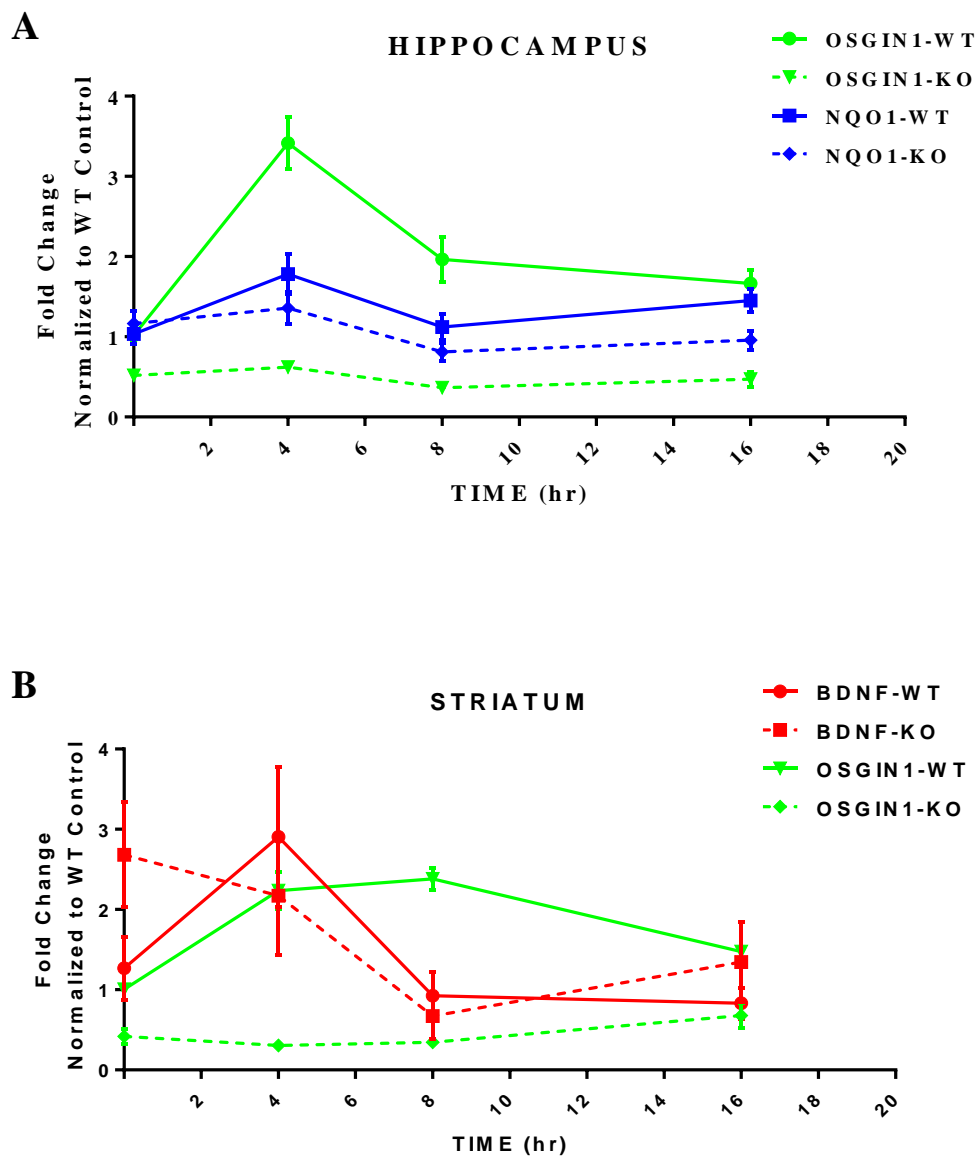


Figure 21. Transcriptional time course with 100 mg/kg DMF in *Nrf2*^{-/-} knockout and wild type mice: CNS tissues.

Transcriptional changes following single 100 mg/kg oral dose of DMF in CNS tissues: Hippocampus (A) and Striatum (B), graphed as changes in selected genes over time. Data are graphed as fold change values normalized to vehicle treated (WT-wildtype) animals, with the starting value of 1 equivalent to the normalized baseline of vehicle treated animals. Graphed genes represent a select panel determined based on gene regulation from the time course study. Refer to Table 15 for statistical analysis.

Table 15. DMF transcriptional time course in *Nrf2*^{-/-} mice.

Tissue	Gene	P-value 0 hrs	P-value 4 hrs	P-value 8 hrs	P-value 16 hrs
Kidney	AKR1B8-WT	-	0.0007	0.0058	0.0286
	AKR1B8-KO	0.1819	0.9683	0.0915	0.8561
	GDF15-WT	-	< 0.0001	0.0053	0.3542
	GDF15-KO	0.0003	0.0069	0.9889	0.0020
	NQO1-WT	-	< 0.0001	< 0.0001	0.0005
	NQO1-KO	0.0003	0.0599	0.7960	0.0063
	OSGIN1-WT	-	0.0400	0.0043	0.2915
	OSGIN1-KO	0.0083	0.6851	0.1179	0.0050
Jejunum	AKR1B8-WT	-	< 0.0001	0.0019	< 0.0001
	AKR1B8-KO	< 0.0001	0.7329	0.9999	0.3252
	NQO1-WT	-	< 0.0001	0.0008	< 0.0001
	NQO1-KO	< 0.0001	0.1502	0.9563	0.0013
	OSGIN1-WT	-	0.0040	0.0617	0.3505
	OSGIN1-KO	0.2371	0.7589	0.9983	0.5581
Striatum	BDNF-WT	-	0.2382	0.6817	0.6546
	BDNF-KO	0.1005	0.6065	0.3476	0.9858
	OSGIN1-WT	-	< 0.0001	< 0.0001	0.0133
	OSGIN1-KO	0.0006	0.0085	0.0004	0.0839
Hippocampus	NQO1-WT	-	0.0329	0.8621	0.0711
	NQO1-KO	0.5377	0.4299	0.3991	0.8776
	OSGIN1-WT	-	< 0.0001	0.0027	0.0037
	OSGIN1-KO	0.0011	0.2886	0.0302	0.0116

Light grey=p<.05 based on one-way analysis of variance (ANOVA) performed with Dunnett's multiple comparison test. p values calculated using WT, vehicle control samples.

2.6 DMF transcriptional regulation translates to protein expression

To confirm that transcriptional regulation of Nrf2 target genes translate to protein following DMF administration, western blot analysis was conducted to analyze protein levels of genes identified to be regulated following transcriptional analysis. Protein levels in tissue extracts from Nrf2^{-/-} knockout and wild type mice 6 hours post 100 mg/kg DMF administration were analyzed for expression changes of NQO1, TXNRD1, GCLC and SQSTM1 in peripheral tissues (Figure 22) and NQO1 and BDNF in CNS tissues (Figure 23). Selection of proteins to be analyzed was determined based on particular interest and success of antibody optimization.

Protein analysis in peripheral tissue extracts identified increased expression of selected proteins following DMF treatment in kidney (Figure 22A) and jejunum (Figure 22B). In the absence of Nrf2, these protein changes were either decreased or lost following DMF administration. In CNS tissues, basal levels of BDNF in the striatum (Figure 23A) and NQO1 in the cortex (Figure 23B) were not altered in the absence of Nrf2; however, although variable, a trend of increased protein expression in the presence of DMF could be identified.

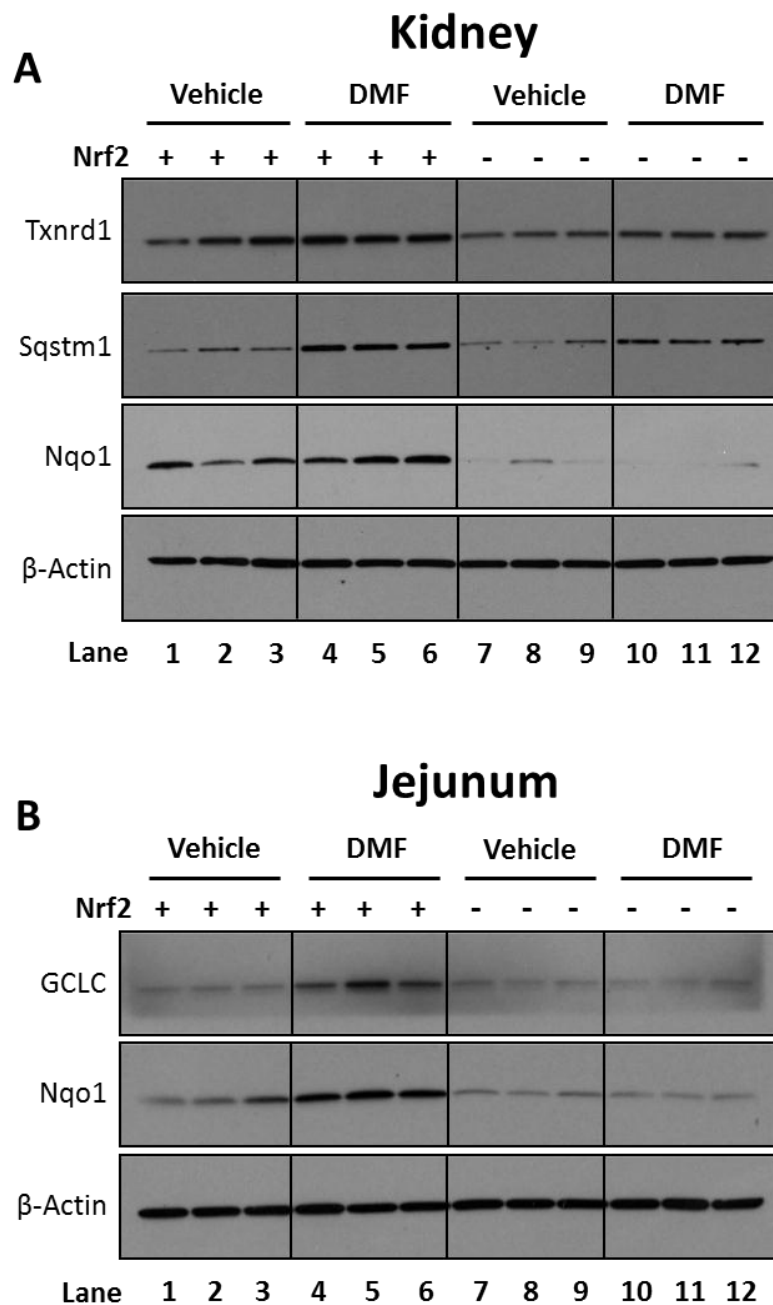


Figure 22. DMF induced Nrf2-dependent protein expression in peripheral tissues.

Nrf2^{-/-} knockout and wild type mice were treated with vehicle or 100 mg/kg DMF in triplicate and tissues harvested at 6 h after compound addition. Relative protein levels of Txnrd1, Sqstm1, Nqo1 and GCLC were assessed and actin control levels measured as an internal control. Protein expression following a single 100 mg/kg oral dose of DMF in Kidney (A) and Jejunum (B).

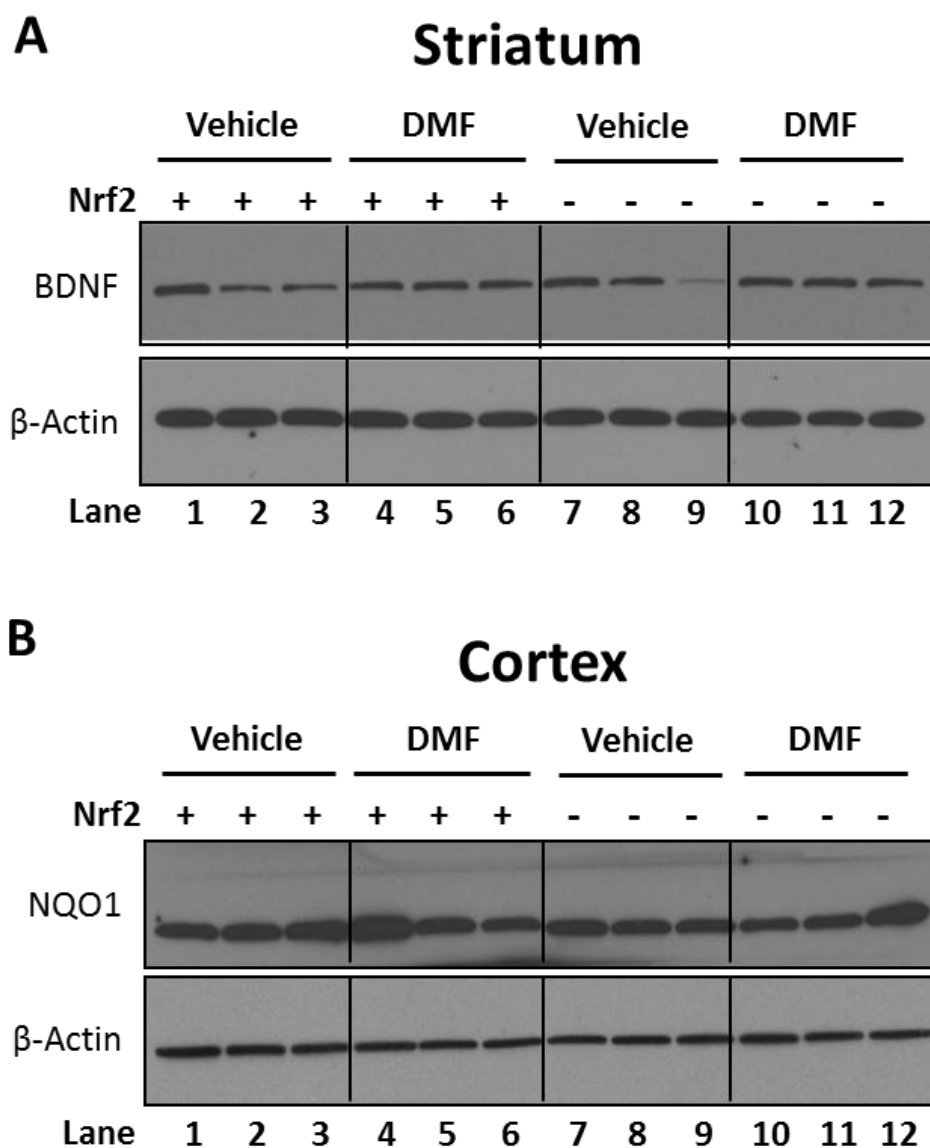


Figure 23. DMF induced protein expression in CNS tissues.

Nrf2^{-/-} and wild type mice were treated with vehicle or 100 mg/kg DMF in triplicate and tissues harvested at 6 h after compound addition. Relative protein levels of Nqo1 and BDNF were assessed and actin control levels measured as an internal control. Protein expression following a single 100 mg/kg oral dose of DMF in Striatum (A) and Cortex (B).

3. Discussion

Recent studies have identified inflammation and generation of excessive oxidative stress as contributing factors in a number of neurodegenerative disorders. Reactive oxygen species (ROS), a natural byproduct of cellular metabolism, exists in all aerobic cells in a physiological balance with neutralizing antioxidants (Andersen et al., 2004). However, when this balance is disrupted and ROS production surpasses antioxidant capacity, toxic free radicals can damage cells leading to oxidative stress (OS) (Orient et al., 2007). Inflammatory processes are also linked to the generation of excessive oxidative stress; the release of significant ROS via a “metabolic burst” mechanism from activated microglia and infiltrating macrophages in the CNS. Disturbances in the normal redox state, either through dysregulation of normal homeostatic processes or from aberrant inflammatory activity in the CNS, are believed to be a common pathogenic mechanism in aging as well as in neurodegenerative diseases such as PD (Jenner, 2007), AD (Emerit et al., 2004), ALS (Carri et al., 2003) and MS (Offen et al., 2004). Previous studies have suggested that targeting the Nrf2 pathway could be a promising therapeutic target for these diseases since this pathway is a ubiquitously expressed defense system for combatting against inflammatory, oxidative and electrophilic stress.

A functional Nrf2 pathway has been shown to be required for DMF protection against toxic oxidative stress in vitro (Scannevin et al, 2012), and for mediating DMF efficacy in vivo in the EAE model (Linker et al, 2011). The primary aim of our current study was to further characterize DMF pharmacodynamic responses throughout the CNS and periphery, and also to understand the requirement for Nrf2 in mediating these

responses. These experiments provide further understanding of the specific genes, onset of expression, duration and relative magnitude of DMF pharmacodynamic responses that occur across many different tissues. These data will help inform the sequence of events involved with DMF-mediated anti-inflammatory effects and cellular protection.

Our results indicate that DMF-induces distinct gene changes within peripheral and CNS tissues, with differentiation in the onset and duration of the response observed between genes and tissue type. These data also confirm earlier studies demonstrating that BG-12 activates transcription of Nrf2-dependent genes in the CNS and periphery. Although many classical Nrf2-dependent genes, such as NQO1, AKR1B8, GCLC, SRXN1 and TRXND1, were found to be regulated across many tissue types, we also identified many gene expression changes specific to certain tissues, including RPB4 in the spleen and BDNF in the striatum (Figures 12A and 13B).

The observations of tissue-specific gene expression indicate additional levels of transcriptional regulation that are specific to individual mRNA and particular cells types. These data also suggest that the dosage of DMF and corresponding relative DMF/MMF exposure may potentially effect transcriptional regulation of specific genes in different tissue types, based on our observation that increased concentrations of DMF can induce unique gene regulation in tissues that were not originally detected at lower doses. In addition to distinct gene changes, most transcriptional changes tended to be transient, with expression levels peaking between 2 and 8 hours post-dose (Figures 11-14). As there was differentiation in the persistence of individual mRNA, even those induced to a similar peak magnitude (Figure 11B. NQO1 vs GCLC), this indicates specific mRNA

stability may be governed by multiple pathways. It is also interesting to note that some of these responses persisted for an extended period of time before returning to baseline (Figures 11A and B; NQO1, AKR1B8).

One of the main goals of this study was to characterize CNS gene regulation following DMF treatment to a greater detail. The presented data indicate that the bioactive metabolite of DMF, MMF, can cross the blood-brain barrier (Figure 10) and induce differential gene expression in various brain regions. Although the regulation of genes in the CNS was not as robust in magnitude or in overall number of genes as within the periphery, we were able to identify small, but significant changes in the classical Nrf2 target gene NQO1 as well as novel expression of OSGIN1 throughout all brain regions (Figure 13 and 14). Although one study identifies OSGIN1 as a candidate Nrf2 target, our analysis is the first to confirm in an in vivo model that Osgin1 expression is mediated via Nrf2 (Chorley et al, 2012). Current literature on OSGIN1 suggests that various splice-variants of this gene interact with p53 to mediate cell death and survival within the cell (Hu et al, 2012). Although we attempted to determine OSGIN1 protein regulation following DMF treatment with commercial antibodies, we were unsuccessful in identifying immune reactive bands that were present or correlated with current literature. This may be due in part to differential regulation of OSGIN1 variants across tissue and cell types.

BDNF was also shown to be regulated in the brain by DMF, specifically within the striatum; however, results from Nrf2^{-/-} studies suggest that BDNF is not Nrf2-dependent. Moreover, it appears that basal expression of BDNF increases in the absence

of Nrf2, and DMF appears to reduce expression levels back to baseline. This line of investigation is currently being further explored as BDNF has demonstrated neurotrophic properties, this may indicate a novel mechanism by which DMF exerts therapeutic effects. BDNF regulation is also of particular interest since the transcriptional expression of this gene is not within the striatum is not widely accepted. Instances where striatal neurons can generate their own BDNF could be significantly beneficial to the health and survival of these cells.

The transcriptional profiling data compiled in this report indicates differential gene regulation across tissue types following treatment with DMF, which gives insight into the unique Nrf2-dependent pathways stimulated, or repressed, within distinct tissues and biofluids. These findings spark particular interest in the regulation of genes in the CNS compared to peripheral tissues, especially in regards to the regulation of OSGIN1 and BDNF in the brain. The activation of distinct cellular genes following DMF treatment may give us insight into the specific pathways that mediate the anti-inflammatory and neuroprotective actions of DMF.

CHAPTER IV

OSGIN1 CONTRIBUTES TO THE CYTOPROTECTIVE PROPERTIES OF MONOMETHYL FUMARATE (MMF)

1. RATIONALE

Previous studies using DMF and its bioactive metabolite, MMF, show Nrf2 stabilization and increased antioxidant protein expression following treatment of human astrocyte and oligodendrocyte cultures (Nguyen et al., 2009, Scannevin et al., 2012). Furthermore, MMF treatment in these cultures systems, as well as in primary mixed neuronal cultures, can protect against oxidative injury induced by hydrogen peroxide. This neuronal protection is also evident in the ability of DMF/MMF to improve clinical score and reduce neuroinflammation in the rat EAE model of MS (Linker et al., 2011). Although there is strong evidence that DMF/MMF increase cellular levels of Nrf2 resulting in antioxidant gene upregulation, it is not known how these alterations result in cellular protection. Therefore, understanding the specific sequence of events involved with Nrf2-mediated cellular protection is crucial for delineating the role fumarates play in these pathways. Following the identification of OSGIN1 as an Nrf2 transcriptional target that is upregulated in the brain following oral administration of DMF (Chapter 3), the importance of OSGIN1 in DMF-mediated cytoprotection was investigated.

2. RESULTS

2.1 MMF induces Nrf2 target genes and is protective against oxidative insult

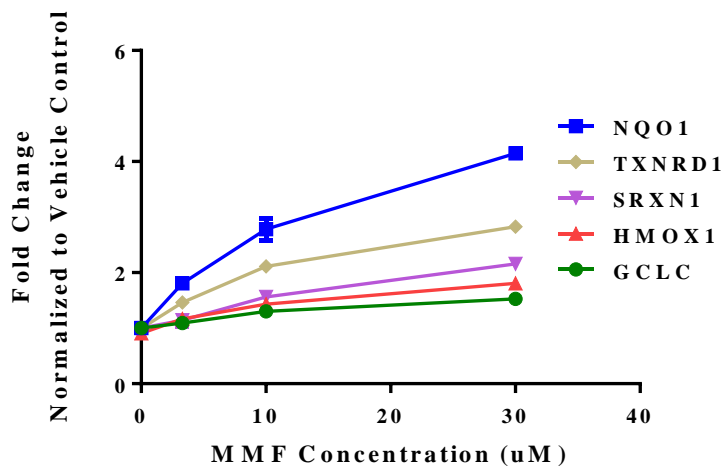
Based on current literature that suggests Nrf2 regulation in the CNS is predominantly via astrocytes, primary human astrocytes were measured for Nrf2 target gene regulation following treatment with MMF (Vargas et al., 2009, Miao et al., 2011). As previously mentioned, DMF is rapidly metabolized to MMF upon oral administration and only MMF exposure is known to be detected in the CNS (Figure 10; Werdenberg et al., 2003); therefore, to parallel *in vivo* studies all *in vitro* cultures were treated with MMF. To confirm that OSGIN1 is endogenously expressed in human astrocytes and confirm OSGIN1 induction with MMF treatment, OSGIN1 and five classical Nrf2 targets were analyzed via q-PCR. Following 24 hour treatment with MMF, q-PCR analysis identified OSGIN1 to be dose-dependently induced approximately 2 fold more than other classical Nrf2 target genes such as NQO1, TXNRD1, SRXN1, GCLC and HMOX1 in the presence of MMF (Figure 24). These results confirm previous *in vivo* studies that OSGIN1 is a MMF-regulated transcriptional target as well as confirm the regulation of Nrf2 target genes in the presence of MMF.

Since the Nrf2 pathway is considered the major cellular response pathway to oxidative and electrophilic stress, the effect of MMF on cellular viability in the presence of oxidative insult was evaluated. Previous studies investigating the cytoprotective effects of MMF have shown this compound to protect human astrocytes from the oxidative insult hydrogen peroxide (H₂O₂) (Scannevin et al., 2012); therefore, to confirm that MMF can indeed protect cells from oxidative damage, human astrocytes were treated with a

titration of MMF for 24 hours followed by oxidative challenge with H₂O₂ (Figure 25). To measure viability of cells following experimentation, LIVE/DEAD analysis was performed. Addition of 300 μ M H₂O₂ to DMSO-treated cells resulted in approximately 85% reduction in LIVE fluorescence intensity measured by calcein-AM incorporation into cells. In the presence of MMF, astrocytes challenged with H₂O₂ were protected against the toxic effects of this insult resulting in only a 50% reduction in cell loss (Figure 25D). To confirm fluorescent intensity quantitative results, images were acquired from samples analyzed in the LIVE/DEAD assay (Figure 25A-C). H₂O₂ challenge alone resulted in a dramatic loss of cell number as well as an increase in dying cells (Figure 25B). In comparison, pre-treatment with MMF was able to preserve cellular viability of astrocytes and reduce cell death (Figure 25C). These data confirm previous studies that MMF is cytoprotective against the effects of oxidative stress *in vitro*. Furthermore, the increases in OSGIN1 (Figure 25B) following MMF treatment correlate with increased cellular survival against H₂O₂, suggesting this gene may play a mechanistic role in this paradigm.

A

q-PCR for Classical Nrf2 Target Genes



B

q-PCR for OSGIN1

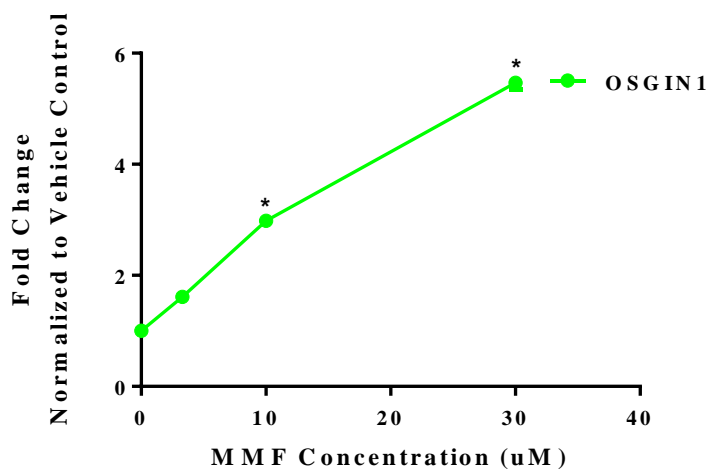


Figure 24. MMF induces Nrf2 target gene expression in human astrocytes.

Human astrocytes were treated with either DMSO or a titration of MMF for 24 hours before RNA extraction and q-PCR analysis. The graph represents triplicate samples; error bars indicate S.D. A, q-PCR analysis of classical Nrf2 target genes. B, OSGIN1 q-PCR analysis. *, $p < 0.001$ of OSGIN1 regulation compared to the other Nrf2 targets using two-way ANOVA with Tukey's multiple comparison's test.

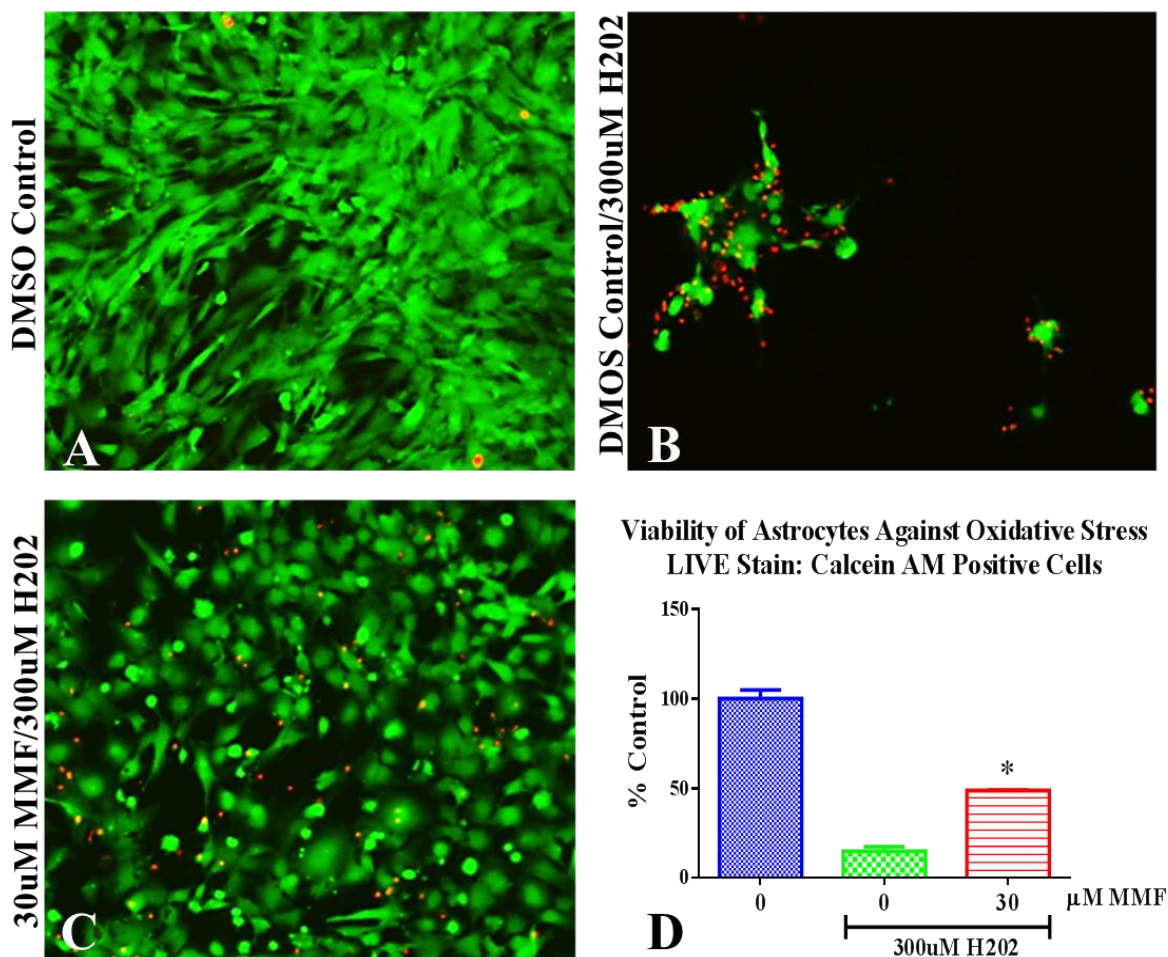


Figure 25. MMF protects human astrocytes from oxidative challenge.

Human astrocytes were treated with DMSO or 30 μM MMF for 24 hours followed by oxidative challenge. A-C, live imaging of LIVE/DEAD labeled cells pretreated with MMF and then challenged with H_2O_2 . LIVE calcein AM (green) and DEAD ethidium homodimer (red) labeling. A, positive control cells treated with DMSO. B, control DMSO-treated and 300 μM H_2O_2 -challenged cells. C, astrocytes pretreated with 30 μM MMF and challenged with 300 μM H_2O_2 . D, quantification of calcein AM fluorescence intensity in LIVE/DEAD labeled cells from A-C. *, $p < 0.001$ compared to control using one-way ANOVA with Tukey's multiple comparison's test. Experiment was repeated three times.

2.2 Loss of Nrf2 abolishes MMF cytoprotection and depletes OSGIN1

Following confirmation of MMF-mediated cytoprotection against oxidative insult, the importance of Nrf2 in this protection was assessed. Human astrocytes were transfected with siRNA targeted against Nrf2 to reduce mRNA and protein levels of this gene. Nrf2 siRNA transfection resulted in an approximate 80% reduction in Nrf2 mRNA levels and almost a complete loss of Nrf2 protein expression (Figure 26B). In the presence of MMF, no significant regulation of Nrf2 transcript was observed in either control or Nrf2 siRNA transfected astrocytes (Figure 26A). Since Nrf2 is constitutively expressed and degraded under normal homeostatic conditions by the protein Keap1 and inhibition of this interaction is believed to regulate Nrf2 protein expression (see section 2.3 of Chapter I; Itoh et al., 1997), no effect on Nrf2 mRNA induction is expected. MMF is believed to interact with the cysteine residues on Keap1 to inhibit the degradation of Nrf2 and allow for Nrf2 accumulation (Linker et al., 2011). Protein accumulation of Nrf2 following MMF treatment was observed with control siRNA and these accumulations were lost in cells transfected with Nrf2 siRNA (Figure 26B). These findings confirm previous findings that MMF regulates Nrf2 expression on a protein level to activate this pathway (Scannevin et al., 2012).

To determine if the loss of Nrf2 expression in human astrocytes correlates with the reduction in OSGIN1 expression seen in Nrf2^{-/-} knockout mice (see section 2.5, Chapter III), q-PCR analysis was conducted to measure OSGIN1 transcript levels following Nrf2 knockdown (Figure 27). Loss of Nrf2 reduced total OSGIN1 expression in astrocytes by greater than 60% and significantly reduced the ability of MMF to induce

OSGIN1 transcript levels. This confirms *in vivo* Nrf2 knockout studies where induction of OSGIN1 was found to be strongly regulated by Nrf2 and Nrf2 was necessary for MMF-mediated regulation of OSGIN1. Although other Nrf2 transcriptional targets have been identified to be mediated by MMF *in vitro* (Scannevin et al., 2012), OSGIN1 is the most significantly regulated Nrf2 target shown to be mediated in the presence of MMF, suggesting that this gene is an important target of Nrf2 (see section 2.5, Chapter III).

In order to determine if activation of the Nrf2 pathway contributes to the cytoprotective properties of MMF, human astrocytes were transfected with Nrf2 siRNA and treated with MMF for 24 hours followed by oxidative challenge with H₂O₂. In the absence of Nrf2, MMF-mediated cytoprotection of human astrocytes was completely abolished, as can be seen in both LIVE/DEAD acquired images and viable nuclear DAPI counts (Figure 28). Nrf2-deficient astrocytes also demonstrated increased sensitivity to oxidative insult as seen in the reduced viability of DMSO-treated cells lacking Nrf2 compared to control transfected cells. These results confirm previous findings from our lab that activation of the Nrf2 pathway is important for MMF-mediated protection against oxidative damage in astrocytes.

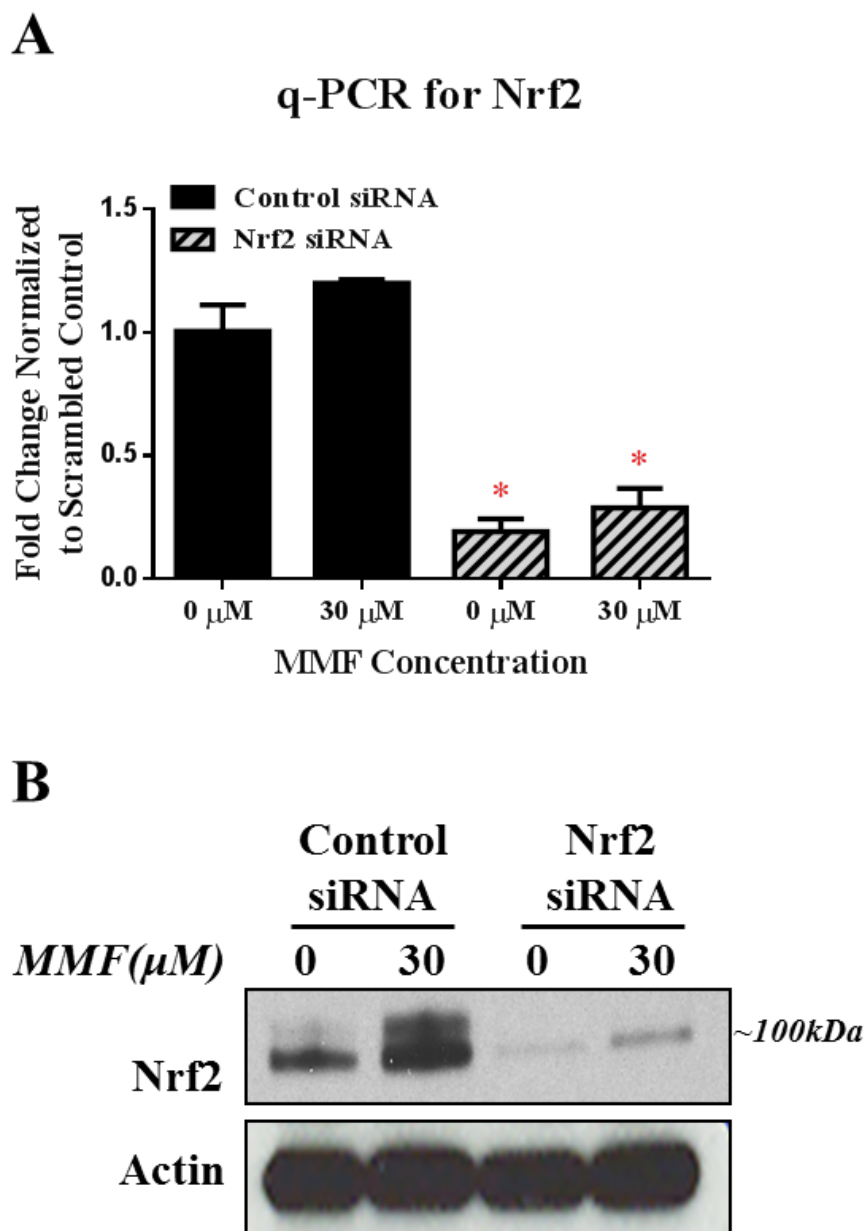


Figure 26. Nrf2 knockdown.

B, q-PCR analysis of human astrocytes treated with 10 nM of control or Nrf2 siRNA and either DMSO or 30 μ M MMF. *, $p < 0.001$ as compared to control siRNA using two-way ANOVA and Tukey's multiple comparison test. B, correlating western blot data with A. Actin is shown as a loading control. Experiment was repeated twice.

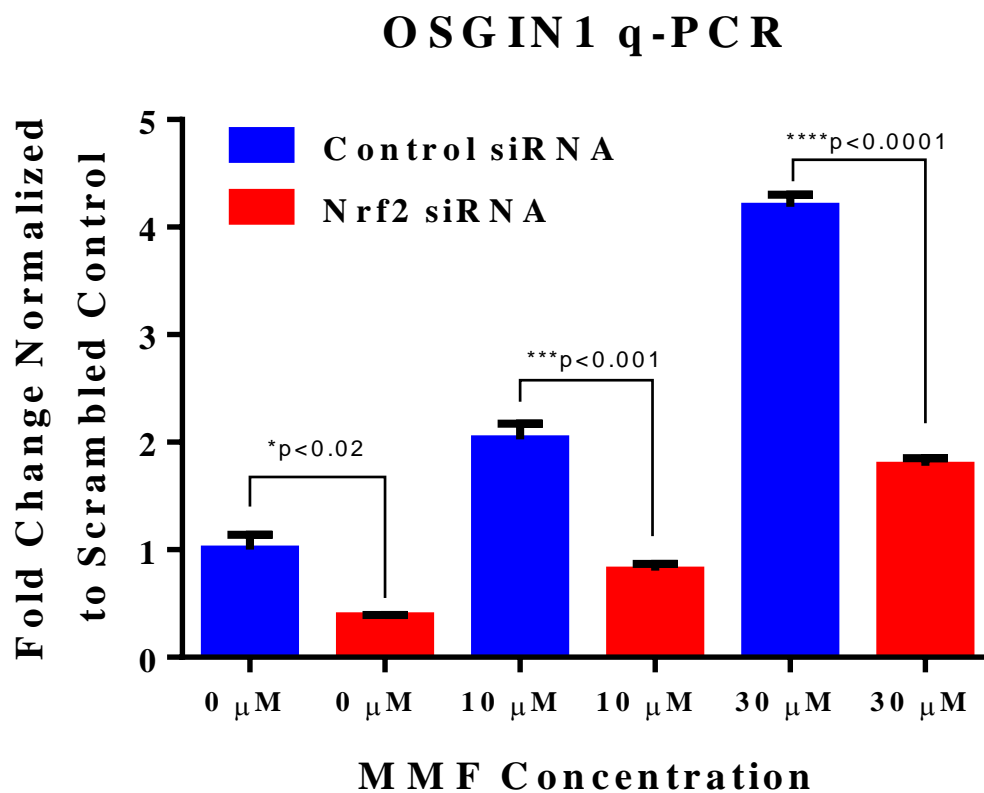


Figure 27. Loss of Nrf2 reduces OSGIN1 expression.

Human astrocytes were transfected with scrambled (control) or Nrf2 siRNA followed by treatment with a titration of MMF. q-PCR analysis was conducted for OSGIN1 transcription. Error bars represent SD and *p* values based on two-way ANOVA with Tukey's post-test for multiple-samples comparisons. Experiment was repeated three times.

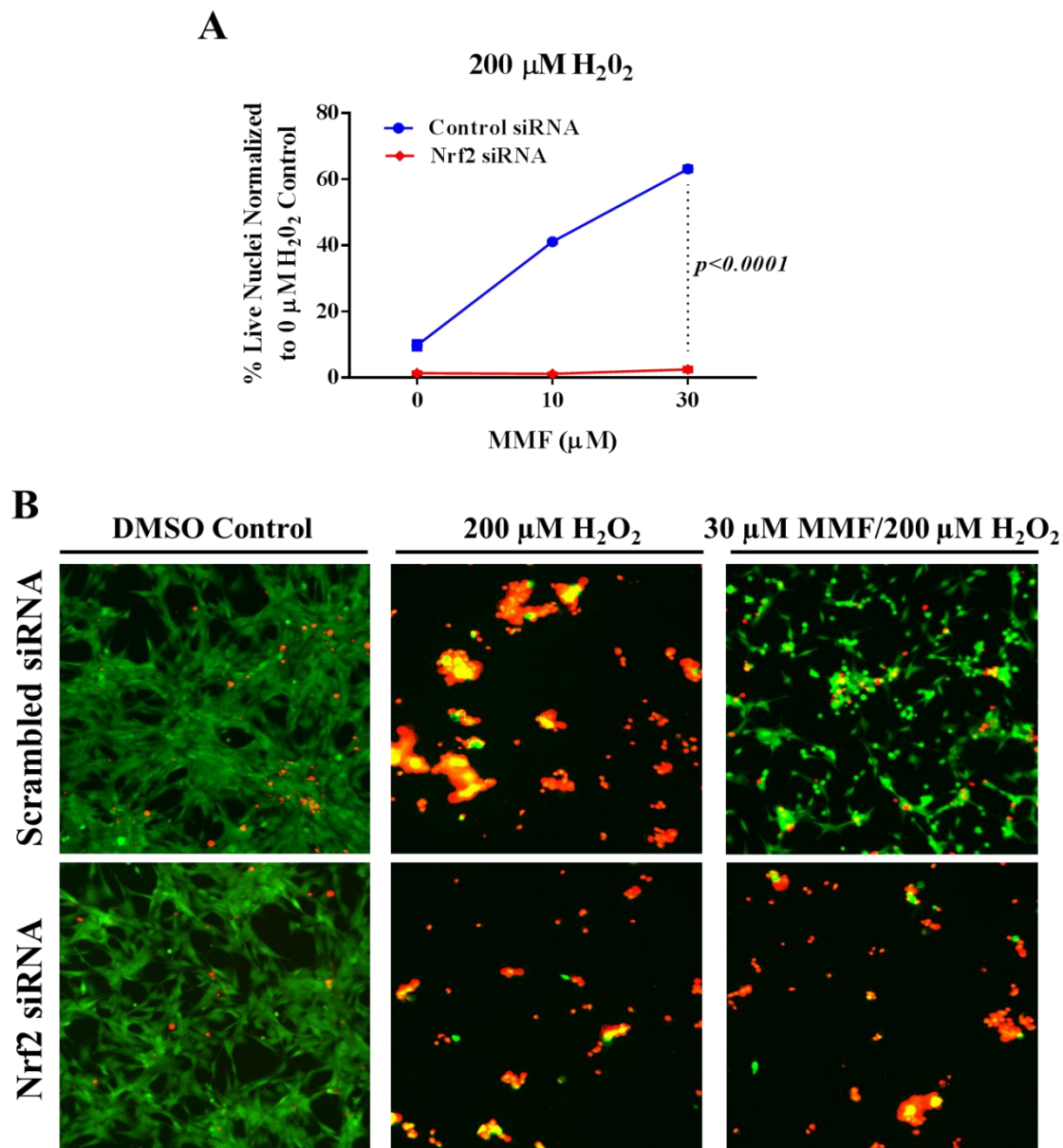


Figure 28. Loss of Nrf2 abolishes MMF-mediated cytoprotection.

Human astrocytes were transfected with scrambled (control) or Nrf2 siRNA and treated with either DMSO or MMF for 24 hours then challenged with H_2O_2 . A, cells fixed and stained with DAPI nuclear dye. Graph represents average cell nuclei counts in 20 fields per well (2 wells averaged in graph). Error bars represent standard deviation (SD) and p values based on two-way ANOVA with Sidak's post-test for multiple-samples comparisons. B, live imaging of LIVE/DEAD labeled cells pretreated with MMF and then challenged with H_2O_2 . LIVE calcein AM (green) and DEAD ethidium homodimer (red) labeling. Experiment was repeated three times.

2.3 Loss of OSGIN1 reduces MMF cytoprotection in the presence of oxidative insult

OSGIN1 was first identified as an Nrf2 target in *in vitro* studies where the loss of Nrf2 inhibited the ability of the oxidation product, Ox-PAPC, to induce OSGIN1 (Li et al, 2006). Although these studies were confirmed in 2014 by Yan et al, further understanding of the role of OSGIN1 as an Nrf2 target has not been thoroughly investigated (Yan et al, 2014). The *in vivo* findings presented in section 2.5 of Chapter III as well as the inability of MMF to induce OSGIN1 in the absence of Nrf2, suggest that OSGIN1 may be involved in mediating some of the protective effects of activating the Nrf2 pathway. To investigate the possibility of a role for OSGIN1 in MMF-mediated cytoprotection, human astrocytes were transfected with OSGIN1 siRNA to diminish OSGIN1 levels and the effect on oxidative challenge was studied as previously described with Nrf2 siRNA knockdown (see section 2.2 of Chapter IV).

siRNA knockdown of OSGIN1 resulted in greater than 70% loss of OSGIN1 transcript levels compared to scrambled siRNA control (Figure 29A). In the presence of MMF, OSGIN1 induction was also significantly diminished following reduction in basal levels of OSGIN1 (Figure 29A). Furthermore OSGIN1 knockdown did not affect the level of Nrf2 transcripts, which is expected since OSGIN1 has already been identified as a downstream target of Nrf2 in section 2.2 of this Chapter (Figure 27B).

To determine if OSGIN1 induction contributes to MMF-mediated cytoprotection, astrocytes transfected with OSGIN1 siRNA were treated with a titration of MMF for 24 hours followed by oxidative challenge with H₂O₂. Knockdown of OSGIN1 resulted in a reduced ability of astrocytes to be protected against H₂O₂ following MMF treatment. This

can be visualized in the increased number of viable cells indicated by LIVE-positive staining and reductions in overall DEAD-positive cells in LIVE/DEAD acquired images (Figure 30A). These findings were further quantified by fluorescence measurement of LIVE-positive cells and viable nuclear DAPI count where an approximately 4 fold decrease in viable cells was observed in the absence of OSGIN1 (Figure 30B and C). In comparison to Nrf2 siRNA transfection (Figure 28), OSGIN1 knockdown did not completely abolish MMF-mediated cytoprotection, with approximately 10% of MMF-mediated cytoprotection maintained. Although this could be a result of incomplete loss of OSGIN1 in this cellular system, it is more likely that other transcriptional targets of Nrf2 also contribute to the protection inferred by MMF.

Interestingly, OSGIN1 siRNA transfection in the presence of H₂O₂ alone tended to be almost 2 fold more resistant to oxidative damage compared to scrambled siRNA control astrocytes (Figure 30). Although there was not a significant difference observed in total cell count between OSGIN1 and control siRNA transfected astrocytes, this could still be due to increased proliferation in the absence of OSGIN1. OSGIN1 has previously been identified to regulate cell cycle and loss of OSGIN1 has been shown to induce proliferation of cancer cell lines (Ong et al., 2004; Huynh et al. 2001, Wang et al., 2005). These aspects of OSGIN1 will be discussed further in section 2.7 of this Chapter.

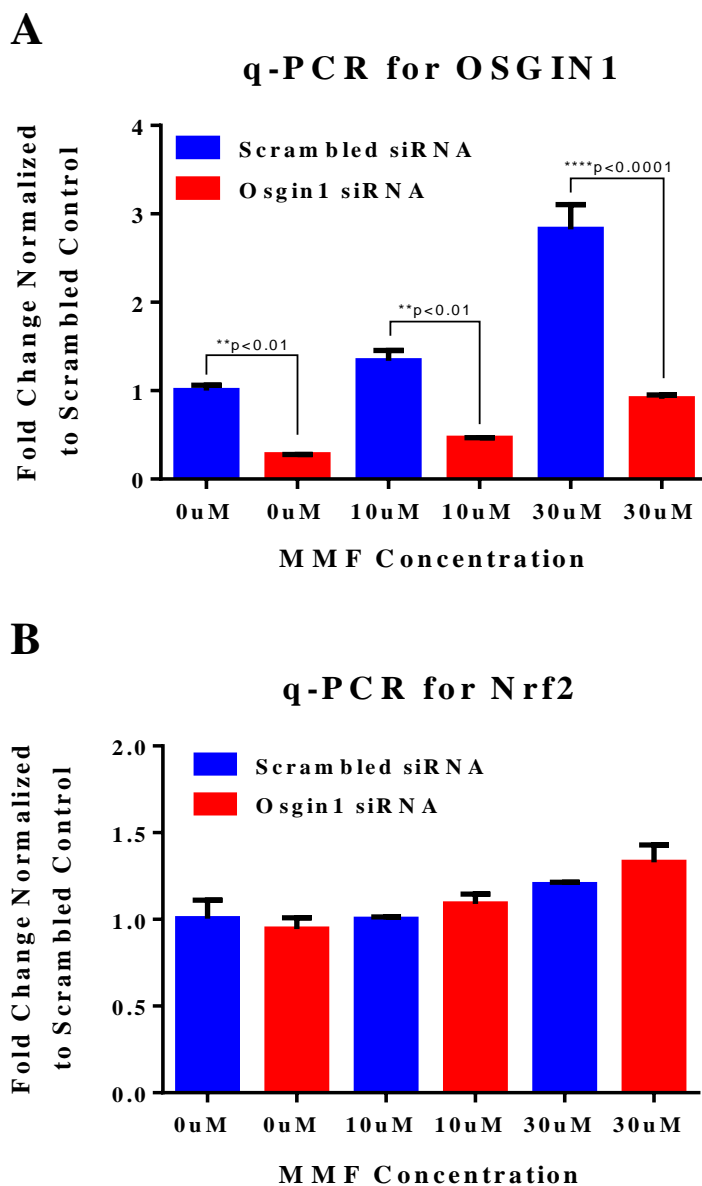


Figure 29. OSGIN1 siRNA knockdown.

Human astrocytes were transfected with scrambled (control) or OSGIN1 siRNA and treated with either DMSO, 10 μ M MMF or 30 μ M MMF for 24 hours before RNA extraction and q-PCR analysis. A, q-PCR analysis for OSGIN1 transcriptional regulation. B, q-PCR analysis for Nrf2 transcriptional regulation. The graphs represent duplicate samples; error bars indicate SD. *p* values based on two-way ANOVA with Tukey's post-test for multiple-samples comparisons. Experiment was repeated three times.

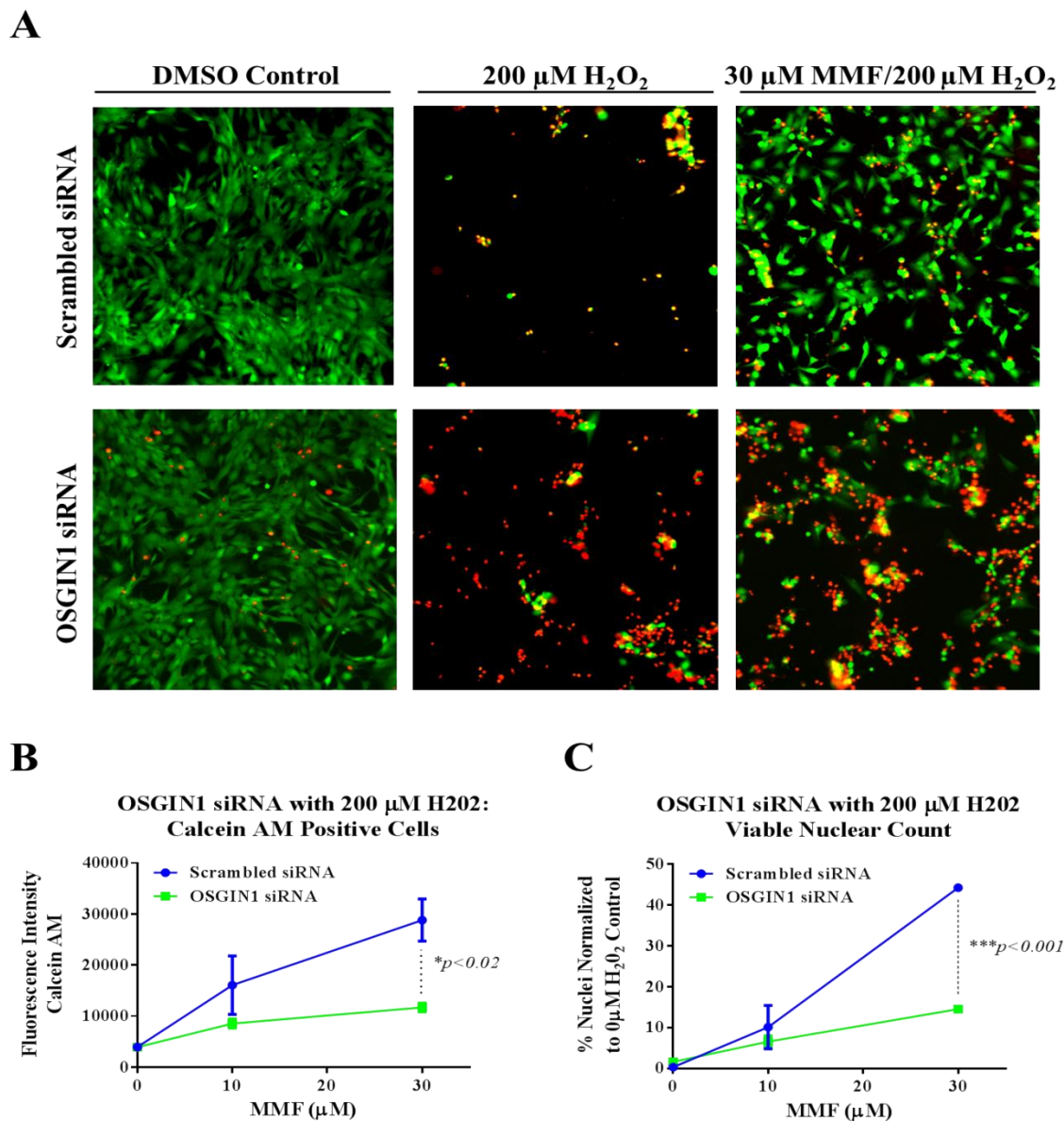


Figure 30. OSGIN1 siRNA knockdown inhibits MMF-mediated cytoprotection.

Human astrocytes were transfected with scrambled (control) or OSGIN1 siRNA and treated with MMF for 24 hours then challenged with H_2O_2 . A, imaging of LIVE/DEAD labeled cells pretreated with MMF and then challenged with H_2O_2 . LIVE calcein AM (green) and DEAD ethidium homodimer (red) labeling. B, quantification of calcein AM fluorescence intensity in LIVE/DEAD labeled cells from A. C, replicate plates as in A fixed and stained with DAPI nuclear dye. Graph represents average cell nuclei counts in 20 fields per well (2 wells averaged in graph). Error bars represent SD and p value based on one-way ANOVA with Tukey's post-test for multiple-samples comparisons. Experiment was repeated three times.

2.4 Identification of OSGIN1 isoform induction in the presence of MMF

2.4.1 Generation of OSGIN1 isoform specific antibodies

As discussed in Chapter I (section 6.1.2), OSGIN1 undergoes alternative splicing to yield various isoforms, three of which have been investigated by researchers (Ong et al., 2004). These include variants encoding for 52 kDa and 61 kDa ORF's, as well as a third isoform encoding a 38 kDa ORF that has been researched but is not accepted as a likely variant. Research investigating the importance of these variants suggests that individual regulation of OSGIN1 isoforms may yield divergent biological functions (Hu et al., 2012). Therefore, following identification of OSGIN1 as a downstream target of Nrf2 that contributes to MMF cytoprotection, investigation into the regulation of OSGIN1 isoforms in the presence of MMF was pursued. To deduce whether OSGIN1 variants are differentially regulated by MMF, three isoform-specific antibodies were generated using affinity purification conducted by New England Peptide (NEP) that recognize the following three human OSGIN1 variants; OSGIN1-38 kDa, OSGIN1-52 kDa and OSGIN1-61 kDa. Based on the splicing characteristics of these isoforms, only the OSGIN1-61 kDa antibody should be unique, with the OSGIN1-52 kDa antibody recognizing both the 52 kDa and 61 kDa forms and the OSGIN1-38 kDa antibody recognizing all three variants (section 1.2.1 of Chapter II; Figure 9).

To determine the specificity of these antibodies, peptide competition studies were conducted. In these studies human astrocyte cell lysates were probed with three different conditions; antibody alone (NP), antibody pre-incubated with antibody specific peptide (P) and antibody pre-incubated with non-specific control peptide (CP) (Figure 31).

Peptides generated against the different isoforms were used as control peptides (example: OSGIN1-52 kDa peptide was a control for OSGIN1-61 kDa antibody optimization). OSGIN1-52 kDa and OSGIN1-61 kDa antibodies detected specific immunoreactive bands that correlated with the appropriate predicted size of their amino acid sequence (Figure 31). Both of these bands were lost when the antibody was pre-incubated with an epitope specific peptide but not with a control peptide. Interestingly, pre-incubation of the OSGIN1-61 kDa antibody with the control peptide (in this case the OSGIN1-52 kDa peptide) resulted in depletion of a lower immunoreactive band (Figure 26B). This could be a result of OSGIN1-52 kDa antibody contamination in the OSGIN1-61 kDa antibody pool, particularly since this band runs at a similar size to the 52 kDa OSGIN1 protein. No immunoreactive bands were identified in the presence of the OSGIN1-38k Da antibody. Since this antibody should pick up all three isoforms, this antibody most likely did not yield successful immunoglobulin.

Following optimization of the OSGIN1-52 kDa and OSGIN1-61 kDa antibodies, siRNA knockdown of OSGIN1 in human astrocytes was conducted to determine if immunoreactive bands associated with these antibodies were depleted in the absence of OSGIN1. Loss of OSGIN1 correlated with depletion of immunoreactive bands identified during optimization, with almost complete loss of the OSGIN1-61 kDa immunoreactive band (Figure 32). Abundance of the OSGIN1-52 kDa immunoreactive band seemed to be higher than that of OSGIN1-61 kDa; however, whether this difference was due to antibody specificity is unclear. However, the modest reduction observed with the

OSGIN1-52 kDa antibody following OSGIN1 knockdown may be indicative of incomplete knockdown and suggest that this isoform is truly more abundant.

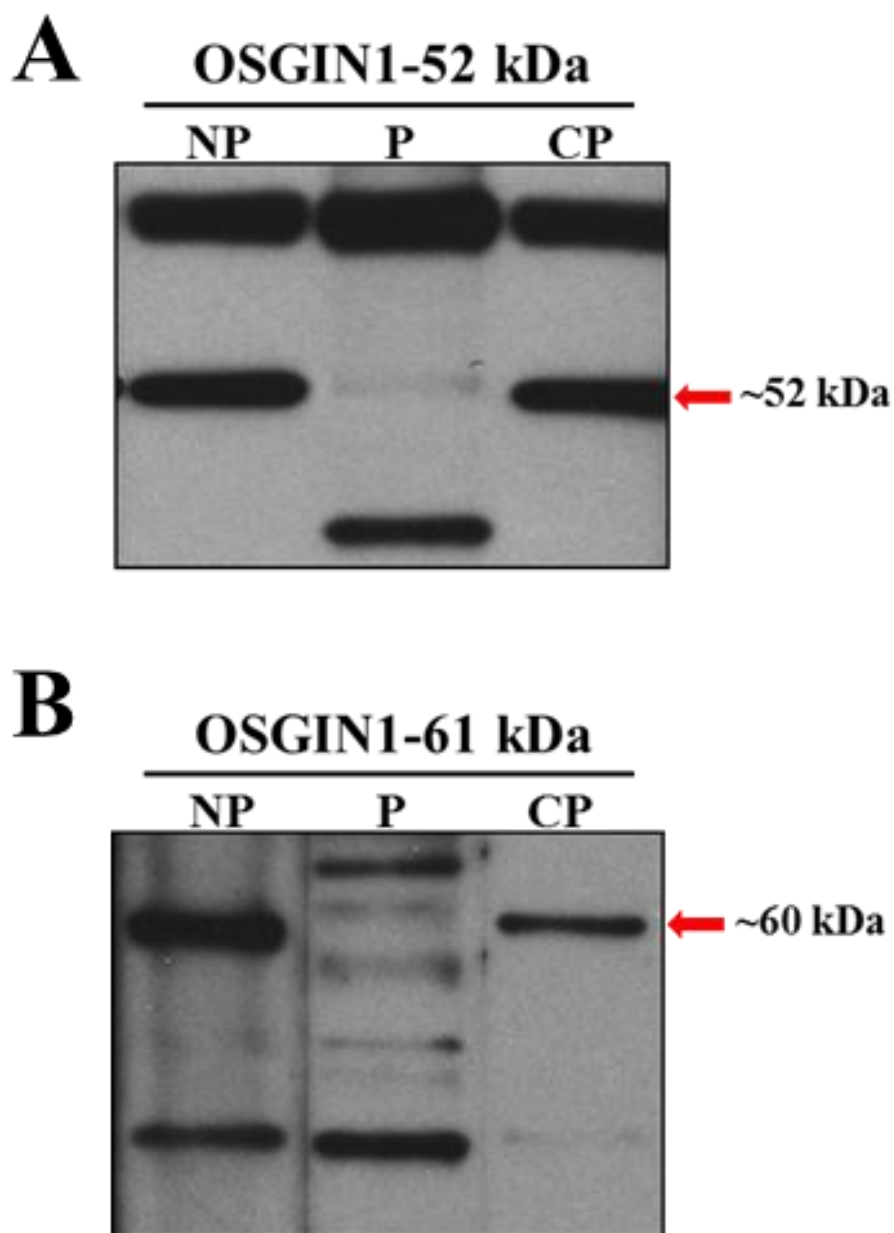


Figure 31. Optimization of OSGIN1-52kDa and OSGIN1-61kDa antibodies.

Human astrocyte cell lysates were probed with three antibody conditions: antibody alone (NP), antibody pre-incubated with epitope specific peptide (P) or non-specific control peptide (CP). A, OSGIN1-52kDa antibody conditions. B, OSGIN1-61kDa antibody conditions. Experiment was repeated twice.

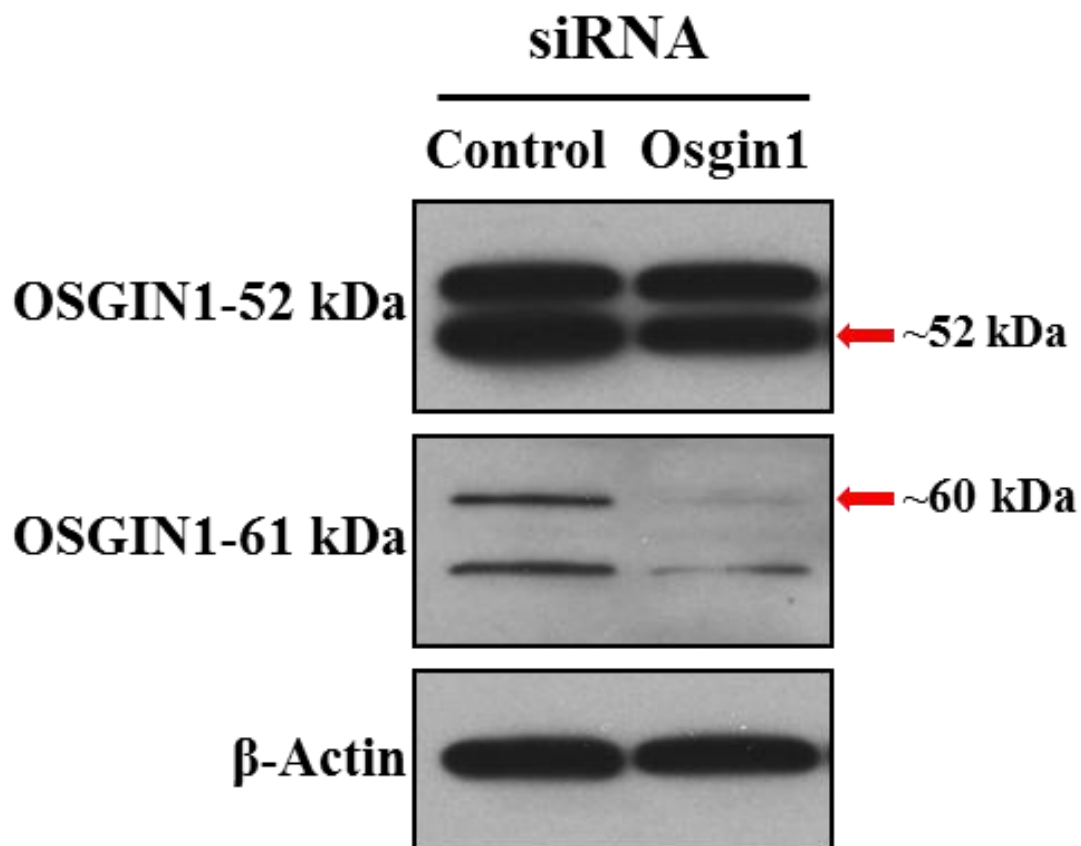


Figure 32. OSGIN1 knockdown depletes OSGIN1 isoform specific immunoreactivity

Human astrocytes were transfected with 10nM of control or OSGIN1 specific siRNA and cell lysates were probed with OSGIN1 isoform-specific antibodies. β -actin is included as a loading control. Experiment was repeated three times.

2.4.2 Evidence for induction of OSGIN1-61 kDa isoform in the presence of MMF

To determine if OSGIN1 isoforms are differentially regulated in the presence of MMF, human astrocytes were transfected with either control or OSGIN1 specific siRNA followed by treatment with MMF for 24 hours. OSGIN1-52 kDa and OSGIN1-61 kDa antibodies were probed against cell lysates via western blot (Figure 33). Although a similar reduction in immunoreactivity was observed with the OSGIN1-52 kDa antibody similar to previous findings, no induction was seen in the presence of MMF (Figure 33A). In contrast, control siRNA transfected astrocytes probed with the OSGIN1-61kDa antibody detected an increase in immunoreactivity in the presence of 30 μ M MMF which was lost in the absence of OSGIN1 (Figure 33B). These findings suggest that addition of MMF to astrocytes specifically induces expression of the 61 kDa encoding OSGIN1 ORF.

Overexpression of the 61 kDa encoding OSGIN1 isoform has been shown to be less toxic to tumorigenic cell lines, suggesting this specific variants may function independently of apoptotic induction and thus may be regulated differentially (Hu et al., 2012). Since OSGIN1 is an Nrf2-regulated target gene and loss of Nrf2 reduces OSGIN1 transcript expression, the regulation of the identified OSGIN1-61 kDa reactive band was examined following Nrf2 depletion. Human astrocytes were transfected with control or Nrf2 specific siRNA and cell lysates were probed with the OSGIN1-61 kDa antibody. Nrf2 knockdown resulted in depletion of OSGIN1-61 kDa immunoreactivity which correlated with OSGIN1 knockdown (Figure 33C), confirming the regulation of this isoform in an Nrf2-dependent manner.

Further examination of both the OSGIN1-52 kDa and OSGIN1-61 kDa generated antibodies was also conducted via immunocytochemistry. Human astrocytes treated with MMF for 24 hours were fixed and probed with either the OSGIN1-52 kDa or OSGIN1-61 kDa antibody. Stained cells were imaged on an automated Thermo HCS Arrayscan technology and immunoreactive puncta were quantified using HCS Studio algorithm software. Total fluorescent spot count indicated a significant increase in immunoreactive puncta probed with the OSGIN1-61 kDa antibody compared to no change seen following identification with OSGIN1-52 kDa immunoreactive puncta (Figure 34). Furthermore, the total fluorescent spot count was observably higher in the 52 kDa group compare to the 61 kDa, providing further evidence that the 61 kDa OSGIN1 isoform is less abundant than the 52 kDa form. However, since the antibodies generated against the OSGIN1-61kDa and OSGIN1-52kDa variants have non-specific immunoreactivity (Figure 31), the absolute spot quantification may not be accurate. Therefore, generation of OSGIN1 variant specific antibodies is necessary to fully understand the contribution of each of these variants to the results identified within this experiment.

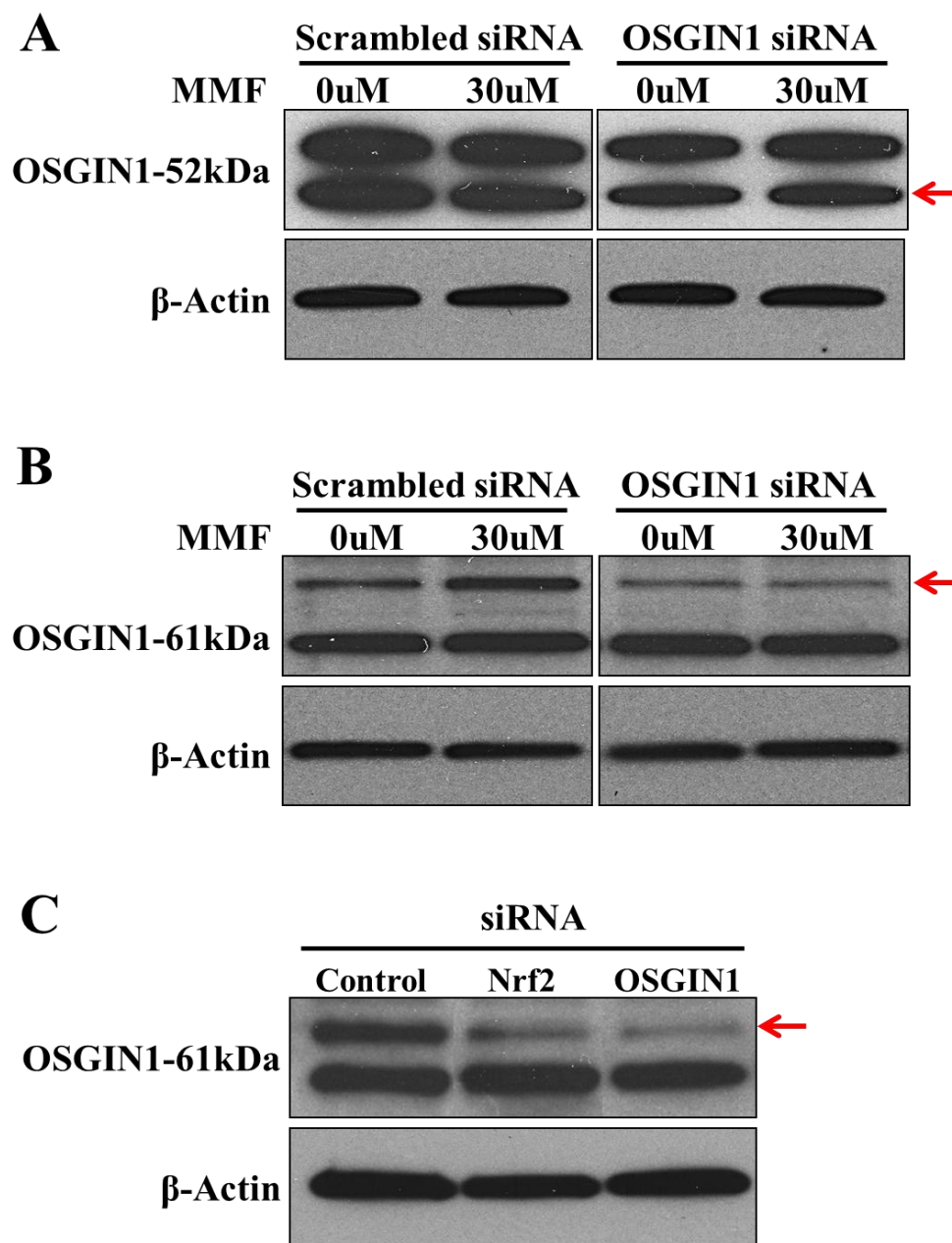


Figure 33. The OSGIN1 61 kDa encoding isoform is regulated via MMF and Nrf2.

Human astrocytes were transfected with either control or OSGIN1 specific siRNA followed by treatment with 30 μ M MMF for 24 hours. A, transfected cell lysates probed with OSGIN1-52 kDa antibody. B, transfected cell lysates probed with OSGIN1-61 kDa antibody. C, human astrocytes transfected with either control or Nrf2 specific siRNA and probed with OSGIN1-61 kDa antibody. β -actin is included in all figures as a loading control. Experiment was repeated three times.

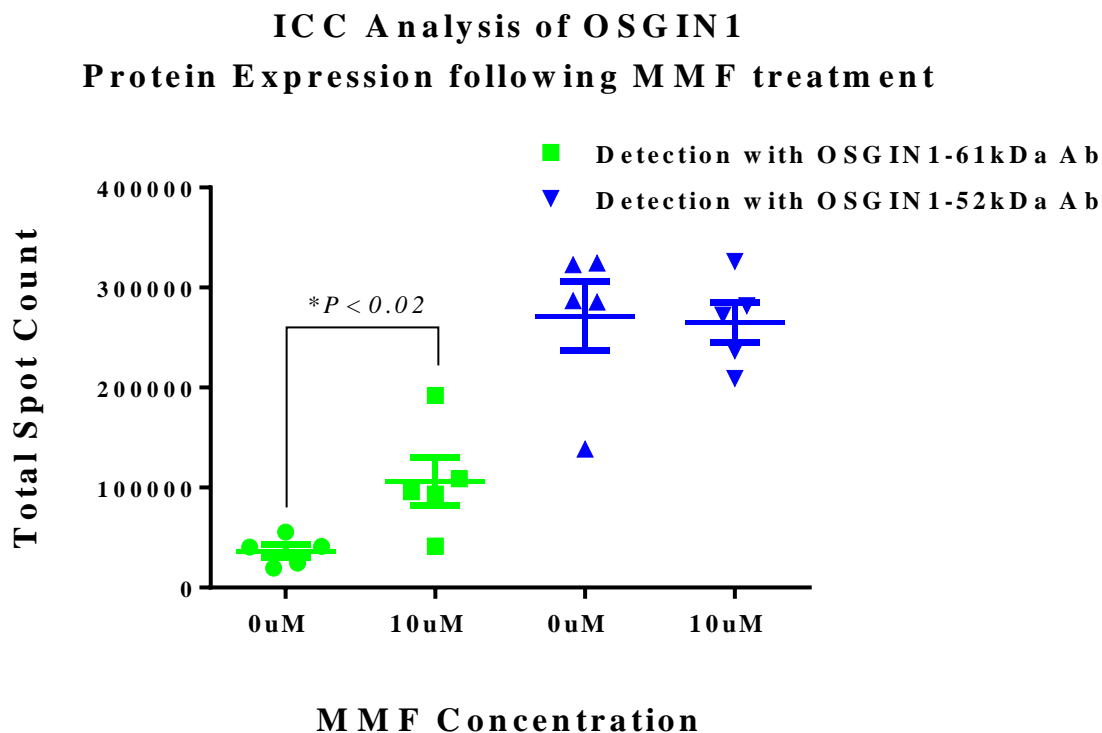


Figure 34. Immunocytochemical analysis of OSGIN1-52 kDa and OSGIN1-61 kDa antibodies.

Human astrocytes were treated with MMF for 24 hours, fixed and then probed with antibodies against OSGIN1-52 kDa and OSGIN1-61 kDa isoforms of OSGIN1. Total fluorescent spot count was accomplished using Thermo HCS Arrayscan technology. *p* values based on one-way ANOVA with Tukey's post-test for multiple sample comparisons.

2.4.3 Alteration in the 5'UTR of OSGIN1 transcripts identified by RACE

Although MMF regulation of the OSGIN1-61kDa isoform was identified via protein analysis, confirmation of this specific transcript was unable to be confirmed via q-PCR based on the location of the primer/probe set within the overlapping region of the OSGIN1 isoforms. Therefore, Northern Blot analysis was attempted to isolate the transcript associated with the identified protein product. As outlined in section 2.7 of Chapter II, RNA probes were generated against the probe sequence used for OSGIN1 q-PCR and probed against human astrocyte purified RNA treated with MMF. Various attempts were made to accurately identify OSGIN1 RNA transcripts; however, these studies were inconclusive. In order to overcome the challenges faced with Northern Blot analysis, rapid amplification of cDNA ends (RACE) was attempted. 3' RACE was performed using RNA extracted from human astrocytes treated with a titration of MMF and probes designed based on the primer/probe sequences used for OSGIN1 q-PCR (see section 1.4.3 in Chapter II). 3' RACE resulted in a 1.3kb sequence that was confirmed to match the 3' end of OSGIN1 following DNA sequencing (Figure 35A). The identified 3' RACE product correlated with an increase in total 3' sequence abundance in the presence of MMF, confirming upregulation of this sequence following MMF treatment (Figure 35A).

Following confirmation of the 3' RACE product by sequencing, primers were generated within the identified 3' sequenced region for 5'RACE analysis (see section 1.4.3 in Chapter II). Similar to 3' RACE, RNA extracted from MMF-treated astrocytes treated was used as a template. 5' RACE analysis identified a 0.6 kb sequence that was

found to match the 5' end of the OSGIN1-52kDa encoding region following DNA sequencing (Figure 30B). Interestingly, the identified 5'RACE product was depleted in a dose-dependent manner in the presence of MMF, suggesting that the 5' end of OSGIN1 in the presence of MMF is differentially regulated. This could potentially be a result of GC enrichment in the 5' region of the longer 61kDa encoding sequence and thus an inability to prime past this region. Furthermore, based on previous results suggesting that the 52kDa is more highly expressed than the 61kDa form, this could simply be a result of low abundance.

Further DNA sequencing analysis of the 0.6 kb 5' RACE product identified two identical transcripts that differed only in two nucleotide substitutions within the 5' region of OSGIN1 (Figure 35B). Alterations in the 5'UTR of OSGIN1 have been previously identified to regulate the protein expression of OSGIN1 (Ong 2007); therefore to determine if MMF differentially regulated these two transcripts, Taqman primer/probe sets specific for each transcript were generated (see section 1.4.2 of Chapter II) and analyzed against human astrocytes treated with and without MMF. q-PCR analysis detected a significant MMF-dependent alteration in expression of these two transcripts suggesting that they are not simply allele variants (Figure 36). Furthermore, MMF induced expression of the "ALT" transcript variant which substitutes a C for an G at position 59 and a G to an A at position 62 of the OSGIN1 sequence (NM_182981.2), which results in a potential ATG start site and a premature stop site (Figure 35B). These findings suggest that alterations in the 5' region of OSGIN1 may be regulated in the presence of MMF, but further investigation of these alterations is necessary.

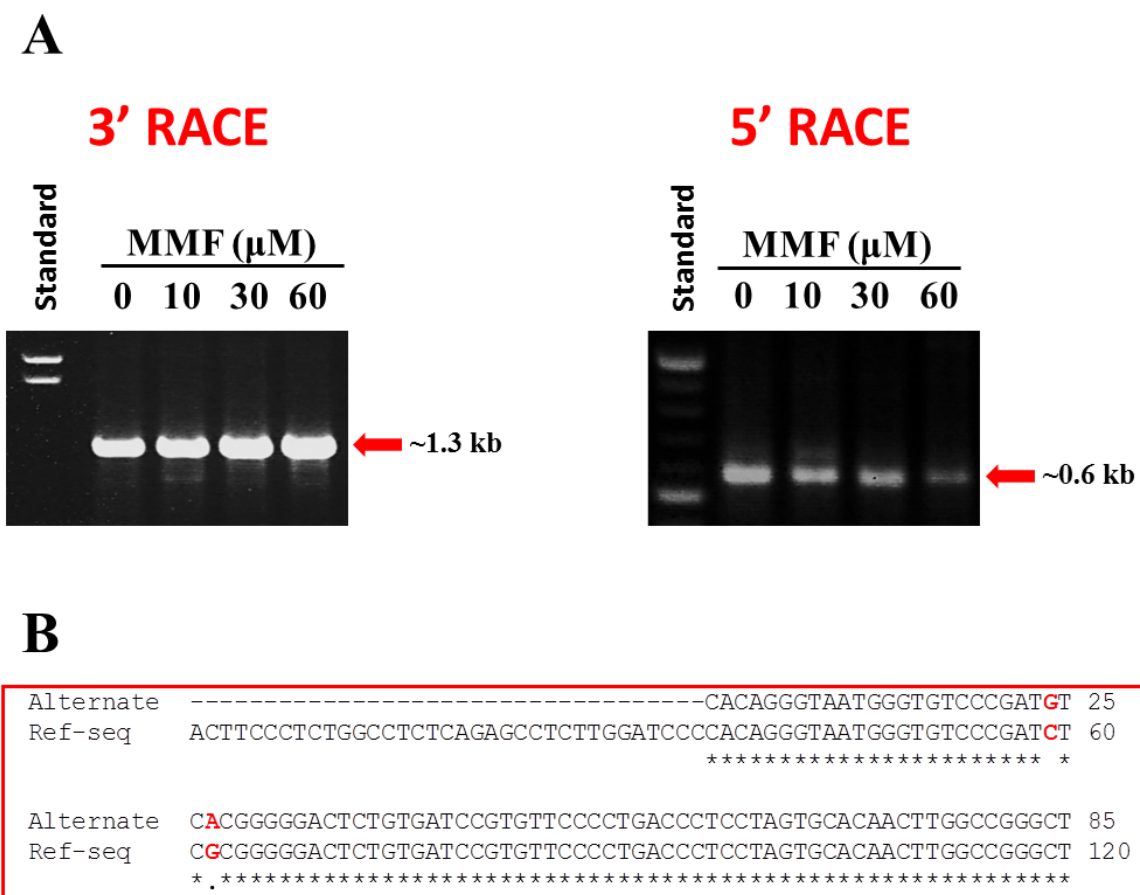


Figure 35. 3' and 5' RACE of OSGIN1 transcript.

RNA extracted from human astrocytes treated with a titration of MMF was subjected to 3' and 5' RACE. A, resulting RACE products analyzed via gel electrophoresis. B, sequencing of 5' RACE products identified two transcript variants of OSGIN1 within the 5' UTR of the OSGIN1-52kDa transcript that differed in two nucleotide substitutions (indicated in red). WT=canonical sequence; ALT=identified 5' RACE sequence with nucleotide substitutions. Dash lined indicates where RACE was terminated.

q-PCR of OSGIN1 5'UTR Transcript Variants in MMF-treated Human Astrocytes

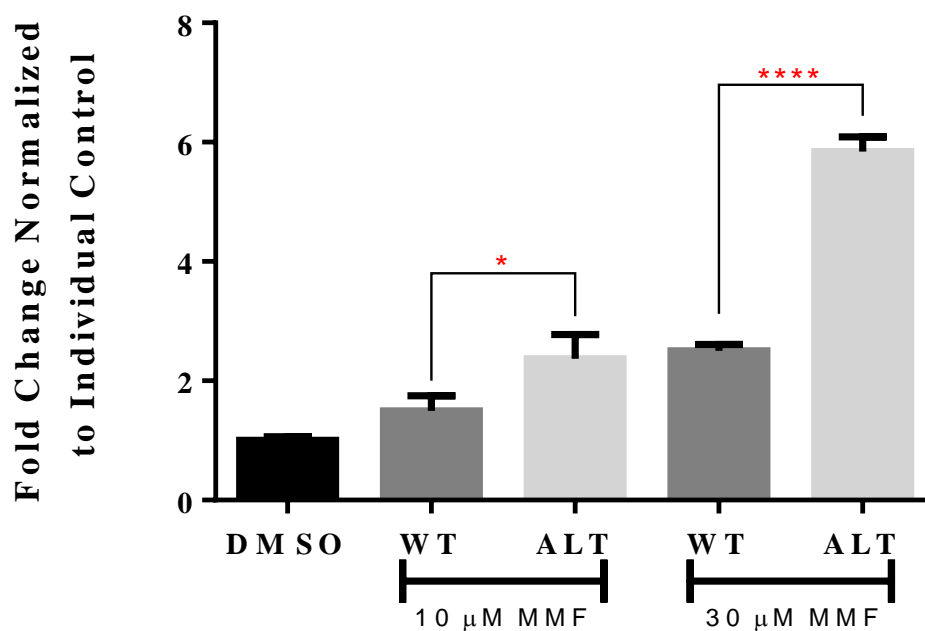


Figure 36. q-PCR analysis of identified 5'RACE transcripts.

RNA was extracted from human astrocytes treated with DMSO or MMF for 24 hours and subjected to q-PCR using primer/probe sets specific to identified 5'RACE transcripts. WT=canonical sequence; ALT=identified 5' RACE sequence with nucleotide substitutions. *, $p < 0.05$ and ****, $p < 0.0001$ based on one-way ANOVA with Tukey's post-test for multiple comparisons. Significance was also identified in the WT (30uM MMF) versus DMSO control ($p < 0.001$).

2.5 p53 is downstream of OSGIN1 and contributes to OSGIN1-mediated cytoprotection

Current literature investigating the role of OSGIN1 describes this gene as a mediator of cell cycle and apoptosis that is believed to be regulated via p53 (Hu et al., 2012; Yao et al., 2008). p53 has been shown to bind to the promoter of OSGIN1 to regulate its transcription as well as interact with OSGIN1 in the cytoplasmic space to induce apoptosis (Hu et al., 2012). To determine if OSGIN1 is transcriptionally regulated by p53, human astrocytes were transfected with siRNA targeted against p53 or OSGIN1 and transcript regulation analyzed. p53 knockdown resulted in an approximate 80% loss of p53 transcript expression (Figure 37A); however, this reduction in p53 did not affect basal transcriptional levels of OSGIN1 (Figure 37C). Furthermore, siRNA knockdown of OSGIN1 had no effect on p53 transcription (Figure 37A). These findings suggest that p53 is not a transcriptional regulator of OSGIN1 in this cell type.

Following 24 hour treatment with MMF, p53 transcript levels were slightly, yet significantly increased in human astrocytes transfected with scrambled (control) as well as Nrf2 siRNA (Figure 37A). This is of particular interest since p53 has been identified within the literature to contribute to Nrf2-mediated transcriptional control and co-regulate the expression of proteins involved in protection against oxidative stress (Toledano et al., 2009); therefore, the effect of p53 knockdown on Nrf2 transcription was also analyzed in human astrocytes. Loss of p53 was found to have no effect on transcriptional regulation of Nrf2 in astrocytes (Figure 37B); however, since Nrf2 regulation is mediated at the protein level and p53 is also believed to be regulated in a similar manner as Nrf2, protein

induction of p53 was investigated (Wakabayashi et al., 2010). In the presence of MMF, control transfected astrocytes exhibited a visible induction of p53 protein that was abolished in p53 knockdown and diminished in astrocytes transfected with OSGIN1 and Nrf2 siRNA (Figure 38A and C). Furthermore, knockdown of p53 did not alter the MMF-mediated accumulation of Nrf2. These findings strongly suggest that p53 is induced downstream of Nrf2 and OSGIN1 in the presence of MMF. Since OSGIN1 has already been identified to be downstream of Nrf2 (Figure 27), regulation of p53 is most likely regulated via an OSGIN1-induced pathway at a protein level.

As mentioned above, p53 protein levels are tightly regulated within cells similar to Nrf2. In resting conditions, p53 protein is maintained at low levels by proteasomal degradation and activation of p53 expression can reduce ROS levels by inducing the expression of anti-oxidative stress proteins (Vurusaner et al., 2012; Levine et al., 2006). Since MMF is known to induce Nrf2 accumulation and translocation into the nucleus, the effect of MMF on p53 nuclear translocation was investigated. Human astrocytes were treated with a titration of MMF for 24 hours followed by fixation and detection with p53 antibody. Plates were imaged using the Thermo HCS Arrayscan and quantification of p53 localization in the nucleus and cytoplasm was accomplished by algorithm creation using HCS Studio software. Addition of MMF to human astrocytes resulted in a significant translocation of p53 protein from the nucleus which correlated with reduced p53 protein levels in the cytoplasm (Figure 39). These results were also confirmed using a p53 nuclear TransAM ELISA which measures cytoplasmic and nuclear cellular fractions in an ELISA with p53 specific DNA sequence bound to the ELISA plate (Figure 40).

Following identification of p53 nuclear translocation with MMF treatment, the importance of p53 in MMF-mediated cytoprotection was evaluated. Human astrocytes were transfected with p53-specific or control siRNA and treated with MMF for 24 hours followed by oxidative challenge with H₂O₂. MMF regulated protection was reduced in this model in the absence of p53 to a similar extent as observed in OSGIN1 knockdown cultures (Figure 41 and Figure 30). These results suggest that the nuclear translocation of p53 may contribute to the cytoprotective properties of MMF.

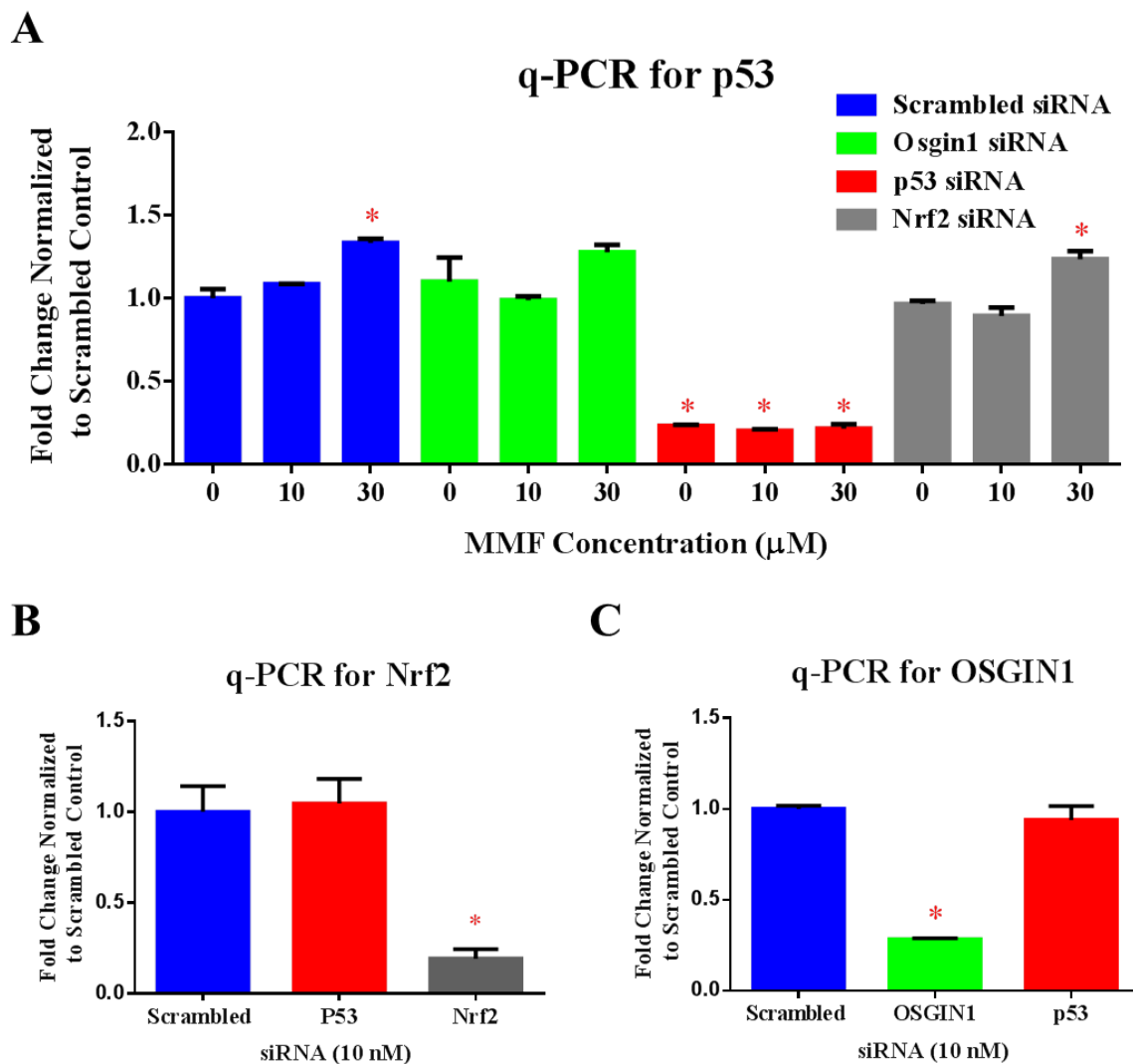


Figure 37. q-PCR of p53 siRNA knockdown.

Human astrocytes transfected with either control (scrambled) or p53 siRNA followed by treatment with DMSO or MMF for 24 hours. A, q-PCR analysis of p53 mRNA levels. *, $p < 0.01$ based on two-way ANOVA with Tukey's post-test for multiple comparisons. B, human astrocytes transfected with either control (scrambled), p53 or Nrf2 siRNA and analyzed for Nrf2 mRNA levels. C, same as B but q-PCR directed against OSGIN1 transcript levels. B/C, *, $p < 0.01$ based on one-way ANOVA with Dunnett's post-test for multiple comparisons. Experiment was repeated three times.

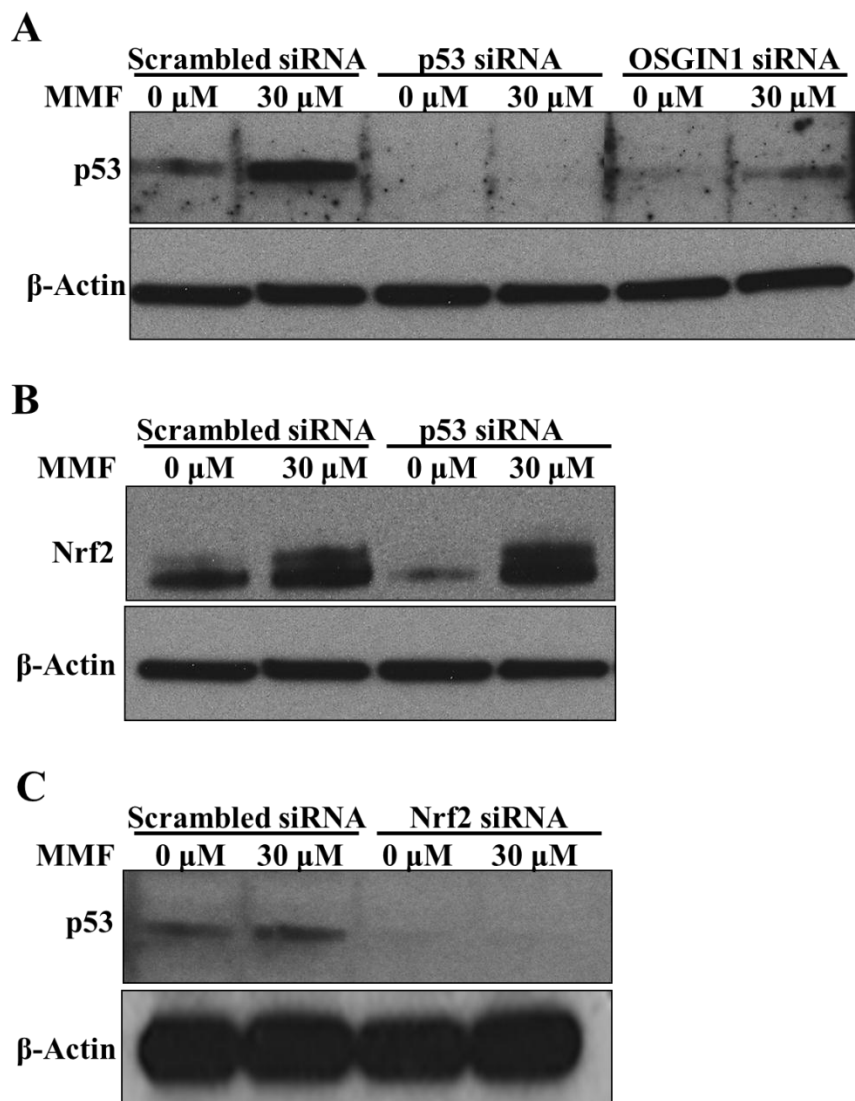


Figure 38. p53 protein is regulated by MMF in an Nrf2 and OSGIN1 dependent manner.

Human astrocytes were transfected with 10 nM control (scrambled), p53, OSGIN1 or Nrf2 siRNA followed by treatment with DMSO or MMF for 24 hours. A, p53 protein measure in scrambled (control), p53 and OSGIN1 siRNA knockdown samples treated with MMF. B, Nrf2 protein measure in scrambled (control) and p53 siRNA knockdown samples treated with MMF. C, Scrambled (control) and Nrf2 siRNA knockdown samples treated with MMF and probed for p53 protein. β -actin is included in all figures as a loading control. Experiment was repeated twice.

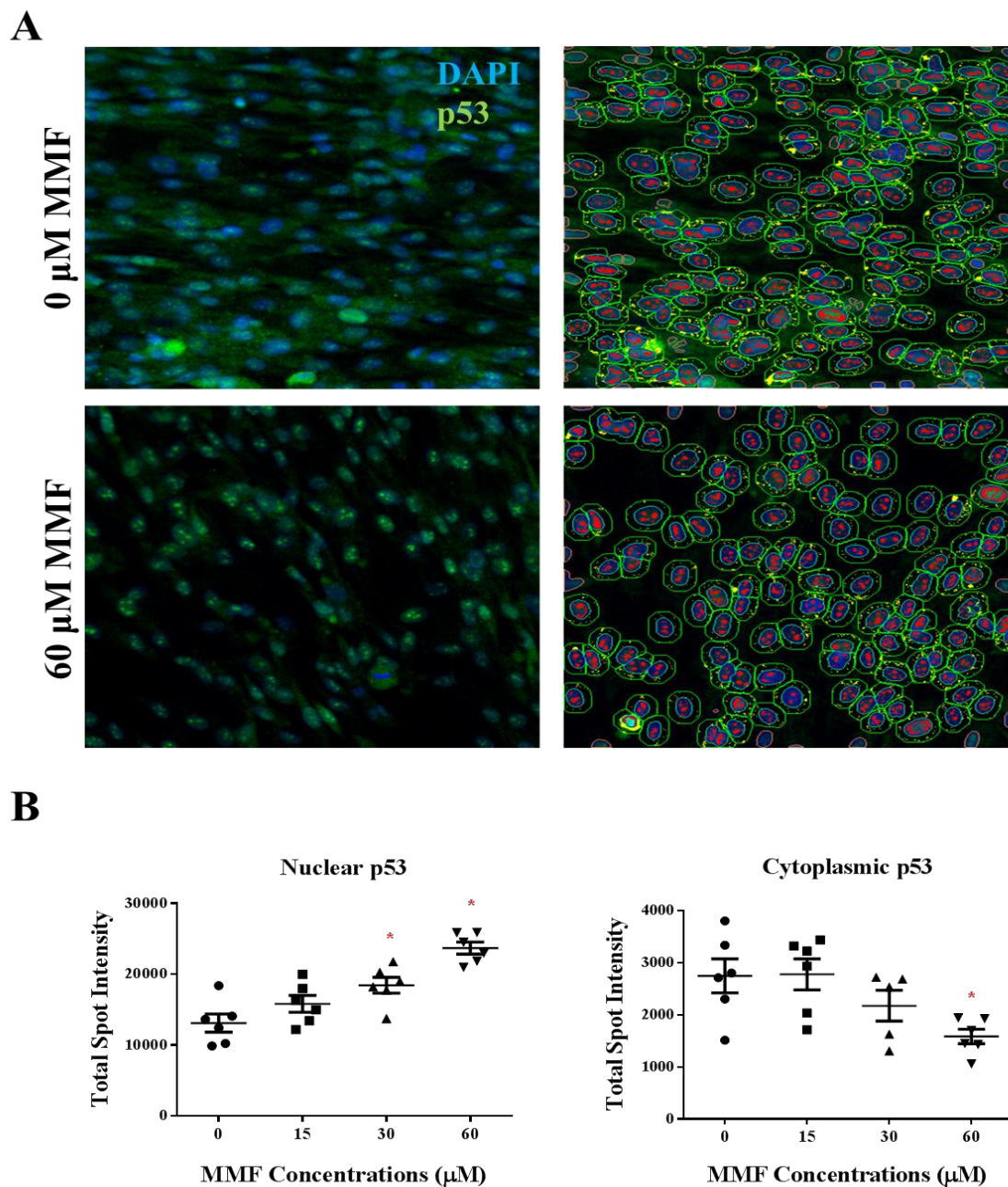


Figure 39. MMF induces nuclear translocation of p53.

Human astrocytes were treated with a titration of MMF for 24 hours followed by fixation and immunocytochemistry (ICC) analysis of p53. A, ICC images acquired using the Thermo HCS Arrayscan and algorithm analysis overlaid. B, Quantification of images in A. Each point represents 20 images from one well; n=6 wells per condition. Statistical analysis was performed using one-way ANOVA with Dunett's multiple comparison post-test (*, $p < 0.05$). Experiment was repeated twice.

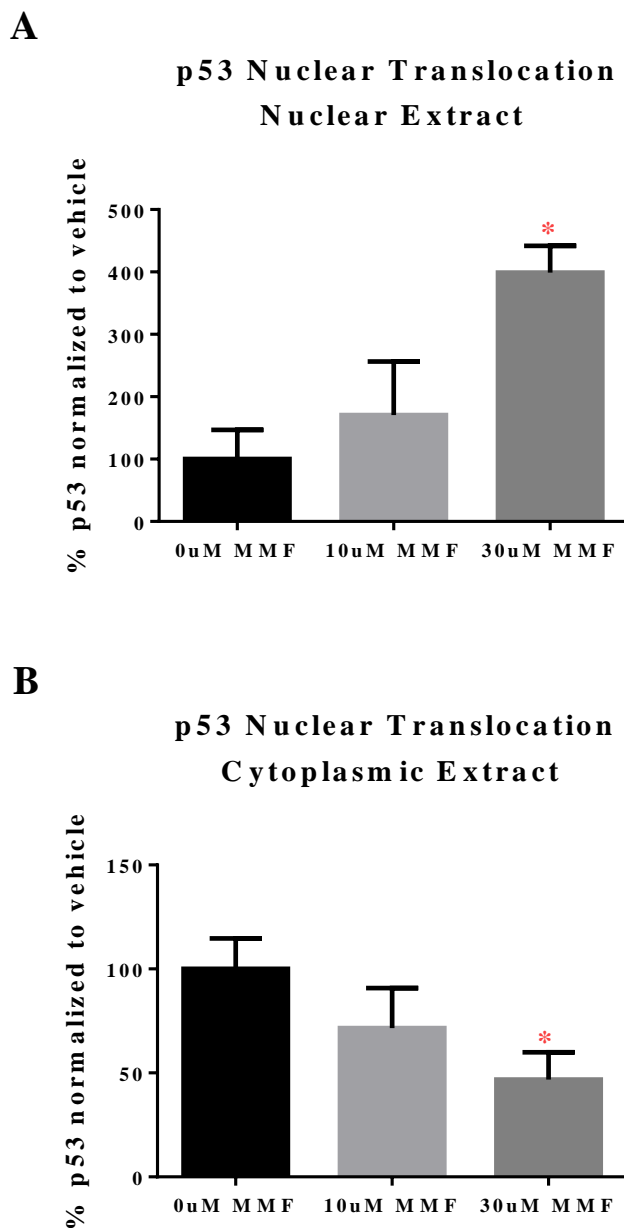


Figure 40. MMF induces nuclear translocation of p53.

Human astrocytes were treated with a titration of MMF for 24 hours followed by analysis of nuclear and cytoplasmic cell extracts for p53 expression. A, nuclear extract quantification. B, cytoplasmic extract quantification. Statistical analysis was performed using one-way ANOVA with Dunnett's multiple comparison post-test (*, $p < 0.05$). Experiment was repeated twice.

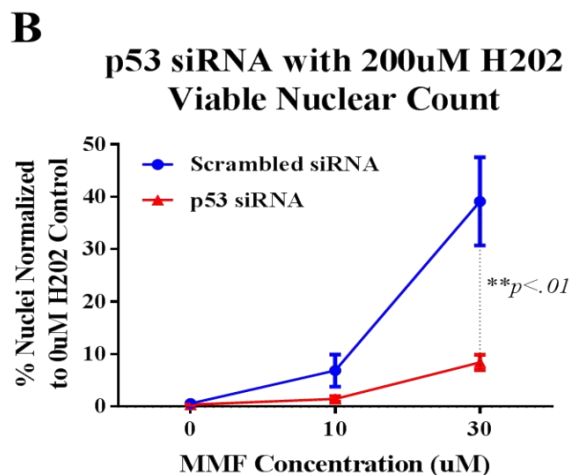
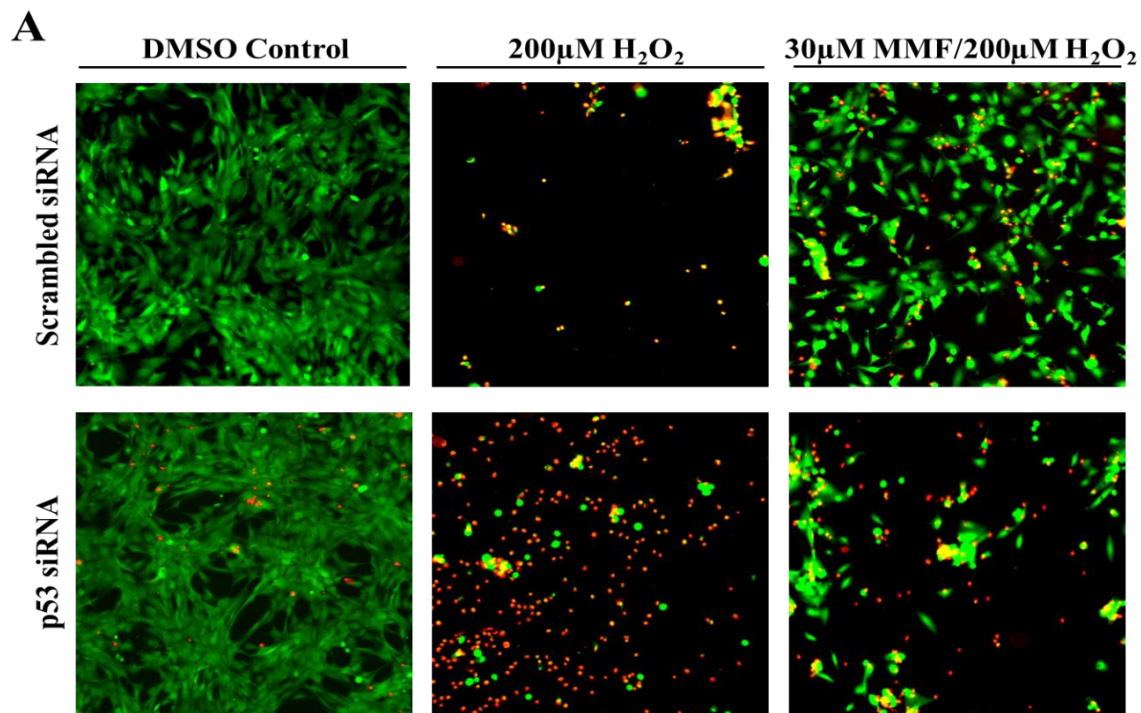


Figure 41. p53 contributes to MMF-mediated cytoprotection.

Human astrocytes were transfected with scrambled (control) or p53 siRNA and treated with MMF for 24 hours then challenged with H₂O₂. A, imaging of LIVE/DEAD labeled cells pretreated with MMF and then challenged with H₂O₂. LIVE calcein AM (green) and DEAD ethidium homodimer (red) labeling. B, quantification of calcein AM fluorescence intensity in LIVE/DEAD labeled cells from A. Error bars represent SD and p value based on one-way ANOVA with Tukey's post-test for multiple-samples comparisons. Experiment was repeated three times.

2.6 MMF time course of OSGIN1, p53, Nrf2 and NQO1.

Sections 2.1 through 2.5 of this chapter have identified OSGIN1, p53 and Nrf2 to contribute to the cytoprotective properties of MMF. In order to confirm the transcript and protein regulation patterns of these genes following MMF treatment, time course analysis was conducted. Human astrocytes were treated with MMF for 3, 6, 9, 12, 24 or 36 hours followed by RNA and protein collection. Transcript expression of OSGIN1 and the classical Nrf2 target, NQO1, were analyzed. Following addition of MMF, OSGIN1 was found to be induced early, peaking at 6 hours and remaining elevated at 36 hours post treatment (Figure 42A). This early, sharp response parallels *in vivo* studies measuring the OSGIN1 time course in mouse brain (Figure 13). In comparison, NQO1 transcript levels elevated in a more gradual manner, peaking at around 24 hours and remaining elevated in a more consistent pattern (Figure 42B). Peak induction of OSGIN1 was almost four fold higher compared to NQO1 induction following MMF treatment.

Since Nrf2 and p53 have only be shown to be predominantly regulated at the protein level, they were measured for protein expression along with NQO1 and OSGIN1 following MMF treatment (Figure 43). Nrf2 accumulated first following MMF addition to human astrocytes beginning at the three hour post-dose and returning to near baseline levels by 36 hours. Interestingly, even though OSGIN1 transcript levels increased first, NQO1 protein levels increased before OSGIN1 with OSGIN1 protein accumulation not occurring to almost 24 hours. This suggests that alterations of OSGIN1 may occur at either the transcript or protein level to eventually lead to protein accumulation after 24 hours. As suggested in section 2.6, p53 protein levels accumulated last between around

36 hours, confirming that p53 protein regulation occurs as a downstream target of Nrf2 and OSGIN1. Together these findings suggest that Nrf2 is activated first in the presence of MMF following by OSGIN1 accumulation and eventually p53 in the nucleus.

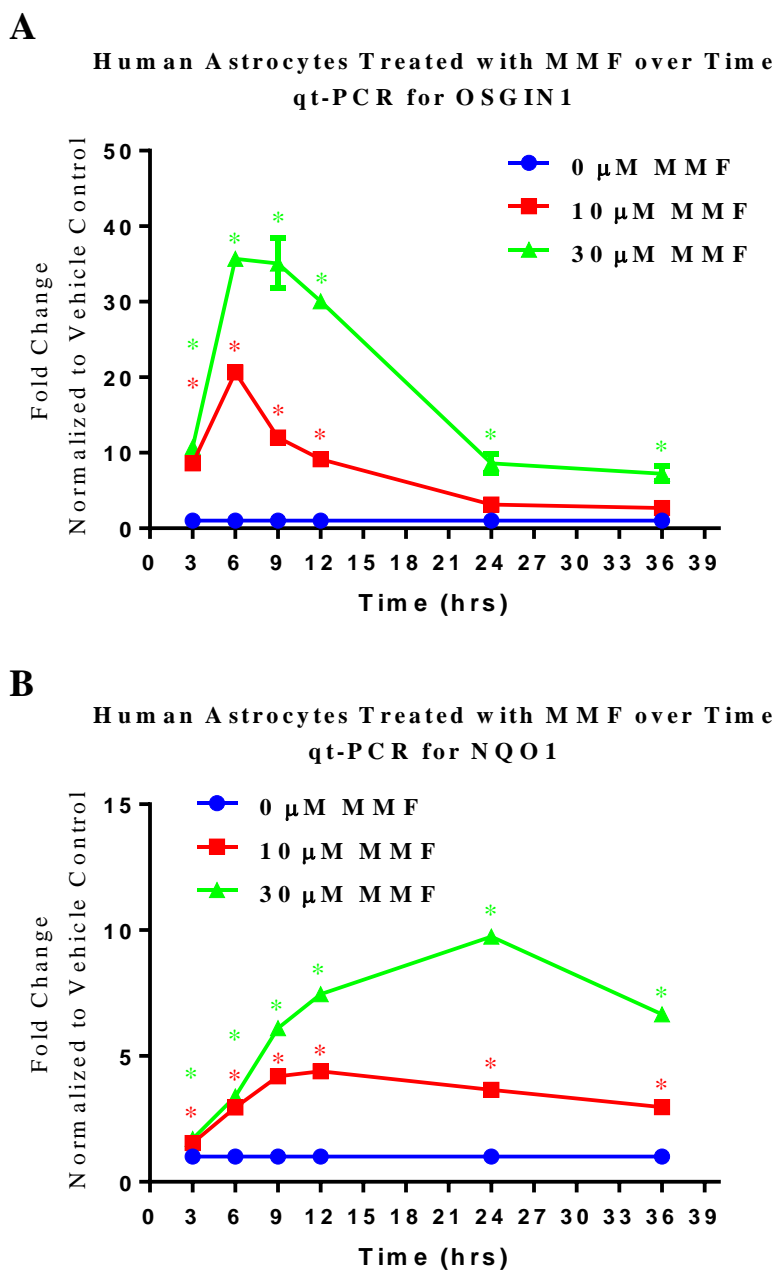


Figure 42. q-PCR time course of NQO1 and OSGIN1.

Human astrocytes were treated with 0, 10 or 30 μM of MMF and analyzed for transcript regulation of OSGIN1 and NQO1 over various time points. A, OSGIN1 time course. B, NQO1 time course. *, $p < 0.001$ based on two-way ANOVA with Tukey's post-test for multiple comparisons using vehicle controls at each time point for comparison.

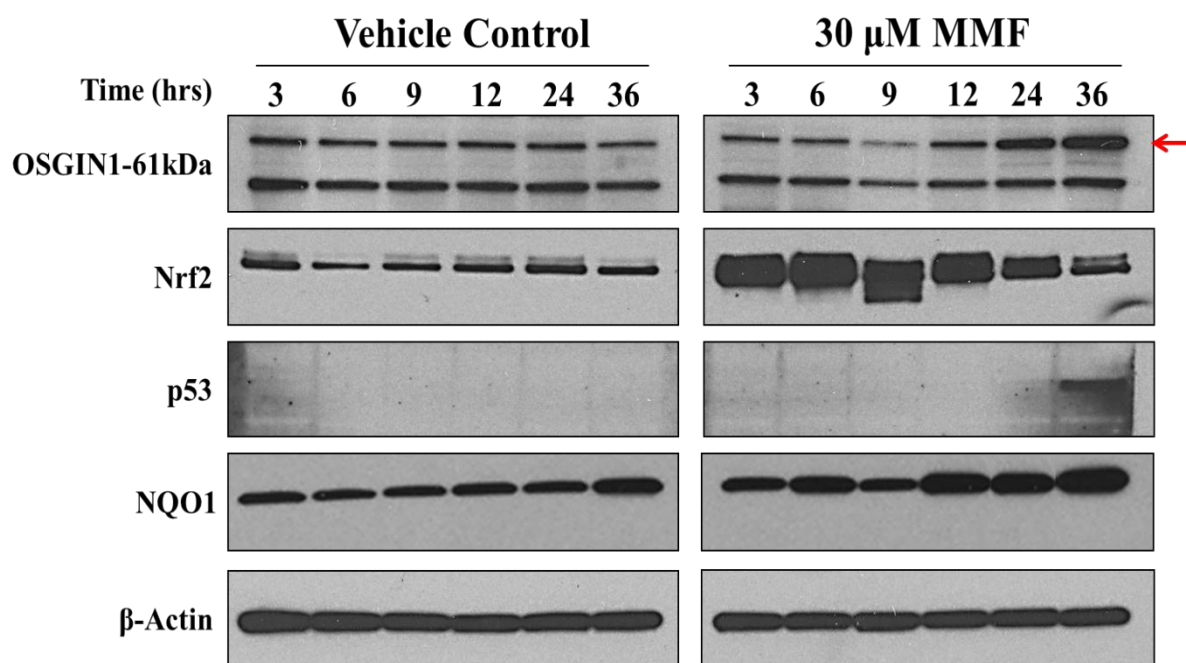


Figure 43. Protein time course of MMF-regulated proteins.

Human astrocytes were treated with 0, 10 or 30 μM of MMF and analyzed for protein regulation of OSGIN1, Nrf2, p53 and NQO1 over various time points. β-actin is included as a loading control. Red arrow indicates OSGIN1-61kDa immune-reactive band confirmed *via* peptide competition.

2.7 MMF inhibits cell proliferation: preliminary studies.

Although OSGIN1 has been shown in the latter studies to contribute to MMF-induced cytoprotection in an Nrf2-dependent and potentially p53-dependent manner, the exact mechanisms associated with the protective characteristics of OSGIN1 are unclear. This section will discuss preliminary data suggesting that OSGIN1 may inhibit cell proliferation following MMF treatment which may contribute to the cytoprotective properties of OSGIN1.

2.7.1 MMF reduces cell proliferation independent of apoptosis

Regulation of cell cycle is considered to be major a cellular pathway controlled by OSGIN1 expression (Liu et al., 2014; Huynh et al., 2001; Ong et al., 2004); however, whether OSGIN1 contributes to cell cycle regulation in astrocytes is unknown. To investigate a role for OSGIN1 in cell cycle regulation, human astrocytes were transfected with scrambled (control) or OSGIN1 siRNA followed by 24 hour treatment with MMF. Astrocytes were pulse labeled with 5-ethynyl-2'-deoxy-uridine (EdU) to label dividing cells and analyzed using the Thermo HCS Arrayscan imaging and algorithm creation technology. Treatment with MMF in control transfected cells resulted in a significant, dose-dependent reduction in total proliferating cells (Figure 44). In the absence of OSGIN1, this effect on proliferation in the presence of MMF was significantly reduced (Figure 44). To confirm that reductions in proliferation in the presence of MMF were independent of apoptosis, transfected astrocytes treated with MMF were analyzed for apoptosis using the TiterTACSTM apoptotic assay. Knockdown of OSGIN1 or p53 did not significantly increase apoptosis compared to control knockdown (Figure 45). These

findings suggest that OSGIN1 may regulate cell proliferation. Interestingly, loss of p53 slightly yet significantly induced apoptosis in the presence of MMF. Since p53 plays a role in various cellular pathways, loss of p53 could place transfected cells in a high state of stress, making them sensitive to compound addition. Whether this is a direct effect of loss of MMF function warrants further investigation.

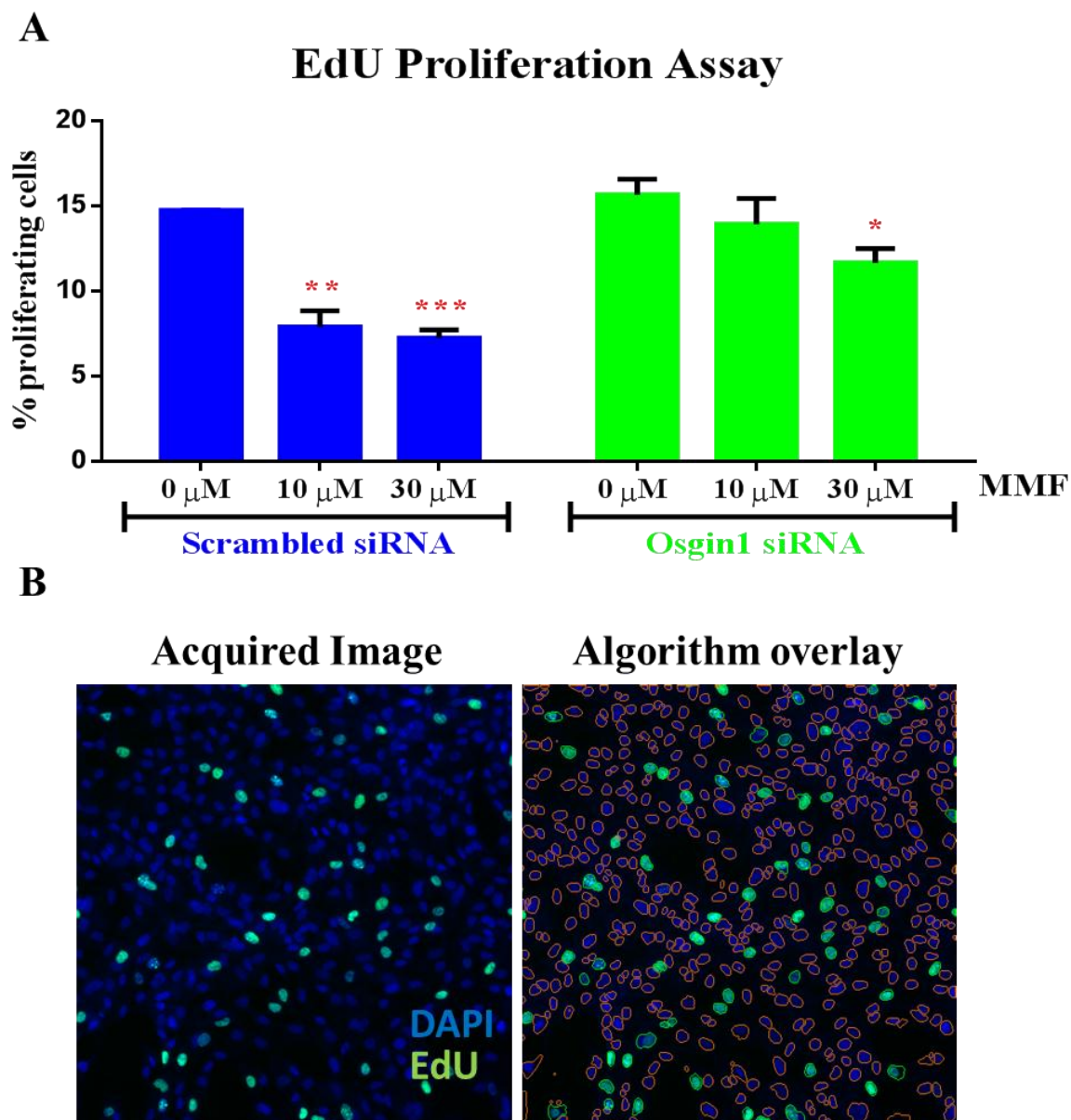


Figure 44. MMF inhibits cell proliferation.

Human astrocytes were transfected with scrambled (control) or OSGIN1 siRNA followed by treatment with 0, 10 or 30 μM MMF and pulse incorporation of EdU. Cells were fixed and EdU incorporated cells were imaged and quantified using a Thermo HCS Arrayscan and HCS Studio software. A, quantification of four wells are averaged in graphs (25 fields/well). *, $p < 0.05$; **, $p < 0.01$; ***, $p < 0.001$ based on two-way ANOVA with Tukey's post-test for multiple comparisons. Experiment was repeated twice.

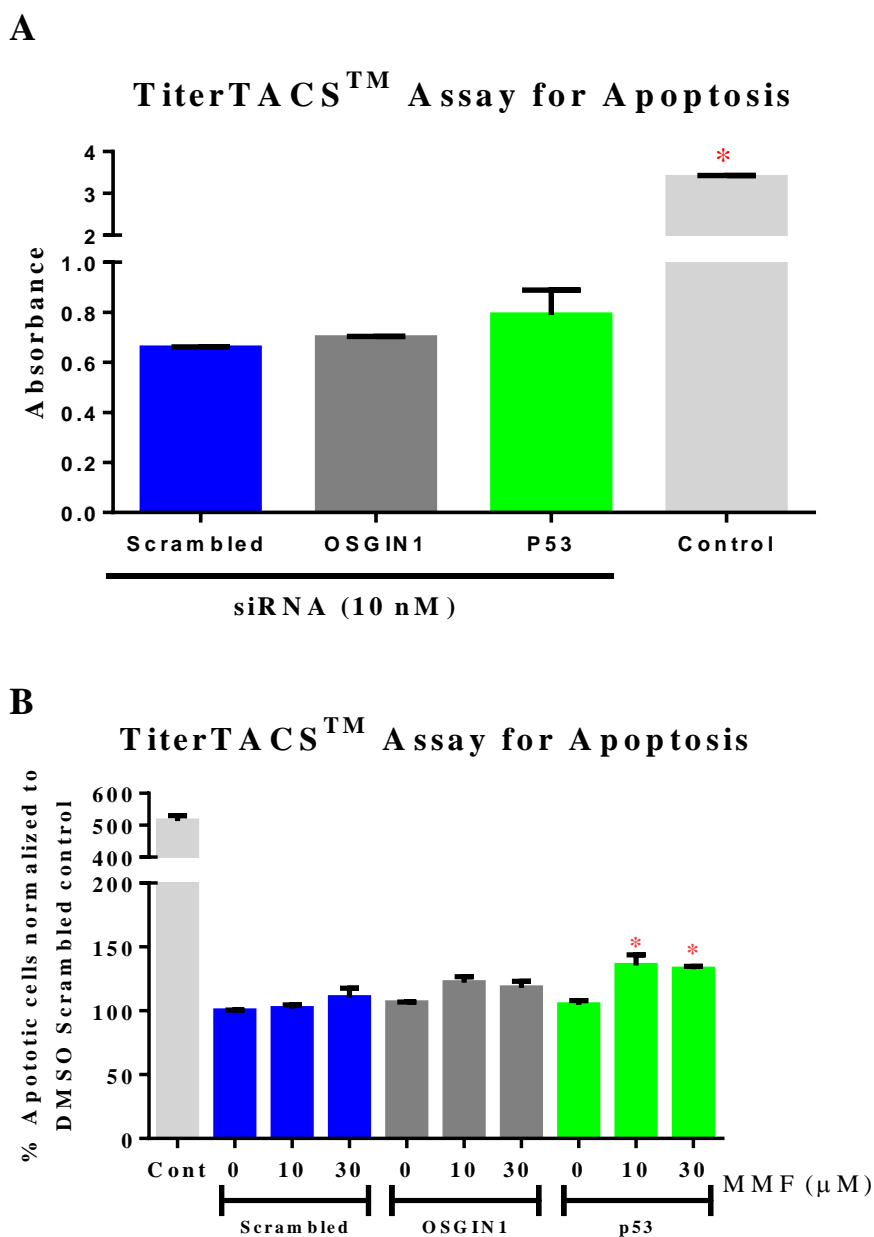


Figure 45. Loss of OSGIN1 does not significantly induce apoptosis.

Human astrocytes transfected with 10 nM scrambled (control), OSGIN1 or p53 siRNA for 48 hours followed by analysis of apoptotic cells using the TiterTACS™ assay. A, siRNA transfection alone. B, siRNA transfection in the presence of MMF treatment for 24 hours. *, $p < 0.01$ based on one-way ANOVA with Dunnett's post-test for multiple comparisons.

2.7.2 *A potential role for PADI4*

As previously mentioned, p53 is cited in the literature to regulate OSGIN1 expression; however, the results discussed in this chapter suggest that OSGIN1 may instead regulate p53 nuclear translocation (Hu et al., 2012). Another protein cited to regulate OSGIN1 expression is peptidyl arginine deiminase type IV (PADI4), which has been shown to negatively regulate OSGIN1 expression (Yao et al., 2008). Furthermore, PADI4 has been shown to regulate gene transcription by regulating the deimination of arginines on histones and antagonizing arginine methylation and may contribute to cell cycle control (Tanikawa et al., 2009; Chang et al., 2011). To determine if PADI4 is transcriptionally regulated following MMF treatment, PADI4 was measured in the previous time course analysis described in section 2.6 of this chapter. PADI4 was demonstrated to be regulated transcriptionally following MMF treatment in a similar manner as NQO1 (Figure 42B), with peak expression occurring at 24 hours and a more gradual induction of expression compared to OSGIN1 (Figure 42A). Since these findings demonstrated PADI4 to be regulated after OSGIN1 induction, PADI4 transcript levels were measured in PADI4, p53 and Nrf2 siRNA knockdown in human astrocytes to determine where PADI4 is targeted. q-PCR analysis of PADI4 levels following siRNA transfection with PADI4, OSGIN1 and p53 resulted in significant reductions in PADI4 expression compared to control samples (Figure 47A). In contrast, Nrf2 knockdown had no effect on PADI4 transcript expression. Furthermore, MMF induction of PADI4 was abolished in the absence of OSGIN1 (Figure 47B). These findings suggest PADI4 is

regulated downstream of p53 since p53 has previously been identified to be regulated downstream of Nrf2 and OSGIN1.

As mentioned above PADI4 has been described in the literature to negatively regulate transcription of OSGIN1 (Yao et al., 2008); however, in the absence of PADI4, no differences in OSGIN1 transcriptional expression were observed (Figure 48A). Furthermore, p53 transcript levels were also not altered in the absence of PADI4 (Figure 48B). Overall, the studies outlined in this section suggest that PADI4 is regulated independently of Nrf2 induction but is also a downstream target of OSGIN1 and p53. Based on the known functions of PADI4 as a mediator of cell proliferation, PADI4 may function to inhibit cell division in the presence of MMF in p53 dependent manner; however, further research is necessary to fully understand the role of PADI4.

**Human Astrocytes Treated with MMF over Time
qt-PCR for PADI4**

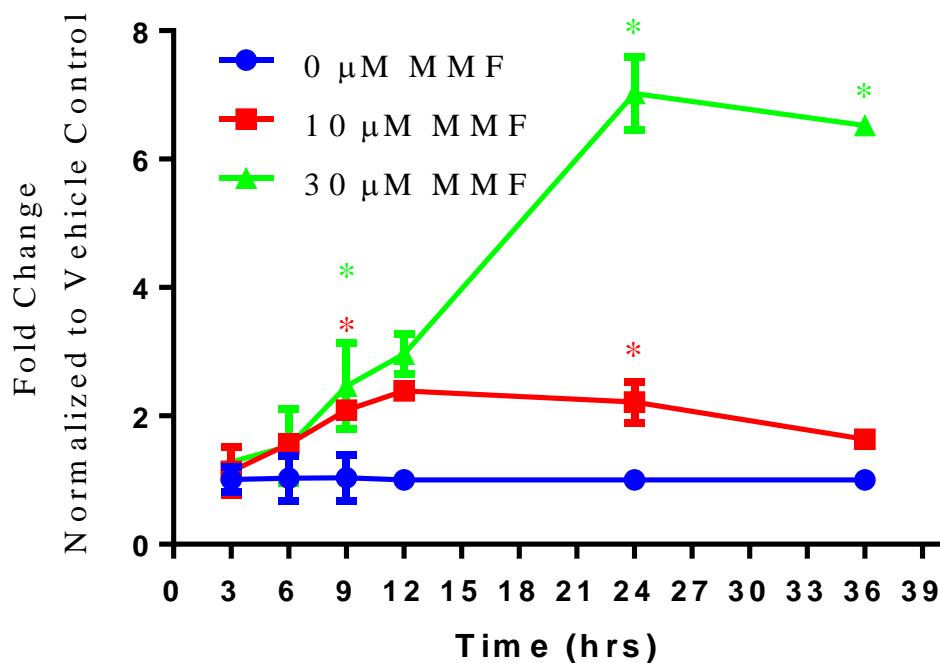


Figure 46. MMF mediated gene induction of PADI4.

Human astrocytes were treated with 0, 10 or 30 μ M of MMF and analyzed for transcriptional regulation of PADI4 over various time points. *, $p < 0.01$ based on two-way ANOVA with Tukey's post-test for multiple comparisons using vehicle controls at each time point for comparison.

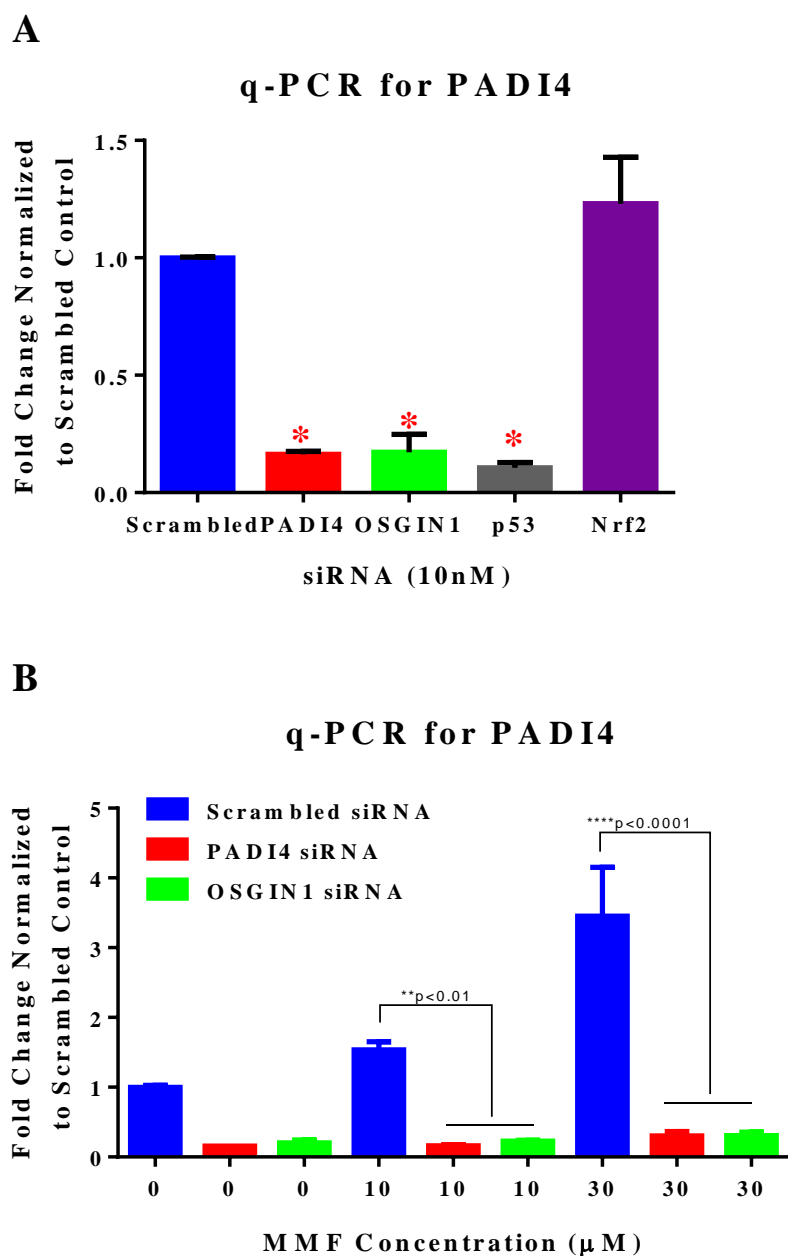


Figure 47. PADI4 is regulated by OSGIN1 and p53.

Human astrocytes were transfected with either scrambled (control), PADI4, OSGIN1, Nrf2 or p53 siRNA followed by q-PCR analysis. A, PADI4 q-PCR. *, $p < 0.0001$ based on one-way ANOVA with Dunnett's post-test for multiple comparisons. B, transfected cells treated with MMF for 24 hours followed by q-PCR for PADI4. p values based on two-way ANOVA with Tukey's post-test for multiple comparisons.

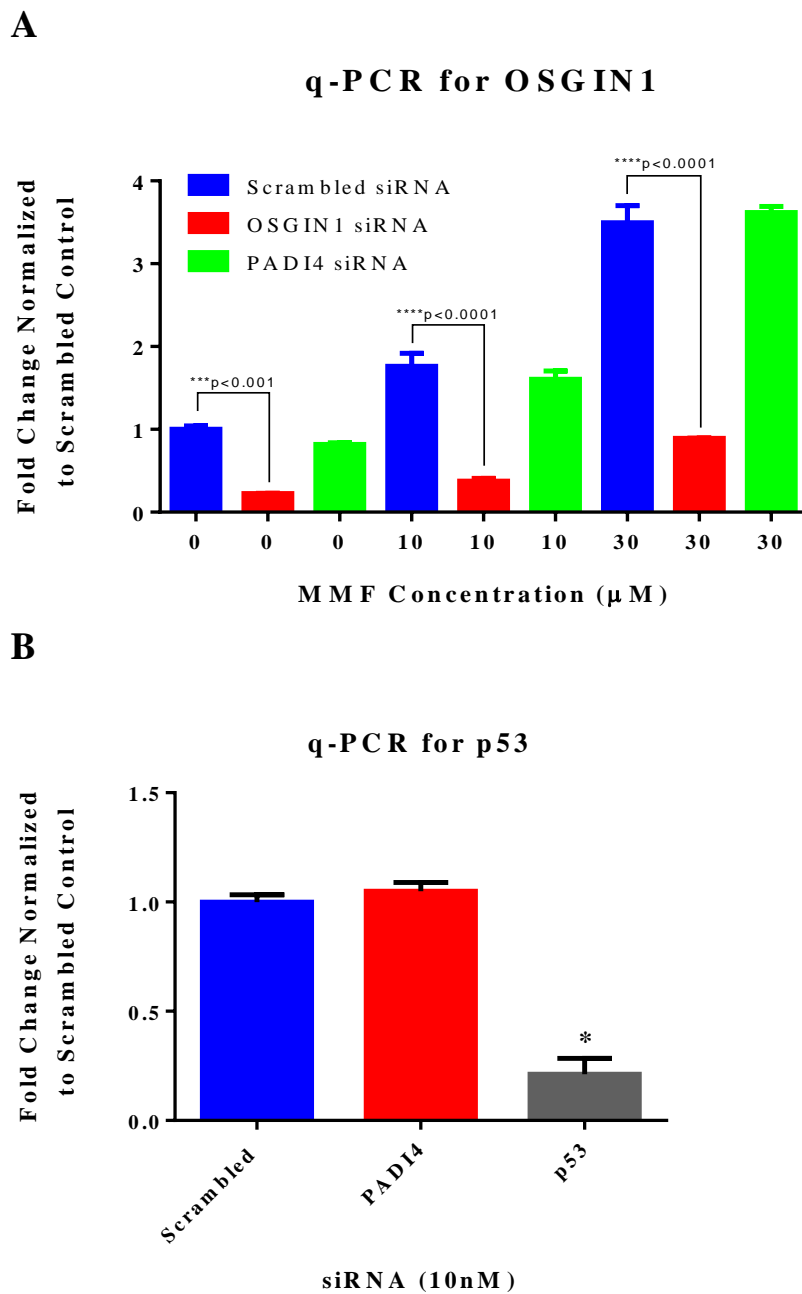


Figure 48. PADI4 does not regulate OSGIN1 or p53.

Human astrocytes were transfected with either scrambled (control), PADI4, OSGIN1 or p53 siRNA followed by q-PCR analysis. A, transfected cells treated with MMF for 24 hours followed by q-PCR for OSGIN1. B, q-PCR for p53. p values based on two-way ANOVA with Tukey's post-test for multiple comparisons. *, $p < 0.001$

3. Discussion

Endogenous regulation of cellular defense systems such as the Nrf2 pathway have become of particular interest to the field of neurodegeneration. A unifying aspect of nervous system disease is the accumulation of ROS leading to an overall state of oxidative stress. Activation of Nrf2 by small-molecule compounds such as DMF has shown to increase antioxidant defense genes leading to cytoprotection in various models of neurodegenerative disease (Linker 2011); however, the exact mechanisms underlying Nrf2-mediated cytoprotection are unclear. In Chapter 3, transcriptional profiling studies were conducted to evaluate gene regulation following oral dosing with DMF in an attempt to identify specific targets of this compound in the CNS. These studies identified the Nrf2 transcriptional target OSGIN1 to be significantly upregulated in the CNS *in vivo*. Current literature describing the biological functions of OSGIN1, describe this gene to be a major mediator of cell apoptosis under the control of the tumor suppressor protein, p53 (Yao et al., 2008; Hu et al., 2012). However, the *in vitro* findings in human astrocytes discussed in this chapter suggest OSGIN1 is significantly regulated by Nrf2 and contributes to the cytoprotective properties of the bioactive metabolite of DMF, MMF, against oxidative insult in human astrocytes.

Regulation of OSGIN1 via an Nrf2-dependent mechanism in contrast to p53-dependent transcriptional control raised the new question of whether splice variants of OSGIN1 contribute to alternate biological functions of this gene. The predominant literature associated with OSGIN1 function has been conducted in tumor cell lines and have identified the shorter OSGIN1 isoforms, OSGIN1-52 kDa and the less accepted

OSGIN1-38 kDa, to be strong inducers of apoptosis under the control of p53 (Hu et al., 2012; Yao et al., 2008). In contrast, the longer OSGIN1-61 kDa isoform is shown to be less toxic to cells and was also the major variant identified to be regulated in astrocytes in the presence of MMF in an Nrf2-dependent manner (Hu et al., 2012). The specific, cytoprotective regulation of OSGIN1-61 kDa under the transcriptional control of Nrf2 supports a mechanism for OSGIN1 independent of the recognized function of this gene in tumor cell lines. These findings suggest that functional domains within OSGIN1 variants may result in differing biological effects regulated under specific cellular conditions. This correlates with findings that OSGIN1 has been identified to contribute to a diverse set of cellular functions other than apoptosis, including anti-inflammatory actions, regulation of cell cycle and protection against oxidative stress (Li et al., 2007; Li et al., 2010; Oguri et al., 2010). Interestingly, we have also identified a role for OSGIN1 in anti-inflammatory effects based on the increased expression of TNF- α following knockdown of OSGIN1 in astrocytes (Figure 49). This correlates with previous findings in other labs that identify OSGIN1 to reduce oxidative stress and inflammation in cells challenged with Ox-PAPC (Romanoski et al., 2011; Li et al., 2007; Hammad et al., 2009). Although these findings have not yet been pursued they support a protective role for OSGIN1.

Although the specific transcript encoding the identified OSGIN1-61 kDa protein product was not detected in RACE analysis, a distinct reduction in expression of the 5'-end of the MMF-induced transcript was identified. DNA sequencing determined the MMF-induced transcript to encode for the 52 kDa OSGIN1 isoform; however, as mentioned previously, this could potentially be a result of GC enrichment in the 5' region

of the known 61kDa encoding sequence or be a result of low abundance of this transcript, resulting in an inability to fully sequence the long form of OSGIN1. In general, these findings suggest that alterations splicing of the 5' region do occur in the presence of MMF. This theory was further supported by identification of two nucleotide substitutions in the 5' end of the identified transcript that were induced following MMF treatment in astrocytes. This is particularly interesting since these nucleotide substitutions resulted in a potential AUG start site encoding a small ORF. Although the Kozak region preceding this new start site was not incredibly strong, there has been evidence in the literature suggesting that upstream AUG sites encoding upstream open reading frames (uORFs) in 5'UTR regions can decrease the frequency of AUG starts sites to initiate transcription in the main open reading frame (Morris and Geballe, 2000). Furthermore, the generation of OSGIN1 small encoding ORFs in the 5'UTR, have been previously identified to negatively control OSGIN1 protein translation (Ong et al., 2007). Therefore, in theory, the regulation of specific OSGIN1 transcripts by Nrf2 could potentially result in selection of the 61 kDa protein over the 52 kDa form through downregulation of OSGIN1-52 kDa protein expression independent of transcript regulation. Preliminary studies in our lab show evidence of reduced OSGIN1-52 kDa protein expression in the presence of MMF; however, further experiments are necessary to confirm these findings as well as thoroughly investigate this theory. Next generation sequencing analysis (RNA-seq) is currently underway to elucidate the various sequences that may be regulated downstream of Nrf2.

As mentioned above, p53 was not shown to regulate OSGIN1 expression in human astrocytes. Instead, studies with MMF in these cell types identified p53 to be a downstream protein target of Nrf2-regulated OSGIN1. This was exemplified by the inability of p53 to accumulate and translocate to the nucleus in the absence of OSGIN1, suggesting this molecule may activate p53-mediated transcriptional control. Previous studies have suggested that p53 and Nrf2 work together to regulate gene expression in the presence of oxidative stress and p53 itself has also been shown to be protective against oxidative damage (Toledano et al. 2009; Chen et al., 2012). Thus, the activation of OSGIN1 by Nrf2 may be a potential mechanism through which Nrf2 regulates p53 during periods of oxidative stress. Since OSGIN1 gene expression is activated before the activation of the gene expression of classical Nrf2 targets, it is possible that the role of OSGIN1 is to induce p53 translocation to the nucleus where it can interact with Nrf2 to regulate other Nrf2 target genes. Previous data from other labs have already identified the ability of p53 and OSGIN1 to interact in the cytoplasm, but there may also be a role for OSGIN1 in inhibiting degradation of p53 similar to the degradation mechanism of Nrf2. One way to investigate these theories would be to conduct p53 pull-down studies to measure the interaction of Nrf2 and OSGIN1 with p53. Furthermore, investigation into the interaction of OSGIN1 with the protein degradation machinery associated with p53 could give insight into whether or not OSGIN1 inhibits p53 degradation.

On the other hand, the translocation of p53 by OSGIN1 may also induce or suppress gene regulation independent of Nrf2. Evidence for this includes the regulation of PADI4 identified in astrocytes to be regulated by p53 but in an Nrf2-dependent

manner. In the preliminary studies described in this chapter, PADI4 was also identified to be transcriptionally regulated by OSGIN1, suggesting that OSGIN1-mediated translocation of p53 induces PADI4 expression. Interestingly, similar to p53, the regulation of PADI4 in association with OSGIN1 contrasts with current literature that suggests PADI4 to be a negative regulator of OSGIN1 (Yao et al., 2008). As discussed above, these alternate functions of OSGIN1 in MMF-treated astrocytes may be due to the expression of the OSGIN1-61 kDa isoform or potentially be due to cell type-specific signaling of OSGIN1. PADI4 has been shown to regulate DNA methylation by citrullination of histone residues to regulate DNA transcription and a role for p53 in this process has been described (Tanikawa et al., 2009). Therefore, the role of PADI4 in our model may be to inhibit DNA transcription in a p53-dependent manner to reduce cell proliferation. This process is independent of apoptosis based on the findings that MMF administration does not induce apoptosis but does reduce cell proliferation. Various studies have identified the inhibition of cell cycle entry to be a protective mechanism within cells, allowing conservation of energy and limiting the probability of DNA damage to be replicated (Price et al., 2003; Giovanni et al., 2005). Contribution of PADI4 to cellular protection in the presence of MMF is currently being further investigated.

Overall, these results indicate a role for the Nrf2 transcriptional target OSGIN1 in MMF-mediated cytoprotection in the presence of oxidative stress. Furthermore, these results lay the groundwork for a potential mechanism of OSGIN1-dependent protection (Figures 50 and 51). This mechanism involves activation of Nrf2 by MMF through inhibition of Keap1 degradation, resulting in the translocation of Nrf2 to the nucleus.

Once inside the nucleus, Nrf2 regulates the transcription of various genes including OSGIN1, which is one of the first Nrf2 transcribed targets. Translation of the OSGIN1-61 kDa protein then results in the accumulation and subsequent translocation of p53 to the nucleus, leading to the induction of PADI4 regulation and potentially inhibition of cell proliferation. Whether p53 also regulates other genes independently or in collaboration with Nrf2 is unknown. Furthermore, the exact importance of inhibiting cell cycle in this paradigm is also not clear, even though there is evidence that this could be a protective mechanism. This inhibition could also involve proliferative inhibition of immune cells and a subsequent inflammatory response since loss of OSGIN1 also increased TNF- α levels. Although many aspects of this theoretical pathway still need further investigation and activation of OSGIN1 is not the sole target of Nrf2, these studies support an important role for OSGIN1 following Nrf2 activation in the presence of MMF. This suggests that Nrf2-mediated cytoprotection is not simply a result of antioxidant induction, but instead consists of a complicated network of pathways that together function to protect the cell during periods of stress.

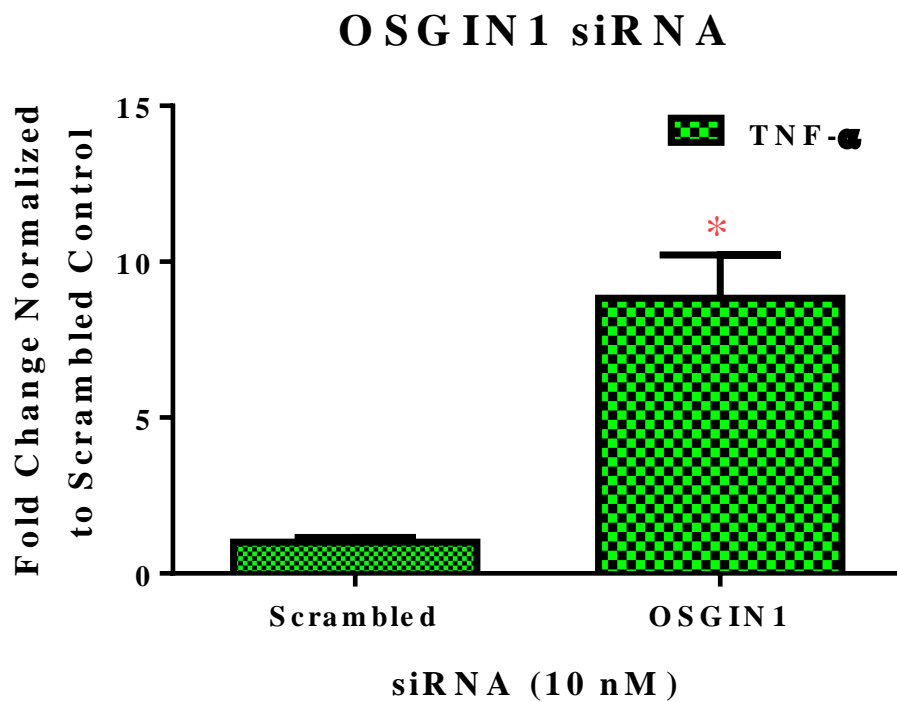


Figure 49. OSGIN1 knockdown induces expression of TNF-alpha.

Human astrocytes were transfected with scrambled (control) or OSGIN1 specific siRNA. Samples were analyzed for alterations in TNF- α transcript levels. *, $p < 0.05$ based on student's t test.

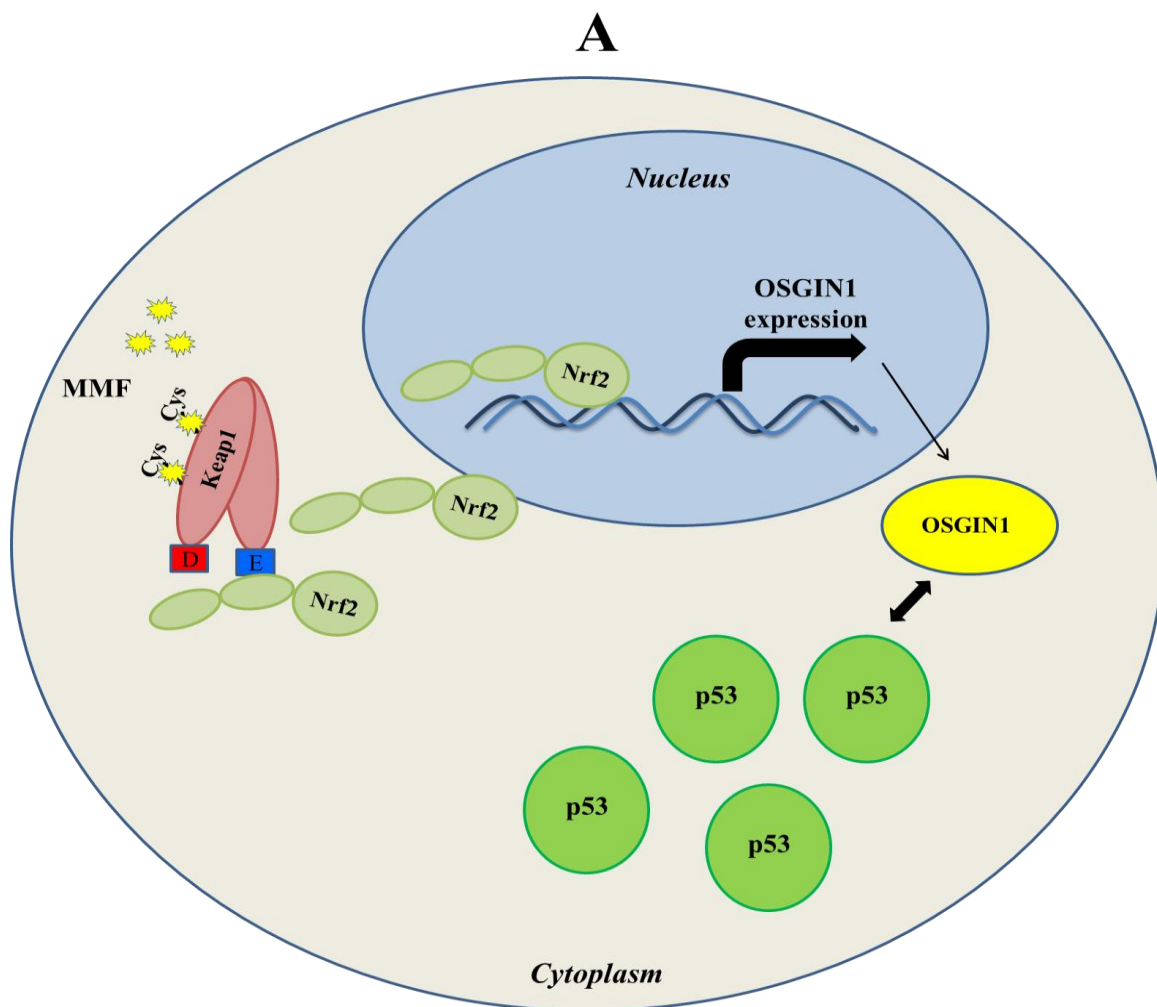


Figure 50. Potential mechanism of action of OSGIN1 mediated cellular protection.

Interaction of MMF with cysteine residues on Keap1 results in allosteric conformational change in the Keap1 protein, resulting in the inability of Nrf2 to be targeted for ubiquitination and subsequent proteasomal degradation. This allows Nrf2 to accumulate in the cytoplasm and translocate to the nucleus where it can regulate the transcription of various genes including OSGIN1. OSGIN1 transcript expression is then translated to a 61kDa protein that can induce the accumulation of p53 in an unknown mechanism. p53 protein can then translocate to the nucleus and induce gene transcription.

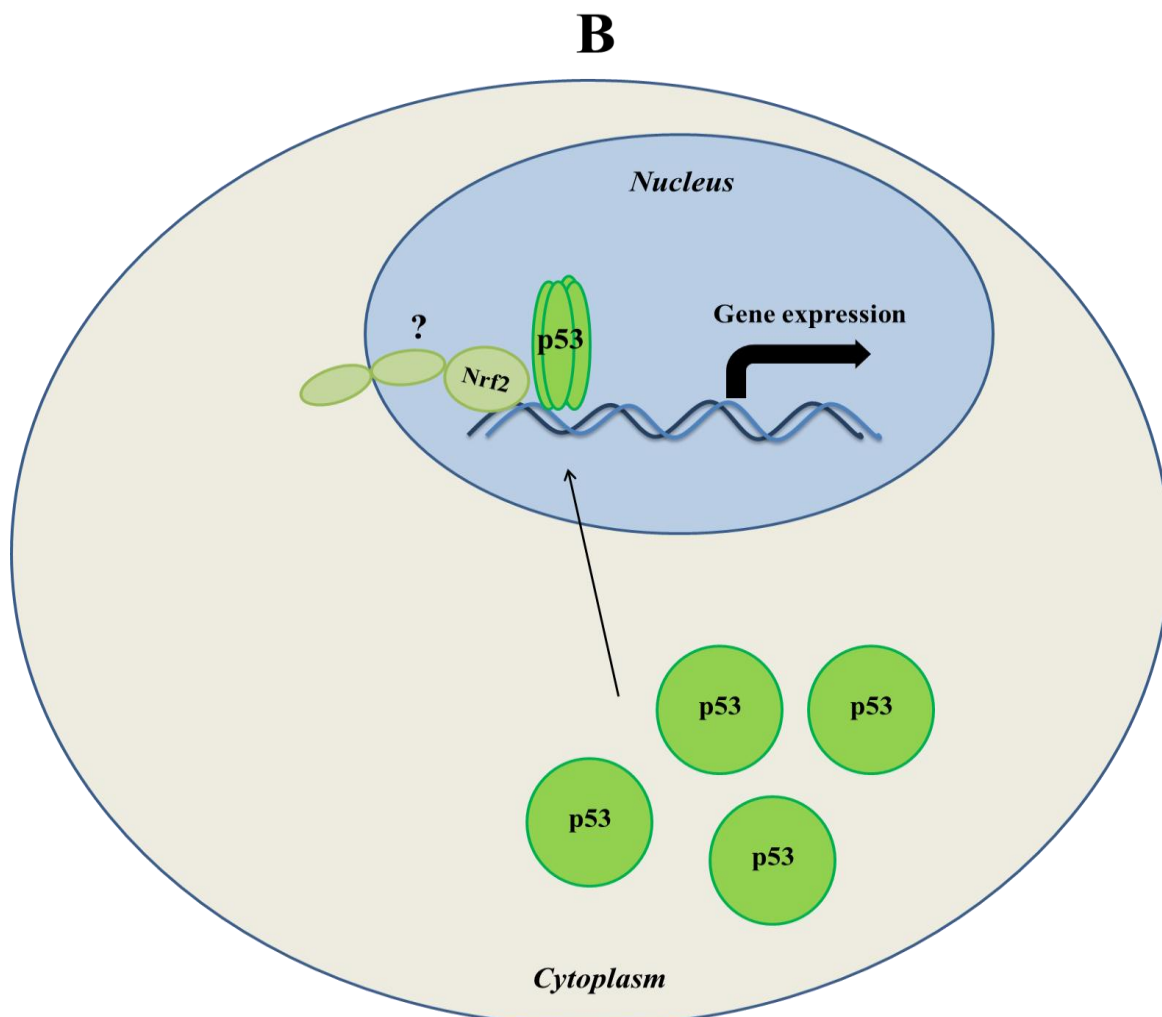


Figure 51. Potential mechanism of action of OSGIN1 mediated cellular protection.

Interaction of MMF with cysteine residues on Keap1 results in allosteric conformational change in the Keap1 protein, resulting in the inability of Nrf2 to be targeted for ubiquitination and subsequent proteasomal degradation. This allows Nrf2 to accumulate in the cytoplasm and translocate to the nucleus where it can regulate the transcription of various genes including OSGIN1. OSGIN1 transcript expression is then translated to a 61kDa protein that can induce the accumulation of p53 in an unknown mechanism. p53 protein can then translocate to the nucleus and induce gene transcription.

CHAPTER V

GENERAL CONCLUSIONS

1. General conclusions

The excessive generation of ROS resulting in a state of oxidative stress is a unifying factor in neurodegenerative disease, which has generated a strong research interest in endogenous pathways that defend against these stresses. Activation of the Nrf2 pathway has been identified as the major endogenous cellular defense system regulated in response to oxidative stress and various small molecules have been shown to activate this pathway. Dimethyl fumarate (DMF) is one such molecule recently approved for the treatment of relapsing forms of MS; however, the exact mechanisms behind Nrf2-mediated cytoprotection of this compound are not well understood. The studies outlined in this dissertation have identified DMF to differentially regulate Nrf2-dependent gene expression across tissue types in both a time and dose-dependent manner. In the CNS, one of the few genes identified to be significantly regulated by DMF was OSGIN1, more specifically OSGIN1-61 kDa, which was found to be Nrf2-dependent. Further analysis of this gene *in vitro* uncovered OSGIN1 as an important mediator of DMF-mediated cellular protection in human astrocytes and outlined a potential mechanism for this gene involving regulation of p53 by the 61 kDa-encoding isoform of OSGIN1. Although further investigation into this gene is necessary to fully understand how OSGIN1 and its splice variants are regulated within the cell to confer protection, these findings contribute further knowledge to the complex pathway associated with Nrf2-mediated cytoprotection.

2. Study limitations

As with every research endeavor, there are study limitations that effect interpretation of the work presented. The major limitation associated with the research outlined in this dissertation was the inability to sequence the OSGIN1-61 kDa transcript following MMF treatment. Although evidence was presented to support the presence of this protein product, the q-PCR probes and siRNA constructs used targeted all variants of OSGIN1. It would be ideal to individually target or knockdown them each isoform individually to look at which one is responsible for the protective effects in the presence of MMF. Although RACE identified alterations in the 5' end of the sequenced transcript, suggesting MMF treatment regulated differential expression or splicing of OSGIN1 transcripts, further experiments are necessary to identify the exact Nrf2-regulated transcript of OSGIN1. As mentioned previously, Next Generation Sequencing is currently underway to assist in answering these questions.

Another study limitation of this research was that the OSGIN1 identified splice variants do not translate back to the mouse. Differential alternative splicing is believed to occur in the mouse that contrasts with splicing of the human OSGIN1 gene and there is no evidence for the long OSGIN1-61 kDa isoform in the mouse (Flicek et al., 2014). Therefore, the specific OSGIN1 sequences regulated in our mouse models may not correlate with what was identified in human cell cultures. This may result in difficulty analyzing this gene *in vivo* unless the human form is expressed. Therefore, further investigation is needed to understand the regulation of OSGIN1 splicing in the mouse. Furthermore, this may also imply that the OSGIN1-mediated cytoprotection mechanism

is unique in human and its *in vivo* validation may be difficult unless human OSGIN1 genome knock-in mice are available for mimicking the physiological expression of human OSGIN1 transcript variants *in vivo*.

siRNA knockdown of p53 also can be considered a study limitation. Since p53 is tightly regulated and is involved with various cellular pathways, general knockdown of this gene may result in altering pathways unassociated with Nrf2 and OSGIN1. It is therefore difficult to determine if knockdown alone of p53 itself reduces protection in an oxidative challenge model or if this effect is solely a result of loss of p53-mediated protection in the presence of MMF.

3. Future directions

Future studies investigating the importance of OSGIN1 in MMF-mediated cytoprotection will be targeted to understand the interactions of OSGIN1 and p53 in cellular protection. One way to approach this would be to tag OSGIN1 splice variants (i.e. GFP) to localize and compare if OSGIN1 variants differentially interact with p53. Ideally, the generation of an OSGIN1-61kDa GFP-tagged DNA would be of greatest interest; however, identification of the full length OSGIN1-61 kDa sequence is necessary to accomplish this. Nonetheless, if accomplished, these tagged proteins could then be investigated in various human neuronal cell lines to determine the cell-specific functions of OSGIN1 variants. This same experimental procedure could also be used to visualize Nrf2 and p53 interactions along with potential pull-down studies.

Investigation of the cell type-specific regulation of Nrf2 signaling is currently underway using a transgenic ARE-luciferase reporter mouse. These mice have been treated with a single dose of DMF and are currently being analyzed via immunohistochemistry (IHC) to locate signal of Nrf2 activation in specific cell types. These studies will give further insight into the localization of Nrf2 signaling within different tissue types, which can be correlated with findings obtained from transcriptional profiling studies in Chapter 3.

Further investigation into the role of PADI4 in OSGIN1/p53 mediated protection and its effects on cell proliferation are important to understand the role of PADI4 downstream of OSGIN1. Although efforts have been made to understand if PADI4 regulation is necessary for MMF-mediated cytoprotection, further studies are necessary to fully elucidate the importance of this gene in Nrf2-p53 signaling.

In vivo analysis of OSGIN1 function would also be of particular interest. The importance of OSGIN1 in regards to immune cell infiltration and astrogliosis in animal models of MS, such as experimental autoimmune encephalomyelitis (EAE), could give insight into the anti-inflammatory and anti-proliferative effects associated with DMF and OSGIN1. Furthermore, generation of transgenic mice overexpressing the human OSGIN1-61 kDa and OSGIN1 knockout mouse models could give further insight into the important biological pathways associated with OSGIN1.

CHAPTER VI

BIBLIOGRAPHY

Abazeed, M. E., Adams, D. J., Hurov, K. E., Tamayo, P., Creighton, C. J., Sonkin, D., et al. (2013). Integrative Radiogenomic Profiling of Squamous Cell Lung Cancer. *Cancer Research*, 73(20), 6289–6298.

Adam-Vizi, V., & Tretter, L. (2013). *Neurochemistry International*. *Neurochemistry International*, 62(5), 757–763.

Alam, J., Stewart, D., Touchard, C., Boinapally, S., Choi, A. M., & Cook, J. L. (1999). Nrf2, a Cap'n'Collar Transcription Factor, Regulates Induction of the Heme Oxygenase-1 Gene*. *The Journal of Biological Chemistry*, (274), 26071–26078.

Alam, Z. I., Jenner, A., Daniel, S. E., Lees, A. J., Cairns, N., Marsden, C. D., et al. (1997). Oxidative DNA Damage in Parkinsonian Brain: An Apparent Selective Increase in 8-Hydroxyguanine Levels in Substantia Nigra. *Journal of Neurochemistry*, 69, 1196–1203.

Altmeyer PJ, Matthes U, Pawlak F, Hoffmann K, Frosch PJ, Ruppert P, Wassilew SW, Horn T, Kreysel HW, Lutz G, et al. (1994). Antipsoriatic effect of fumaric acid derivatives. Results of a multicenter double-blind study in 100 patients. *Journal of American Academy of Dermatology*, 30(6):977-81.

Ansari MA, Scheff SW. (2010). Oxidative stress in the progression of Alzheimer disease in the frontal cortex. *Journal of Neuropathology and Experimental Neurology*. 69(2):155-67.

Apostolova, N., Garcia-Bou, R., Hernandez-Mijares, A., Herance, R., Rocha, M., & Victor, V. M. (2011). Mitochondrial Antioxidants Alleviate Oxidative and Nitrosative Stress in a Cellular Model of Sepsis. *Pharmaceutical Research*, 28(11), 2910–2919.

Baird, L., Lieres, D., Swift, S., & Dinkova-Kostova, A. T. (2013). Regulatory flexibility in the Nrf2-mediated stressresponse is conferred by conformational cycling of the Keap1-Nrf2 protein complex. *Proceedings of the National Academy of Sciences*, 110(38), 15259–15264.

Baird, L., Swift, S., Llères, D., & Dinkova-Kostova, A. T. (2014). *Biotechnology Advances*. *Biotechnology Advances*, 1–12.

Balogun, E., Hoque, M., Gong, P., Killeen, E., Green, C. J., & Foresti, R. (2003). Curcumin activates the haem oxygenase-1 gene via regulation of Nrf2 and the antioxidant-responsive element. *Biochemical Journal*, (371), 887–895.

- Beal, M. F., Brouillet, E., Jenkins, B. G., Ferrante, R. J., Kowall, N. W., Miller, J. M., et al. (1993). Neurochemical and Histologic Characterization of Striatal Excitotoxic Lesions Produced by the Mitochondrial Toxin 3-Nitropropionic Acid. *The Journal of Neuroscience*, 13(10), 4181–4192.
- Beckman, J. S. (1996). Oxidative Damage and Tyrosine Nitration from Peroxynitrite. *Chemical Research in Toxicology*, 9, 836–844.
- Bell, K. F., Al-Mubarak, B., Fowler, J. H., Baxter, P. S., Gupta, K., Tsujita, T., et al. (2011). Mild oxidative stress activates Nrf2 in astrocytes, which contributes to neuroprotective ischemic preconditioning. *Proceedings of the National Academy of Sciences*, 108(1), E1–E2.
- Bogdanov, M. B., Andreassen, O. A., Dedeoglu, A., Ferrante, R. J., & Beal, M. F. (2001). Increased oxidative damage to DNA in a transgenic mouse model of Huntington's Disease. *Rapid Communication*, 79, 1246–1249.
- Braun, A., Dang, J., Johann, S., Beyer, C., & Kipp, M. (2009). Selective regulation of growth factor expression in cultured cortical astrocytes by neuro-pathological toxins. *Neurochemistry International*, 55(7), 610–618.
- Brieger, K., Schiavone, S., Miller, J., & Krause, K. H. (2012). Reactive oxygen species: from health to disease. *Swiss Medical Weekly*.
- Brouillet, E., Jacquard, C., Bizat, N., & Blum, D. (2005). 3-Nitropropionic acid: a mitochondrial toxin to uncover physiopathological mechanisms underlying striatal degeneration in Huntington's disease. *Journal of Neurochemistry*, 95(6), 1521–1540.
- Browne SE, Ferrante RJ, Beal MF. (1999). Oxidative stress in Huntington's disease. *Brain Pathology*, 9(1):147-63.
- Bruijn, L. I., Beal, M. F., Becher, M. W., Schulz, J. B., Wong, P. C., DL, P., & Cleveland, D. W. (1997). Elevated free nitrotyrosine levels, but not protein-bound nitrotyrosine or hydroxyl radicals, throughout amyotrophic lateral sclerosis (ALS)-like disease implicate tyrosine nitration as an aberrant in vivo property of one familial ALS-linked superoxide dismutase 1 mutant. *Proceedings of the National Academy of Sciences*, 94, 7606–7611.
- Bryan, H. K., Olayanju, A., Goldring, C. E., & Park, B. K. (2013). Biochemical Pharmacology. *Biochemical Pharmacology*, 85(6), 705–717.
- Bryla J, Gardas A. (1965). Coupling factors and high-energy intermediates of oxidative phosphorylation. *Postepy Biochemistry*. 11(4):395-411.

Butterfield DA, Drake J, Pocernich C, Castegna A. (2001). Evidence of oxidative damage in Alzheimer's disease brain: central role for amyloid beta-peptide. *Trends in Molecular Medicine* 7(12):548-54.

Calkins, M. J., Jakel, R. J., Johnson, D. A., Chan, K., & Wai Kan, Y. (2005). Protection from mitochondrial complex II inhibition in vitro and in vivo by Nrf2-mediated transcription. *Proceedings of the National Academy of Sciences*, 102(1), 244–249.

Cente M1, Filipcik P, Pevalova M, Novak M. (2006) Expression of a truncated tau protein induces oxidative stress in a rodent model of tauopathy. *European Journal of Neuroscience*. 24(4):1085-90.

Cente M1, Filipcik P, Mandakova S, Zilka N, Krajciova G, Novak M. (2009) Expression of a truncated human tau protein induces aqueous-phase free radicals in a rat model of tauopathy: implications for targeted antioxidative therapy. *Journal of Alzheimer's Disease*. 17(4):913-20.

Chan, J. Y., Kwong, M., Lu, R., Chang, J., Wang, B., Yen, T. S. B., & Kan, Y. W. (1998). Targeted disruption of the ubiquitous CNC-bZIP transcription factor, Nrf-1, results in anemia and embryonic lethality in mice. *The EMBO Journal*, 17(6), 1779–1787.

Chan K, Lu R, Chang JC, Kan YW. (1996) NRF2, a member of the NFE2 family of transcription factors, is not essential for murine erythropoiesis, growth, and development. *Proceedings of the National Academy of Sciences United States of America*. 26;93(24):13943-8.

Chanas, S. A., Jiang, Q., McMahon, M., McWalter, G. K., McLellan, L. I., Elcombe, C. R., et al. (2002). Loss of the Nrf2 transcription factor causes a marked reduction in constitutive and inducible expression of the glutathione S-transferase *Gsta1*, *Gsta2*, *Gstm1*, *Gstm2*, *Gstm3* and *Gstm4* genes in the livers of male and female mice. *Biochemical Journal*, 365, 405–416.

Chen, C.-M., Wu, Y.-R., Cheng, M.-L., Liu, J.-L., Lee, Y.-M., Lee, P.-W., et al. (2007). Increased oxidative damage and mitochondrial abnormalities in the peripheral blood of Huntington's disease patients. *Biochemical and Biophysical Research Communications*, 359(2), 335–340.

Chen, H., Assmann, J. C., Krenz, A., Rahman, M., Grimm, M., Karsten, C. M., et al. (2014). Hydroxycarboxylic acid receptor 2 mediates dimethyl fumarate's protective effect in EAE. *Journal of Clinical Investigation*, 124(5), 2188–2192.

Chen, L., Kwong, M., Lu, R., Ginzinger, D., Lee, C., Leung, L., & Chan, J. Y. (2003). Nrf1 Is Critical for Redox Balance and Survival of Liver Cells during Development. *Molecular and Cellular Biology*, 23(13), 4673–4686.

Chen, W., Sun, Z., Wang, X.-J., Jiang, T., Huang, Z., Fang, D., & Zhang, D. D. (2009). Direct Interaction between Nrf2 and p21Cip1/WAF1 Upregulates the Nrf2-Mediated Antioxidant Response. *Molecular Cell*, 34(6), 663–673.

Chen, Z.-H., Saito, Y., Yoshida, Y., Sekine, A., Noguchi, N., & Niki, E. (2005). 4-Hydroxynonenal Induces Adaptive Response and Enhances PC12 Cell Tolerance Primarily through Induction of Thioredoxin Reductase 1 via Activation of Nrf2. *Journal of Biological Chemistry*, 280(51), 41921–41927.

Chien, W.-L., Lee, T.-R., Hung, S.-Y., Kang, K.-H., Wu, R.-M., Lee, M.-J., & Fu, W.-M. (2013). Free Radical Biology and Medicine. *Free Radical Biology and Medicine*, 58(C), 160–169.

Chowdhry, S., Zhang, Y., McMahon, M., Sutherland, C., Cuadrado, A., & Hayes, J. D. (2012). Nrf2 is controlled by two distinct b-TrCP recognition motifs in its Neh6 domain, one of which can be modulated by GSK-3 activity. *Oncogene*, 32(32), 3765–3781.

Clements, C. M., McNally, R. S., Conti, B. J., Mak, T. W., & Ting, J. P. (2006). DJ-1, a cancer- and Parkinson's disease-associated protein, stabilizes the antioxidant transcriptional master regulator Nrf2. *Proceedings of the National Academy of Sciences*, 103(41), 15091–15096.

Cooper, C. E., Patel, R. P., Brookes, P. S., & Darley-Usmar, V. M. (2002). Nanotransducers in cellular redox signaling: modification of thiols by reactive oxygen and nitrogen species. *Trends in Biochemical Sciences*, 27(10), 489–492.

Cook AL, Vitale AM, Ravishankar S, Matigian N, Sutherland GT, Shan J, Sutharsan R, Perry C, Silburn PA, Mellick GD, Whitelaw ML, Wells CA, Mackay-Sim A, Wood SA. (2011) NRF2 activation restores disease related metabolic deficiencies in olfactory neurosphere-derived cells from patients with sporadic Parkinson's disease. *PLoS One*. 6(7):e21907.

Copple IM, Goldring CE, Kitteringham NR, Park BK. (2010). The keap1-nrf2 cellular defense pathway: mechanisms of regulation and role in protection against drug-induced toxicity. *Handbook of Experimental Pharmacology*. 2010;(196):233-66.

Cross, A. H., Manning, P. T., Richard, K., Schmidt, R. E., & Misko, T. P. (1998). Peroxynitrite formation within the central nervous system in active multiple sclerosis. *Journal of Neuroimmunology*, (88), 45–56.

Cross, A. H., San, M., Stern, M., Richard, K., Salvemini, D., & Misko, T. P. (2000). A catalyst of peroxynitrite decomposition inhibits murine experimental autoimmune encephalomyelitis. *Journal of Neuroimmunology*, (107), 21–28.

Csiszar A, Toth J, Peti-Peterdi J, Ungvari Z. (2007) The aging kidney: role of endothelial oxidative stress and inflammation. *Acta Physiologica Hungaria*. 94(1-2):107-15.

Cullinan, S. B., Zhang, D., Hannink, M., Arvisais, E., Kaufman, R. J., & Diehl, J. A. (2003). Nrf2 Is a Direct PERK Substrate and Effector of PERK-Dependent Cell Survival. *Molecular and Cellular Biology*, 23(20), 7198–7209.

Dasuri, K., Le Zhang, & Keller, J. N. (2013). *Free Radical Biology and Medicine*. *Free Radical Biology and Medicine*, 62(C), 170–185.

Dawson, T. M. (2003). Molecular Pathways of Neurodegeneration in Parkinson's Disease. *Science*, 302(5646), 819–822.

David DC, Hauptmann S, Scherping I, Schuessel K, Keil U, Rizzu P, Ravid R, Dröse S, Brandt U, Müller WE, Eckert A, Götz J. (2005) Proteomic and functional analyses reveal a mitochondrial dysfunction in P301L tau transgenic mice. *Journal of Biological Chemistry*. 280(25):23802-14.

Deby, C., & Goutier, R. (1990). New Perspectives on the Biochemistry of Superoxide Anion and the Efficiency of Superoxide Dismutases. *Biochemical Pharmacology*, 39(3), 399–405.

DeNicola, G. M., Karreth, F. A., Humpton, T. J., Gopinathan, A., Wei, C., Frese, K., et al. (2011). Oncogene-induced Nrf2 transcription promotes ROS detoxification and tumorigenesis. *Nature*, 475(7354), 106–109.

DeNicola, G. M., Karreth, F. A., Humpton, T. J., Gopinathan, A., Wei, C., Frese, K., et al. (2012). Oncogene-induced Nrf2 transcription promotes ROS detoxification and tumorigenesis. *Nature*, 475(7354), 106–109.

Derjuga, A., Gourley, T. S., Holm, T. M., Heng, H. H. Q., Shivdasani, R. A., Ahmadi, S., et al. (2004). Complexity of CNC Transcription Factors As Revealed by Gene Targeting of the Nrf3 Locus. *Molecular and Cellular Biology*, 24(8), 3286–3294.

Dexter DT, Jenner P. (2013) Parkinson disease: from pathology to molecular disease mechanisms. *Free Radical Biological Medicine*. 62:132-44.

Dhakshinamoorthy, S. (2000). Small Maf (MafG and MafK) Proteins Negatively Regulate Antioxidant Response Element-mediated Expression and Antioxidant Induction of the NAD(P)H:Quinone Oxidoreductase1 Gene. *Journal of Biological Chemistry*, 275(51), 40134–40141.

Dinkova-Kostova, A. T., Holtzclaw, W. D., Cole, R. N., Itoh, K., Wakabayashi, N., Katoh, Y., et al. (2002). Direct evidence that sulfhydryl groups of Keap1 are the sensors regulating induction of phase 2 enzymes that protect against carcinogens and oxidants. *Proceedings of the National Academy of Sciences*, 99(18), 11908–11913.

Dorsey ER, Beck CA, Darwin K, Nichols P, Brocht AF, Biglan KM, Shoulson I. (2013) Natural history of Huntington disease. *JAMA Neurology*. 70(12):1520-30.

Dringen R, Gutterer JM, Hirrlinger J. (2000) Glutathione metabolism in brain metabolic interaction between astrocytes and neurons in the defense against reactive oxygen species. *European Journal of Biochemistry*. 267(16):4912-6.

Dumont, M., & Beal, M. F. (2010). Neuroprotective strategies involving ROS in Alzheimer disease. *Free Radical Biology and Medicine*, 1–13.

Eggler AL, Liu G, Pezzuto JM, van Breemen RB, Mesecar AD. (2005) Modifying specific cysteines of the electrophile-sensing human Keap1 protein is insufficient to disrupt binding to the Nrf2 domain Neh2. *Proceedings of the National Academy of Sciences United States of America*. 102(29):10070-5.

Elipenahli C, Stack C, Jainuddin S, Gerges M, Yang L, Starkov A, Beal MF, Dumont M. (2012) Behavioral improvement after chronic administration of coenzyme Q10 in P301S transgenic mice. *Journal of Alzheimers Disease*. 28(1):173-82.

Escartin, C., Joon Won, S., Malgorn, C., Auregan, G., Berman, A. E., Chen, P. C., et al. (2011). Nuclear Factor Erythroid 2-Related Factor 2 Facilitates Neuronal Glutathione Synthesis by Upregulating Neuronal Excitatory Amino Acid Transporter 3 Expression. *Journal of Neuroscience*, 31(20), 7392–7401.

Federico, A., Cardaioli, E., Da Pozzo, P., Formichi, P., Gallus, G. N., & Radi, E. (2012). *Journal of the Neurological Sciences*. *Journal of the Neurological Sciences*, 322(1-2), 254–262.

Fernández-Vizarra, E., Tiranti, V., & Zeviani, M. (2009). *Biochimica et Biophysica Acta*. *BBA - Molecular Cell Research*, 1793(1), 200–211.

Finkel, T. (1998). Oxygen radicals and signaling Toren Finkel. *Current Opinion in Cell Biology*, (10), 248–253.

Flicek et al. (2014) Ensembl 2014. *Nucleic Acids Res*. 42(Database issue):D749-55. doi: 10.1093/nar/gkt1196. Epub 2013 Dec 6.

Forman, M. S., Trojanowski, J. Q., & Lee, V. M.-Y. (2004). Neurodegenerative diseases: a decade of discoveries paves the way for therapeutic breakthroughs. *Nature Medicine*, 10(10), 1038–1113.

- Forstermann, U., & Sessa, W. C. (2012). Nitric oxide synthases: regulation and function. *European Heart Journal*, 33(7), 829–837.
- Fox, S. H., & Brotchie, J. M. (2010). The MPTP-lesioned non-human primate models of Parkinson. *Progress In Brain Research*, 184(133–157).
- Furuta S, Hashimoto T. (1995) Purification and properties of 3-hydroxyacyl coenzyme A dehydrogenase-binding protein from rat liver mitochondria. *Journal of Biochemistry*. 118(4):810-8.
- Gabbita SP, Lovell MA, Markesbery WR. (1998) Increased nuclear DNA oxidation in the brain in Alzheimer's disease. *Journal of Neurochemistry*. 71(5):2034-40.
- Gan, L., Johnson, D. A., & Johnson, J. A. (2010). Keap1-Nrf2 activation in the presence and absence of DJ-1. *European Journal of Neuroscience*, 31(6), 967–977.
- Garg, R., Gupta, S., & Maru, G. B. (2008). Dietary curcumin modulates transcriptional regulators of phase I and phase II enzymes in benzo[a]pyrene-treated mice: mechanism of its anti-initiating action. *Carcinogenesis*, 29(5), 1022–1032.
- Geisler S, Holmström KM, Treis A, Skujat D, Weber SS, Fiesel FC, Kahle PJ, Springer W. (2010) The PINK1/Parkin-mediated mitophagy is compromised by PD-associated mutations. *Autophagy*. 6(7):871-8.
- Gold R, Linker RA, Stangel M (2012) Fumaric acid and its esters: an emerging treatment for multiple sclerosis with antioxidative mechanism of action. *Clinical Immunology*. 142(1):44-8.
- Gorsky, L. D., Koop, D. R., & Coon, M. J. (1984). On the Stoichiometry of the Oxidase and Monooxygenase Reactions Catalyzed by Liver Microsomal Cytochrome P-450. *The Journal of Biological Chemistry*, 259(11), 6812–6817.
- Groneberg, D., König, P., Koesling, D., & Friebe, A. (2011). Nitric Oxide–Sensitive Guanylyl Cyclase Is Dispensable for Nitroergic Signaling and Gut Motility in Mouse Intestinal Smooth Muscle. *Gastroenterology*, 140(5), 1608–1617.
- Hadjipanayi, E., & Schilling, A. F. (2013). Hypoxia-based strategies for angiogenic induction: The dawn of a new era for ischemia therapy and tissue regeneration. *Organogenesis*, 9(4), 261–272.
- Hafler, D. A. (2004). Multiple sclerosis. *Journal of Clinical Investigation*, 113(6), 788–794.

Hamilton, M. L., Remmen, H. V., Drake, J. A., Yang, H., Guo, Z. M., Kewitt, K., et al. (2001). Does oxidative damage to DNA increase with age? *Proceedings of the National Academy of Sciences*, 98(18), 10469–10474.

Han, D., Ybanez, M. D., Ahmadi, S., Yeh, K., & Kaplowitz, N. (2009). Redox Regulation of Tumor Necrosis Factor Signaling. *Antioxidants & Redox Signaling*, 11(9), 2245–2263.

Hand CK, Rouleau GA.. (2002) Familial amyotrophic lateral sclerosis. *Muscle Nerve*. 25(2):135-59.

Hayes JD, Chanas SA, Henderson CJ, McMahon M, Sun C, Moffat GJ, Wolf CR, Yamamoto M. (2000) The Nrf2 transcription factor contributes both to the basal expression of glutathione S-transferases in mouse liver and to their induction by the chemopreventive synthetic antioxidants, butylated hydroxyanisole and ethoxyquin. *Biochemistry Society Transactions*. 28(2):33-41.

Hohlfeld, R., & Wekerle, H. (2004). Autoimmune concepts of multiple sclerosis as a basis for selective immunotherapy: From pipe dreams to (therapeutic) pipelines. *Colloquium*, 101(2), 14599–14606.

Holland, R., & Fishbein, J. C. (2010). Chemistry of the Cysteine Sensors in Kelch-Like ECH-Associated Protein 1. *Antioxidants & Redox Signaling*, 13(11), 1749–1761.

Holland, R., Hawkins, A. E., Egger, A. L., Mesecar, A. D., Fabris, D., & Fishbein, J. C. (2008). Prospective Type 1 and Type 2 Disulfides of Keap1 Protein. *Chemical Research in Toxicology*, 21(10), 2051–2060.

Holley, J. E., Newcombe, J., Winyard, P. G., & Gutowski, N. J. (2007). Peroxiredoxin V in multiple sclerosis lesions: predominant expression by astrocytes. *Multiple Sclerosis*, 13(8), 955–961.

Honjo, Y., Ito, H., Horibe, T., Takahashi, R., & Kawakami, K. (2010). Protein disulfide isomerase-immunopositive inclusions in patients with Alzheimer disease. *Brain Research*, 1349(C), 90–96.

Hoozemans JJ, Veerhuis R, Rozemuller JM, Eikelenboom P. (2005) Neuroinflammation and regeneration in the early stages of Alzheimer's disease pathology. *International Journal of Development Neuroscience*. 24(2-3):157-65.

van Horssen J, Schreibelt G, Drexhage J, Hazes T, Dijkstra CD, van der Valk P, de Vries HE. (2008) Severe oxidative damage in multiple sclerosis lesions coincides with enhanced antioxidant enzyme expression. *Free Radical Biological Medicine*. 45(12):1729-37.

Hu, J., Yao, H., Gan, F., Tokarski, A., & Wang, Y. (2012). Interaction of OKL38 and p53 in Regulating Mitochondrial Structure and Function. *PLoS One*, 7(8), e43362.

Huang, H. C. (2002). Phosphorylation of Nrf2 at Ser-40 by Protein Kinase C Regulates Antioxidant Response Element-mediated Transcription. *Journal of Biological Chemistry*, 277(45), 42769–42774.

Hubbs, A. F., Benkovic, S. A., Miller, D. B., O'Callaghan, J. P., Battelli, L., Schwegler-Berry, D., & Ma, Q. (2007). Vacuolar Leukoencephalopathy with Widespread Astrogliosis in Mice Lacking Transcription Factor Nrf2. *The American Journal of Pathology*, 170(6), 2068–2076.

Hur, W., Sun, Z., Jiang, T., Mason, D. E., Peters, E. C., Zhang, D. D., et al. (2010). A Small-Molecule Inducer of the Antioxidant Response Element. *Chemistry & Biology*, 17(5), 537–547.

Huynh, H., Ng, C. Y., ONG, C. K., LIM, K. B., & CHAN, T. W. (2001). Cloning and Characterization of a Novel Pregnancy- Induced Growth Inhibitor in Mammary Gland. *Endocrinology*, 142(8), 3607–3615.

Ichimura, Y., Waguri, S., Sou, Y.-S., Kageyama, S., Hasegawa, J., Ishimura, R., et al. (2013). Phosphorylation of p62 Activates the Keap1-Nrf2 Pathway during Selective Autophagy. *Molecular Cell*, 51(5), 618–631.

Imitola J, Chitnis T, Khoury SJ. (2005) Cytokines in multiple sclerosis: from bench to bedside. *Pharmacological Therapeutics*. 106(2):163-77.

Innamorato NG, Jazwa A, Rojo AI, García C, Fernández-Ruiz J, Grochot-Przeczek A, Stachurska A, Jozkowicz A, Dulak J, Cuadrado A. (2010) Different susceptibility to the Parkinson's toxin MPTP in mice lacking the redox master regulator Nrf2 or its target gene heme oxygenase-1. *PLoS One*. 5(7):e11838.

Irizarry MC, Hyman BT (2003) Brain isoprostanes: a marker of lipid peroxidation and oxidative stress in AD. *Neurology*. 61(4):436-7.

Ischiropoulos, H., & Beckman, J. S. (2003). Oxidative stress and nitration in neurodegeneration: Cause, effect, or association? *Journal of Clinical Investigation*, 111(2), 163–169.

Itoh, K., Chiba, T., Takahashi, S., Ishii, T., Igarashi, K., Katoh, Y., et al. (1997). An Nrf2/Small Maf Heterodimer Mediates the Induction of Phase II Detoxifying Enzyme Genes through Antioxidant Response Elements. An Nrf2/Small Maf Heterodimer Mediates the Induction of Phase II Detoxifying Enzyme Genes Through Antioxidant Response Elements. *Biochemical and Biophysical Research Communications*, 236(2), 313–322.

Itoh, K., Igarashi, K., Hayashi, N., Nishizawa, Y., & Yamamoto, M. (1995). Cloning and Characterization of a Novel Erythroid Cell-Derived CNC Family Transcription Factor Heterodimerizing with the Small Maf Family Proteins. *Molecular and Cellular Biology*, 15(8), 4184–4193.

Itoh, K., Tong, K. I., & Yamamoto, M. (2004). Molecular mechanism activating nrf2–keap1 pathway in regulation of adaptive response to electrophiles. *Free Radical Biology and Medicine*, 36(10), 1208–1213.

Itoh, K., Wakabayashi, N., Katoh, Y., Ishii, T., Igarashi, K., Engel, J. D., & Yamamoto, M. (1999). Keap1 represses nuclear activation of antioxidant responsive elements by Nrf2 through binding to the amino-terminal Neh2 domain. *Genes & Development*, 13, 76–86.

Itoh, K., Wakabayashi, N., Katoh, Y., Ishii, T., O'Connor, T., & Yamamoto, M. (2003). Keap1 regulates both cytoplasmic-nuclear shuttling and degradation of Nrf2 in response to electrophiles. *Genes to Cells*, (8), 379–391.

Jack, C., Antel, J., Brück, W., & Kuhlmann, T. (2007). Contrasting potential of nitric oxide and peroxynitrite to mediate oligodendrocyte injury in multiple sclerosis. *Glia*, 55(9), 926–934.

Jacobs, A. T., & Marnett, L. J. (2010). Systems Analysis of Protein Modification and Cellular Responses Induced by Electrophile Stress. *Accounts of Chemical Research*, 43(5), 673–683.

Jain, A., Lamark, T., Sjøttem, E., Bowitz Larsen, K., Atesoh Awuh, J., Overvatn, A., et al. (2010). p62/SQSTM1 Is a Target Gene for Transcription Factor NRF2 and Creates a Positive Feedback Loop by Inducing Antioxidant Response Element-driven Gene Transcription. *Journal of Biological Chemistry*, 285(29), 22576–22591.

Jazwa A, Rojo AI, Innamorato NG, Hesse M, Fernández-Ruiz J, Cuadrado A. (2011) Pharmacological targeting of the transcription factor Nrf2 at the basal ganglia provides disease modifying therapy for experimental parkinsonism. *Antioxidant and Redox Signaling*. 14(12):2347-60.

Jenner, P. (2003). Oxidative stress in Parkinson's disease. *Annals of Neurology*, 53(S3), S26–S38.

Johnson, J. A., Johnson, D. A., Kraft, A. D., Calkins, M. J., Jakel, R. J., Vargas, M. R., & Chen, P.-C. (2008). The Nrf2-ARE Pathway. *Annals of the New York Academy of Sciences*, 1147(1), 61–69.

Joselin, A. P., Hewitt, S. J., Callaghan, S. M., Kim, R. H., Chung, Y. H., Mak, T. W., et al. (2012). ROS-dependent regulation of Parkin and DJ-1 localization during oxidative stress in neurons. *Human Molecular Genetics*, 21(22), 4888–4903.

Joshi G, Johnson JA. (2012) The Nrf2-ARE pathway: a valuable therapeutic target for the treatment of neurodegenerative diseases. *Recent Patterns in CNS Drug Discovery*. 7(3):218-29.

Juge N1, Mithen RF, Traka M (2007) Molecular basis for chemoprevention by sulforaphane: a comprehensive review. *Cellular and Molecular Life Sciences*. 64(9):1105-27.

Kang, M.-I., Kobayashi, A., Wakabayashi, N., Kim, S.-G., & Yamamoto, M. (2004). Scaffolding of Keap1 to the actin cytoskeleton controls the function of Nrf2 as key regulator of cytoprotective phase 2 genes. *Proceedings of the National Academy of Sciences*, 101(7), 2046–2051.

Kanninen, K., Heikkinen, R., Malm, T., Rolova, T., Kuhmonen, S., Leinonen, H., et al. (2009). Intrahippocampal injection of a lentiviral vector expressing Nrf2 improves spatial learning in a mouse model of Alzheimer's disease. *Proceedings of the National Academy of Sciences*, 106(38), 16505–16510.

Kappos, L., Gold, R., Miller, D. H., MacManus, D. G., Havrdova, E., Limmroth, V., et al. (2008). Efficacy and safety of oral fumarate in patients with relapsing-remitting multiple sclerosis: a multicentre, randomised, double-blind, placebo-controlled phase IIb study. *The Lancet*, 372(9648), 1463–1472.

Kato, Y., Itoh, K., Yoshida, E., Miyagishi, M., Fukamizu, A., & Yamamoto, M. (2001). Two domains of Nrf2 cooperatively bind CBP, a CREB binding protein, and synergistically activate transcription. *Genes to Cells*, (6), 857–686.

Kesarwani, P., Murali, A. K., Al-Khami, A. A., & Mehrotra, S. (2013). Redox Regulation of T-Cell Function: From Molecular Mechanisms to Significance in Human Health and Disease. *Antioxidants & Redox Signaling*, 18(12), 1497–1534.

Kim, H. J., & Vaziri, N. D. (2010). Contribution of impaired Nrf2-Keap1 pathway to oxidative stress and inflammation in chronic renal failure. *AJP: Renal Physiology*, 298(3), F662–F671.

Kim, H. J., Sato, T., Rodriguez-Iturbe, B., & Vaziri, N. D. (2011). Role of Intrarenal Angiotensin System Activation, Oxidative Stress, Inflammation, and Impaired Nuclear Factor-Erythroid-2-Related Factor 2 Activity in the Progression of Focal Glomerulosclerosis. *Journal of Pharmacology and Experimental Therapeutics*, 337(3), 583–590.

- Klepac, N., Relja, M., Klepac, R., Hećimović, S., Babić, T., & Trkulja, V. (2007). Oxidative stress parameters in plasma of Huntington's disease patients, asymptomatic Huntington's disease gene carriers and healthy subjects. *Journal of Neurology*, 254(12), 1676–1683.
- Kobayashi, A., Kang, M. I., Okawa, H., Ohtsuji, M., Zenke, Y., Chiba, T., et al. (2004). Oxidative Stress Sensor Keap1 Functions as an Adaptor for Cul3-Based E3 Ligase To Regulate Proteasomal Degradation of Nrf2. *Molecular and Cellular Biology*, 24(16), 7130–7139.
- Kobayashi, M. (2010). Harnessing the Antioxidant Power with ARE-Inducing Compounds. *Chemistry & Biology*, 17(5), 419–420.
- Kraft, A. D., Lee, J.-M., Johnson, D. A., Kan, Y. W., & Johnson, J. A. (2006). Neuronal sensitivity to kainic acid is dependent on the Nrf2-mediated actions of the antioxidant response element. *Journal of Neurochemistry*, 98(6), 1852–1865.
- Kumar, P., Kalonia, H., & Kumar, A. (2010). Huntington's disease: pathogenesis to animal models. *Pharmacological Reports*, 62, 1–14.
- Kurosaki R, Muramatsu Y, Michimata M, Matsubara M, Kato H, Imai Y, Itoyama Y, Araki T. (2002) Role of nitric oxide synthase against MPTP neurotoxicity in mice. *Neurology Research*. 24(7):655-62.
- Kuthan, H., & Ullrich, V. (1982). Oxidase and Oxygenase Function of the Microsomal Cytochrome. *European Journal of Biochemistry*, (126), 583–588.
- Langsdorf, E. F., Mao, X., & Chang, S. L. (2011). A role for reactive oxygen species in endotoxin-induced elevation of MOR expression in the nervous and immune systems. *Journal of Neuroimmunology*, 236(1-2), 57–64.
- Lass, A., Agarwal, S., & Sohal, R. (1997). Mitochondrial Ubiquinone Homologues, Superoxide Radical Generation, and Longevity in Different Mammalian Species. *Journal of Biological Chemistry*, 272(31), 19199–19204.
- Lau, A., Wang, X. J., Zhao, F., Villeneuve, N. F., Wu, T., Jiang, T., et al. (2010). A Noncanonical Mechanism of Nrf2 Activation by Autophagy Deficiency: Direct Interaction between Keap1 and p62. *Molecular and Cellular Biology*, 30(13), 3275–3285.
- Lee, J. M. (2001). Phosphatidylinositol 3-Kinase, Not Extracellular Signal-regulated Kinase, Regulates Activation of the Antioxidant-Responsive Element in IMR-32 Human Neuroblastoma Cells. *Journal of Biological Chemistry*, 276(23), 20011–20016.

Lee, J., Kosaras, B., Signore, S. J., Cormier, K., McKee, A., Ratan, R. R., et al. (2010). Modulation of lipid peroxidation and mitochondrial function improves neuropathology in Huntington's disease mice. *Acta Neuropathologica*, 121(4), 487–498.

Leung, L. (2003). Deficiency of the Nrf1 and Nrf2 Transcription Factors Results in Early Embryonic Lethality and Severe Oxidative Stress. *Journal of Biological Chemistry*, 278(48), 48021–48029.

Levine AJ, Hu W, Feng Z. (2006) The P53 pathway: what questions remain to be explored? *Cell Death and Differentiation*. 13(6):1027-36.

Li, J. (2004). Stabilization of Nrf2 by tBHQ Confers Protection against Oxidative Stress-Induced Cell Death in Human Neural Stem Cells. *Toxicological Sciences*, 83(2), 313–328.

Li, J., Schneebeli, S. T., Bylund, J., Farid, R., & Friesner, R. A. (2011). IDSite: An Accurate Approach to Predict P450-Mediated Drug Metabolism. *Journal of Chemical Theory and Computation*, 7(11), 3829–3845.

Li, R., Chen, W., Yanes, R., Lee, S., & Berliner, J. A. (2006). OKL38 is an oxidative stress response gene stimulated by oxidized phospholipids. *The Journal of Lipid Research*, 48(3), 709–715.

Li, R., Ning, Z., Majumdar, R., Cui, J., Takabe, W., Jen, N., et al. (2010). Ultrafine particles from diesel vehicle emissions at different driving cycles induce differential vascular pro-inflammatory responses: Implication of chemical components and NF- κ B signaling. *Particle and Fibre Toxicology*, 7(1), 6.

Li, W., & Kong, A.-N. (2009). Molecular mechanisms of Nrf2-mediated antioxidant response. *Molecular Carcinogenesis*, 48(2), 91–104.

Li, Y., & Jaiswal, A. K. (1992). Regulation of Human NAD(P)H:Quinone Oxidoreductase Gene. *The Journal of Biological Chemistry*, 267(21), 15097–15104.

Lim, G. P., Chu, T., Yang, F., Beech, W., Frautschy, S. A., & Cole, G. M. (2001). The Curry Spice Curcumin Reduces Oxidative Damage and Amyloid Pathology in and Alzheimer Transgenic Mouse. *The Journal of Neuroscience*, 21(21), 8370–8377.

Kim JK, Choi SJ, Cho HY, Kim YJ, Lim ST, Kim CJ, Kim EK, Kim HK, Peterson S, Shin DH. (2011) Ipomoea batatas attenuates amyloid β peptide-induced neurotoxicity in ICR mice. *Journal of Medicinal Food*. 14(3):304-9

Linker, R. A., Lee, D. H., Ryan, S., van Dam, A. M., Conrad, R., Bista, P., et al. (2011). Fumaric acid esters exert neuroprotective effects in neuroinflammation via activation of the Nrf2 antioxidant pathway. *Brain*, 134(3), 678–692.

- Litjens, N. H. R., Burggraaf, J., van Strijen, E., van Gulpen, C., Mattie, H., Schoemaker, R. C., et al. (2004). Pharmacokinetics of oral fumarates in healthy subjects. *British Journal of Clinical Pharmacology*, 58(4), 429–432.
- Liu, D. H., Yuan, F. G., Hu, S. Q., Diao, F., Wu, Y. P., Zong, Y. Y., et al. (2013). Endogenous nitric oxide induces activation of apoptosis signal-regulating kinase 1 via s-nitrosylation in rat hippocampus during cerebral ischemia–reperfusion. *Neuroscience*, 229(C), 36–48.
- Liu, M., Li, Y., Chen, L., Chan, T. H. M., Song, Y., Fu, L., et al. (2014). *Gastroenterology*, 1–93. doi:10.1053/j.gastro.2013.12.041
- Loewen CA, Feany MB. (2010) The unfolded protein response protects from tau neurotoxicity in vivo. *PLoS One*. 5(9). pii: e13084.
- López Salon M1, Morelli L, Castaño EM, Soto EF, Pasquini JM (2000) Defective ubiquitination of cerebral proteins in Alzheimer's disease. *Journal of Neuroscience Research*. 62(2):302-10.
- Ma, Q., Battelli, L., & Hubbs, A. F. (2006). Multiorgan Autoimmune Inflammation, Enhanced Lymphoproliferation, and Impaired Homeostasis of Reactive Oxygen Species in Mice Lacking the Antioxidant-Activated Transcription Factor Nrf2. *The American Journal of Pathology*, 168(6), 1960–1974.
- MacManus DG, Miller DH, Kappos L, Gold R, Havrdova E, Limmroth V, Polman CH, Schmierer K, Yousry TA, Eraksoy M, Meluzinova E, Dufek M, Yang M, O'Neill GN, Dawson K. (2011) BG-12 reduces evolution of new enhancing lesions to T1-hypointense lesions in patients with multiple sclerosis. *Journal of Neurology*. 258(3):449-56.
- Maher, J., & Yamamoto, M. (2010). The rise of antioxidant signaling-The evolution and hormetic actions of Nrf2. *Toxicology and Applied Pharmacology*, 244(1), 4–15.
- Marchler-Bauer, A., Zheng, C., Chitsaz, F., Derbyshire, M. K., Geer, L. Y., Geer, R. C., et al. (2012). CDD: conserved domains and protein three-dimensional structure. *Nucleic Acids Research*, 41(D1), D348–D352.
- Marcus DL, Thomas C, Rodriguez C, Simberkoff K, Tsai JS, Strafci JA, Freedman ML. (1998) Increased peroxidation and reduced antioxidant enzyme activity in Alzheimer's disease. *Experimental Neurology*. 150(1):40-4.
- Martien S, Abbadie C. (2007) Acquisition of oxidative DNA damage during senescence: the first step toward carcinogenesis? *Annals, The New York Academy of Sciences*. 1119:51-63.

- Mas S, Gassó P, Trias G, Bernardo M, Lafuente A. (2012) Sulforaphane protects SK-N-SH cells against antipsychotic-induced oxidative stress. *Fundamental Clinical Pharmacology*. (6):712-21.
- Matsuura, E., Lopez, L. R., Shoenfeld, Y., & Ames, P. R. J. (2012). Autoimmunity Reviews. *Autoimmunity Reviews*, 12(2), 241–249.
- Matusheski NV, Juvik JA, Jeffery EH. (2004) Heating decreases epithiospecifier protein activity and increases sulforaphane formation in broccoli. *Phytochemistry*. 65(9):1273-81.
- McGeer, P. L., & McGeer, E. G. (2002). Innate Immunity, Local Inflammation, and Degenerative Disease. *Peer Reviewed*, 1–9.
- McMahon M, Thomas N, Itoh K, Yamamoto M, Hayes JD. (2006) Dimerization of substrate adaptors can facilitate cullin-mediated ubiquitylation of proteins by a "tethering" mechanism: a two-site interaction model for the Nrf2-Keap1 complex. *Journal of Biological Chemistry*. 281(34):24756-68.
- Melo, A., Monteiro, L., Lima, R. M. F., de Oliveira, D. M., de Cerqueira, M. D., & El-Bachá, R. S. (2011). Oxidative Stress in Neurodegenerative Diseases: Mechanisms and Therapeutic Perspectives. *Oxidative Medicine and Cellular Longevity*, 2011(3), 1–14.
- Miao, W. (2005). Transcriptional Regulation of NF-E2 p45-related Factor (NRF2) Expression by the Aryl Hydrocarbon Receptor-Xenobiotic Response Element Signaling Pathway: Direct Cross-talk Between phase I and II Drug-metabolizing Enzymes. *Journal of Biological Chemistry*, 280(21), 20340–20348.
- Miao, Y., Qiu, Y., Lin, Y., Miao, Z., Zhang, J., & Lu, X. (2010). Protection by pyruvate against glutamate neurotoxicity is mediated by astrocytes through a glutathione-dependent mechanism. *Molecular Biology Reports*.
- Miller, A. A., De Silva, T. M., Judkins, C. P., Diep, H., Drummond, G. R., & Sobey, C. G. (2010). Augmented Superoxide Production By Nox2-Containing NADPH Oxidase Causes Cerebral Artery Dysfunction During Hypercholesterolemia. *Stroke*, 41(4), 784–789.
- Miller AT, Wilcox HM, Lai Z, Berg LJ. (2004) Signaling through Itk promotes T helper 2 differentiation via negative regulation of T-bet. *Immunity*. 21(1):67-80.
- Misra JR1, Horner MA, Lam G, Thummel CS. (2011) Transcriptional regulation of xenobiotic detoxification in *Drosophila*. *Genes and Development*. ;25(17):1796-806.

Mittal, M., Siddiqui, M. R., Tran, K., Reddy, S. P., & Malik, A. B. (2014). Reactive Oxygen Species in Inflammation and Tissue Injury. *Antioxidants & Redox Signaling*, 20(7), 1126–1167.

Mittler, R., Vanderauwera, S., Suzuki, N., Miller, G., Tognetti, V. B., Vandepoele, K., et al. (2011). ROS signaling: the new wave? *Trends in Plant Science*, 16(6), 300–309.

Mitsuishi Y, Motohashi H, Yamamoto M. (2012) The Keap1-Nrf2 system in cancers: stress response and anabolic metabolism. *Front Oncol.* 2:200.

Mizuno K1, Kume T, Muto C, Takada-Takatori Y, Izumi Y, Sugimoto H, Akaike A. (2011) Glutathione biosynthesis via activation of the nuclear factor E2-related factor 2 (Nrf2)--antioxidant-response element (ARE) pathway is essential for neuroprotective effects of sulforaphane and 6-(methylsulfinyl) hexyl isothiocyanate. *Journal of Pharmacological Sciences.* 115(3):320-8.

Mochizuki H, Yasuda T. (2012) Iron accumulation in Parkinson's disease. *Journal of Neural Transmission.* 119(12):1511-4.

Mohler J, Vani K, Leung S, Epstein A. (1991) Segmentally restricted, cephalic expression of a leucine zipper gene during *Drosophila* embryogenesis. *Mechanisms of Development.* 34(1):3-9.

Moi P, Chan K, Asunis I, Cao A, Kan YW. (1994) Isolation of NF-E2-related factor 2 (Nrf2), a NF-E2-like basic leucine zipper transcriptional activator that binds to the tandem NF-E2/AP1 repeat of the beta-globin locus control region. *Proceedings of the National Academy of Sciences United States of America.* 91(21):9926-30.

Møller IM, Sweetlove LJ. (2010) ROS signalling--specificity is required. *Trends in Plant Science.* 15(7):370-4.

Montushci, P. (2004). Isoprostanes: markers and mediators of oxidative stress. *The FASEB Journal*, 18(15), 1791–1800.

Morris DR1, Geballe AP. (2000) Upstream open reading frames as regulators of mRNA translation. *Molecular and Cellular Biology.* 2000 Dec;20(23):8635-42.

Mouawad, C. A., Mrad, M. F., Al-Hariri, M., Soussi, H., Hamade, E., Alam, J., & Habib, A. (2013). Role of Nitric Oxide and CCAAT/Enhancer-Binding Protein Transcription Factor in Statin-Dependent Induction of Heme Oxygenase-1 in Mouse Macrophages. *PLoS One*, 8(5), e64092.

Mrowietz and Asadullah (2005). Dimethylfumarate for psoriasis: more than a dietary curiosity. *Trends in Molecular Medicine.* 11(1):43-8.

van Muiswinkel FL1, Kuiperij HB. (2005) The Nrf2-ARE Signalling pathway: promising drug target to combat oxidative stress in neurodegenerative disorders. *Current Drug Targets-CNS and Neurological Disorders*. 4(3):267-81.

Mukherjee B1, Telang N, Wong GY. (2009) Growth inhibition of estrogen receptor positive human breast cancer cells by Taheebo from the inner bark of *Tabebuia avellandae* tree. *International Journal of Molecular Medicine*. 24(2):253-60.

Murphy P, Sharp A, Shin J, Gavriyuk V, Dello Russo C, Weinberg G, Sharp FR, Lu A, Heneka MT, Feinstein DL. (2001) Suppressive effects of ansamycins on inducible nitric oxide synthase expression and the development of experimental autoimmune encephalomyelitis. *Journal of Neuroscience Research*. 67(4):461-70.

Nair, S., Doh, S. T., Chan, J. Y., Kong, A.-N., & Cai, L. (2008). Regulatory potential for concerted modulation of Nrf2- and Nfkb1-mediated gene expression in inflammation and carcinogenesis. *British Journal of Cancer*, 99(12), 2070–2082.

Nathan, C., & Cunningham-Bussel, A. (2013). Beyond oxidative stress: an immunologist's guide to reactive oxygen species. *Nature Publishing Group*, 13(5), 349–361.

Nguyen, T. (2000). Transcriptional Regulation of the Antioxidant Response Element. Activation by Nrf2 and Repression by MafK. *Journal of Biological Chemistry*, 275(20), 15466–15473.

Nguyen, T., Nioi, P., & Pickett, C. B. (2009). The Nrf2-Antioxidant Response Element Signaling Pathway and Its Activation by Oxidative Stress. *Journal of Biological Chemistry*, 284(20), 13291–13295.

Nguyen, T., Sherratt, P. J., & Pickett, C. B. (2003). Regulatory Mechanisms Controlling Gene Expression Mediated by the Antioxidant Response Element. *Annual Review of Pharmacology and Toxicology*, 43(1), 233–260.

Nguyen, T., Sherratt, P. J., Nioi, P., Yang, C. S., & Pickett, C. B. (2005). Nrf2 Controls Constitutive and Inducible Expression of ARE-driven Genes through a Dynamic Pathway Involving Nucleocytoplasmic Shuttling by Keap1. *Journal of Biological Chemistry*, 280(37), 32485–32492.

Niki, E. (2012). Do antioxidants impair signaling by reactive oxygen species and lipid oxidation products? *FEBS Letters*, 586(21), 3767–3770.

Niki, E., Omata, Y., Fukuhara, A., Saito, Y., & Yoshida, Y. (2008). Assessment of Radical Scavenging Capacity and Lipid Peroxidation Inhibiting Capacity of Antioxidant. *Journal of Agricultural and Food Chemistry*, 56(18), 8255–8260.

- Nioi, P., Nguyen, T., Sherratt, P. J., & Pickett, C. B. (2005). The Carboxy-Terminal Neh3 Domain of Nrf2 Is Required for Transcriptional Activation. *Molecular and Cellular Biology*, 25(24), 10895–10906.
- Nishinaka, T., & Yabe-Nishimura, C. (2005). Transcription Factor Nrf2 Regulates Promoter Activity of Mouse Aldose Reductase (AKR1B3) Gene. *Journal of Pharmacological Science*, 97, 43–51.
- Ockenfels, H. M., Schultewolter, T., Ockenfels, G., Funk, R., & Goos, M. (1998). The antipsoriatic agent dimethylfumarate immunomodulates T-cell cytokine secretion and inhibits cytokines of the psoriatic cytokine network. *British Journal of Dermatology*, 139, 390–395.
- Ohtsubo, T., Kamada, S., Mikami, T., Murakami, H., & Tsujimoto, Y. (1999). Identification of NRF2, a member of the NF-E2 family of transcription factors, as a substrate for caspase-3(-like) proteases. *Cell Death and Differentiation*, 6, 865–872.
- Omura S1, Koike E, Kobayashi T. (2009) Microarray analysis of gene expression in rat alveolar epithelial cells exposed to fractionated organic extracts of diesel exhaust particles. *Toxicology*. 262(1):65-72.
- Ong, C. K., Leong, C., Tan, P. H., Van, T., & Huynh, H. (2006). The role of 5' untranslated region in translational suppression of OKL38 mRNA in hepatocellular carcinoma. *Oncogene*, 26(8), 1155–1165.
- Ong, C. K., Ng, C. Y., Leong, C., Ng, C. P., Foo, K. T., Tan, P. H., & Huynh, H. (2004). Genomic Structure of Human OKL38 Gene and Its Differential Expression in Kidney Carcinogenesis. *Journal of Biological Chemistry*, 279(1), 743–754.
- Oreja-Guevara, C., Ramos-Cejudo, J., Aroeira, L. S., Chamorro, B., & Diez-Tejedor, E. (2012). TH1/TH2 Cytokine profile in relapsing-remitting multiple sclerosis patients treated with Glatiramer acetate or Natalizumab. *BMC Neurology*, 12(1), 1–1.
- Osborne, S. A., & Tonissen, K. F. (2001). Genomic organisation and alternative splicing of mouse and human thioredoxin reductase I genes. *BMC Genomics*, 2(10), 1471–2164.
- Osburn, W. O., Karim, B., Dolan, P. M., Liu, G., Yamamoto, M., Huso, D. L., & Kensler, T. W. (2007). Increased colonic inflammatory injury and formation of aberrant crypt foci in Nrf2-deficient mice upon dextran sulfate treatment. *International Journal of Cancer*, 121(9), 1883–1891.
- Pacher, P., Beckman, J. S., & Liaudet, L. (2007). Nitric Oxide and Peroxynitrite in Health and Disease. *Physiological Research*, 87(1), 315–424.

Paonessa, J. D., Ding, Y., Randall, K. L., Munday, R., Argoti, D., Vouros, P., & Zhang, Y. (2011). Identification of an Unintended Consequence of Nrf2-Directed Cytoprotection against a Key Tobacco Carcinogen plus a Counteracting Chemopreventive Intervention. *Cancer Research*, 71(11), 3904–3911.

Park HM, Kim JA, Kwak MK. (2009) Protection against amyloid beta cytotoxicity by sulforaphane: role of the proteasome. *Archives of Pharmacal Research*. 32(1):109-15.

Pehar, M., Vargas, M. R., Robinson, K. M., Cassina, P., Diaz-Amarilla, P. J., Hagen, T. M., et al. (2007). Mitochondrial Superoxide Production and Nuclear Factor Erythroid 2-Related Factor 2 Activation in p75 Neurotrophin Receptor-Induced Motor Neuron Apoptosis. *Journal of Neuroscience*, 27(29), 7777–7785.

Pendyala, S., & Natarajan, V. (2010). Redox regulation of Nox proteins. *Respiratory Physiology & Neurobiology*, 174(3), 265–271.

Priyadarshini, M., Orosco, L. A., & Panula, P. J. (2013). Oxidative Stress and Regulation of Pink1 in Zebrafish (*Danio rerio*). *PLoS One*, 8(11), e81851.

Qu, Z.-W., Miao, W.-Y., Hu, S.-Q., Li, C., Zhuo, X.-L., Zong, Y.-Y., et al. (2012). N-Methyl-D-Aspartate Receptor-Dependent Denitrosylation of Neuronal Nitric Oxide Synthase Increase the Enzyme Activity. *PLoS One*, 7(12), e52788.

Querfurth HW, LaFerla FM. (2010) Alzheimer's disease. *New England Journal of Medicine*. 362(4):329-44.

Rada, P., Rojo, A. I., Evrard-Todeschi, N., Innamorato, N. G., Cotte, A., Jaworski, T., et al. (2012). Structural and Functional Characterization of Nrf2 Degradation by the Glycogen Synthase Kinase 3/ -TrCP Axis. *Molecular and Cellular Biology*, 32(17), 3486–3499.

Ramachandran, B., Yu, G., & Gulick, T. (2008). Nuclear Respiratory Factor 1 Controls Myocyte Enhancer Factor 2A Transcription to Provide a Mechanism for Coordinate Expression of Respiratory Chain Subunits. *Journal of Biological Chemistry*, 283(18), 11935–11946.

Ramos-Gomez, M., Kwak, M.-K., Dolan, P. M., Yamamoto, M., Talalay, P., & Kensler, T. W. (2001). Sensitivity to carcinogenesis is increased and chemoprotective efficacy of enzyme inducers is lost in nrf2 transcription factor-deficient mice. *Proceedings of the National Academy of Sciences*, 98(6), 3410–3415.

Ramsey, C. P., Glass, C. A., Montgomery, M. B., Lindl, K. A., Ritson, G. P., Chia, L. A., et al. (2008). Expression of Nrf2 in Neurodegenerative Diseases. *Journal of Neuropathology and Experimental Neurology*, 66(1), 75–85.

Rashba-Step J, Cederbaum AI. (1994) Generation of reactive oxygen intermediates by human liver microsomes in the presence of NADPH or NADH. *Molecular Pharmacology*. 45(1):150-7.

Ray, P. D., Huang, B.-W., & Tsuji, Y. (2012). Reactive oxygen species (ROS) homeostasis and redox regulation in cellular signaling. *Cellular Signalling*, 24(5), 981–990.

Rea SL1, Walsh JP, Layfield R, Ratajczak T, Xu J. (2013) New insights into the role of sequestosome 1/p62 mutant proteins in the pathogenesis of Paget's disease of bone. *Endocrine Reviews*. 34(4):501-24.

Rejdak, K., Eikelenboom, M. J., Petzold, A., Thompson, E. J., Stelmasiak, Z., Lazeron, R. H. C., et al. (2004). CSF nitric oxide metabolites are associated with activity and progression of multiple sclerosis. *Neurology*, 63(8), 1439–1445.

Rejdak, K., Petzold, A., Stelmasiak, Z., & Giovannoni, G. (2008). Cerebrospinal fluid brain specific proteins in relation to nitric oxide metabolites during relapse of multiple sclerosis. *Multiple Sclerosis*, 14(1), 59–66.

Resende, R., Moreira, P. I., Proença, T., Deshpande, A., Busciglio, J., Pereira, C., & Oliveira, C. R. (2008). Brain oxidative stress in a triple-transgenic mouse model of Alzheimer disease. *Free Radical Biology and Medicine*, 44(12), 2051–2057.

Reynolds, M. R., Berry, R. W., & Binder, L. I. (2007). Nitration in Neurodegeneration: Deciphering the “Hows” and “Whys”. *Biochemistry*, 46(25), 7325–7336.

Riou, P., Saffroy, R., & Cornoy, J. (2002). Investigation in Liver Tissues and Cell Lines of the Transcription of 13 Genes Mapping to the 16q24 Region That Are Frequently Deleted in Hepatocellular Carcinoma. *Clinical Cancer Research*, (8), 3178–3168.

Romanoski, C. E., Che, N., Yin, F., Mai, N., Pouldar, D., Civelek, M., Pan, C., Lee, S., Vakili, L., Yang, W. P., Kayne, P., Mungrue, I. N., Araujo, J. A., Berliner, J. A., & Lusis, A. J. (2011a). Network for Activation of Human Endothelial Cells by Oxidized Phospholipids: A Critical Role of Heme Oxygenase 1. *Circulation Research*, 109(5), e27–e41.

Romanoski, C. E., Che, N., Yin, F., Mai, N., Pouldar, D., Civelek, M., Pan, C., Lee, S., Vakili, L., Yang, W. P., Kayne, P., Mungrue, I. N., Araujo, J. A., Berliner, J. A., & Lusis, A. J. (2011b). Network for Activation of Human Endothelial Cells by Oxidized Phospholipids: A Critical Role of Heme Oxygenase 1. *Circulation Research*, 109(5), e27–e41.

Rosen, D. R., Siddique, T., & Patterson, D. (1993). Mutations in Cu/Zn superoxide dismutase gene are associated with familial amyotrophic lateral sclerosis. *Letters to Nature*, 362, 59–62.

Rundlöf AK, Fernandes AP, Selenius M, Babic M, Shariatgorji M, Nilsson G, Ilag LL, Dobra K, Björnstedt M. (2007) Quantification of alternative mRNA species and identification of thioredoxin reductase 1 isoforms in human tumor cells. *Differentiation*. 75(2):123-32.

Rushmore, T. H., Morton, M. R., & Pickett, C. B. (1991). The Antioxidant Responsive Element. *The Journal of Biological Chemistry*, 266(18), 11632–11639.

Rushworth, S. A., Zaitseva, L., Murray, M. Y., Shah, N. M., Bowles, K. M., & MacEwan, D. J. (2012). The high Nrf2 expression in human acute myeloid leukemia is driven by NF- κ B and underlies its chemo-resistance. *Blood*, 120(26), 5188–5198.

Sacson, R. A., Bunton-Stasyshyn, R. K. A., Fisher, E. M. C., & Fratta, P. (2013). Is SOD1 loss of function involved in amyotrophic lateral sclerosis? *Brain*, 136(8), 2342–2358.

Salminen A, Kaarniranta K, Haapasalo A, Hiltunen M, Soininen H, Alafuzoff I. (2012) Emerging role of p62/sequestosome-1 in the pathogenesis of Alzheimer's disease. *Progress in Neurobiology*. 96(1):87-95.

Sangokoya, C., Telen, M. J., & Chi, J. T. (2010). microRNA miR-144 modulates oxidative stress tolerance and associates with anemia severity in sickle cell disease. *Blood*, 116(20), 4338–4348.

Sato Y, Yoshizato T, Shiraishi Y, Maekawa S, Okuno Y, Kamura T, Shimamura T, Sato-Otsubo A, Nagae G, Suzuki H, Nagata Y, Yoshida K, Kon A, Suzuki Y, Chiba K, Tanaka H, Niida A, Fujimoto A, Tsunoda T, Morikawa T, Maeda D, Kume H, Sugano S, Fukayama M, Aburatani H, Sanada M, Miyano S, Homma Y, Ogawa S. (2013) Integrated Molecular Analysis of Clear-cell Renal Cell Carcinoma. *Nature Genetics*. 45(8):860-7.

Scannevin, R. H., Chollate, S., Jung, M. Y., Shackett, M., Patel, H., Bista, P., et al. (2012). Fumarates Promote Cytoprotection of Central Nervous System Cells against Oxidative Stress via the Nuclear Factor (Erythroid-Derived 2)-Like 2 Pathway. *Journal of Pharmacology and Experimental Therapeutics*, 341(1), 274–284.

Schilling, S., Goelz, S., Linker, R., Luehder, F., & Gold, R. (2006). Fumaric acid esters are effective in chronic experimental autoimmune encephalomyelitis and suppress macrophage infiltration. *Clinical and Experimental Immunology*, 145(1), 101–107.

- Schimrigk, S., Brune, N., Hellwig, K., Lukas, C., Bellenberg, B., Rieks, M., et al. (2006). Oral fumaric acid esters for the treatment of active multiple sclerosis: an open-label, baseline-controlled pilot study. *European Journal of Neurology*, 13(6), 604–610.
- Schieber M, Chandel NS. (2014) ROS Function in Redox Signaling and Oxidative Stress. *Current Biology*. 24(10):R453-R462.
- Schipper, H. M. (2010). Biological Markers and Alzheimer Disease: A Canadian Perspective. *International Journal of Alzheimer's Disease*, 2010(2), 1–7. doi:10.1002/pmic.200300475
- Schrottmaier, W., Oskolkova, O. V., Schabbauer, G., & Afonyushkin, T. (2014). Accepted Manuscript. *Atherosclerosis*, 1–34. Schweckendiek (1959)
- Segal BM. (2003) Experimental autoimmune encephalomyelitis: cytokines, effector T cells, and antigen-presenting cells in a prototypical Th1-mediated autoimmune disease. *Current Allergy and Asthma Reports*. 3(1):86-93.
- Sharief MK, Hentges R. (1991) Association between tumor necrosis factor-alpha and disease progression in patients with multiple sclerosis. *New England Journal of Medicine*. 325(7):467-72
- Shih, A. Y., Imbeault, S., Barakauskas, V., Erb, H., Jiang, L., Li, P., & Murphy, T. H. (2005). Induction of the Nrf2-driven Antioxidant Response Confers Neuroprotection during Mitochondrial Stress in Vivo. *Journal of Biological Chemistry*. 280(24), 22925–22936.
- Shih, A. Y., Johnson, D. A., Wong, G., Kraft, A. D., Jiang, L., Erb, H., et al. (2003). Coordinate Regulation of Glutathione Biosynthesis and Release by Nrf2-Expressing Glia Potently Protects Neurons from Oxidative Stress. *Journal of Neuroscience*. 23(8), 3394–3406.
- Shivdasani, R. A., & Orkin, S. H. (1995). Erythropoiesis and globin gene expression in mice lacking the transcription factor NF-E2. *Proceedings of the National Academy of Sciences*. 92, 8690–8694.
- Siebert, A., Desai, V., Chandrasekaran, K., Fiskum, G., & Jafri, M. S. (2009). Nrf2 activators provide neuroprotection against 6-hydroxydopamine toxicity in rat organotypic nigrostriatal cocultures. *Journal of Neuroscience Research*. 87(7), 1659–1669.
- Sies, H. (2014). Role of Metabolic H₂O₂ Generation: Redox Signaling and Oxidative Stress. *Journal of Biological Chemistry*, 289(13), 8735–8741.
- Sies, H (1985). Oxidative stress: damage to intact cells and organs. *Philosophical Transactions of the Royal Society*, 311(1152), 617-3

- Singh, A., Misra, V., Thimmulappa, R. K., Lee, H., Ames, S., Hoque, M. O., et al. (2006). Dysfunctional KEAP1–NRF2 Interaction in Non-Small-Cell Lung Cancer. *PLoS Medicine*, 3(10), e420.
- Sofic E, Sapcanin A, Tahirovic I, Gavrankapetanovic I, Jellinger K, Reynolds GP, Tatschner T, Riederer P. (2006) Antioxidant capacity in postmortem brain tissues of Parkinson's and Alzheimer's diseases. *Journal of Neural Transmission*. (71):39-43.
- Stamer K, Vogel R, Thies E, Mandelkow E, Mandelkow EM. (2002) Tau blocks traffic of organelles, neurofilaments, and APP vesicles in neurons and enhances oxidative stress. *Journal of Cell Biology*. 2002 Mar 18;156(6):1051-63.
- Stefano, G. B., & Kream, R. M. (2009). Dopamine, Morphine, and Nitric Oxide: An Evolutionary Signaling Triad. *CNS Neuroscience & Therapeutics*. 16(3):124-137.
- Stoof TJ, Flier J, Sampat S, Nieboer C, Tensen CP, Boorsma DM. (2001) The antipsoriatic drug dimethylfumarate strongly suppresses chemokine production in human keratinocytes and peripheral blood mononuclear cells. *British Journal of Dermatology*. 144(6):1114-20.
- Suzuki, T., Shibata, T., Takaya, K., Shiraishi, K., Kohno, T., Kunitoh, H., et al. (2013). Regulatory Nexus of Synthesis and Degradation Deciphers Cellular Nrf2 Expression Levels. *Molecular and Cellular Biology*, 33(12), 2402–2412.
- Sykoti, G. P., & Bohmann, D. (2010). Stress-Activated Cap“n”collar Transcription Factors in Aging and Human Disease. *Science Signaling*, 3(112), re3–re3.
- Szabó, C., Ischiropoulos, H., & Radi, R. (2007). Peroxynitrite: biochemistry, pathophysiology and development of therapeutics. *Nature Reviews Drug Discovery*, 6(8), 662–680. doi:10.1038/nrd2222
- Szarka, A., Bánhegyi, G., & Sümegi, B. (2014). Mitochondria, oxidative stress and aging. *Orvosi Hetilap*, 155(12), 447–452.
- Tannenberg RK, Scott HL, Tannenberg AE, Dodd PR. (2006) Selective loss of synaptic proteins in Alzheimer's disease: evidence for an increased severity with APOE varepsilon4. *Neurochemistry International*. 49(7):631-9.
- Tarozzi, A., Angeloni, C., Malaguti, M., Morroni, F., Hrelia, S., & Hrelia, P. (2013). Sulforaphane as a Potential Protective Phytochemical against Neurodegenerative Diseases. *Oxidative Medicine and Cellular Longevity*, 2013(5), 1–10.
- Thimmulappa, R. K., Mai, K. H., & Srisuma, S. (2002). Identification of Nrf2-regulated Genes Induced by the Chemopreventive Agent Sulforaphane by Oligonucleotide Microarray. *Cancer Research*, 62, 5196–5203.

- Toki, T., Itoh, J., Kitazawa, J., Arai, K., Hatakeyama, K., Akasaka, J.-I., et al. (1997). Human small Maf proteins form heterodimers with CNC family transcription factors and recognize the NF-E2 motif. *Oncogene*, 14, 1901–1910.
- Toledano MB. (2009) The guardian recruits cops: the p53-p21 axis delegates prosurvival duties to the Keap1-Nrf2 stress pathway. *Molecular Cell*. 34(6):637-9.
- Tong, K. I., Katoh, Y., Kusunoki, H., Itoh, K., Tanaka, T., & Yamamoto, M. (2006). Keap1 Recruits Neh2 through Binding to ETGE and DLG Motifs: Characterization of the Two-Site Molecular Recognition Model. *Molecular and Cellular Biology*, 26(8), 2887–2900.
- Touil T, Deloire-Grassin MS, Vital C, Petry KG, Brochet B. (2001) In vivo damage of CNS myelin and axons induced by peroxynitrite. *Neuroreport*. 12(16):3637-44.
- Toki T1, Itoh J, Kitazawa J, Arai K, Hatakeyama K, Akasaka J, Igarashi K, Nomura N, Yokoyama M, Yamamoto M, Ito E. (1997) Human small Maf proteins form heterodimers with CNC family transcription factors and recognize the NF-E2 motif. *Oncogene*. 14(16):1901-10.
- Trinh, K., Andrews, L., Krause, J., Hanak, T., Lee, D., Gelb, M., & Pallanck, L. (2010). Decaffeinated Coffee and Nicotine-Free Tobacco Provide Neuroprotection in Drosophila Models of Parkinson's Disease through an NRF2-Dependent Mechanism. *Journal of Neuroscience*, 30(16), 5525–5532.
- Tully, M., & Shi, R. (2013). New Insights in the Pathogenesis of Multiple Sclerosis—Role of Acrolein in Neuronal and Myelin Damage. *International Journal of Molecular Sciences*, 14(10), 20037–20047.
- Turner, M. R., Bowser, R., Bruijn, L., Dupuis, L., Ludolph, A., McGrath, M., et al. (2013). Mechanisms, models and biomarkers in amyotrophic lateral sclerosis. *Amyotrophic Lateral Sclerosis and Frontotemporal Degeneration*, 14(S1), 19–32.
- van der Veen, R. C., Hinton, D. R., Incardonna, F., & Hofman, F. M. (1997). Extensive peroxynitrite activity during progressive stages of central nervous system inflammation. *Journal of Neuroimmunology*, (77), 1–7.
- van Muiswinkel, F. L., de Vos, R. A. I., Bol, J. G. J. M., Andringa, G., Jansen Steur, E. N. H., Ross, D., et al. (2004). Expression of NAD(P)H:quinone oxidoreductase in the normal and Parkinsonian substantia nigra. *Neurobiology of Aging*, 25(9), 1253–1262.
- Vargas, M. R., & Johnson, J. A. (2009). The Nrf2–ARE cytoprotective pathway in astrocytes. *Expert Reviews in Molecular Medicine*, 11.

- Vargas, M. R., Johnson, D. A., Sirkis, D. W., Messing, A., & Johnson, J. A. (2008). Nrf2 Activation in Astrocytes Protects against Neurodegeneration in Mouse Models of Familial Amyotrophic Lateral Sclerosis. *Journal of Neuroscience*, 28(50), 13574–13581.
- Vargas, M. R., Pehar, M., Cassina, P., Beckman, J. S., & Barbeito, L. (2006). Increased glutathione biosynthesis by Nrf2 activation in astrocytes prevents p75^{NTR}-dependent motor neuron apoptosis. *Journal of Neurochemistry*, 97(3), 687–696.
- Venugopal R, Jaiswal AK. (1996) Nrf1 and Nrf2 positively and c-Fos and Fra1 negatively regulate the human antioxidant response element-mediated expression of NAD(P)H:quinone oxidoreductase1 gene. *Proceedings of the National Academy of Sciences United States of America*. 93(25):14960-5.
- Vernon, P. J., & Tang, D. (2013). Eat-Me: Autophagy, Phagocytosis, and Reactive Oxygen Species Signaling. *Antioxidants & Redox Signaling*, 18(6), 677–691.
- Vehviläinen P, Koistinaho J, Gundars G. (2014) Mechanisms of mutant SOD1 induced mitochondrial toxicity in amyotrophic lateral sclerosis. *Frontiers in Cellular Neuroscience*. 8:126. eCollection 2014.
- Vila, B., Jaradat, Z. W., Marquardt, R. R., & Frohlich, A. A. (2002). Effect of T-2 toxin on in vivo lipid peroxidation and vitamin E status in mice. *Food and Chemical Toxicology*, 40, 479–486.
- Vila, E., Jyrkkänen, H. K., & Levonen, A. L. (2012). *Free Radical Biology & Medicine*. *Free Radical Biology and Medicine*, 52(6), 973–982.
- Vistoli, G., De Maddis, D., Cipak, A., Zarkovic, N., Carini, M., & Aldini, G. (2013). Advanced glycoxidation and lipoxidation end products (AGEs and ALEs): an overview of their mechanisms of formation. *Free Radical Research*, 47(S1), 3–27.
- Vurusaner B1, Poli G, Basaga H. (2012) Tumor suppressor genes and ROS: complex networks of interactions. *Free Radical Biological Medicine*. 52(1):7-18.
- Wakabayashi N, Itoh K, Wakabayashi J, Motohashi H, Noda S, Takahashi S, Imakado S, Kotsuji T, Otsuka F, Roop DR, Harada T, Engel JD, Yamamoto M. (2003) Keap1-null mutation leads to postnatal lethality due to constitutive Nrf2 activation. *Nature Genetics*. 35(3):238-45.
- Wang, H., Liu, K., Geng, M., Gao, P., Wu, X., Hai, Y., et al. (2013). RXR Inhibits the NRF2-ARE Signaling Pathway through a Direct Interaction with the Neh7 Domain of NRF2. *Cancer Research*, 73(10), 3097–3108.

Wang, T. (2004). Bone Marrow Stromal Cell-derived Growth Inhibitor Inhibits Growth and Migration of Breast Cancer Cells via Induction of Cell Cycle Arrest and Apoptosis. *Journal of Biological Chemistry*, 280(6), 4374–4382.

Wang, T., Zhang, X., & Li, J. J. (2002). The role of NF- κ B in the regulation of cell stress responses. *International Immunopharmacology*, 2, 1509–1520.

Werdenberg D1, Joshi R, Wolfram S, Merkle HP, Langguth P. (2003) Presystemic metabolism and intestinal absorption of antipsoriatic fumaric acid esters. *Biopharmaceutics and Drug Disposition*. 24(6):259-73.

Wild AC, Moinova HR, Mulcahy RT. (1999) Regulation of gamma-glutamylcysteine synthetase subunit gene expression by the transcription factor Nrf2. *Journal of Biological Chemistry*. 274(47):33627-36.

Wohlgemuth SE, Calvani R, Marzetti E. (2014) The interplay between autophagy and mitochondrial dysfunction in oxidative stress-induced cardiac aging and pathology. *Journal of Molecular and Cellular Cardiology*. 71C:62-70.

Wruck, C. J., Gotz, M. E., Herdegen, T., Varoga, D., Brandenburg, L. O., & Pufe, T. (2008). Kavalactones Protect Neural Cells against Amyloid Peptide-Induced Neurotoxicity via Extracellular Signal-Regulated Kinase 1/2-Dependent Nuclear Factor Erythroid 2-Related Factor 2 Activation. *Molecular Pharmacology*, 73(6), 1785–1795.

Xu, C. (2006). Inhibition of 7,12-Dimethylbenz(a)anthracene-Induced Skin Tumorigenesis in C57BL/6 Mice by Sulforaphane Is Mediated by Nuclear Factor E2-Related Factor 2. *Cancer Research*, 66(16), 8293–8296.

Yamamoto, T., Suzuki, T., Kobayashi, A., Wakabayashi, J., Maher, J., Motohashi, H., & Yamamoto, M. (2008). Physiological Significance of Reactive Cysteine Residues of Keap1 in Determining Nrf2 Activity. *Molecular and Cellular Biology*, 28(8), 2758–2770.

Yan X, Lee S, Gugiu BG, Koroniak L, Jung ME, Berliner J, Cheng J, Li R. (2014) Fatty acid epoxyisoprostane E2 stimulates an oxidative stress response in endothelial cells. *Biochemical and Biophysical Research Communications*. 444(1):69-74.

Yang, C., Zhang, X., Fan, H., & Liu, Y. (2009). Curcumin upregulates transcription factor Nrf2, HO-1 expression and protects rat brains against focal ischemia. *Brain Research*, 1282(C), 133–141.

Yao, H., Li, P., Venters, B. J., Zheng, S., Tompson, P. R., Pugh, B. F., & Wang, Y. (2008). Histone Arg Modifications and p53 Regulate the Expression of OKL38, a Mediator of Apoptosis. *The Journal of Biological Chemistry*, 283(29), 1–9.

Yia-Herttuala, S., Palinski, W., Rosenfield, M. E., Parthasarathy, S., Carew, T. E., Butler, S., et al. (1989). Evidence for the Presence of Oxidatively Modified Low Density Lipoprotein in Atherosclerotic lesions of Rabbit and Man. *Journal of Clinical Investigation*, 84, 1086–1095.

Yoh K, Itoh K, Enomoto A, Hirayama A, Yamaguchi N, Kobayashi M, Morito N, Koyama A, Yamamoto M, Takahashi S. (2001) Nrf2-deficient female mice develop lupus-like autoimmune nephritis. *Kidney International*. 60(4):1343-53.

Yoon JI, Bang SH, Park JS, Chang ST, Kim YH, Min J. (2010) Increased in vitro lysosomal function in oxidative stress-induced cell lines. *Applied Biochemistry and Biotechnology*. 163(8):1002-11.

Yu, R., Lei, W., Mandlekar, S., Weber, M. J., Der, C. J., Wu, J., & Kong, A.-N. (1999). Role of a Mitogen-activated Protein Kinase Pathway in the Induction of Phase II Detoxifying Enzymes by Chemicals*. *The Journal of Biological Chemistry*, (274), 27545–27552.

Zangar, R. (2004). Mechanisms that regulate production of reactive oxygen species by cytochrome P450. *Toxicology and Applied Pharmacology*, 199(3), 316–331.

Zecca, L., Berg, D., Arzberger, T., Ruprecht, P., Rausch, W. D., Musicco, M., et al. (2005). In vivo detection of iron and neuromelanin by transcranial sonography: A new approach for early detection of substantia nigra damage. *Movement Disorders*, 20(10), 1278–1285.

Zepeda AB, Pessoa A Jr, Castillo RL, Figueroa CA, Pulgar VM, Farías JG. (2013) Cellular and molecular mechanisms in the hypoxic tissue: role of HIF-1 and ROS. *Cell Biochemistry and Function*. 31(6):451-9.

Zipper LM, Mulcahy RT. (2002) The Keap1 BTB/POZ dimerization function is required to sequester Nrf2 in cytoplasm. *Journal of Biological Chemistry*. 277(39):36544-52.

Zoghi S, Amirghofran Z, Nikseresht A, Ashjazadeh N, Kamali-Sarvestani E, Rezaei N. (2011) Cytokine secretion pattern in treatment of lymphocytes of multiple sclerosis patients with fumaric acid esters. *Immunology Investigation*. 40(6):581-96.

CURRICULUM VITAE

MELANIE SHACKETT BRENNAN (b. 1984)

7 Linden Street Apt 2, Brookline, MA 02445

203-376-5897 · melaniesbrennan@gmail.com

EDUCATION

Boston University, Graduate Program in Neuroscience, Boston, MA

PhD in Neuroscience, September 2014

- *Coursework*: Behavioral Neuropharmacology, Developmental Neurobiology, Computational Neuroscience, Neuropharmacology, Neuroinflammation, Drug Discovery. GPA 3.93 out of 4.0.
- *Dissertation Title*: “The Nrf2 Transcriptional Target, Osgin1, Contributes to the Cytoprotective Properties of Dimethyl Fumarate”

University of Hartford, Program in Neuroscience, West Hartford, CT

MS in Neuroscience, June 2008

- *Coursework*: Neurophysiology, Neuroanatomy, Neuropharmacology, Clinical Neurology, Histology, Pathophysiology, Statistics. GPA 3.94 out of 4.0. Neuroscience Fellowship 2006-2008.
- *Master’s Thesis*: “Effects of Dietary Restriction and Exercise on Cognition and Oxidative Stress in Type 2 Diabetes”

University of Connecticut, Storrs, CT

BS in Biological Sciences, May 2006. Minor in History.

PROFESSIONALEXPERIENCE

Senior Associate Scientist, Pharmacology, Neurobiology Department

12/2013-present

Biogen Idec, Cambridge, MA

Associate Scientist III, Pharmacology, Neurobiology Department

02/2010-present

Biogen Idec, Cambridge, MA

- Investigated the mechanism of action of BG-12 which assisted in the program strategy for Tecfidera. This work was presented at various research meeting and will be published.
- Responsible for stable and primary cell-line assay development (ELISA, ICC, FLIPR Calcium Flux, Thermo Arrayscan Live/Fixed Cell Imaging Platform, RT-PCR) for multiple projects.

- Organization and execution of *in vivo* and *in vitro* pharmacology studies for downstream studies, including transcriptional profiling and protein quantification.
- Routinely conducted the *in vivo* screening/characterization assay (e.g. ELISA) for potential compound candidates in extracted/purified brain, plasma, and CSF from multiple animal models.
- Head the Thermo Arrayscan VTI technology: assist in assay development and algorithm creation
- Successfully prepared and delivered research updates/presentations at internal/external meetings
- Tissue culture manager

Associate Scientist II, Pharmacology, Neurobiology Department
07/2008-02/2010

Biogen Idec, Cambridge, MA

- Routinely conducted the *in vivo* screening/characterization assay (e.g. ELISA) for potential compound candidates in extracted/purified brain, plasma, and CSF from multiple animal models.
- Consistently executed weekly *in vitro* compound screening using cell-based assays (e.g. ELISA, viability assay)
- Used well-established statistical analysis for compound assessment and routinely presented results at weekly/monthly meetings
- Assisted with assay development as well as *in vivo* pharmacology studies

Graduate Research Assistant, Dr. Jacob P. Harney's Laboratory
12/2006-07/2008

University of Hartford, West Hartford, CT

- Conducted grant-funded research on ROS-deficient, diabetic mice (ALS/Lt strain). Performed *in vivo* glucose/insulin testing, cognition/depression testing, perfusion/fixation and tissue sectioning.
- Conducted protein analysis of *in vivo* samples using SDS-PAGE, Western Blot, and immunohistochemistry.
- Analyzed data using SPSS statistical analysis and presented findings at the annual Northeast Under/Graduate Research Organization for Neuroscience.

Graduate Research Assistant, Dr. Joanna Borucinska's Histology Laboratory
12/2007-07/2008

University of Hartford, West Hartford, CT

- Awarded a grant to research melanomacrophage centers (MMC) in shark livers.
- Assisted in shark dissection, tissue sampling and data collection in 3 sport fishing tournaments.
- Analyzed liver MMC using Spot Advanced software for histological methods and presented results at the annual Northeast Fish and Wildlife Conference.

ADDITIONAL EXPERIENCE

Head Teaching Assistant, Biology Department**08/2006-05/2008**

University of Hartford, West Hartford, CT

- Coordinated introductory biology and animal physiology labs. Planned and executed laboratory assignments, homework and exams for more than 60 students per semester. Instructed the neurophysiology lab for Master's students.

Horticultural Technician, Research Greenhouses**09/2002-05/2006**

University of Connecticut, Storrs, CT

- Trained in care, maintenance and propagation of rare and exotic plants. Identified abnormal plant conditions and performed tree surgeries. Assisted graduate students.

Medical Technician, Student Health Services**09/2003-05/2006**

University of Connecticut, Storrs, CT

- Formed productive liaison between medical professionals and patients. Routinely autoclaved, assisted nurses and handled medical records.

TECHNICAL AND LABORATORY EXPERTISE

Biochemistry and Molecular Biology: Protein analysis (e.g., SDS-PAGE, Western Blot, ELISA); Protein purification (e.g., immunoprecipitation, solid-phase extraction, SEC); RNA purification from cells and tissue, RACE, Northern Blot, Reverse-Transcription, RT-PCR, primer/probe set development; Assay development

In Vivo Techniques: Tissue harvest and sectioning, including brain microdissection; sterile surgery; dosing (e.g. PO/IP), cardiac puncture, *in vivo* cognition testing (e.g. Morris water maze and radial arm maze), *in vivo* depression testing, perfusion/fixation, immunohistochemistry, paraffin sectioning. Experience with rodent (e.g. rat, mouse), frog and shark.

Cell Biology: Sterile technique; Stable cell and primary cell culture (neuronal, astrocyte, microglial, macrophage and mixed cultures); Cell transfection (viral, liposomal, nucleofection); Cell-based assay development; Immunocytochemistry; Live/fixed cell imaging (Fluorescence and Confocal microscopy); Cell quantification/imaging (Cellomics Arrayscan); FLIPR Calcium Flux Assay

PUBLICATIONS

Melanie Shackett Brennan, Hiral Patel, Mi-Young Jung, Sarah Ryan, Matvey Lukashev, Pradeep Bista, Norm Allaire, Alice Thai, Patrick Cullen, Kenneth J. Rhodes, Robert H. Scannevin (2014). “BG-12 (delayed-release dimethyl fumarate) pharmacodynamic responses have distinct temporal and dose-dependent profiles and are Nrf2-dependent” *In preparation*.

Robert H. Scannevin, Sowmya Chollate, Mi-young Jung, **Melanie Shackett**, Hiral Patel, Pradeep Bista, Wei-ke Zeng, Sarah Ryan, Masayuki Yamamoto, Matvey Lukashev, and Kenneth J. Rhodes (2012). “Fumarates Promote Cytoprotection of Central Nervous System Cells against Oxidative Stress via the Nuclear Factor (Erythroid-Derived 2)-Like 2 Pathway” *Journal of Pharmacology and Experimental Therapeutics*. 341(1):274-284.

Hairuo Peng, Tina Talreja, Zhili Xin, J. Hernan Cuervo, Gnanasambandam Kumaravel, Michael J. Humora, Lin Xu, Ellen Rohde, Lawrence Gan, Mi-young Jung, **Melanie N. Shackett**, Sowmya Chollate, Anthone W. Dunah, Pamela A. Snodgrass-belt, H. Moore Arnold, Arthur G. Taveras, Kenneth J. Rhodes, and Robert H. Scannevin (2011). “Discovery of BIIB042, a Potent, Selective, and Orally Bioavailable γ -Secretase Modulator” *ACS Medicinal Chemistry Letters*. 2:786-791.

Zhili Xin, Hairuo Peng, Andrew Zhang, Tina Talreja, Gnanasambandam Kumaravel, Lin Xu, Ellen Rohde, Mi-young Jung, **Melanie N. Shackett**, David Kocisko, Sowmya Chollate, Anthone W. Dunah, Pamela A. Snodgrass-Belt, H. Moore Arnold, Arthur G. Taveras, Kenneth J. Rhodes, Robert H. Scannevin (2011). “Discovery of 4-aminomethylphenylacetic acids as c-secretase modulators via a scaffold design approach” *Bioorganic and Medicinal Chemistry Letters*. 21:7277-7280.

Borucinska JD, **Shackett M**, Kotran K, Barker T (2009). “Melanomacrophages in three species of free-ranging sharks from the northwestern Atlantic, the blue shark *Prionace glauca* (L.), the shortfin mako, *Isurus oxyrinchus Rafinesque*, and the thresher, *Alopias vulpinus* (Bonnaterre)” *Journal of fish diseases*. 32(10):883-891.

ABSTRACTS (2011-present)

M. S. Brennan, M.F. Matos, C. Sun, S. Szak, R.H. Scannevin (2014). “The Nrf2 transcriptional target, OSGIN1, contributes to the cytoprotective properties of monomethyl fumarate” *2014 Society for Neuroscience Meeting (Poster)*.

M. S. Brennan, N. Allaire, D.J. Huss, P. Cullen, A. Thai, S. Szak, A.M. Thomas, D. Gianni, J.P. Carulli, J.D. Fontenot, B.T. Wipke, K.J. Rhodes, R.H. Scannevin (2014). “Dimethyl Fumarate and Monomethyl Fumarate are Distinguished by Nonoverlapping Pharmacodynamic Effects In Vivo” *2014 Annual Meeting of the American Academy of Neurology (Poster)*.

Melanie S. Brennan, Maria Matos, Xiaoping Hronowski, Benbo Gao, Peter Juhasz, Kenneth J. Rhodes and Robert H. Scannevin (2014). “Dimethyl Fumarate and Monoethyl Fumarate Exhibit Differential Effects on Glutathione, Keap1 and Nrf2 Activation In Vitro” *2014 Annual Meeting of the American Academy of Neurology (Poster)*.

M. S. Brennan, H. Patel, S. Ryan, M. Lukashev, P. Bista, S. Glass, N. Allaire, A. Thai, P. Cullen, K.J. Rhodes, R.H. Scannevin (2013). “BG-12 (Dimethyl Fumarate) pharmacodynamic responses have distinct temporal and dose-dependent profiles and are Nrf2-dependent” *2013 Society for Neuroscience Meeting (Nanosymposium speaker)*.

M. S. Brennan, N. Allaire, D. Huss, P. Cullen, A. Thai, S. Szak, A. Thomas, D. Gianni, J. P. Carulli, J. Fontenot, B. Wipke, K. P. Rhodes, R. H. Scannevin (2013). “Dimethyl fumarate and monomethyl fumarate are distinguished by non-overlapping pharmacodynamic effects in vivo” *2013 European Committee for Treatment and Research in Multiple Sclerosis (Poster)*.

Melanie N. Shackett, M.S., Hiral Patel, M.S., Mi-Young Jung, Ph.D., Sarah Ryan, B.A., Matvey Lukashev, Ph.D., Pradeep Bista, Ph.D., Kenneth J. Rhodes, Ph.D., Robert H. Scannevin, Ph.D. (2013). “BG-12 Pharmacodynamic Responses Have Distinct Temporal Profiles and are Dose-Dependent” *65th Annual Meeting of the American Academy of Neurology (Poster)*.

Melanie N. Shackett, M.S., Hiral Patel, M.S., Mi-Young Jung, Ph.D., Sarah Ryan, B.A., Matvey Lukashev, Ph.D., Pradeep Bista, Ph.D., Kenneth J. Rhodes, Ph.D., Robert H. Scannevin, Ph.D. (2012). “BG-12 Pharmacodynamic Responses Have Distinct Temporal Profiles and are Dose-Dependent” *2012 European Committee for Treatment and Research in Multiple Sclerosis (Poster)*.

ACTIVITIES AND HONORS

Society for Neuroscience, Member, 2012-present

Women in Neuroscience (WIN), Member, 2012-present

HBA Boston 2012 Mentoring Program, Accepted as a Mentee for the 2012 Program

Community Lab Volunteer, Volunteer at the BIIB science lab for middle/high school students, 2009-present.

Community Lab Mentor, mentor to HS student for science project, Sept 2010-Feb 2011.

Society Member, National Honors Society of Leadership and Success, 2007-2008

Chairman, Dean’s Graduate Student Advisory Board, 2006-2008

Grant Recipient, Women’s Education and Leadership Fund, 2007, 2008

Research Presenter, Northeast Under/Graduate Research Organization for Neuroscience. 2007, 2008

Research Presenter, Northeast Fish and Wildlife Conference, 2008.

Research Presenter, University of Hartford Graduate Research/Creativity Symposium, 2008.

SKILLS

Computer: Proficient in MS Office, GraphPad Prism, SPSS, Axiovision, Thermo Arrayscan Software (vHCS Scan and View), SoftMaxPro, Primer Express. Working knowledge of Accord for Excel, Spot Advanced.

Technologies: Thermo Arrayscan VTI, Confocal Imaging, JANUS liquid handler, PerkinElmer Envision and Enspire, QuantStudio 12k-flex, Kodak Image Station, FLIPR